ACTIVITY AND STRUCTURE OF AUDITORY BRAIN NEURONS UNDERLYING PHONOTACTIC BEHAVIOUR IN FEMALE CRICKETS

Xinyang Zhang

King's College

This dissertation is submitted for the degree of Doctor of Philosophy in

University of Cambridge

September 2020

PREFACE

This dissertation is the result of my own work and includes nothing which is the outcome of work done in collaboration except as declared in the Preface and specified in the text. It is not substantially the same as any that I have submitted, or is being concurrently submitted for a degree of diploma or other qualification at the University of Cambridge or any other University or similar institution except as declared in the Preface and specified in the text.

This thesis contains 59248 words which does not exceed the prescribed word limit for the Degree Committee.

ACKNOWLEDGEMENTS

I would like to express my sincerest gratitude to my supervisor Dr. Berthold Hedwig for his patient guidance and support throughout my PhD study. Dr. Hedwig has always been very supportive no matter what difficulty I was encountering. Thank you for accompanying me and strengthening my inner power along this fantastic journey. You are really a good friend, a caring advisor and a great mentor to me.

Thanks to my friends and colleagues in Hedwig Lab for their constant support. I would also like to thank Cambridge Trust, Trinity college, and the Department of Zoology for providing financial support for my PhD study.

Most importantly, I want to express my thanks and love to my parents for their unwavering support and encouragement. You have always been there for me no matter what tribulations I have gone through in my life. Your love infuses vitality, happiness and courage into my little life and always leads me to pursue my dream. My love, in return, will now guard your sweet dreams through every long night of your life.

TABLE OF CONTENTS

Preface **2**

Acknowledgements **3**

Table of contents **4**

Summary **5**

Chapter 1: General Introduction **7**

Chapter 2: Morphology of the auditory neuropil **15**

Introduction 15

Materials and methods 17

Results 21

Discussion 31

Chapter 3: The effects of changing interval durations within a chirp on processing by the pattern recognition circuit **34**

Introduction 34

Materials and methods 37

Results 44

Discussion 114

Chapter 4: The effects of changing pulse durations within a chirp on processing by the pattern recognition circuit **124**

Introduction 124

Materials and methods 126

Results 129

Discussion 219

Chapter 5: General Discussion **234**

Bibliography 245

SUMMARY

A long standing question in cricket neurobiology is what kind of neuronal mechanism the females use, to recognise the temporal pattern of the male calling song. A delay-line and coincidence detector circuit with five neurons underlying auditory pattern recognition in the bi-spotted cricket *Gryllus bimaculatus* was identified by Schöneich et al (2015). My results here confirmed the morphology of the five identified neurons. Moreover, the group labelling of the auditory neuropil in cricket brain shown in my thesis demonstrated that there are at least 51 neurons in the auditory neuropil. The cell bodies are grouped into six clusters with five in the hemisphere ipsilateral and one in the hemisphere contralateral to the ring structure.

In the previous researches the mechanisms underlying the temporal processing were mostly explored by testing sound patterns with varied pulse period. Recent behavioural tests were performed by systematically varying single pulse durations or inter-pulse intervals, which also led to the design of a chirp pattern with 5-20-50 ms pulses that is attractive when played forward, but non-attractive when the same pulses are played backwards as a 50-20-5 ms chirp pattern. In this thesis, I used these sound paradigms to explore the mechanism underlying the processing of individual pulses and intervals by recording the identified neurons in the pattern recognition circuit in cricket brain. The recordings of the pattern recognition circuit reveal the neurophysiological response properties of the five neurons in response to these sound paradigms. The pattern recognition circuit filters the temporal patterns of the chirps progressively. The tuning of the coincidence detector (LN3) and the feature detector (LN4) to the stimuli with varied intervals matched the behavioural tuning but did not reflect the behavioural responses when the duration of pulses were varied. The results also demonstrate that the mechanisms underlying the filtering of pulses or intervals in the pattern recognition circuit may be different. The processing of a train of pulses was accumulative and the activity elicited by a sound pulse in the pattern recognition circuit influences the subsequent responses. One single long interval is sufficient for a reduced activity in LN4 compared to the normal chirp. However, when intervals were kept constant, it required at least three consecutive long pulses

for LN4 to respond differently compared to the normal pulses. The attractive and non-attractive patterns elicited very similar level of activity in the feature detector LN4 in terms of AP/chirp. Further exploration is required to clarify the possible reason for this discrepancy between the neural and behavioural activity.

CHAPTER 1: GENERAL INTRODUCTION

Acoustic signaling occurs in many species of vertebrates and invertebrates. It supports mate attraction at night and in cluttered environments and over large distances when population densities are low. In insect acoustic signaling has evolved in several taxa, and is most prominent in cicada, moths, grasshoppers, crickets and bush-crickets (Hedwig 2014). Signals are generated by stridulatory (grasshoppers, crickets) or timbal mechanisms (cicada, moths). Acoustic signals are often stereotypical repetitive sequences of sound patterns generated by simple motor programs driving the "musical instruments". The song patterns are species-specific, and species may use different signals for mate attraction, territorial and rivalry behaviour and courtship displays and accordingly are generally labelled as calling, rivalry and courtship songs. Acoustic signaling comes with the evolution of hearing organs and auditory pathways, which in insects may have different shapes and design and structure (Fullard &Yack 1993, Yager 1999).

In insects' acoustic signals are part of communication systems in which generally the males are the sender of the signal. In uni-directional systems (e.g. crickets, some bushcrickets) males generate a calling song, while the mute females, which are ready to mate, will approach the singing male guided by the song pattern of the male. In bi-directional systems (Phaneopterine bush-crickets, cicada, acridid grasshoppers, Eneopterine crickets) the females remain stationary and respond to the singing male by a response song of her own, or by a vibratory signal and it is up to the male to approach the female. In this case, both males and females are sender as well as receiver of a signal. In any case, the receiver have to solve two fundamental problems: they need to recognise if the song pattern is a conspecific calling song and they need to approach the sender using just the acoustic signal for orientation, in a behaviour called phonotaxis.

The sounds of insects have attracted the attention of naturalists in different cultures since centuries (Roesel von Rosenhof 1748) and in China singing bush crickets were kept as pets for amusement (Laufer 1927). In more modern times, acoustically communicating insects became "model" animals for scientists to analyse the biomechanical and neural mechanisms of signal generation and auditory processing (Elsner and Popov 1978, Huber et al. 1989, Gerhardt and Huber 2002, Ronacher 2019). While there are about 600 extant cricket species, especially

Teleogryllus oceanicus, *Acheta domesticus* and the sister species *Gryllus campestris* and *Gryllus bimaculatus* became model organisms for behavioural and neurobiological studies (Hoy 1978, Huber et al. 1989, Horch et al. 2017).

Male crickets generate their songs by rhythmically rubbing the front wings together. Each closing movement of the front wings generates a sound pulse of 15-20 ms duration, in the range of 3-6 kHz and which in some species may reach up to 95 dB SPL. In *G. bimaculatus* and *A. domesticus* 3-5 pulses are grouped into chirps with pulse intervals of 15-20 ms. During a calling song, 2-3 chirps are produced per second, while the songs may continue with brief pauses for many hours. Rivalry songs are only generated during aggressive encounters with conspecific males and contain 8-12 pulses while courtship songs in front of females consist of low amplitude, high frequency sound pulses of 12-16 kHz which are repeated at the rate of chirps (Kutsch and Otto 1972). Song patterns in other species like *Teleogryllus* are more complex, as pulses of slightly different durations and pulse periods are grouped into chirps and trills. Females, which are ready to mate, walk or fly towards the singing conspecific males, using their sound patterns for orientation.

Various approaches have been developed and employed to analyse the behavioural responses of females towards the male calling song. Tschuch (1976) using arena experiments and Popov and Shuvalov (1977) using a Y-maze were the first to systematically characterise female cricket preferences to different song patterns and reported that *G. bimaculatus* females prefer pulse periods of about 36 ms and chirp durations of about 130-170 ms. More systematic quantitative studies were possible with the development of walking compensators, which allowed the cricket specimen to walk freely on top of a trackball in closed loop systems, while the movements of the trackball were compensated by an optoelectronic feedback system (Wendler et al. 1980, Weber and Thorson 1989). In open-loop systems tethered crickets rotate a small lightweight sphere while exposed to different sound patterns. In both cases the movements of the trackball indicate the movements of the cricket. The quantitative measurements indicate the walking speed and walking direction of the tested specimen (Doherty and Pires 1987, Hedwig and Poulet 2005, Hedwig 2017) and allow to characterise the temporal tuning of female crickets to different pulse patterns (Thorson et al. 1982, Hedwig 2006, Hennig 2003). In the sister species *G. campestris* and *G. bimaculatus* temporal preferences for pulse patterns relate to a band pass filter. Females do not respond to pulses presented at short pulse periods of 5-20 ms, they perform phonotaxis well at pulse periods of 34-42 ms and then

their phonotactic response decreases again, when chirps with pulse periods longer than 50 ms are presented.

As female crickets and bush-crickets are selectively attracted to the conspecific male calling song, their nervous system must have neuronal processing mechanisms that allow the identification of the song pattern and the subsequent phonotactic orientation. Cricket acoustic communication is used as a neuroethological model system, with the aim to explore the neurobiological basis of a "simple" behaviour and link it to the structure and function of identified neurons and to the network properties of the central nervous system (Huber et al. 1989, Gerhardt and Huber 2002, Horch et al. 2017).

Crickets carry their hearing organs in the tibia of their front legs. Sound acts on the auditory organ via a tympanal membrane at the posterior of the tibia and also via an auditory trachea, which runs from its opening in the lateral prothoracic body segment towards the hearing organ in the front leg. The 40-60 auditory afferents are not attached to the tympanic membrane but are located on the auditory trachea and linearly arranged in the *crista acustica*. The axons of the primary afferent neurons project towards the prothoracic ganglion, with terminals ending in the anterior ventrally located auditory neuropil.

The prothoracic auditory interneurons are well characterised (Rheinlaender et al. 1976, Wohlers and Huber 1982, Boyan and Williams 1982). Besides the local Omega shaped ON1 neurons, which support directional processing, the ascending interneurons AN1 and AN2 forward auditory information towards the brain. Whereas AN1 is tuned towards the carrier frequency of the male calling song, AN2 responds to high frequency signals and is linked to bat avoidance behaviour (Nolen and Hoy 1984). Only one AN1 and one AN2 occur at each side of the central nervous system, and AN1 seems to be the only neuron that forwards auditory information related to the calling song towards the brain. Both AN1 and AN2 neurons terminate in the anterior ventral protocerebrum, especially the axonal terminals of AN1 form a confined ring-like structure close to the surface of the brain. Also, AN2 sends axonal branches into the ring-like neuropil, but it projects more widely in the lateral areas of the brain and towards the optical stalk (Schildberger 1984). From the prothoracic ganglion a descending interneuron (DN1) that also reliably copies the song pattern projects posteriorly towards the meso- and metathoracic ganglion and a T-fibre neuron, with very transient phasic responses projects anteriorly and posteriorly in the CNS. Furthermore, local non-spiking prothoracic auditory neurons have been described (Stiedl et al. 1997).

The neural network for auditory pattern recognition is located in the brain. Local brain neurons have been identified (Schildberger 1984, 1988, Boyan1981, 1984, Kostarakos and Hedwig 2012, Schöneich et al. 2015), which are likely involved in higher level of auditory processing. The picture for the descending neurons, which may provide the commands for phonotactic motor control are net yet very clear. Although descending neurons have been described which respond to acoustic stimuli, a clear link to the control of phonotactic walking behaviour has not yet been established. This may be because phonotactic behaviour is not controlled by a single command neuron for phonotactic walking, but rather by a population of descending neurons. Information is still very sparse on descending interneurons, which may integrate auditory responses. Such neurons are required to carry the phonotactic motor commands to the thoracic system to drive the phonotactic behaviour (Boyan and Williams 1981, Böhm and Schildberger 1992, Staudacher and Schildberger 1998, Zorovic and Hedwig 2013).

Three main concepts have been put forward to explain the basis of temporal pattern recognition, which can be summarised as *template matching*, *band-pass filtering* and *delay-line coincidence-detection* (Weber and Thorson 1989, Kostarakos and Hedwig 2015). Alexander (1962) speculated that the neuronal structures that are used for song production in the male, would reside in the females and could be used for auditory pattern recognition. Based on this idea Hoy (1978) suggested that a feature detector for the conspecific song pattern could be established by comparing the auditory neuronal input pattern with an internal template, based on a corollary discharge from the singing CPG, which at a very low level would also be active in mute females. The neuronal network for song pattern generation, however resides in the abdominal ganglia chain of the males (Schöneich and Hedwig, 2012, Jacob and Hedwig 2019) and there is no structural overlap between the motor network controlling singing and the auditory pathway. Pattern recognition using a cross-correlation with an internal template was suggested by Hennig (2003) and suggested oscillatory properties of neurons, which would be compared to the auditory signal over physiological time windows. In bush-crickets oscillatory properties of a pattern recognition network have been made plausible by behavioural experiments (Bush and Schul 2006), although the underlying neurons have not been identified.

Based on neurophysiological recordings of the omega neurons (ON1) Wiese and Eilts (1985) and Wiese and Albrecht (1990) suggested that the band pass filtering of the song pattern occurs already at the thoracic level, based on the time constants of the reciprocal inhibition between the ON1 neurons and a proposed postinhibitory rebound. This hypothesis of a thoracic

filtering mechanism was not supported by further evidence. Recordings of the ascending interneuron AN1 did not show evidence for temporal filtering of the pulse pattern at the thoracic level (Wohlers and Huber 1982). The AN1 spike activity rather copies any sound pattern and forwards the information towards the brain, indicating that the recognition of the species-specific song pattern must happen in the brain. Auditory brain neurons were recorded for the first time by Boyan (1981), and by Schildberger (1984), who proposed that the spike activity of local brain neurons indicated filtering of the pulse pattern by low-pass and high-pass neurons, which in sequential combination would set-up the band-pass filter properties, underlying the phonotactic tuning of the females. This band-pass filter hypothesis was inspired by data in frogs (Rose and Capranica 1983) and for some time became the text book hypothesis for auditory pattern recognition in crickets (Carew 2000).

Recent neurophysiological experiments however, support the hypothesis of a delay-line and coincidence-detector mechanisms for the filtering of the calling song pulse pattern (Kostarakos and Hedwig 2012, Schöneich et al. 2015). Evidence is based on the response properties of local auditory brain neurons located in the ring-like structure, which have been characterised as coincidence detector neurons. These neurons respond weakly, if only one cricket sound pulse is presented, but respond with an enhanced excitation and spikes when two pulses are presented at the normal pulse interval of the calling song. This property is supported, by a non-spiking interneuron that generates a delayed post-inhibitory rebound with a time course matching the pulse period of the *G. bimaculatus* calling song. Temporal filtering is thought to be based on the coincidence of the delayed post-inhibitory rebound signal and a direct non-delayed signal, both carried forward to the coincidence detector neuron.

As the delay-line coincidence-detection circuitry forms the crucial background to my thesis, I want to give a more detailed account of its function and organisation, which follows the general concept outlined by Weber and Thorson (1989) and the details given by Schöneich et al. (2015). The underlying neuronal circuit occurs on each side of the anterior protocerebrum and includes the ascending neuron AN1, and four local neurons (LN): an inhibitory neuron LN2, a non-spiking neuron LN5, a coincidence detector LN3 and a feature detector LN4 (Fig. 1A). The ascending neuron AN1 receives input from auditory afferents in the prothoracic ganglion (Hennig 1988) and forwards the information to both the inhibitory neuron LN2 and the coincidence detector LN3. The neuron LN2 tightly follows AN1 activity with a latency of about of 2 ms, and in response to sound pulses it inhibits the non-spiking neuron LN5 and the feature

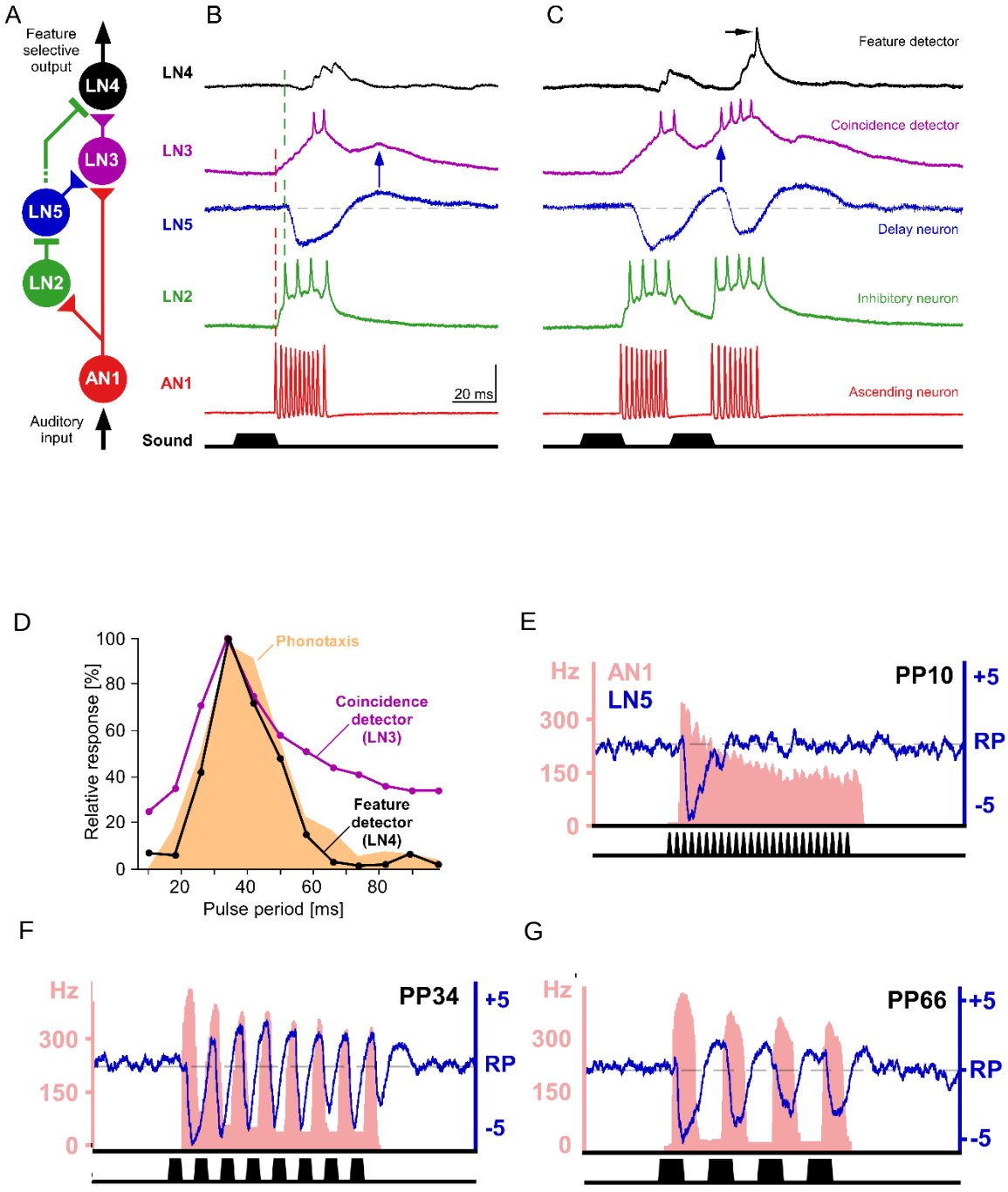

Fig. 1 The pattern recognition circuitry and its tuning to different pulse period. **A.** The pattern recognition circuitry proposed by Schoeneich et. al (2015). **B-C.** The typical responses of the five auditory neurons to a single (B) and a pair (C) of sound pulses with a 20-ms interval. **D.** Tuning of the coincidence detector (LN3), the feature detector LN4, and the phonotactic behaviour toward chirps with different pulse periods. **E-G.** Instantaneous spike rate of AN1 (red shade) and changes in the membrane potential of LN5 (blue trace) for chirps with different pulse period (pulse period = 10 ms, 34 ms, and 66 ms). PP34 is the same as in the normal calling song of *Gryllus bimaculatus*. The figures are derived from Schoeneich et. al (2015).

detector LN4. The non-spiking neuron LN5 responds with a pronounced inhibition and subsequently generates a post-inhibitory rebound (PIR), with a delay of about 40 ms after the start of a sound pulse. The excitatory activity caused by the post-inhibitory rebound is carried forward to the coincidence detector neuron LN3 (Fig. 1A). In this way the coincidence-detector LN3 receives a direct excitatory input from AN1 and a delayed excitatory input from the PIR of LN5. Due to the coincidence of both inputs LN3 responds stronger and passes the integrated information to the feature detector LN4 (Fig. 1A). The PIR is considered as the most crucial element in this pattern recognition circuit (Schöneich et al. 2015). When one sound pulse is presented, AN1 spikes excite the coincidence detector LN3, while the PIR of LN5 activates the coincidence detector with a delayed graded depolarisatison following the AN1 input (Fig. 1B). When a second pulse follows the first pulse with an interval of 20 ms, the activity of AN1 caused by the second pulse transiently overlaps with the graded depolarisation of the PIR in LN5 caused by the previous pulse (Fig. 1C). The coincidence detector LN3 now receives the two excitatory inputs from AN1 and LN5 at the same time, and their temporal summation causes a stronger response to the second sound pulse. The temporal tuning of this circuit depends on the delay and the time course of the PIR and is adapted to the pulse period of the natural calling song.

The feature detector neuron (LN4) integrates inhibition from LN2 and excitation from LN3. In case of the first sound pulse the excitation from LN3 is not sufficient to overcome the inhibition, however when LN3 responds to the second pulse and later pulses, its enhanced activity causes spiking in LN4. Consequently, LN4 selectively responds best to the species-specific sound pattern and matches the tuning of the phonotactic behaviour when the circuit is tested with different pulse periods (Schöneich et al. 2015, Fig. 1D). The time course of the delayed graded rebound potential in LN5 and whether it coincides at the coincidence detector LN3 with the direct input from AN1 is key to the temporal tuning of the pattern recognition network and works best, when the pulse period is between 34 and 42 ms, corresponding to the natural calling song of *G. bimaculatus* (Fig. 1E-G). The coincidence detection mechanisms underlying the processing of temporal patterns were also reported in other animals like bats (Covey and Faure 2005). The pattern recognition in bats comes from the coincidence between the responses to the onset and offset of the sound pulses. Moreover, the temporal processing based on the interplay between inhibition and excitation in the auditory neurons was also reported in frogs (Leary et al. 2008).

The neuronal circuit of the delay-line and coincidence-detector circuit is confined to the local interneurons in the ring-like neuropil. The total number of neurons projecting into this neuropil is not well understood and it is not clear if the identified neurons are represented by single neurons of by groups of neurons, performing the same/similar function. Using an extracellular labelling method with surface electrodes (Kostarakos and Hedwig 2017) demonstrated that neurons of three different clusters project into the ring-like structure, which all could contribute to auditory processing.

In the previous research the mechanisms underlying the temporal processing were explored by testing sound patterns with varied pulse period, and this overlooked the different roles of pulses and intervals within a chirp. The mechanism underlying the processing of individual pulses and intervals can be revealed by exploring the response properties of the identified neurons in the pattern recognition circuit with individual pulses and intervals of a chirp varied.

The processing of the pulses in a chirp with different intervals and pulses should reflect the proposed principle of the delay-line and coincidence detection mechanism based on the overlap between the post-inhibitory rebound and the AN1 spikes. It should also reveal the dynamics of neuronal responses depending on the pulse duration and intervals.

What my research aims at is to explore the possible effect of individual intervals and pulses on the activity of the neural network proposed by Schoneich et al. (2015) and evaluate its link to the phonotactic tuning of female *G. bimaculatus* obtained by Hedwig and Sarmiento-Ponce (2017).

CHAPTER 2: NEURONS OF THE RING-LIKE AUDITORY NEUROPIL

INTRODUCTION

In crickets, the external auditory signals are carried to the central nervous system by the auditory afferents which terminate in the prothoracic ganglion. To recognize the conspecific calling song, the nervous system of female crickets is required to analyze not only the carrier frequency but, more crucially, the temporal structure of the calling song produced by males. Experimental evidence indicates that the filtering of the temporal pattern of auditory signals does not occur at the level of thoracic processing but rather in the brain (Schildberger et al. 1989, Hedwig, 2014). We now have a good understanding of the auditory pathway and its neural components in the nervous system. Two types of neurons with their cell bodies located in the prothoracic ganglion have axons ascending to the brain of *Gryllus bimaculatus*: the ascending neurons AN1 and AN2 (Wohlers and Huber 1982). AN1 copies the auditory patterns presented at the conspecific carrier frequency with high fidelity whereas the response of AN2 does not represent sound patterns at this carrier frequency. This points towards AN1 to be a crucial element for auditory processing and pattern recognition of the calling song in the cricket brain (Schildberger 1984; Schildberger et al. 1989). In *G. bimaculatus* the axonal terminals of AN1 form a ring-like pattern in the anterior ventral protocerebrum where some local auditory brain neurons with temporal selectivity were described (Boyan and Williams 1982; Schildberger 1984). Recently four specific local neurons were identified (LN2 to LN5) and proposed to establish a delay-line and coincidence detector mechanism for pattern recognition (Kostarakos and Hedwig 2012; Schöneich et al. 2015). The cell bodies of these local neurons locate in the lateral protocerebrum with a primary neurite projecting highly similar to the ring-like pattern of AN1. The primary neurites of the local brain neurons split into two branches forming a similar ring structures overlapping with the AN1 arborizations. Besides these common features, each of the identified auditory neurons shows slightly different arborisations. The arborizations of LN2 and LN5 form a close-up ring pattern, whereas LN3 and LN4 show an arborization with seperation between the dendritic and axonal neurites, and have some neurites which project to the midline of the brain. A crucial question here is, whether the five neurons (AN1, LN2, LN3, LN4 and LN5) identified by intracellular recordings represent the complete neuronal network underlying auditory pattern recognition or if the ring-like auditory neuropil that houses the local brain neurons is composed of more neurons that also could be involved in the processing and filtering

the auditory signals?

Although the neurons mentioned above all possess the ring-like arborisation, their cell bodies locate at slightly different positions. Do neurons with cell bodies at different locations function differently? Therefore, it is important to clarify 1. How many neurons are there with their arborisations mingled in the auditory neuropil? 2. Do they all belong to the same morphological group in terms of the location of their cell bodies? Recordings of the auditory neurons exhibit some variability in their responses. This may be explained by the fact that recordings from different parts of a neuron give different responses, however, it may also be an indication of the existance of more than one individual of the identified neuron playing a similar role in auditory processing.

The structure of central neurons in crickets has mainly been obtained by loading fluorescent dyes intracelluarly into individual neurons. This technique can be difficult and is not efficient for the identification of groups of neurons. To stain different auditory neurons simultaneously, additionally two approaches were used in my experiment. First, I used blunt glass microelectrodes to ionophoretically inject dyes whenever the electrode picked up clear signals from multiple auditory neurons. The advantage of this approach is that it allows labelling of closely adjacent auditory neurons at the same time with high resolution since the electrode is placed very close to the neurites.

The second approach I used to label groups of auditory neurons was based on a method by Isaacson and Hedwig (2017) that is to stain neurons by electrophoretic dye delivery using a surface electrode. By attaching the surface electrode to the intact sheath, groups of neurons were labelled simultaneously by delivering different fluorescent dyes into the central nervous system. By attaching surface electrodes to the brain and iontophoretically delivering fluorescent dyes, the ring-like neuropil with three clusters of cell bodies in the protocerebrum have been revealed (Kostarakos and Hedwig, 2017). This approach allows group-labelling in a much wider range of auditory neurons compared to using the blunt electrode. However, the resolution of the stainings obtained (Kostarakos and Hedwig, 2017) did not allow a detailed analysis due to the background fluorescent signals generated by the diffusion of the dyes in the brain tissue. To increase the resolution of the spatial dimensions of the auditory neurons in the ring-like neuropil, refinements on the diameter of the electrode tip, the position and time for dye delivery were required. Therefore, I improved the technique by developing electrodes-pulling programs, fine-tuned the dye-loading position and the time for dye-injection. With the optimised technique,

I aimed to label the population of neurons in the ring-like auditory neuropil and the location of their cell bodies.

METHODS

For intracellular staining, I applied dye-injection for ten AN1, two LN2, four LN5, four LN3 and five LN4 neurons. However, only five AN1, one LN2, one LN5, and two LN4/LN3 were successfully labelled. For blunt microelectrode staining, one clear staining of three neurons was obtained. A total of 43 female *G. bimaculus* were used for the surface electrode method, 15 preparations were stained clearly and examined with confocal microscopy.

Animals

Adult female crickets (*Gryllus bimaculatus* DeGeer), at 10 - 25 days post-ecdysis with intact tympanal membranes and spiracles were used for the experiments. Last instar nymphs were separated from the colony at the Department of Zoology/Cambridge and kept individually in plastic containers at 28ºC with a 12h/12h light/dark cycle, and isolated from singing males. Cricket food contained a mixture of muesli, fish food and cat food, and water was provided ad libitum. All experiments were performed at 23-24°C.

Electrodes

Different glass microelectrodes were used for the three different labelling techniques described above.

Intracellular microelectrodes and labelling:

Microelectrodes were pulled from borosilicate glass capillaries (Harvard Apparatus Ltd., UK; 1 mm OD, 0.58 mm ID) using a DMZ-Universal micropipette puller (Zeitz Instruments, Martinsried, Germany). The microelectrodes were filled with 2 M potassium acetate providing resistances of 40-60 MΩ for intracellular recordings. For staining, the tips of the electrodes were filled with 5% Lucifer yellow CH (Sigma-Aldrich) dissolved in 0.2 M lithium chloride (LiCl). The shaft was backfilled with 0.5 M LiCl, giving a resistance of 60-120 MΩ.

Blunt microelectrodes for extracellular labelling:

The blunt microelectrodes used in the staining experiment were obtained by breaking the tip of the intracellular electrodes. The tips of the electrodes were filled with 0.5% Alexa 568 hydrazide (Invitrogen) dissolved in water and the shaft was backfilled with 2 M potassium acetate. The size of the opening could not be controlled, however, the electrodes had resistances in the range of 20-40 MΩ.

Surface electrodes for population labelling:

The surface electrodes with tip diameters of 20 µm, 60 µm and 80 µm were pulled from borosilicate glass capillaries with two different inner diameters: 0.58 mm and 0.7 mm (Harvard Apparatus Ltd., UK; 1 mm OD) using a DMZ-Universal micropipette puller (Zeitz Instruments, Martinsried, Germany).

The tip of the electrode was filled with 4% Lucifer Yellow CH (Sigma-Aldrich) and 4% Tylose in H_2O, and the shaft was filled with a solution of 4% Tylose (Tylose H200 YG4, ShinEtsu, Wiesbaden, Germany) dissolved in cricket saline, composition in mmol/ L: NaCl 140; KCl 10; $CaCl_2$ 7; $NaHCO_3$ 8; $MgCl_2$ 1; TES 5; D-trehalose dehydrate 4, adjusted to pH 7.4. Tylose was used to increase the viscosity of the solutions and prevented leaking. The microelectrodes were inserted into a customised electrode holder that connected to a syringe for applying suction to the electrode. A platinum wire was inserted into the cavity of the electrode holder as contact (Isaacson and Hedwig 2017) (Fig. 2A). The amplitude of the current and the injection time determined the amount of Lucifer yellow injected.

Sound stimuli

Test pulses of 250 ms duration at a carrier frequency of 4.8 kHz with 75 dB SPL intensity were used in all approaches to evoke field potentials and activate auditory neurons. They were generated with Cool Edit Pro 2000 and were delivered via a speaker (Sinus live NEO 13 s, Conrad Electronics, Hirschau, Germany) positioned 50 cm to the front of the cricket.

Recordings

The head of a cricket was fixed facing forward in a modified 2 ml Eppendorf tube using a mixture of beeswax and collophonium. The brain was exposed by removing the cuticle between the compound eyes and was rinsed and covered by insect saline. A stainless-steel platform with an optic fiber embedded was placed under the dorsal side of the brain for support and

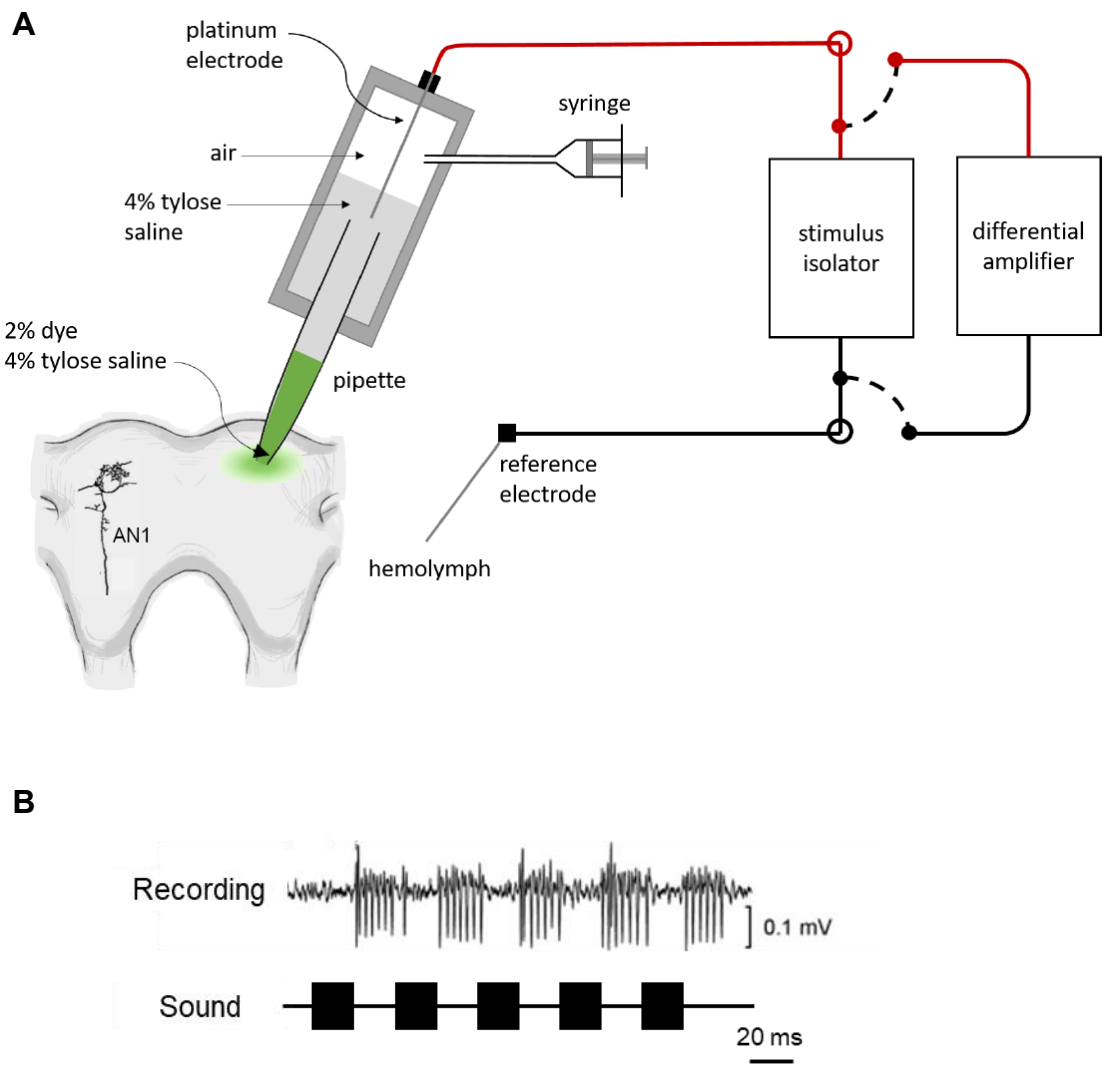

Fig. 2 Setup for the surface microelectrode staining technique. A. Electrode holder and circuitry. The electrode tip was filled with dye and tylose, the electrode holder was filled with tylose saline and a platinum wire was inserted in the electrode holder. A syringe is connected to the electrode holder to apply suction on the electrode tip. A reference electrode was inserted in the hemolymph next to the brain. The dye-releasing site is at the axonal terminals of AN1 on the brain, as indicated in the diagram. **B.** AN1 activity recorded by surface electrodes in response to a chirp with 20 ms pulses separated by 20 ms intervals presented at 75 dB SPL.

illumination. The position of the electrode was controlled by a Leitz micromanipulator (model M; Leica Microsystems, Wetzlar, Germany). Microelectrode depth was monitored with a digital depth indicator (Digimatic, ID-C125MB; Mitutoyo Corporation, Japan).

For the intracellular and the blunt electrode recording, the electrodes were inserted into the brain through the sheath using the micromanipulator. The platform served as a reference electrode. A tungsten ring was gently placed on the ventral side of the brain to stabilize its position. Recorded signals were amplified by a DC amplifier (BA-01X, NPI Electronic, Germany). For surface electrode staining the electrode was attached to the ventral surface of an intact brain in the area of the ring-like neuropil applying slight pressure. A platinum wire was used as reference electrode and placed into the saline next to the brain. The neuronal activity recorded was amplified and filtered between 300 Hz and 5 kHz with a differential amplifier (Model 1700, A-M Systems, Carlsborg, WA), (Fig. 2A).

For all three approaches, the amplified signal was digitized at a sampling rate of 20 kHz per channel using a CED Micro3-1401 controlled by Spike 2 software (Cambridge Electronics Design, Cambridge, UK). All experiments were performed at 24°C.

Staining

Dye-injection procedures were different for the three approaches.

Intracellular staining: After recording the physiological activity of a neuron 5% Lucifer yellow CH (Sigma-Aldrich) dissolved in 0.2 M lithium chloride (LiCl) was iontophoretically injected for 1 - 5 min by hyperpolarizing current (1.5-3 nA).

Blunt electrode staining: The blunt electrode was placed where the neurites of the identified auditory neurons might mingle together. Whenever a recording of auditory responses was obtained, the fluorescent dye (0.5% Alexa 568 hydrazide) was iontophoretically injected into the neurons for 2 - 10 min by hyperpolarizing current (1 - 5 nA).

Surface staining: The position for dye release was determined by obtaining a good extracellular recording of AN1 spike activity (Fig. 2B), then 4% Lucifer Yellow CH (Sigma-Aldrich) in Tylose was iontophoretically released into the brain through the sheath for 20 s by a hyperpolarizing current (-20 μA) delivered by a constant current source (Stimulus Isolator A-360, WPI, Sarasota, FL).

After dye-injection, the brain was dissected and fixed in 4% paraformaldehyde, dehydrated in a series of ethanol at 70%, 90%, 95%, and 100%, and cleared in methyl salicylate. The morphology of the stained neuron was examined using either a Zeiss Axiophot epifluorescence microscope (Axiophot, Carl Zeiss, Germany) with Zeiss filter sets 63 HE attached with a digital SLR camera (Canon EOS 350D; Canon) or a confocal microscope (Leica SP5, Wetzlar, Germany). Neurons were reconstructed manually from image stacks using ImageJ (National Institutes of Health, Bethesda, MD) and Photoshop CS4 (Adobe Systems) software. Neurons were identified according to their morphology and response patterns (Kostarakos and Hedwig 2012, Schöneich et al. 2015).

RESULTS

The structure of individual neurons of the pattern recognition circuit was revealed by intracellular staining, while groups of neurons were labelled with blunt microelectrodes and surface electrodes.

Intracellular labelling of auditory neurons

By injecting fluorescent dyes (Lucifer Yellow and Alexa) while doing intracellular recordings in the ring-like branches of the pattern recognition neurons, the morphologies of the neurons are confirmed. In the experiment, there are more than 10 AN1, 2 LN3 and 2 LN4 stained clearly intracellularly. Fig. 3 shows the morphology of the neurons (AN1, LN3 and LN4) in the pattern recognition circuit. The axon of the ascending neuron AN1 projects to the brain and forms a ring-like arborization (Fig. 3A). The cell bodies of all the other pattern recognition neurons (for example, LN3 and LN4) all locate laterally next to the optical nerve (Fig. 3B). The neurites project medially and make a loop overlapping with the axonal ring-like structure of AN1 (Fig. 3B). The morphologies of these neurons are in accordance with the previous description by Kostarakos and Hedwig (2015).

Group labelling of auditory neurons using blunt microelectrodes

I used blunt microelectrodes to inject dye at the connecting point between the ring structure and the lateral neurite (Fig. 4A, injecting site) once an extracellular recording of activity of several auditory neurons was obtained. A staining of three local auditory neurons was obtained and visualized with confocal microscopy, their cell bodies are labeled as cb1, cb2 and cb3 (Fig. 4A). Their arborisations all form a ring-like pattern, overlap with each other and follow very similar

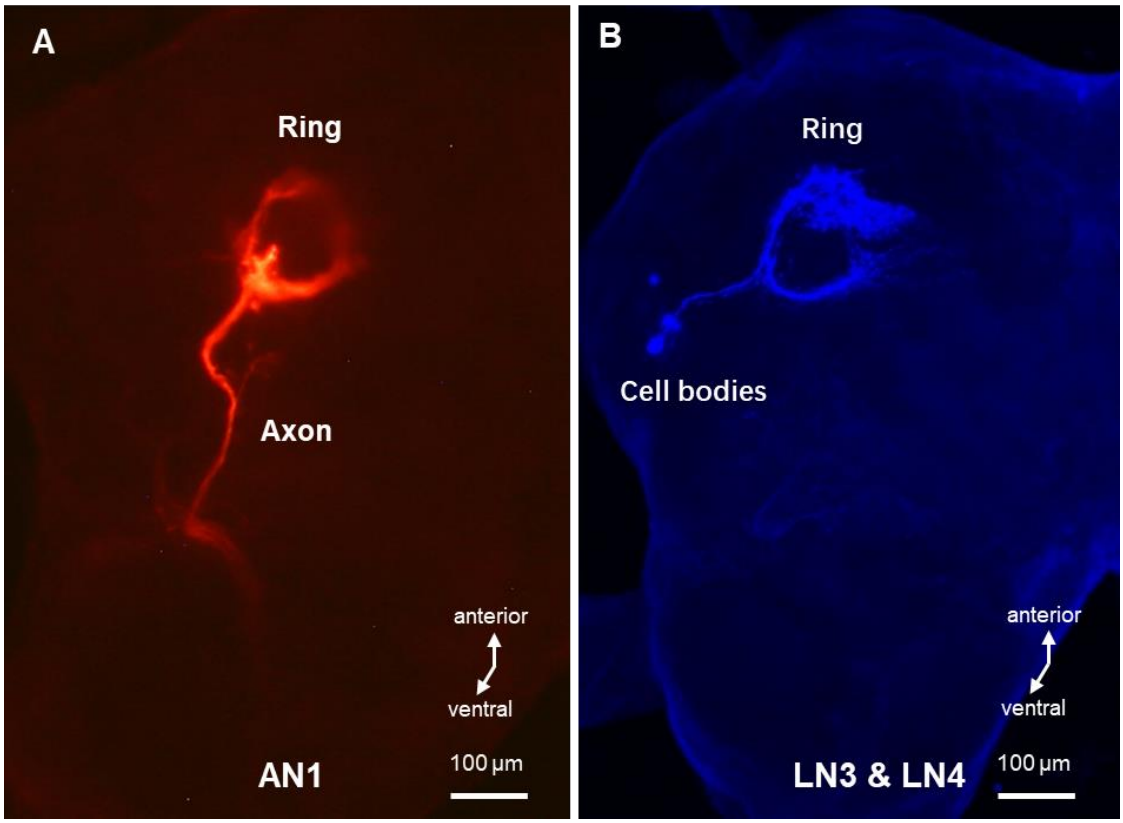

Fig. 3 Intracellular staining of AN1, LN3 and LN4. A. Intracellular staining of AN1 in the brain. Only the axon was shown in this figure and the terminal arborization forms a ring-like pattern. **B.** Intracellular staining of LN3 and LN4. Both neurons showed a ring-like arborization. The neurons were stained by Lucifer Yellow and the photos are in red and blue due to different digital filters in ImageJ software.

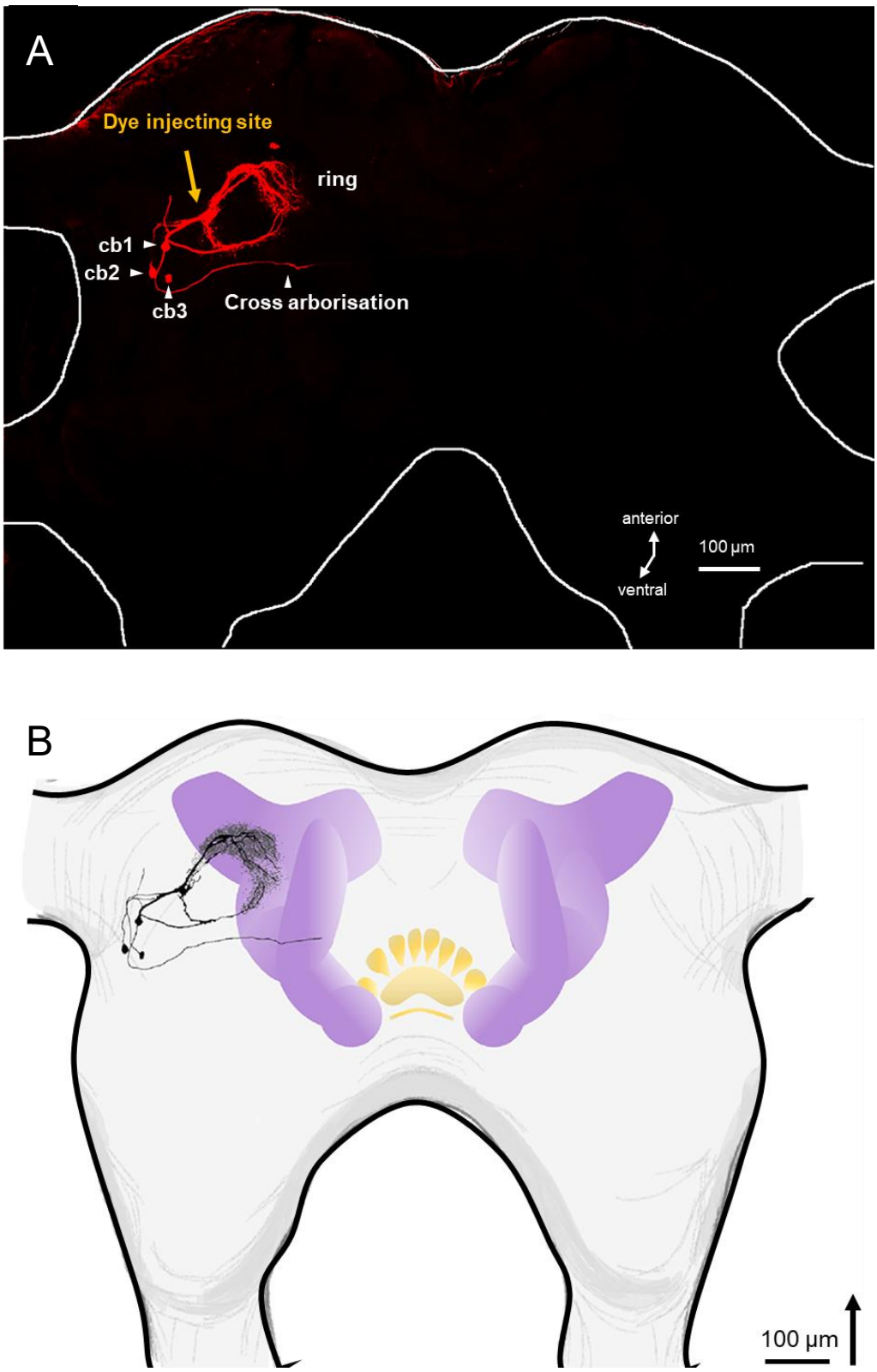

Fig. 4 Auditory neurons labelled using a blunt microelectrode. A. Three auditory neurons with a ring-like arborization in the anterior protocerebrum were revealed by Alexa 568 hydrazide. The cell bodies were labelled as cb1, cb2 and cb3. One of the neurons has a neurite crossing the midline of the brain. **B.** Relative position of the neuronal arborisations relative and frontal to the mushroom body.

projection pattern around a central neuropil, the function of which is not yet clear (Fig. 4A). One of the neurons has a neurite projecting towards the midline (Fig. 4A, cross arborisation). By comparing the morphologies of the identified auditory neurons to these three neurons, neuron 1 (cb1) and neuron 2 (cb2) can be in the same group with LN2 or LN5, and neuron 3 (cb3) may belong to the same group as BLC-3 (Kostarakos and Hedwig, 2012).

The three neurons were drawn in Fig. 4B to show their projections relative to the main neuropils, the mushroom bodies (purple) and the central complex (yellow). All three neurons have their cell bodies laterally located next to the optical nerve. The transversal view based on the confocal imaging reveals that the cell bodies are all close to the ventral surface of the brain. The major neurites of the neurons are mingled together, and the ring-like neurite structures are curved towards the ventral surface of the brain. The medial end of the ring-like structure lays right behind the ventral sheath of the brain. Fig. 5 reveals more details of the three neurons. The brain was scanned with confocal microscopy and planes in three dimensions were reconstructed using ImageJ software: transversal, sagittal and frontal planes. In my results, the ventral-dorsal projections were defined as the frontal planes. In order to provide references for measurements I define the most frontal plane as the top of the ventral surface of the brain as $Ventral_{REF}$, the most transversal plane as the anterior end of the brain between the two hemispheres as $Anterior_{REF}$ and the most sagittal plane at the entry point of the optical nerve and the most lateral part of the antennal lobes as $Lateral_{REF}$ (Fig. 5B and C).

Fig. 5A shows the morphology of the three neurons which were derived from a stack of 80 slices from the ventral surface of the brain (0 µm) to a depth of 248.8 µm (3.11 µm/slice). The closest terminals of the ring neuropil to the ventral surface of the brain were at 34.21 µm, and the deepest neurite of the ring structure reached 236.36 µm. The most anterior end of the ring structure lies at 187.23 µm from the $Anterior_{REF}$, and the ring structure ends at 304.72 µm to the $Anterior_{REF}$ (Fig. 5, T-a, T-c). The most lateral part of the ring structure was at 178.75 µm and the medial end lies at 275.77 µm to the $Lateral_{REF}$ (Fig. 5, S-e and S-f). Therefore, the overall size of the ring structure is approximately 202.15 µm (ventral-dorsal), 117.49 µm (anterior-posterior) and 97.02 µm (lateral-medial).

The cell body (cb1) was 266.06 µm from anterior, 94.61 µm from lateral and 286.12 µm from the ventral reference plane (Fig. 5A, S-c). The cell body (cb2) located at 223.92 µm ($Ventral_{REF}$), 313.81 µm ($Anterior_{REF}$) (Fig. 5A, T-c and T-d), and 69.59 µm ($Lateral_{REF}$) (Fig. 5A, S-a); the cell body (cb3) located at 298.56 ($Ventral_{REF}$), 323.67 µm ($Anterior_{REF}$) (Fig. 5A,

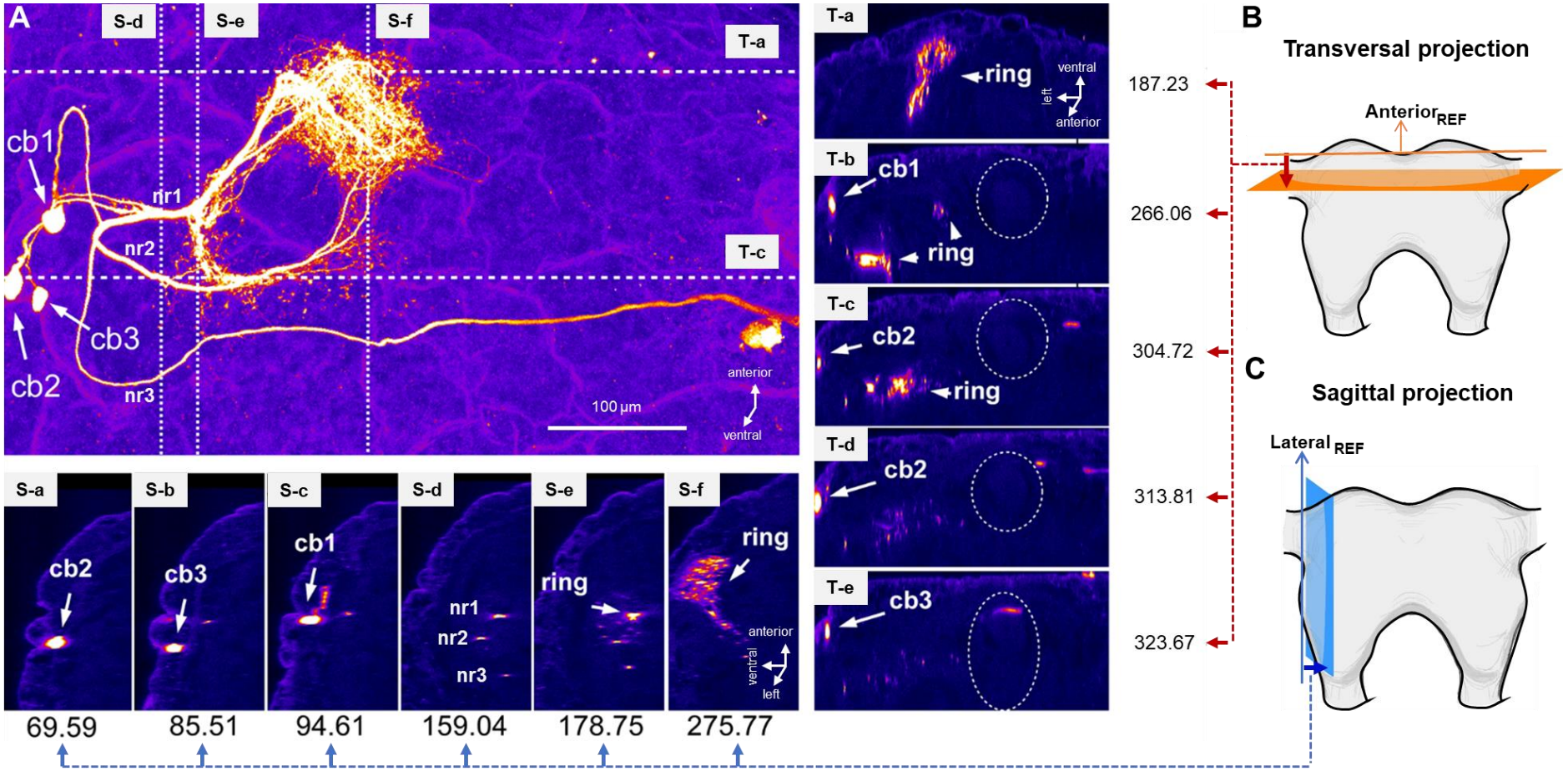

Fig. 5 Position of the auditory neurons labelled using a blunt microelectrode.

Fig. 5 Position of the auditory neurons labelled using a blunt microelectrode. A. The frontal view of the three neurons obtained with a confocal microscope. The three cell bodies were labelled as cb1, cb2 and cb3. The three neurites were labelled as nr1, nr2 and nr3. 6 sagittal sections are shown and labeled as S-a, S-b, S-c, S-d, S-e and S-f and 5 transversal sections are labeled as T-a, T-b, T-c, T-d and T-e. Positions of the cell bodies are given in S-a: cb2; S-b: cb3; S-c: cb1. S-d: the relative position of the three neurites; S-e: lateral end of the ring structure; S-f: medial end of the ring structure. T-a: anterior end of the ring structure; T-b: cb1; T-c: posterior end of the ring structure; T-d: cb2; T-e: cb3. The white dotted circles in T-b to T-e indicate the position of the mushroom body. The depth (μm) was labelled next to each slice. **B.** Diagram showing the transversal reference. **C.** Diagram showing the sagittal reference. For the reference planes see suggestion in main text.

T-e), and 85.51 µm ($Lateral_{REF}$) (Fig. 5A, S-b). Overall, the three cell bodies distribute at the range of 223.92 µm – 298.56 µm to the $Ventral_{REF}$, 266.06 µm - 323.67 µm to the $Anterior_{REF}$, and 69.59 µm -159.04 µm to the $Lateral_{REF}$ planes. Cb1 located most anteriorly and most medially, cb3 located most posteriorly. Cb2 located most laterally. The cell bodies are 84.14 µm (cb1) -109.16 µm (cb2) away from the lateral end of the ring structure. The position and size of the three neurons as determined by these measurements correspond to the features of the auditory neurons reported before (Kostarakos and Hedwig 2012).

Group labelling of auditory neurons by surface staining using suction electrode

To explore how many neurons and clusters of cell bodies contribute to the auditory neuropil, I used surface electrodes to inject dye electrphoretically through the intact sheath of the brain (Fig. 6).

The spiking activity of the ascending neuron AN1 in response to auditory stimuli could be picked up clearly when the tip of the surface electrode was positioned on the brain surface of the anterior protocerebrum where the axon of AN1 terminates (Fig. 2B). Lucifer yellow was injected into the underlying neuropil by applying hyperpolarising current through the surface electrode.

In 12 experiments, the major structure of the ringlike branches and the position of the cell bodies of the auditory neurons were revealed. The neurons are all located in the protocerebrum with the medial part of the ring partially overlapping with the mushroom body, when viewed from frontal (Fig. 6A and B). It is not clear what neuropil lies within the ring structure. In 6 experiments the lateral and posterior cluster of cell bodies were clearly stained, the anterior cluster was revealed in 2 staining. Since the dye-injection point was at the anterior part of the ring, the signal-to-noise ratio of the staining in that area of the brain was poorer due to the overload of the dye in the brain tissue.

A total of 51 cell bodies was revealed. Four major and one minor cluster of cell bodies were located in the same hemisphere as the ring structure, and a bundle of 3 neurites projected across the midline with cell bodies positioned in the contralateral hemisphere (Fig. 6A and B). The clusters of cell bodies ipsilateral to the ring may be divided into anterior, lateral and posterior cluster (Fig. 6A, C). The anterior cluster (ant-C) contained 30 cell bodies and was located anterior to the medial part of the ring. It covered 39.6 µm from anterior to posterior (Fig. 7a, b), and 39.6µm from lateral to medial (Fig. 7o, p).

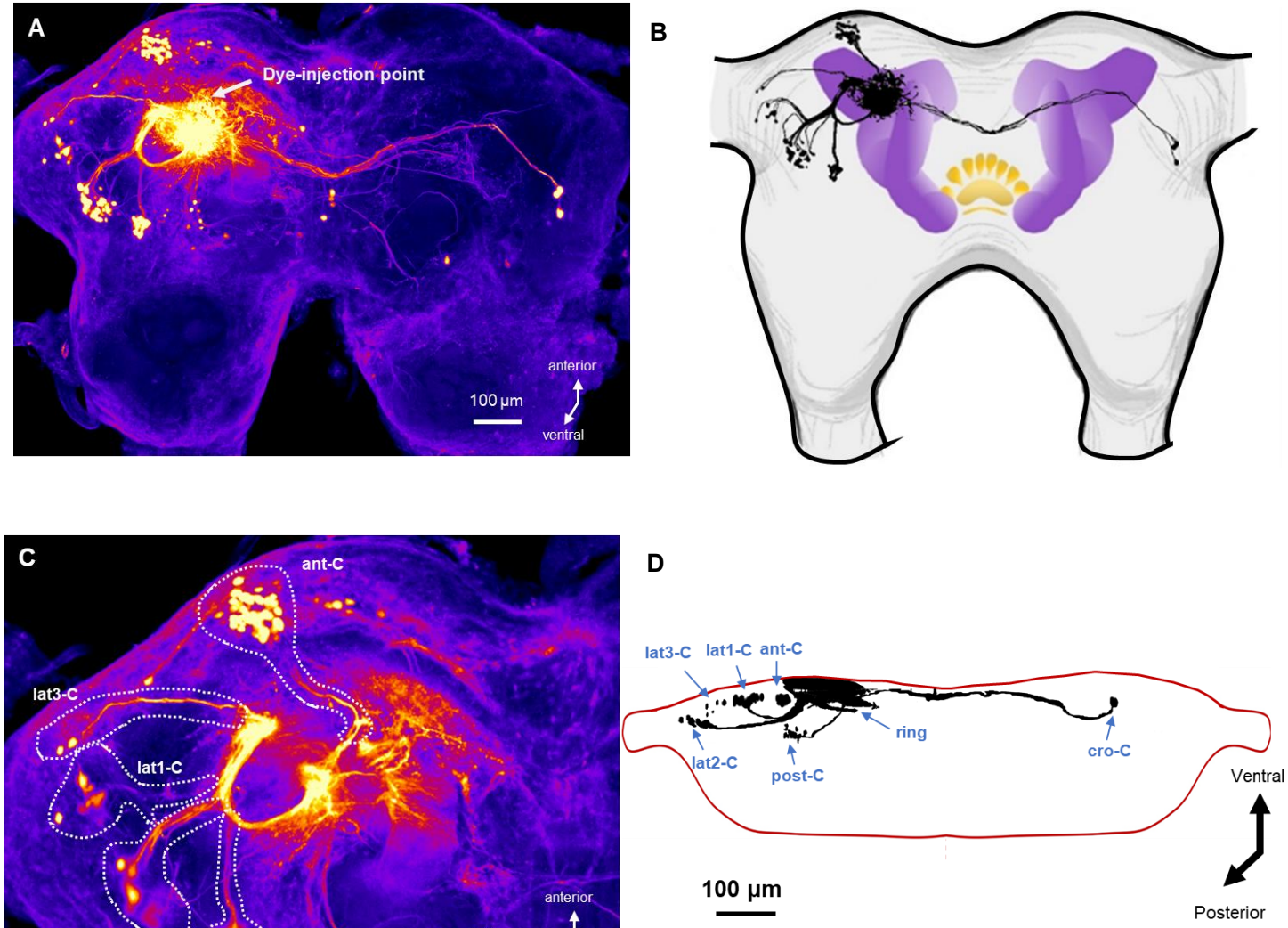

Fig. 6 Auditory neurons stained using a surface microelectrode. A. Frontal view of the auditory neurons obtained with confocal microscopy. **B.** Relative position of the projection of the neurons and the central neuropils. **C.** Image showing the five clusters of cell bodies stained in the hemisphere ipsilateral to the ring structure with their bundles of neurites. The anterior cluster is named ant-C; the three lateral clusters are named lat1-C, lat2-C and lat3-C; the posterior cluster is named post-C. **D.** Transversal view of the position of the neurons in the brain. The cluster of cell bodies located in the hemisphere contralateral to the ring structure is named cont-C.

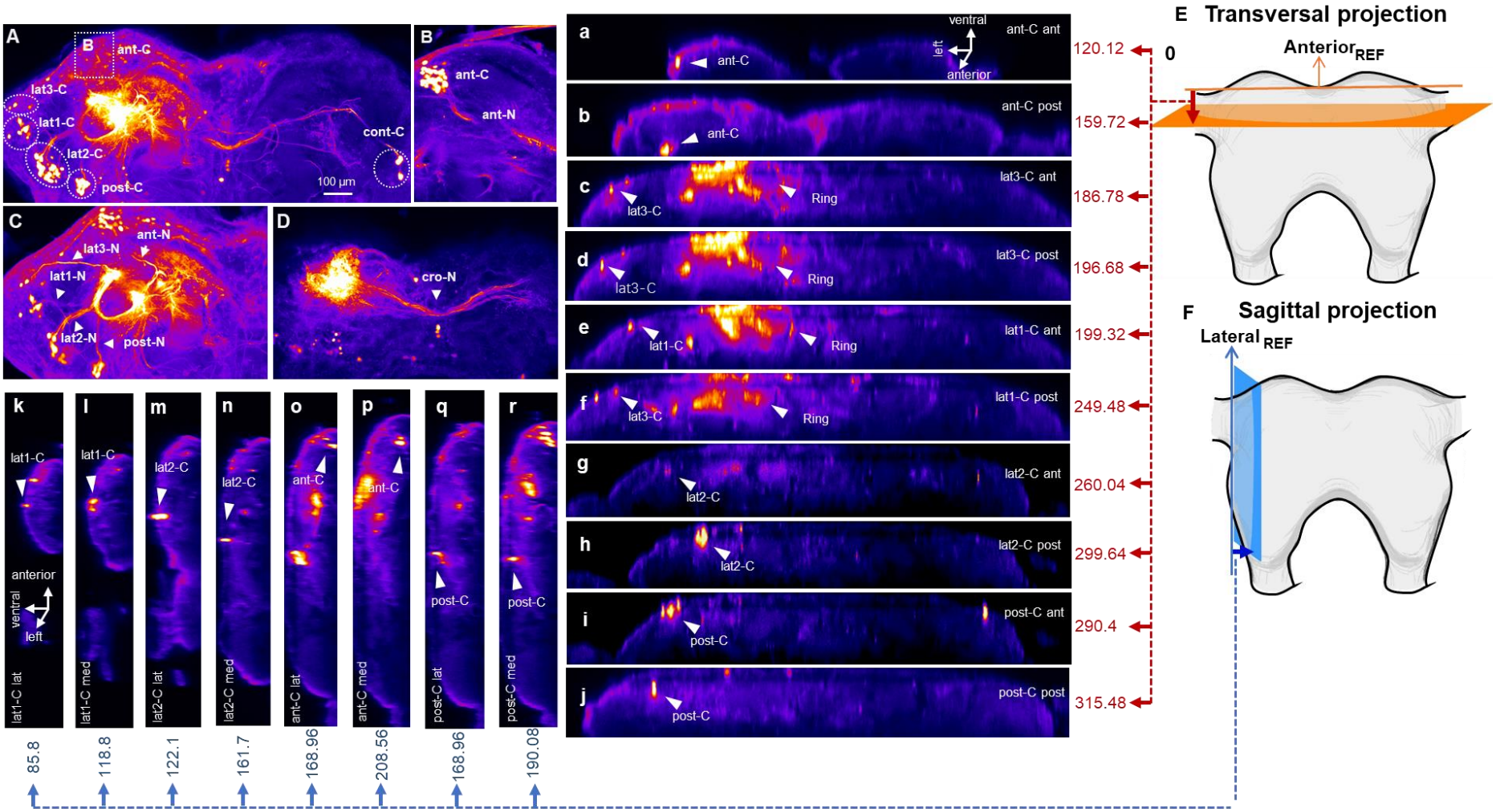

Fig. 7 Position and size of the auditory neurons labelled using a surface microelectrode.

Fig. 7 Position and size of the auditory neurons labelled using a surface microelectrode. A. Image showing the clusters of cell bodies stained in both hemispheres except for the ant-C. The cluster located in the contralateral hemisphere to the ring structure is named cont-C. **B.** The anterior cluster of cell bodies and its neurites. **C.** The clusters and neurites located lateral to the ring structure. The neurites are labeled as ant-N, lat1-N, lat2-N, lat3-N and post-N. **D.** The contralateral cluster with neurites crossing the midline. **E.** Diagram showing the transversal reference. **F.** Diagram showing the sagittal reference. For the reference planes see suggestion in main text. **a.** anterior end of ant-C; **b.** posterior end of ant-C; **c.** anterior end of lat3-C; **d.** posterior end of lat3-C; **e.** anterior end of lat1-C; **f.** posterior end of lat1-C; **g.** anterior end of lat2-C; **h.** posterior end of lat2-C; **i.** anterior end of post-C; **j.** posterior end of post-C; **k.** lateral end of lat1-C; **l.** medial end of lat1-C; **m.** lateral end of lat2-C; **n.** medial end of lat2-C; **o.** lateral end of ant-C; **p.** medial end of ant-C; **q.** lateral end of post-C; **r.** medial end of post-C. The depth (μm) was labelled next to each slice.

There were 3 lateral clusters. The lateral cluster (lat3-C) is the most anterior of the three clusters and contained 5 cell bodies. It was located anterior and next to the optical nerve about 85 µm from the $Lateral_{REF}$ plane (Fig. 7A). The cluster covered 9.9 µm anterior to posterior (Fig. 7c and d) and 33 µm from lateral to medial. Also, cluster lat1-C was positioned lateral and next to the optical nerve, it contained 8 cell bodies (Fig. 7A). The cluster extends from 199.32 to 249.48 µm from the $Anterior_{REF}$ plane, covering 50.19 µm anterior to posterior (Fig. 7e and f) and stretches over 33 µm from lateral to medial (Fig. 7k and l). Cluster lat2-C with 25 cell bodies is positioned lateral posterior to the ring (Fig. 7A). It extended over 39.6 µm anterior to posterior (Fig. 7g and h) and about 36.3µm lateral to medial (Fig. 7m and n). The cluster post-C with 9 cell bodies is positioned posterior to the ring (Fig. 7A), covering 25.08 µm from anterior to posterior (Fig. 7i and j) and about 21.1µm from lateral to medial (Fig. 7q and r). One cluster cont-C containing 4 cell bodies occurred in the contralateral hemisphere, its position mirrored the position of the lat2-C. The transversal view of the brain (Fig. 6D) revealed that cluster lat1-C is closer to the ventral surface of the brain than the other clusters and the lat1-C is the most laterally located cluster.

The transversal projections show that the ring structure is curved towards the surface of the brain. Corresponding to the locations of the cell body cluster, the primary neurites projected along different routes towards the ring. The neurites from the ant-C projected to the medial anterior end of the ring. The neurites from lat3-C run towards the anterior lateral end of the ring structure (Fig. 7C), neurites from lat2-N projected to the lateral and posterior part of the ring, while a bifurcated branch from lat1-C connected to its lateral part (Fig. 7C). The post-C neurites connected to the ring structure at its most posterior end (Fig. 7C). From cont-C a bundle of 4-5 neurites crossed the midline and entered the median part of the ring structure. These neurites were running right beneath the ventral surface of the brain (Fig. 6D).

DISCUSSION

The group labelling techniques

Group labelling with blunt electrodes were used in my experiment. The shape and size of the tip of a broken electrode however can not be standardized leading to variability in the experiments. Also finding an optimal spot for dye delivery is not always guaranteed. However, as an advantage of this technique the resolution of the staining can be quite high since the dye

is taken up into the neurons at a very close distance or even intracellularly through an injured membrane. If successful neurons with a close spatial relationship will be labelled from a particular spot. As the number of labelled neurons is small, their structural relationship can be analysed in great detail.

The surface staining approach allowed exploration of the spatial organisation of the auditory neurons in the cricket brain. To increase the resolution of the method and reduce the number of neurons labelled, I improved the technique by developing electrodes-pulling programs, fine-tuned the dye-loading position and the time for dye-injection. With the optimised technique, the population of neurons contributing to the ring-like neuropil could be labelled more clearly with less fluorescent background.

The morphology of the auditory neurons shows a ring-like structure

The blunt and surface glass capillaries were used to label groups of auditory neurons by releasing fluorescent dye into the cricket brain. The auditory neuropil in the protocerebrum showed a ring-like structure. The medial part of the ring-like structure located very close to the ventral surface of the brain, the neuropil structure inside the ring is not yet characterised. The auditory ring structure is however located anteriorly to the mushroom body. Labelling a small group of neurons revealed that their neurites closely mingle together in the auditory neuropil, providing the basis for synaptic contacts and local processing right in the area of the AN1 axonal terminals. Projections to the contralateral ring-structure are few and seem to occur only via one bundle of neurites, these may correspond to the B-LC-3 neurons (Kostarakos and Hedwig, 2012).

There are more neurons besides the identified auditory neurons in the auditory neuropil

In the delay-line and coincidence detector circuit, five neurons were proposed to function as a pattern recognition circuit. In my experiment, more than 50 cell bodies were stained with neurites projecting towards the auditory neuropil. The cell bodies formed five different clusters. There are be three different possibilities for the organization of these neurons:

The four identified brain neurons (LN2, LN3, LN5 and LN4) may be sufficient for the pattern recognition, and other neurons may play different roles in driving the phonotacitc behaviour. For example, integrating the information in both hemispheres or generating descending signals to the motor system.

The four local neurons (LN2, LN3, LN5 and LN4) may be representatives of four different types of neurons sharing the same function. Neurons with their cell bodies located in the same cluster may be similar in their functions. By comparing the morphology of the identified auditory neurons obtained from intracellular staining (Kostarakos and Hedwig 2012) it can be seen that LN2, LN3 and LN4 have their cell bodies in the cluster lat2-C, which contains 25 cell bodies in total. The cell body of LN5 (Schöneich et al. 2015) belongs to the cluster lat1-C, with 8 cell bodies. Therefore, for all identified neurons there may be more than one individual having the same or a similar role in the pattern recognition and these neurons may rather be functional types.

The population stainings also indicate that further local neurons may be involved in pattern recognition, which have not yet been identified. Evidence from the intracellular recordings supporting this possibility will be presented in the later chapters. Thus, the pattern recognition circuit may encompass more neurons and may be more complex than currently described. This provides a wider and different morphological aspect for a more comprehensive understanding of the neural mechanism underlying the pattern recognition network.

CHAPTER 3: THE EFFECTS OF CHANGING INTERVAL DURATIONS WITHIN A CHIRP ON PROCESSING BY THE PATTERN RECOGNITION CIRCUIT

INTRODUCTION

The network for pattern recognition in the cricket brain was derived from intracellular recordings of the auditory neurons while the insects were stimulated with sequences of chirps with changing intervals, pulse durations or pulse periods; during these tests all pulses and intervals were altered at the same time (Kostarakos and Hedwig 2012, Schöneich et al. 2015). The intracellular recording of the auditory neurons in the brain revealed different responses of the neurons to sound patterns with different intervals (Kostarakos and Hedwig, 2012), e.g. the feature detector neuron, appears to be specifically tuned to chirps with every interval being 20 ms. However, testing the system in this way may overlook the possible roles of the specific intervals and pulse durations within a chirp. On the basis of the proposed delay-line and coincidence detector network, Hedwig and Sarmiento-Ponce (2017) explored whether changes in the duration of single pulses or intervals (Fig. 8) would lead to different levels of phonotaxis in *G. bimaculatus*. They tested the phonotactic responses of females to chirps containing three pulses and systematically varied the first (I1) or the second (I2) interval (Fig. 9A and B), or the duration of one of the three pulses P1, P2 and P3 (shown in the next Chapter). The phonotactic tuning curves to the I1- and I2-tests exhibited a band-pass shape with peak responses at intervals of 20 ms, but different degrees of phonotactic response at very long intervals (Fig. 9C). The responses were compared to a reference level, defined as the response to a 2-pulse chirp. While the females responded to long I2-intervals in the same way as to the reference chirp, the response to long I1-intervals was significantly lower. To explore the neural basis underlying the corresponding phonotactic tuning, I tested the response properties of the neurons in the pattern recognition circuit with sound patterns, which were varied either in a single interval or single pulse duration of a chirp, to reveal their functional implications for temporal pattern recognition.

My approach follows the behavioural experiments by Hedwig and Sarmiento-Ponce (2017), who tested the phonotactic behaviour of *G. bimaculatus* in response to chirps with varied intervals (Fig. 9). In this chapter, I focus on investigating what impact changing the intervals I1 and I2 may have on the processing within the pattern recognition circuit? I additionally use a paradigm in which the duration of all intervals is altered at the same time,

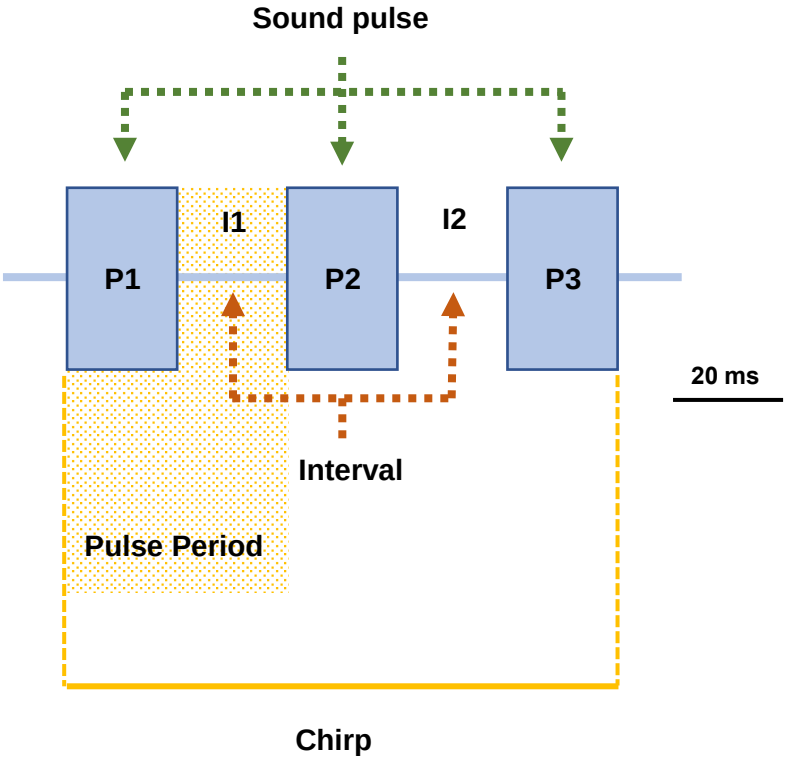

Fig. 8 Temporal structure of an artificial chirp of the calling song of *G. bimaculatus*. The chirp consists of three sound pulses, which are labelled as P1, P2 and P3, and the two pulse intervals labeled as I1 and I2. The duration of each sound pulse and each pulse interval is 20 ms. The pulse period of this chirp is 40 ms containing one sound pulse and one interval. The chirp period is 330 ms.

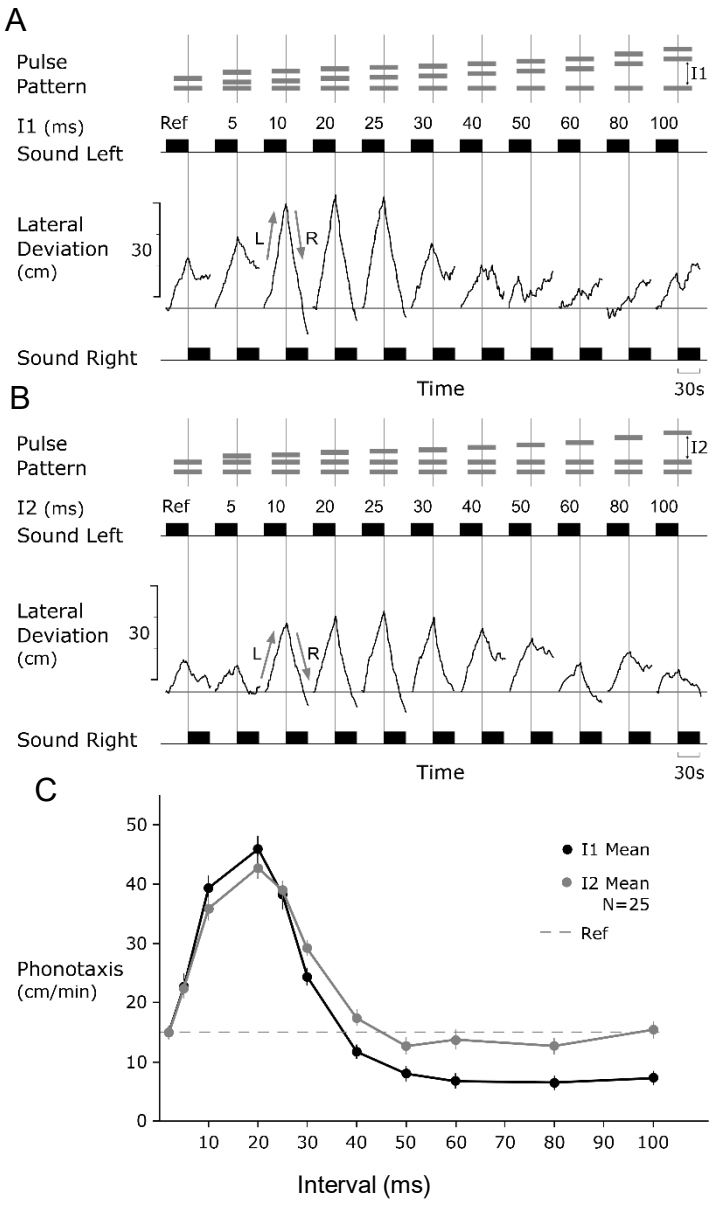

Fig. 9 The behavioural tuning of female *Gryllus bimaculatus* to the patterns with varied intervals (I1- and I2-tests) A. Chirp patterns with increasing duration of I1 (top); each pattern is presented as a sequence for 30 s from the left and right side (black rectangles). The lateral deviation (middle) indicates the phonotactic steering of a female towards the left (L, upwards) and then to the right (R, downwards) as the active speaker changes. **B.** Chirp patterns with increasing duration of I2 (top) and phonotactic steering of a female towards 30 s sequences of chirp patterns with increasing duration of I2 (middle). **C.** Characteristic responses for 25 females to changes in I1 (black line) and to changes in I2 (grey line). Hedwig and Sarmiento-Ponce, 2017.

following Kostarakos and Hedwig (2012).

MATERIALS AND METHODS

Animals

Adult female crickets (*Gryllus bimaculatus* DeGeer) at 10 - 25 days post-ecdysis with intact tympanal membranes and spiracles were used for the experiments. Last instar nymphs were separated from the colony at the Department of Zoology/Cambridge and kept individually in plastic containers at 28ºC with a 12h/12h light/dark cycle, and isolated from singing males. Cricket food contained a mixture of muesli, fish food and cat food, and water was provided ad libitum. All experiments were performed at 23-24°C.

Acoustic stimulation

All experiments are based on chirps with 3 sound pulses (P1 to P3) and correspondingly two intervals (I1 and I2) (Fig. 8). As in previous experiments the chirp with both the duration of the pulses and the intervals being 20 ms (pulse period is 40 ms) is referred to as a "normal chirp", which is in the range of pulse durations and intervals of *G. bimaculatus* songs under the natural condition (Verburgt et. al 2011). Three acoustic paradigms with a carrier frequency of 4.8 kHz and an intensity of 75 dB SPL were designed to analyse the interval selectivity of auditory neurons (Fig. 10-12; Hedwig and Sarmiento-Ponce, 2017). The chirp period was 330 ms.

I1-test: For chirps in this test, the first interval (I1) was systematically changed between 5 ms and 80 ms while keeping the duration of three pulses (P1, P2 and P3) and the second interval (I2) constant at 20 ms. For example, in I1-5, interval I1 was 5 ms whereas P1, P2, P3 and I2 were all 20 ms, resulting in a chirp duration of 85 ms. The first interval in this test includes 5, 10, 20, 25, 30, 40, 50 and 80 ms (Fig. 10).

I2-test: The second interval (I2) was systematically changed while keeping the duration of the pulses (P1 - P3) and the first interval (I1) constant at 20 ms. For example, in I2-5, interval I2 was 5 ms whereas P1, P2, P3 and I1 were all 20 ms. The second interval in this test includes 5, 10, 20, 25, 30, 40, 50 and 80 ms (Fig. 11).

Pulse-interval (PI) test: Chirps consisting of four pulses and three intervals were used. For

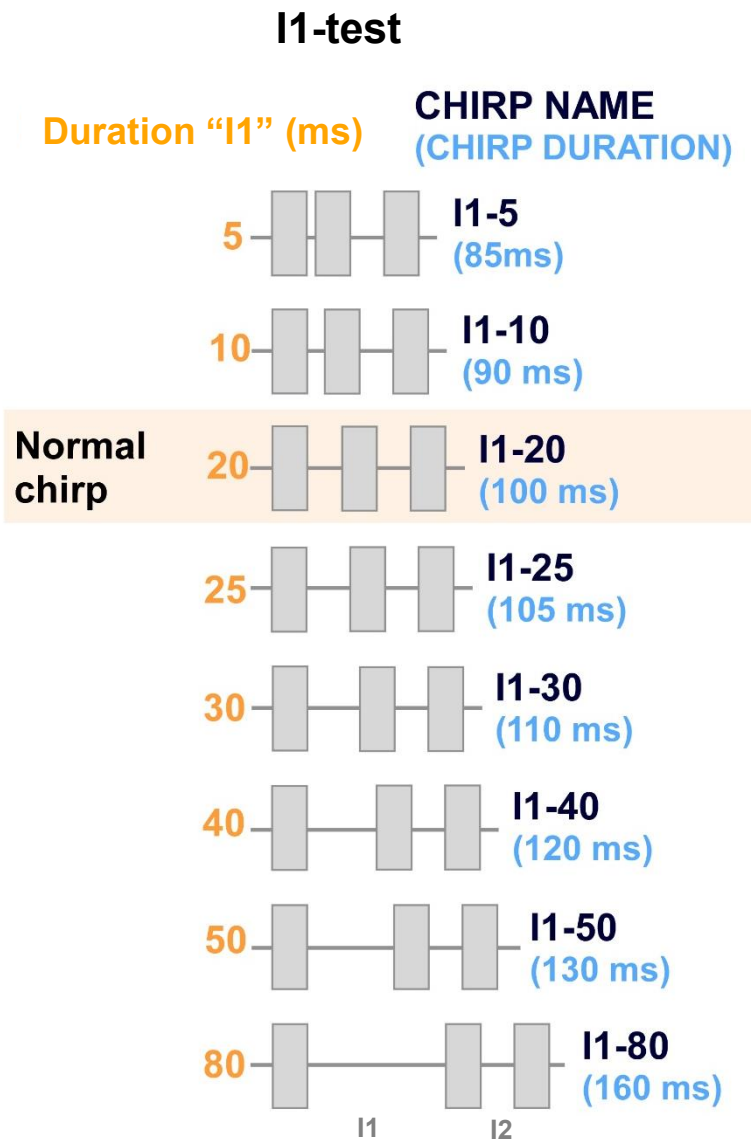

Fig. 10 Chirps with the first pulse interval varied (I1-test). Each chirp contains three sound pulses, for 8 chirps the interval I1 is varied from 5, 10, 20, 25, 30, 40, 50 to 80 ms. The chirps are named correspondingly as I1-5, I1-10, I1-20, I1-25, I1-30, I1-40, I1-50 and I1-80. The duration of the chirps then becomes 85, 90, 100, 105, 110, 120, 130 and 160 ms, respectively. The duration of all pulses was set at 20 ms. The normal chirp is composed of 20-ms pulses and 20-ms intervals and is based on the calling song of *Gryllus bimaculatus*. The carrier frequency is 4.8 kHz and sound intensity is calibrated to 70dB SPL.

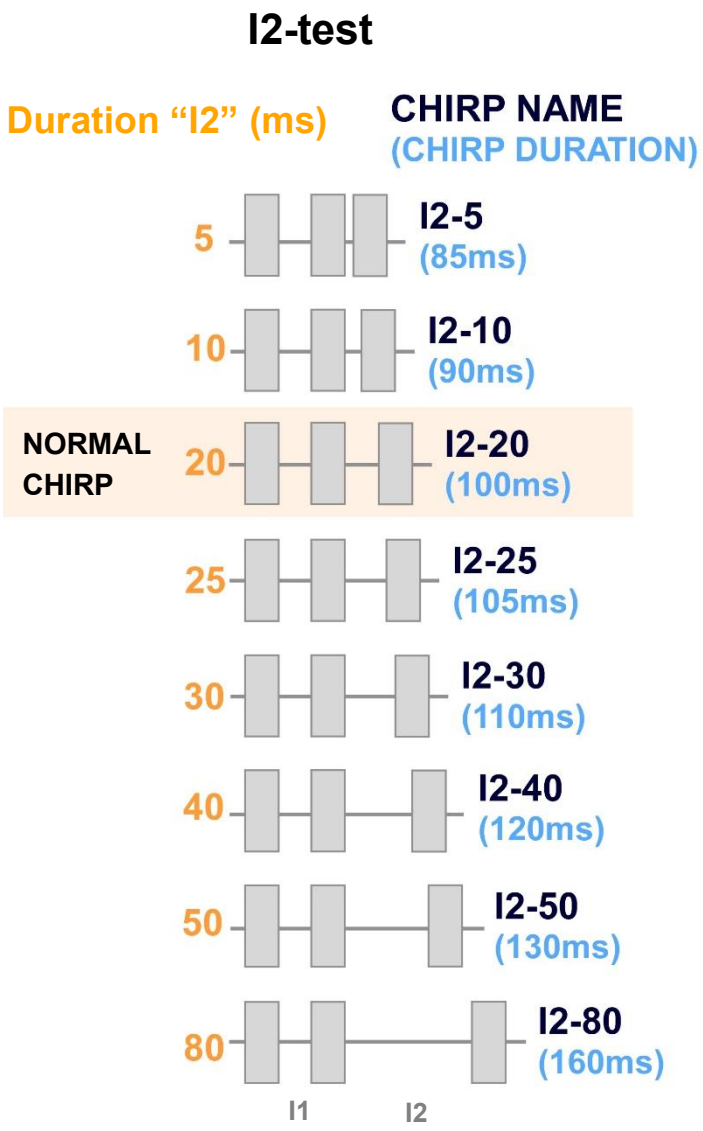

Fig. 11 Chirps with the second pulse interval varied (I2-test). Each chirp contains three sound pulses, for 8 chirps the interval I2 is varied from 5, 10, 20, 25, 30, 40, 50 to 80 ms. The chirps are named correspondingly as I2-5, I2-10, I2-20, I2-25, I2-30, I2-40, I2-50 and I2-80. The duration of the chirps is 85, 90, 100, 105, 110, 120, 130 and 160 ms, respectively. Interval I1 and the duration of the pulses was set at 20 ms. The normal chirp indicates a chirp with 20-ms pulses and separated by 20-ms intervals. The carrier frequency was set to 4.8 kHz and sound intensity was calibrated to 70dB SPL.

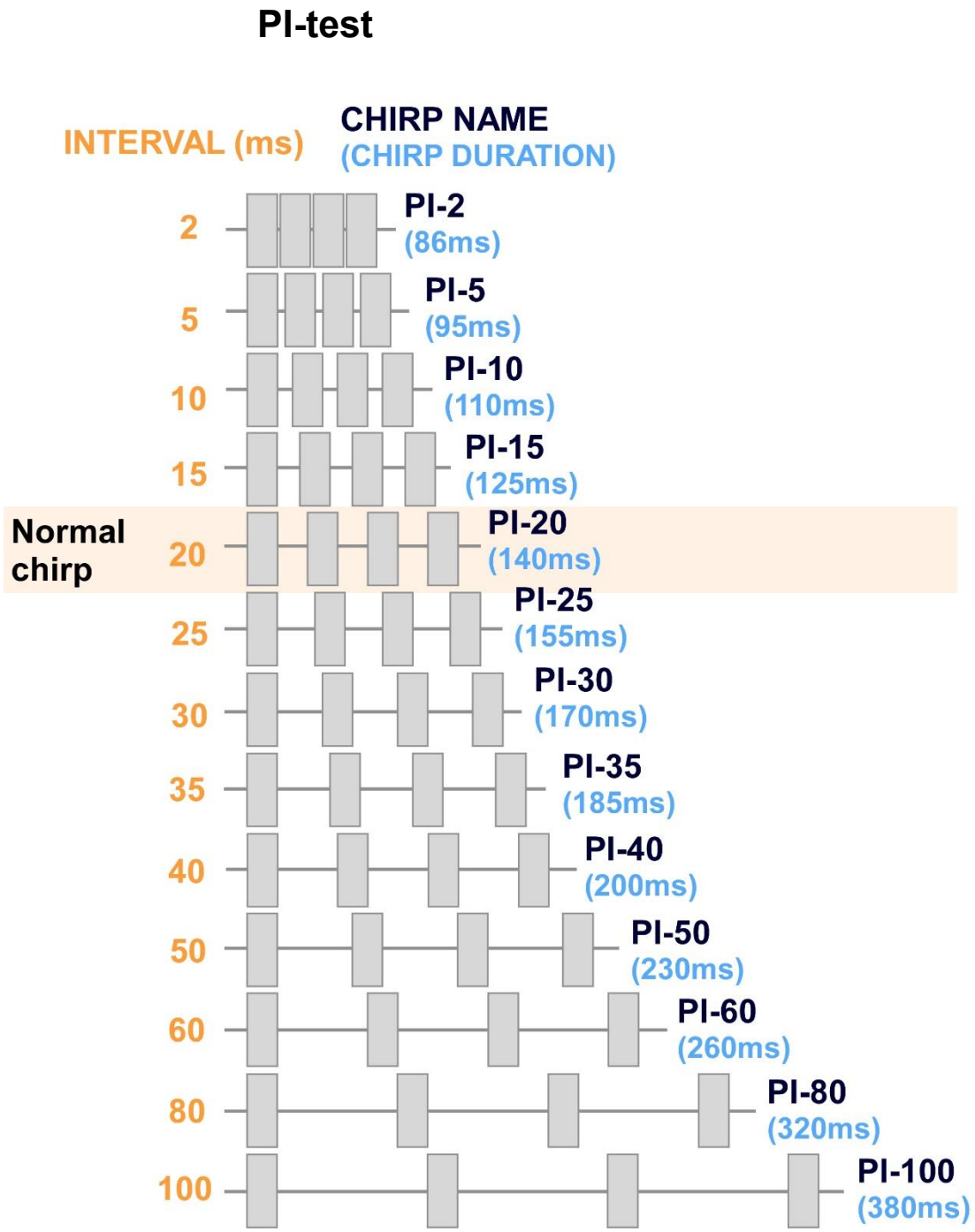

Fig. 12 Chirps with all pulse intervals varied (PI-test). Each chirp contains four sound pulses. For each chirp the duration of all pulse intervals was varied from 2, 5, 10, 15, 20, 25, 30, 35, 40, 50, 60, 80 to 100 ms. The 13 chirps were named as PI-2, PI-5, PI-10, PI-15, PI-20, PI-25, PI-30, PI-40, PI-50, PI-60, PI-80 and PI-100. The duration of the chirps was 86, 95, 110, 125, 140, 155, 170, 185, 200, 230, 260, 320 and 380 ms, respectively. The duration of the pulses was 20 ms. The normal chirp indicates a chirp with 20 ms pulses and separated by 20-ms intervals.

chirps in this test, all four pulses were kept constant at 20 ms whereas all the intervals were changed. For example, in PI-2 four 20 ms pulses were separated by three 2-ms intervals, giving a chirp duration of 86 ms. The interval in this test include 2, 5, 10, 15, 20, 25, 30, 35, 40, 50, 60, 80 and 100 ms (Fig. 12, Kostarakos and Hedwig, 2012).

In all paradigms, the rising and falling ramps for sound pulses were 2 ms. Sound stimuli were designed with Cool Edit Pro 2000 software (Syntrillium, Phoenix, AZ, USA). Sound signals were presented by two speakers (Sinus live NEO 13s, Conrad Electronics, Hirschau, Germany) placed frontal to the cricket at an angle of 45º from the left and the right to the animal's long axis. Sound intensity was calibrated to 75 dB SPL relative to 20 μPa at the location of the cricket using a Brüel&Kjær measuring amplifier and a 1/2-inch free field microphone (models 2610 and 4939, respectively; Nærum, Denmark).

In behavioural test each chirp pattern was presented for a total of 60 times. Due to the difficulty of the neuronal recordings and the limited test times, I presented test sequences containing all varied chirps, each chirp occurred only once in each sequence, while the sequences were looped and repeated several times.

Intracellular recordings and staining of the neurons

The head of a cricket was fixed facing forward in a modified 2 ml Eppendorf tube using beeswax (Fig. 13A). Animals were placed on a trackball to allow free walking during the intracellular recordings (Fig. 13B) although no neuronal activity could be recorded during behaviour due to rare occurrence of phonotaxis after the dissection. The brain was exposed by removing the cuticle between the compound eyes. It was rinsed and covered by insect saline, composition in mmol/L: NaCl 140; KCl 10; $CaCl_2$ 7; $NaHCO_3$ 8; $MgCl_2$ 1; TES 5; D-trehalose dehydrate 4, adjusted to pH 7.4. A stainless-steel platform with an optic fibre embedded was placed under the dorsal side of the brain for support and illumination. The platform also served as a reference electrode for intracellular recordings. A tungsten ring was gently placed on the ventral side of the brain to stabilize its position (Fig. 13B).

Microelectrodes were pulled from borosilicate glass capillaries (Harvard Apparatus Ltd., UK; 1 mm OD, 0.58 mm ID) using a DMZ-Universal micropipette puller (Zeitz Instruments, Martinsried, Germany). The microelectrodes were filled with 2 M potassium acetate providing resistances of 40-60 MΩ for intracellular recordings. For in vivo staining, the tips of the electrodes were filled with 5% Lucifer yellow CH (Sigma-Aldrich) dissolved in 0.2

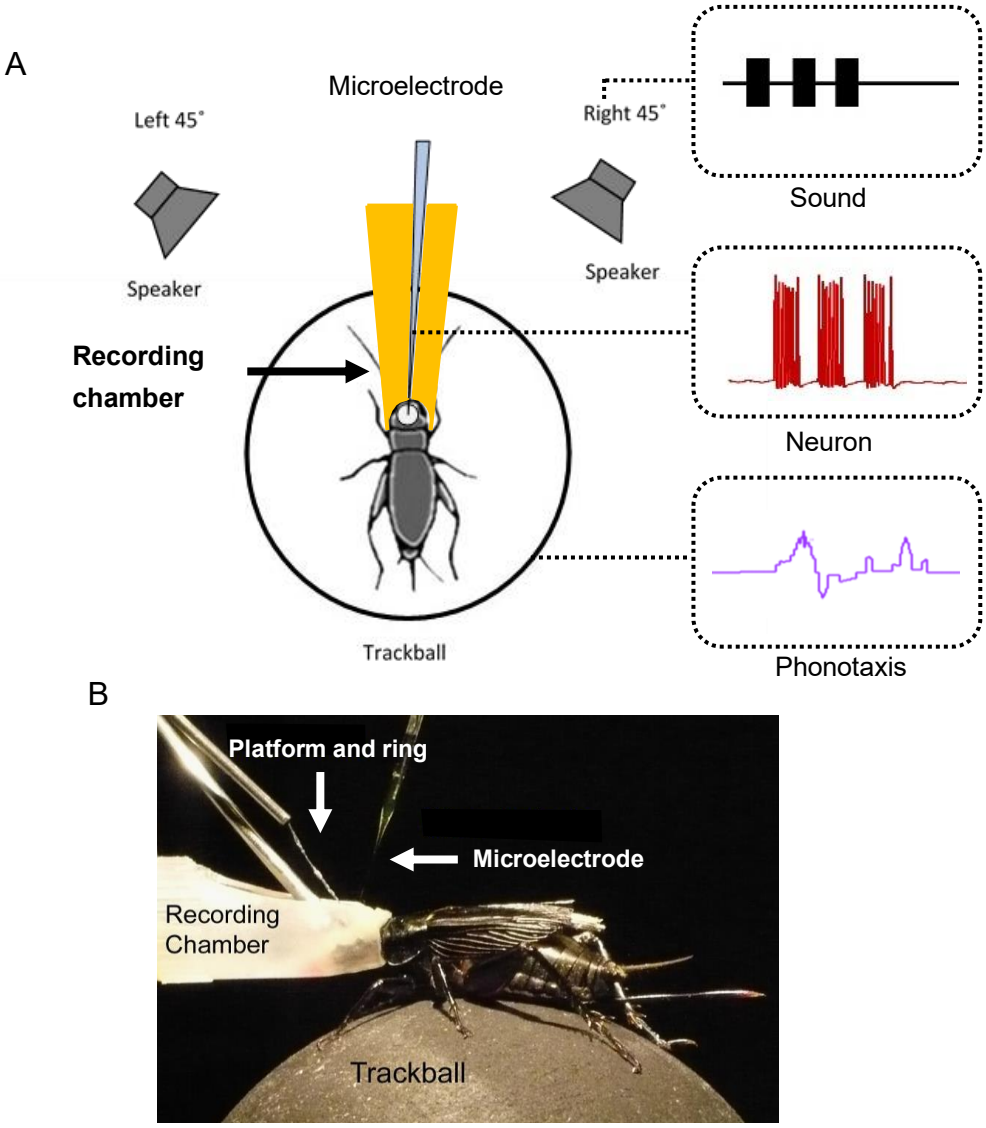

Fig. 13 Experimental set-up for intra-cellular recording. A. Crickets were tethered to a customized recording chamber by placing bees wax around the head (yellow shade). The speakers were placed at 45° left and right to its body length and the sound stimuli were played from left or right side depending on the recording position. The cuticle between the compound eyes was removed to expose the brain. A microelectrode was inserted to the brain for neuronal recording and the phonotactic steering was recorded by the trackball system. **B.** A stainless steel platform with an optic fibre embedded was placed under the dorsal side of the brain for support and illumination. The platform also served as a reference electrode for the intracellular recordings. A tungsten ring was gently placed on the ventral side of the brain to stabilize it.

M lithium chloride. The shaft was backfilled with 0.5 M lithium chloride, giving a resistance of 80-120 MΩ. The position of the microelectrode was controlled by a Leitz micromanipulator (model M; Leica Microsystems, Wetzlar, Germany). Electrode depth was monitored with a digital depth indicator (Digimatic, ID-C125MB; Mitutoyo Corporation, Japan). Intracellular recordings lasted from 1 min to more than 60 min. Recorded signals were amplified by a DC amplifier (BA-01X, NPI Electronic, Germany). Test pulses of 250 ms duration at a carrier frequency of 4.8 kHz were used as "search" pulses to evoke field potentials and activate auditory neurons.

For anatomical identification, 5% Lucifer yellow CH (Sigma Aldrich) dissolved in ddH_2O, or 0.5% Alexa 568 hydrazid (Invitrogen) dissolved in 0.2M lithium chloride (LiCl) were iontophoretically injected into the neurons for 2–20 min by hyperpolarizing current injection (1.5-3 nA). The brain was then dissected and fixed in 4% paraformaldehyde, dehydrated in a series of ethanol at 70%, 90%, 95%, and 100%, and cleared in methyl salicylate. The morphology of the stained neuron was examined using either a Zeiss Axiophot epifluorescence microscope (Axiophot, Carl Zeiss, Germany) with Zeiss filter sets 63 HE attached with a digital SLR camera (Canon EOS 350D; Canon) or a confocal microscope (Leica SP5, Wetzlar, Germany). Neurons were reconstructed manually from image stacks using ImageJ (National Institutes of Health, Bethesda, MD) and Photoshop CS4 (Adobe Systems) software. Neurons were identified according to their morphology and response patterns (Kostarakos and Hedwig 2012, Schöneich et al. 2015).

Data recording and analysis

All recording channels (intracellular recordings, sound, current and trackball) were digitized at 20 kHz sampling rate using a CED 1401 data acquisition interface (Micro1401 mk II, CED, Cambridge, UK). Neural recordings were displayed on an analogue oscilloscope (Tektronix 5440, Bracknell, UK) and a computer screen using Spike 2 software (Cambridge Electronic Design) and were monitored using headphones. Data were saved to the hard disc of a PC for off-line analysis. Recorded data were analyzed with Neurolab software (Knepper & Hedwig, 1997), Spike 2, Prism (GraphPad Software) and Excel (Microsoft).

A different number of neurons was recorded (N) and a different number of stimulus repeats (n) may be presented in each case. For the characteristic responses of the neurons elicited by 20-ms pulses and normal chirps, 10 repeats of AN1 (N=5, n=10), 10 repeats of LN2

(N=2, n=10), 10 repeats of LN5 (N=4, n=10), 10 repeats of LN3 (N=5, n=10) and 5 repeats of LN4 (N=5, n=5) were analysed. For the I1-test, 5 repeats of AN1 (N=5, n=5), 2 repeats of LN2 (N=2, n=2), 18 repeats of LN5 (N=4, n=18), 13 repeats of LN3 (N=5, n=13) and 5 repeats of LN4 (N=5, n=5) were analysed. The data shown in the behavioural tests form intervals (PI) were performed by Adam Bent, the data shown for I1- and I2-tests (Fig. 9) were derived from Hedwig and Sarmiento-Ponce (2017).

To compare the neural activity to the phonotactic behaviour, I calculated the number of AP per chirp generated by the four spiking neurons of the circuit: AN1, LN2, LN3 and LN4 together with the standard error of the mean for each neuron. For LN2, only two recordings were obtained, I plotted the average number of spikes of both recordings. For LN3, I also analysed the number of spikes elicited by each sound pulse within a chirp. For LN4, I calculated the number of spikes caused by the second and the third pulse, since the first pulse does not elicit any spiking activity. Besides the absolute response also the relative neuronal response was calculated to allow comparisons, i.e. in these cases for all neurons the number of spikes was normalised to the activity evoked by the normal chirp. To characterise the level of activity in the circuit at different stages of processing, I compared the mean spiking response of LN2, LN3 and LN4 to the activity of AN1.

I measured the latency of the first spike in AN1; for LN2 and LN3 I measured the latency of the EPSPs elicited by the first sound pulse and the first spike; for LN4 the latency of the inhibition was determined. For the non-spiking neuron LN5, I calculated the amplitude between the resting potential and the point where the post-inhibitory rebound (PIR) was cut off by the subsequent inhibition and named as PIR1, PIR2 and PIR3. This is explained in the Result part in detail. The standard error of the mean was calculated for each amplitude. I also calculated the summed amplitude of the first and the second post-inhibitory rebound to compare the overall output from LN5 with the phonotactic behaviour. The differences in the amplitude of adjacent PIRs over time were calculated and named the ‘slope’ of the PIRs. This is explained with figures in the Result part. In all experiments, the different responses towards different test patterns were analysed by Repeated Measure ANOVA with Tuckey’s post hoc if the data were parametric, and Friedman test with Dunn’s multiple comparisons test if the data were nonparametric if the data were non-parametric. Results with a “p” value less than 0.05 are considered to be significant. The relation between the sound paradigm and the change in number of spikes was analysed by calculating Pearson’s correlation coefficient.

RESULTS

In the following I will present the five neurons of the pattern recognition circuit and their responses to the I1-test and I2-test. At the end of each part I will compare the tuning curves and the responses to elucidate the flow of auditory processing. General features of the neurons e.g. latency of the responses, which are identical for all tests, will only be given for the I1-test.

Response of the pattern recognition network neurons to chirps with different first intervals: I1-test

Taking the tuning of the phonotactic behaviour as a reference, for the description of the neuronal responses I use categories of short, medium and long intervals. I will focus on the neuronal responses to chirps with short I1-intervals (I1-5 and I1-10) as the phonotactic behaviour increases over these chirps. I will refer to chirps with medium I1-intervals in the range of 20 to 30 ms (I1-20 to I1-30), as these cover the strongest phonotactic response. I finally will present the neuronal responses to chirps with longI1-intervals in the range of 40 to 80 ms (I1-40 to I1-80), as phonotaxis decreases and is particular low for long I1-intervals.

The number of recordings of the neurons are: 10 repeats of AN1 (N=5, n=10), 10 repeats of LN2 (N=2, n=10), 10 repeats of LN5 (N=4, n=10), 10 repeats of LN3 (N=5, n=10) and 5 repeats of LN4 (N=5, n=5) for the characteristic responses of the neurons elicited by 20-ms pulses and normal chirps, and 5 repeats of AN1 (N=5, n=5), 2 repeats of LN2 (N=2, n=2), 18 repeats of LN5 (N=4, n=18), 13 repeats of LN3 (N=5, n=13) and 5 repeats of LN4 (N=5, n=5) for the I1-test.

The ascending neuron – AN1

The ascending interneuron AN1 responds to sound pulses with a consistent spike activity and forwards the auditory information to the inhibitory neuron LN2 and the coincidence detector LN3 (Fig. 14A).

<u>AN1 response to a single 20 ms sound pulse and the normal chirp</u>

The neuron responded to 20 ms pulses with an activity of 6.5±0.0 AP/pulse, spiking activity lasted for 22.1±0.2 ms (n=10). In response to a normal chirp, AN1 had a latency of 18.9±0.1

Table 1. Latencies and the duration of activities of the neurons to each sound pulse of a normal chirp

Latencies to each sound pulse and the duration of activities				
Neuron		**1st pulse (ms)**	**2nd pulse (ms)**	**3rd pulse (ms)**
AN1	**LAT_{spikes}**	**18.9±0.1**	**18.4±0.2**	**19.6±0.1**
	$DURA_{spikes}$	22.1±0.2		
LN2	**LAT_{depo}**	**19.9±0.2**	**21.7±0.5**	**22.5±0.5**
	LAT_{spikes}	**22.2±0.2**	**24.5±0.5**	**26.4±0.5**
	$DURA_{depo}$	39.2±0.7	40.6±0.6	54.9±1.9
	$DURA_{spikes}$	25.0±1.0	20.5±1.7	10.0±0.7
	$DURA_{depo\text{-}single}$	58.4±3.8		
	$DURA_{spikes\text{-}single}$	25.0±1.9		
	$DURA_{initial\ spikes}$	10.3±0.2		
LN5	**LAT_{inh}**	**26.4±0.2**	**25.7±0.5**	**26.2±0.4**
	$LAT_{max\ inh}$	**36.4±0.5**	**35.4±1.0**	**36.9±0.3**
	$LAT_{peak\text{-}single}$	**89.4±2.2**		
	$DURA_{PIR\ decay}$	**177.9±1.8**		
LN3	**LAT_{depo}**	**23.2±0.4**	**23.4±0.4**	**24.0±0.2**
	LAT_{spikes}	**34.1±0.8**	**27.3±0.4**	**29.8±0.5**
	$DURA_{depo}$	33.8±0.3	33.7±1.3	41.5±2.1
	$DURA_{spikes}$	6.7±0.6	16.7±1.3	14.2±0.8
	$DURA_{depo\text{-}single}$	54.0±0.3		
	$DURA_{spikes\text{-}single}$	8.7±0.1		
LN4	**$LAT_{onset\ inh/spikes}$**	**24.9±0.3**	**30.3±0.5**	**29.1±0.2**
	$DURA_{hyper\text{-}single}$	75.6±1.2		
	$DURA_{depo}$		19.3±0.5	30.6±2.0
	$DURA_{spikes}$		9.7±1.4	16.5±1.1

LAT_{depo}: the latency of the depolarisation to each sound pulse of a normal chirp.

LAT_{spike}: the latency of the spikes to each sound pulse of a normal chirp.

$DURA_{depo}$: the duration of the depolarisation elicited by each sound pulse of a normal chirp.

$DURA_{spikes}$: the duration of the spiking activity elicited by each sound pulse of a normal chirp.

$DURA_{depo\text{-}single}$: the duration of the depolarisation elicited by a single 20 ms pulse.

$DURA_{spikes\text{-}single}$: the duration of the spiking activity elicited by a single 20 ms pulse.

$DURA_{hyper\text{-}single}$: the duration of the hyperpolarisation caused by a single 20 ms pulse.

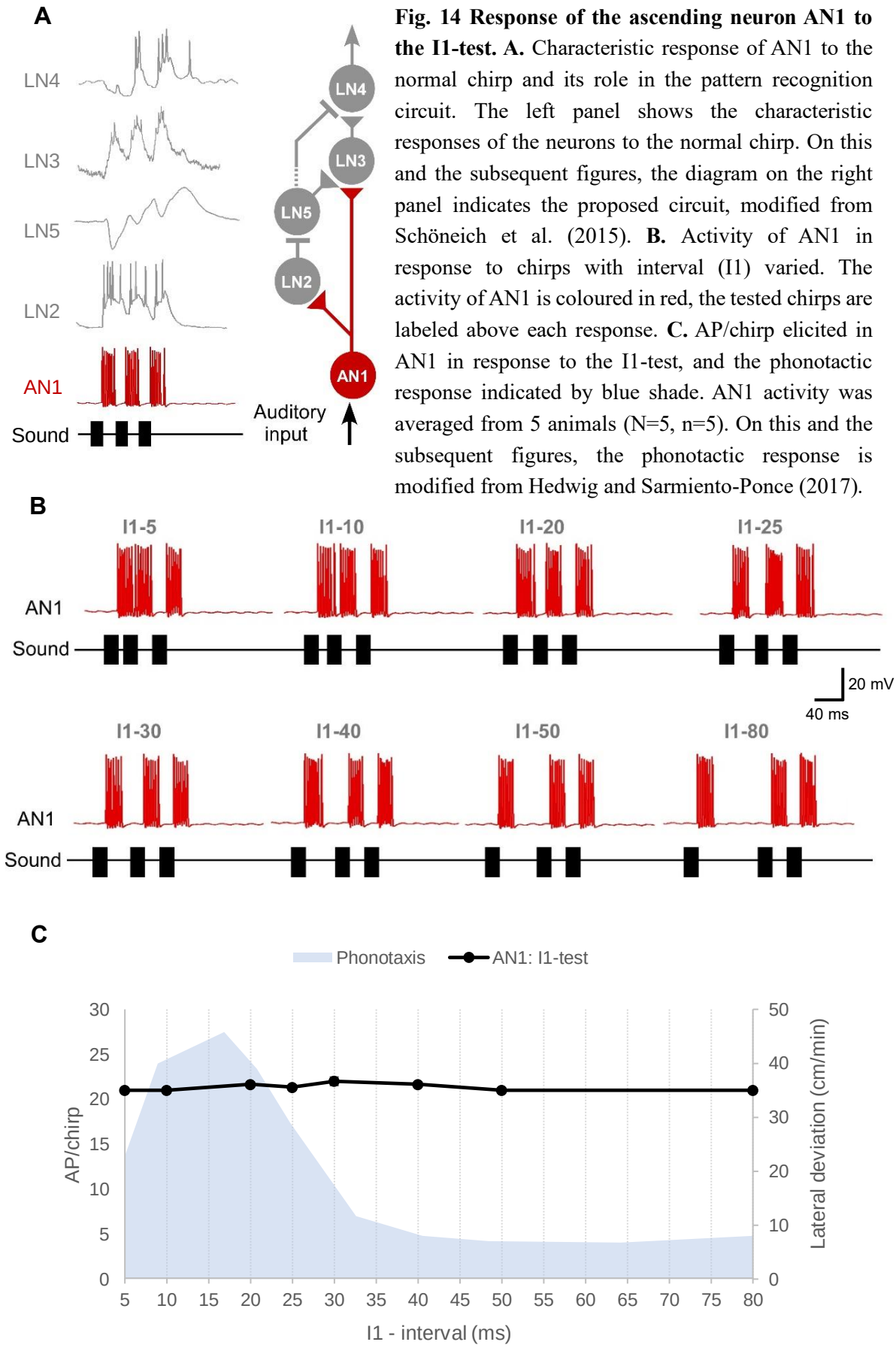

Fig. 14 Response of the ascending neuron AN1 to the I1-test. A. Characteristic response of AN1 to the normal chirp and its role in the pattern recognition circuit. The left panel shows the characteristic responses of the neurons to the normal chirp. On this and the subsequent figures, the diagram on the right panel indicates the proposed circuit, modified from Schöneich et al. (2015). **B.** Activity of AN1 in response to chirps with interval (I1) varied. The activity of AN1 is coloured in red, the tested chirps are labeled above each response. **C.** AP/chirp elicited in AN1 in response to the I1-test, and the phonotactic response indicated by blue shade. AN1 activity was averaged from 5 animals (N=5, n=5). On this and the subsequent figures, the phonotactic response is modified from Hedwig and Sarmiento-Ponce (2017).

ms for the first, 18.4±0.2 for the second and 19.6±0.1 for the third sound pulse (Table. 1).

AN1 response to I1-chirps

When stimulated with the chirps of the I1-5 pattern, the spike response of AN1 to the first and the second pulse merged and the 5 ms interval between the pulses was not obvious (Fig. 14B). When the intervals were equal to or larger than 10 ms, AN1 reliably copied the temporal pattern of the pulses (Fig. 14B). For short, medium and long I1-intervals every chirp led to a very similar number of spikes ranging from 21.0±0.0 to 22.0±0.5 AP/chirp, since AN1 copies the duration of sound pulses and every chirp in the I1-test came with three 20 ms pulses (Fig. 14C)($p=0.1526$, Friedman test, N=5, n=5). The highly similar spiking activity across the I1-test does not match the phonotactic behaviour (Fig. 14C, blue shaded area), which is tuned towards I1-20. AN1 however, plays a crucial role in forwarding accurate temporal information of the sound stimuli to the brain. In summary, AN1 copied the sound pattern but did not reflect the behavioural tuning curve in terms of temporal filtering.

The inhibitory neuron – LN2

The local neuron LN2 is driven by the AN1 activity and inhibits both the non-spiking neuron LN5 and the feature detector LN4 (Fig. 15A).

LN2 response to a single 20 ms sound pulse

The spiking activity evoked by a 20 ms pulse lasted for 25.0±1.9 ms, the underlying depolarisation, however, only slowly declined after the spikes and overall lasted for 58.4±3.8 ms from the onset to the end (Table. 1). Therefore, the first two depolarisations elicited by a normal chirp did not return to the resting membrane potential (Fig. 15B, I1-20).

LN2 response to the normal chirp

In response to the normal chirp LN2 generated 8.4±0.1 AP (Fig. 15B, I1-20). LN2 responded to the first sound pulse of each chirp with a phasic spike activity, reaching spike rates of 236.15±6.48 Hz for the initial 3 spikes. This strong transient activity lasted 10.3±0.2 ms. The dendritic recordings obtained demonstrate a prominent depolarisation with a latency of 19.9±0.2 ms and spiking with a latency of 22.2±0.2 ms to the first sound pulse. The depolarisation lasted for 39.2±0.7 ms and the spiking activity lasted 25.0±1.0 ms. The latencies of the depolarisation and the spiking to the second sound pulse were 21.7±0.5 and 24.5±0.5 ms.

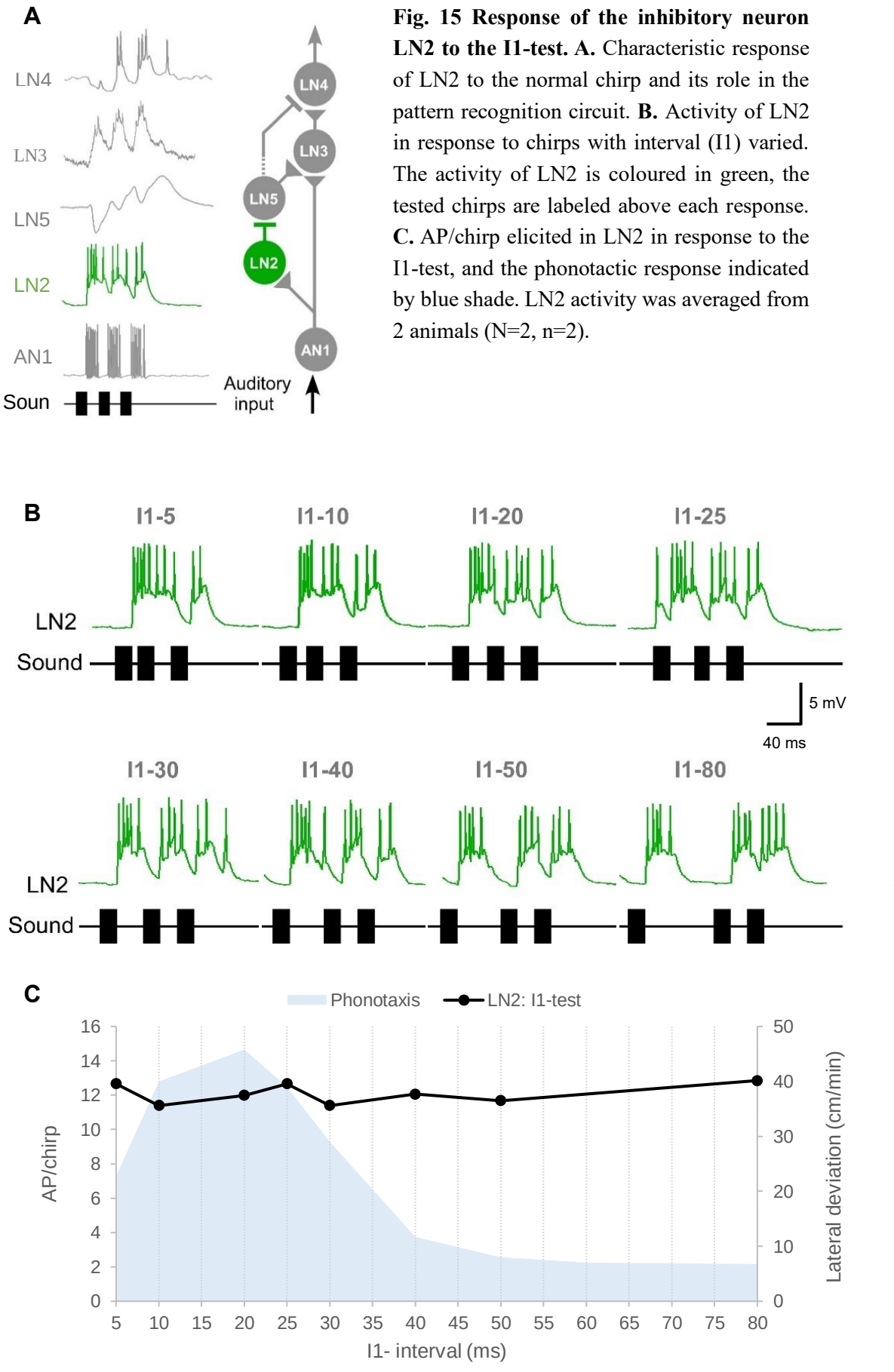

Fig. 15 Response of the inhibitory neuron LN2 to the I1-test. A. Characteristic response of LN2 to the normal chirp and its role in the pattern recognition circuit. **B.** Activity of LN2 in response to chirps with interval (I1) varied. The activity of LN2 is coloured in green, the tested chirps are labeled above each response. **C.** AP/chirp elicited in LN2 in response to the I1-test, and the phonotactic response indicated by blue shade. LN2 activity was averaged from 2 animals (N=2, n=2).

The duration of the second depolarisation was very similar to the first one which was 40.6±0.6 ms whereas the spiking activity became shorter as 20.5±1.7 ms (p=0.018, t-test, n=10). The latencies of the depolarisation and the spikes elicited by the third sound pulse were 22.5±0.5 and 26.4±0.5 ms, respectively. The depolarisation lasted for 54.9±1.9 ms, while the spiking activity was further reduced in terms of duration to 10.0±0.7 ms (P2 vs. P3: p=0.001, t-test, n=10)(Fig. 15B, I1-20).The spiking activity elicited by the first, the second and the third sound pulse follow AN1 by about 3.3, 6.1 and 6.8 ms, respectively. Compared to AN1, LN2 responded to each pulse with a longer spiking activity (AN1: 22.1±0.2 ms; LN2: 25.0±1.9 ms, both n=10).

LN2 response to I1-chirps

When LN2 was stimulated with short I1-intervals (I1-5 and I1-10 chirps) its spike activity occurred on a plateau-like depolarisation and generated 8.8 AP/chirp when stimulated with I1-5 and 7.9 AP/chip for I1-10. As the repolarising phase of the LN2 depolarisation took longer than the varied interval the response to the first (P1) and second sound pulse (P2) merged (Fig. 15B). For medium I1 between 20 and 30 ms, LN2 responded to the second sound pulse with an independent EPSP and spikes, but responses were not completely separated from the first response. For example, in response to the normal chirp, i.e. a chirp with 20 ms pulses and 20 ms intervals, LN2 generated 12.0 AP/chirp. The response to the first pulse (5.3±0.1 AP) was always stronger than the response to the third pulse (2.4±0.1 AP), possibly due to adaptation in the auditory pathway (N=2, n=60) (Fig. 15B, I1-20). In response to these chirps, the membrane potential did not return to the level of the resting potential (Fig. 15B, I1-20 to I1-30). When LN2 was exposed to chirps with long I1-intervals between 40 and 80 ms the membrane potential at the end of the first burst repolarised to the resting potential and the neuron generated three bursts of spikes coupled to the sound pulses (Fig. 15B, I1-40: 12.1 AP/chirp; I1-50: 11.7 AP/chirp; I1-80: 12.8 AP/chirp).

Given the different response patterns of LN2, the number of spikes elicited by each chirp was almost constant and led to a relatively flat tuning curve, shown for the mean response of two repeats (Fig. 15C). The activity of LN2 remained similar across the I1-test, showing only a difference of 1.4 spikes in total (I1-10: 11.4 AP/chirp and I1-80: 12.8 AP/chirp), (Fig. 15C). The resulting tuning curve of LN2 does not reflect the phonotactic behaviour, indicating no temporal selectivity at this stage.

LN2 response compared with AN1 response

Compared to AN1, LN2 responded to each pulse with a longer depolarisation and spiking activity (AN1 duration of spike activity: 22.1±0.2 ms, n=10; LN2 duration of spiking activity: 25.0±1.9 ms, LN2 duration of depolarisation: 58.4±3.8 ms, n=10). In the mean LN2 copied the sound pattern with a 43.3±1.1% lower number of spikes when compared to AN1 (AN1: 21.3±0.1 AP/chirp; LN2: 12.1±0.2 AP/chirp). This may be an indication of the refinement of the activity received from AN1 for a higher efficiency.

All in all, LN2 converts its excitatory response to an inhibitory output towards to the pattern recognition circuit following the activity of AN1.

The non-spiking neuron – LN5

The non-spiking neuron LN5 plays a key role in the circuit. Triggered by each sound pulse, in response to the inhibition from LN2, it generates a delayed post-inhibitory rebound (PIR), which is forwarded to the coincidence detector LN3 (Fig. 16A).

LN5 responses to the normal chirp

Before the LN5 response is discussed in detail, I refer to its typical response to a normal chirp i.e. a chirp with 20 ms pulses and 20 ms intervals to introduce its properties. The LN5 membrane potential showed a rhythmic oscillation driven by the pulse pattern with a typical sequence of inhibitions and post-inhibitory-rebound depolarisations, here labelled as INH1 to INH3 and PIR1 to PIR3 (Fig. 16B). The inhibitions are elicited by the sound pulses, and the rebound potentials always start to develop from the peak (i.e. the lowest point) of the inhibition. Due to the nature of the timing PIR1 occurs after P2, and PIR 2 and PIR3 occur after the third sound pulse P3 (Fig. 16B). While INH1 starts from resting membrane potential, the inhibitions INH2 and INH3 start to develop from the peak of the rebound PIR1 and PIR2, respectively. Only the last rebound PIR3 is not terminated by an inhibition. The latency of the start of the LN5 inhibitory response to the first sound pulse was 26.4±0.2 ms (Table. 1). The latencies of the second and the third inhibition to the second and the third sound pulses were very similar (Table. 1). The three inhibitory responses reached a maximum amplitude relative to the resting potential all with a latency around 36.2 ms, which is about 10 ms after the start of each inhibition (INH1: -4.4±0.1 mV occurring with a latency of 36.4±0.5 ms to the start of P1. INH2: 1.4±0.1 mV at 35.4±1.0ms to the start of P2 and INH3: 3.3±0.3 mV occurring at 36.9±0.3ms to the start of P3). The time for the inhibition to reach its maximum indicates the time it requires to develop (~10 ms) and this may be related to the onset spiking activity in LN2, it is stable although the

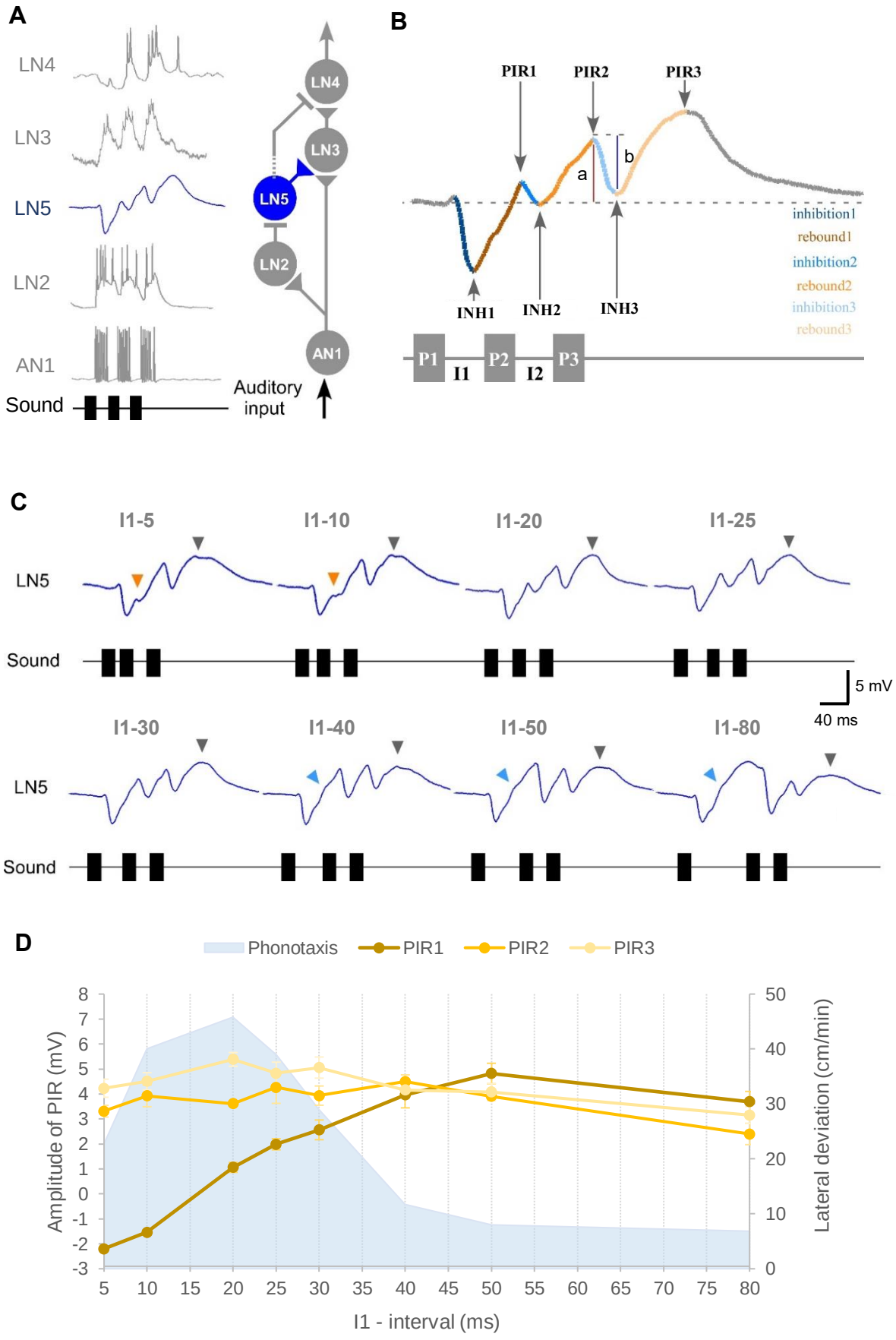

Fig. 16 Activity of LN5 elicited by I1-test and the tuning of the amplitude of PIRs.

Fig. 16 Activity of LN5 elicited by the I1-test and the tuning of the amplitude of PIRs. **A.** Diagram showing characteristic activity of LN5 to the normal chirp and its role in the pattern recognition circuit. **B.** Activity elicited in LN5 in response to a normal chirp. P1, P2 and P3 represent the three sound pulses, I1 and I2 refer to the two intervals. LN5 responds to the three pulses with three inhibitions (inhibition1, inhibition2 and inhibition3) and three rebounds (rebound1, rebound2 and rebound3). The maximum amplitudes of the inhibitions are labelled as INH1, INH2 and INH3. The highest membrane potential of rebound1 (brown) and rebound2 (orange) are marked as PIR1 and PIR2, they are reached before the following inhibition (blue and light blue). The peak amplitude of rebound3 (light yellow) is labelled as PIR3. **C.** Average responses of LN5 to the I1 test (N=4, n=18). The activity of LN5 is colored in blue, the names of the chirps are given above each recording. Orange arrowheads represent the premature rebound1 in response to I1-5 and I1-10. Blue arrowheads represent the deflections during rebound1 in response to I1-40, I1-50 and I1-80. Grey arrowheads represent the peak of the last post-inhibitory rebound (PIR3), which is the only complete rebound in response to 3-pulses chirps. **D.** Maximum amplitude of the rebounds over the I1-test. The PIR1, PIR2 and PIR3 are colored in dark to light yellow. The data are averaged from 10 recordings. Error bar indicates the standard error mean (SEM). The phonotactic tuning is indicated by blue shade.

LN2 activity declines over the sound pulses.

Due to the post-inhibitory rebound (PIR) activity each inhibition leads to a subsequent depolarisation. Since each rebound depolarisation was interrupted by the following inhibition, the peak of each PIR elicited by the normal chirp was also the start of the following inhibition. For example, PIR1 was also the start of the second inhibition INH2. According to the delay-line and coincidence detector mechanism, the overlap between the activity in the direct pathway (the AN1 activity elicited by P2) and the delayed pathway (the first rebound elicited by P1) is crucial for achieving the coincidence. It is noteworthy that although P1 initiates the first inhibition and the first rebound, the peak of the first rebound (PIR1) and the overlap area between the first rebound and the second AN1 activity are defined by P2 due to the cut-off effect generated by the second inhibition on the first rebound. Besides, both PIR2 and PIR3 occur after the third sound pulse P3. Therefore, the latency of PIR1 in LN5 will be given in relation to the onset of the second sound pulse (P2). Similarly, the latency of PIR2 and PIR3 will be measured from the start of the third sound pulse (P3).

The PIRs reached a maximum amplitude of PIR1: 1.1±0.2, PIR2: 3.6±0.1, and PIR3: 5.4±0.3 mV, at 25.7±0.5 (latency to P2), 26.2±0.4 (latency to P3) and 79.9±3.1 ms (latency to P3) (Table. 1). Since the rising phase of the post-inhibitory rebound was interrupted by the second and the third inhibition, the AN1 activity and the post-inhibitory rebound overlapped for about 7 ms before the subsequent inhibition kicked in (PIR1 in LN5 and the second AN1: 26.4±0.2 vs. 18.4±0.2 ms; PIR2 in LN5 and the third AN1: 25.7±0.5 vs. 19.6±0.1 ms) (Table. 1). This allows about 3-4 spikes of AN1 to coincide with the post-inhibitory rebound. The amplitude of the PIRs was measured between the resting potential and the peak of the PIR, as indicated for the amplitude of PIR2 (Fig. 16B, a). The amplitude of the inhibition was measured from the starting point of the inhibition (i.e. resting potential for INH1; or the peak of the previous PIR for INH2 and INH3) to the lowest point as shown for the amplitude of INH3 (Fig. 16B, b). The peak of the post-inhibitory rebound elicited by a single sound pulse occurred with a latency of 89.4±2.2 ms (measured from I1-80).

LN5 responses to I1-chirps

In all tests the amplitude and timing of the LN5 inhibitory response to the first sound pulse P1 was not affected by changing I1 (Fig. 16C), the membrane potential of INH1 reached a minimum of -4.43±0.07 mV with a latency of 36.4±0.5 ms (Table. 1). The response of LN5 to

the second (P2) and the third pulse (P3) of the I1-chirps depended on the duration of I1. For I1-5 and I1-10 the interval was too short for LN5 to generate a pronounced PIR after INH1. The PIR1 resulted in only a small 'bump' with an amplitude of -2.2±0.1 (I1-5) and -1.5±0.1 mV (I1-10) occurring with a latency of 23.8±0.8 and 27.5±0.3 ms to the onset of the second sound pulse, and driven by a small inhibition caused by P2 (Fig. 16C, I1-5 and I1-10, orange arrows).

Although the second inhibition (INH2) was not clearly expressed, the second rebound (PIR2) continued from the first rebound to depolarise and eventually overshot the resting potential with an amplitude of 3.3±0.2 mV (I1-5) and 3.9±0.4 mV (I1-10). These peaks occurred with a latency of 26.7±1.3 (I1-5) and 28.1±0.5 ms(I1-10) to the third sound pulse (Fig. 16C, I1-5 and I1-10). The third inhibition (INH3) was pronounced and reached an amplitude of 3.9±0.4 mV (I1-5) and 3.8±0.3 mV (I1-10). The subsequent rebound (PIR3) was always the largest and the most prolonged one, which gradually declined as it was not terminated by an inhibition (Fig. 16C, I1-5 & I1-10, grey arrows). The maximum of PIR3 reached 4.2±0.4 mV (I1-5) and 4.5±0.3 mV (I1-10), while the peaks occurred with a latency of 78.4±1.5 and 79.1±0.7ms to the onset of the third sound pulse, respectively. The major features of the LN5 response for short I1 are: 1. The first inhibition was prolonged, since LN5 responded to the first two sound pulses as one pulse. 2. Only the second and the third PIR were pronounced and reached their maximum above the resting potential. 3. The PIR3 amplitude was slightly higher than PIR2.

In response to chirps with medium I1 (I1-20, I1-25 and I1-30), PIR1 reached a maximum above the resting potential with 1.1±0.2, 2.0±0.2 and 2.6±0.4 mV, respectively (Fig. 16C). The second inhibition (INH2) of LN5 became more pronounced, and reached 1.4±0.1, 2.0±0.6 and 2.9±0.4 mV, respectively, also PIR2 became more pronounced with 3.6±0.1 (I1-20), 4.3±0.6 (I1-25) and 3.9±0.4 (I1-30) mV. Finally, the third rebound (PIR3) peaked at an even higher membrane potential, with 5.4±0.3 (I1-20), 4.8±0.4 (I1-25) and 5.1±0.4 (I1-30) mV, revealing an overall continuous build-up of the peak amplitudes of the three PIRs over the time course of the chirps (Fig. 16C, I1-20, I1-25 and I1-30, grey arrows). The response of LN5 to medium I1 is characterised by 3 features: 1. Each of the three sound pulses elicited a separate PIR with a peak above the resting potential. 2. The amplitude of the three PIRs progressively increased. 3. The membrane potential over a chirp gradually built up by alternating effects from inhibition and PIRs.

When exposed to chirps with long I1-intervals the PIR1 developed for longer time and reached peak amplitudes of 4.0±0.5 (I1-40), 4.8±0.4 mV (I1-50) and 4.4±0.4 mV (I1-80) (Fig.

16C). A deflection in the course of the membrane potential occurred during the depolarising rebound phase with a latency of 66.7±0.6 ms to the onset of the first sound pulse, which is 40.3 ms after the onset of the inhibition. This was not directly linked to a sound pulse but matched the pulse period of a normal chirp (Fig. 16C, I1-40 - I1-80, blue arrows). The responses of LN5 to each of these chirps show slight differences. For I1-40, the amplitude of PIR2 was 4.5±0.3 mV, and larger than that of PIR1 and the INH2 reached an amplitude (4.5±0.3 mV). The amplitude of PIR3 was 4.2±0.3 mV and the smallest among the three PIRs. For I1-50, the amplitude of PIR2 was 3.9±0.2 mV, and the smallest among the three PIRs; INH2 was 6.2±0.2 mV, and PIR3 was 4.1±0.3 mV. At I1-80 the time course of the first rebound (PIR1) is exposed in more detail. It reached a broad peak of 4.4±0.4 mV at 112.0 ms after the onset of the first sound pulse with is 85.64 ms after the beginning of the first inhibition, and it then started already to repolarise when INH2 kicked in. The second inhibition (INH2) reached an amplitude of 7.1±0.4 mV, which is similar to the first inhibition (INH1). The amplitude of PIR2 was the smallest with 2.4±0.4 mV as the final broad maximum of PIR3 reached an amplitude of 3.2±0.3 mV.

The responses of LN5 to long I1-intervals are characterised by 3 features: 1. Three PIRs crossed the resting potential. With increasing I1, PIR1 became more pronounced and at I1-80 started to repolarise. 2. The amplitude of the three PIRs did not increase over the chirps; the second and the third PIRs decreased in amplitude. 3. A deflection in the membrane potential occurred in the rising phase of the first post-inhibitory rebound (blue arrows).

For a quantitative analysis of the LN5 activity I compared the responses across all the chirps, I plotted the amplitudes of the three post-inhibitory rebounds (PIR1 to PIR3) over the duration of I1 (Fig. 16D) and aligned and superimposed the responses of LN5 to both the first and the last sound pulse (Fig. 17A,B).

As the first sound pulse always had a duration of 20 ms, the first inhibition generated in LN5 was not affected by changing I1, all reaching a minimum of -4.43±0.07 mV at 36.4±0.5 ms (Fig. 17A) and starting the rebound. The amplitude of PIR1 showed the strongest change among the three PIRs, with increasing I1 the time when the INH2 kicked in and interrupted the first rebound was delayed and this left more time for the first rebound to develop. This is shown clearly when aligning the responses of LN5 to the onset of the second sound pulse (P2) (Fig. 17B). The amplitude of PIR1 increased from -2.2±0.05 to 1.1±0.2 mV with a slope of m=0.2193 (R^2=0.9807, Pearson correlation coefficient) when I1 increased from 5 to 20 ms (Fig. 16D).

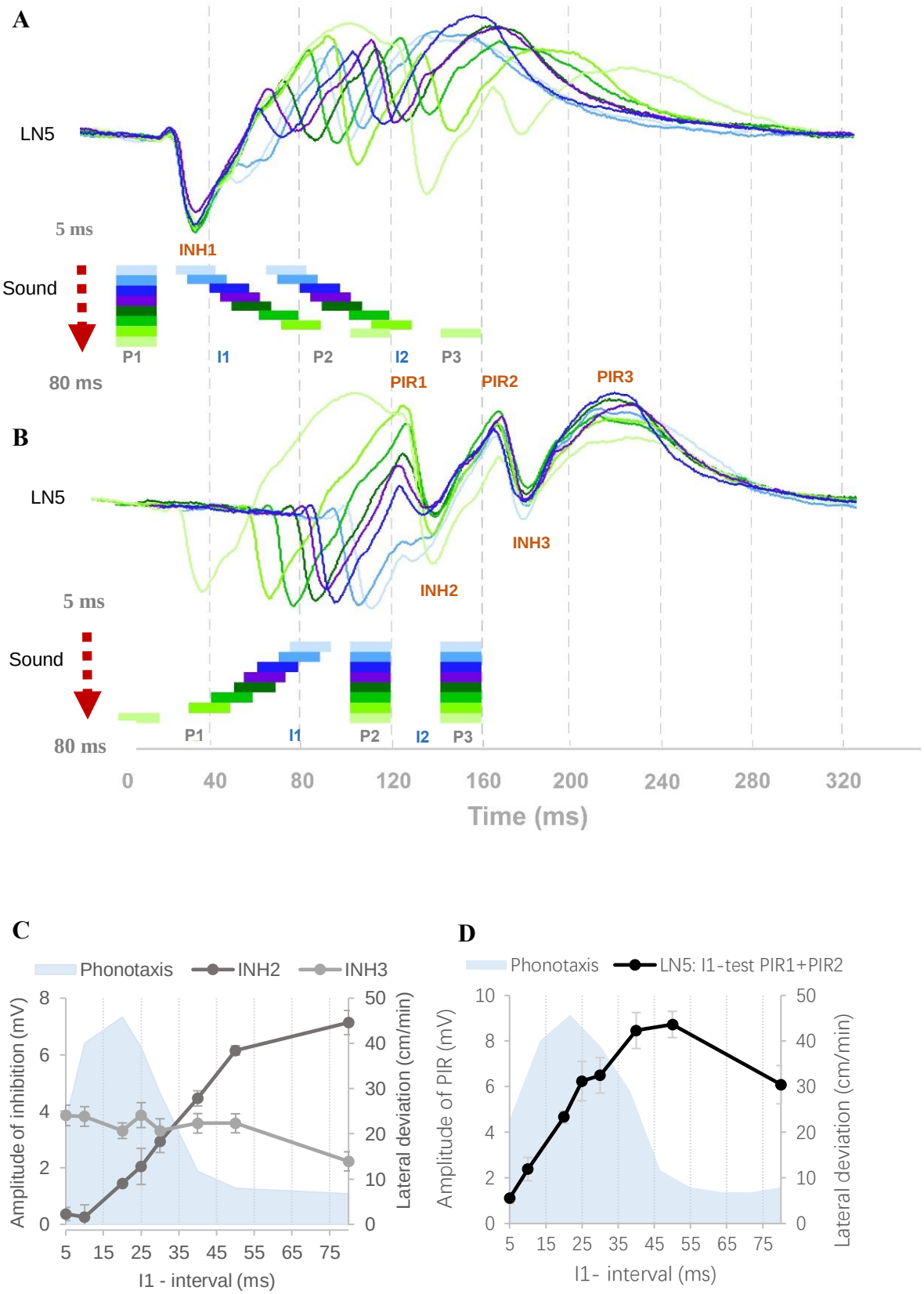

Fig. 17 LN5 activity elicited by I1-test aligned to the first or the last sound pulses and the tuning curves of inhibitions and summed PIRs.

Fig. 17 LN5 activity elicited by the I1-test aligned to the first or the second sound pulse, and the tuning curves of inhibitions and summed PIRs. A. Averaged LN5 activity in response to the I1-test aligned to the onset of P1 (N=4, n=18). **B.** Averaged LN5 activity in response to the I1-test aligned to the onset of P2. When interval I1 is smaller than 30 ms, the chirps and LN5 responses (I1-5, I1-10, I1-20 and I1-25) are colored as light to dark blue and purple, respectively. For I1 equal to or larger than 30 ms, chirps and LN5 responses (I1-30, I1-40, I1-50 and I1-80) are colored as dark to light green, respectively. Responses in dark blue and purple are to chirps I1-20 and I1-25 that elicit the best phonotactic behavior. **C.** Maximum of INH1 and INH2 over the I1-test, colored in dark and light grey. **D.** Sum of PIR1 and PIR2 over the I1-test. Error bar indicate the standard error mean (SEM). The phonotactic tuning is indicated by blue shade.

This increase was in accordance with the phonotactic tuning curve in the range of I1-5 to I1-20 although the PIR1 amplitude elicited by short I1 did not increase as sharply as the phonotactic response. The amplitude of PIR1 then increased linearly from 2.0±0.2 to 4.8±0.4 mV but with a slower rate (slope: m=0.116) (R^2=0.989, Pearson correlation coefficient) when I1 was between 20 ms and 50 ms, which exhibits an opposite trend to the phonotactic tuning within this range. The amplitude of PIR1 then slightly declined at I1-80 to 4.4±0.4 mV but was still higher than that at I1-40 (Fig. 16D). In the I1-test, the interval between the second and the third pulse was constant at 20 ms, but I1 did also have an impact on PIR2 and PIR3 (Fig. 17B). The amplitude of PIR2 showed a rather flat tuning, it remained almost constant at 3.5 mV up to I1-50 and then declined to 2 mV at I1-80 (Fig. 16D), which was not in accordance with the behavioural tuning. PIR3 increased in amplitude from 4.2±0.4 to 5.4±0.3 mV when I1 was increased from 5 to 20 ms and then decreased to 4.2±0.3 mV when I1 further increased to 40 ms, resulting in a peak amplitude at I1-20. For long I1, the amplitude decreased to 3.2±0.3 mV (I1-80) (Fig. 16D). The overall tuning curve of the amplitude of PIR3 showed a qualitatively similar shape to the phonotactic tuning with a peak at I1-20 and a slow decrease from I1-40. Since the third rebound (PIR3) was the only one that was completed without cut-off by a subsequent inhibition, its peak amplitude indicates the current depolarisation state of the cell after processing the preceding sound pulses and also the state of the cell to respond to any following sound pulses. However, the difference of the amplitude elicited by I1-5 (4.2±0.4mV) and I1-20 (5.4±0.3 mV) was only 1.2 mV and the maximum differences in the amplitude was about 2.2 mV (I1-20: 5.4±0.3 mV vs. I1-80: 3.2±0.3 mV). In summary, none of the tuning curves of the three PIRs reflects the tuning of the phonotactic behaviour.

I also analysed the inhibitory responses of LN5. The strength of the INH2 showed a similar tuning as the amplitude of PIR1 (Fig. 17C). From I1-5 to I1-25 ms, it increased from 0.4±0.2 to 2.0±0.6 mV with a slope of m=0.091 (R^2=0.9219, correlation coefficient); as I1 further increased to 50 ms, INH2 increased to 6.2±0.2 mV with a larger slope of m=0.1626 (R^2=0.9994, correlation coefficient) and up to I1-80 the amplitude of the inhibition increased to 7.1±0.4 mV, however with a with a slower rate. Therefore, the amplitude of INH2 increased as I1 increased. On the contrary, the amplitude of INH3 was very stable at about 3.5 mV in the range of I1-5 to I1-50, it dropped to 2 mV at I1-80 (Fig. 17C) and overall was similar to the response to PIR3 (Fig. 16D).

The response of the coincidence detector LN3 depends on the level of overlap of the

direct and delayed activity forwarded by AN1 and LN5. According to the function of the pattern recognition network (Schöneich et al. 2015) in three-pulse chirps, only the rebounds elicited by the first two pulses are effective in driving the activity of the coincidence detector LN3. Therefore, the sum of PIR1 and PIR2 may determine the overall strength of the input received in the coincidence detector LN3. I therefore summed the amplitudes of PIR1 and PIR2 and plotted these in Fig. 17D. Similar to the increasing trend of the phonotactic tuning, the summed amplitude initially increased from 1.1±0.2 to 4.7±0.3 mV when I1 increased from 5 to 20 ms; and it then further increased to 8.7±0.6 mV at I1-50. Only when I1 was 80 ms did the summed PIR amplitude decrease to 6.8±0.8 mV, but it was still higher than the amplitude at I1-30 (Fig. 17D). Thus, also the summed activity of PIR1 and PIR2 did not reveal a tuning corresponding to the behavioural response.

A feature that has not been reported before is the trend in the change of the peak amplitude of the three PIRs over the time course of the chirps (Fig. 18, illustrated by arrows 1 to 3). The overall trend is shown for four I1-chirps from the start of the resting membrane potential to the peak of PIR1 (slope 1), from the peak of PIR1 to the peak of PIR2 (slope 2) and from the peak of PIR2 to the peak of PIR3 (slope 3). In response to I1-5 (Fig. 18, I1-5) the PIR1 has a low amplitude and the initial trend is negative (arrow 1), however PIR2 and PIR3 are both increasing revealing a subsequent increase in the response (Fig. 18, I1-5, arrows 2,3). In response to the normal chirp, the amplitudes of the PIRs continuously increased over the chirp (Fig. 17, I1-20). For I1 of 50 ms (Fig. 18, I1-50) the maxima of the PIRs are of similar amplitudes and reveal a plateau stage (arrow 2), with a marginal decrease for PIR3 (arrow 3). In case of I1-80 (Fig. 18, I1-80), PIR1 (arrow 1) gave the largest response whereas the amplitude of PIR2 (arrow 2) and PIR3 (arrow 3) was considerably lower, indicating an overall decrease of the PIR maxima towards the end of the chirp. The development of the PIR maxima over the time course of the chirps demonstrates that compared to the normal chirp, the PIR amplitudes elicited by chirps containing short or long I1 exhibit different trends. Only for the normal chirp did a continuous increase of the peak amplitude and the overall membrane potential of LN5 occur.

The trend of the change in the peak amplitude of the three PIRs in response to different I1-chirps can be compared by averaging their slopes. For example, the slope 1 in response to I1-20 is the differences in the membrane potential between the resting level and the PIR1 over the duration of t1. The overall slope for a particular chirp is averaged from slopes 1, 2 and 3.

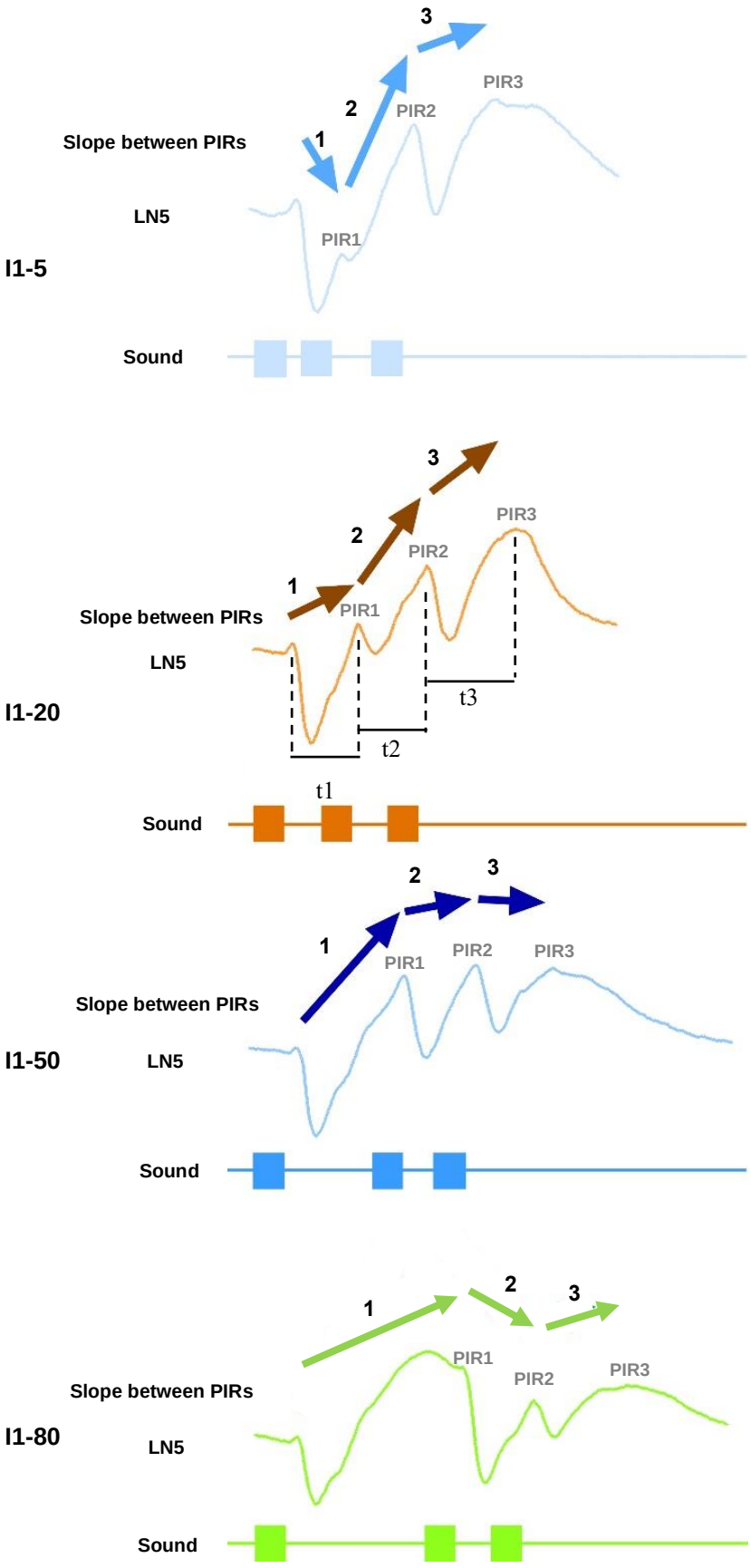

Fig. 18 The changes in the amplitude of adjacent PIRs over time (slope between PIRs) in I1-test.

Fig. 18 The changes in the amplitude of adjacent PIRs over time (slope between PIRs) in I1-test. The changes in the maximum amplitude of adjacent rebounds over time in response to four example chirps (I1-5. I1-20, I1-50 and I1-80) of the I1-test (N=4, n=18). The arrows indicate the change and slope between two adjacent peaks of the rebounds over the time between the two PIRs (t1, t2 and t3), which are named as slope1, slope2 and slope3. The slope1 and slope2 were directly influenced by varying interval I1.

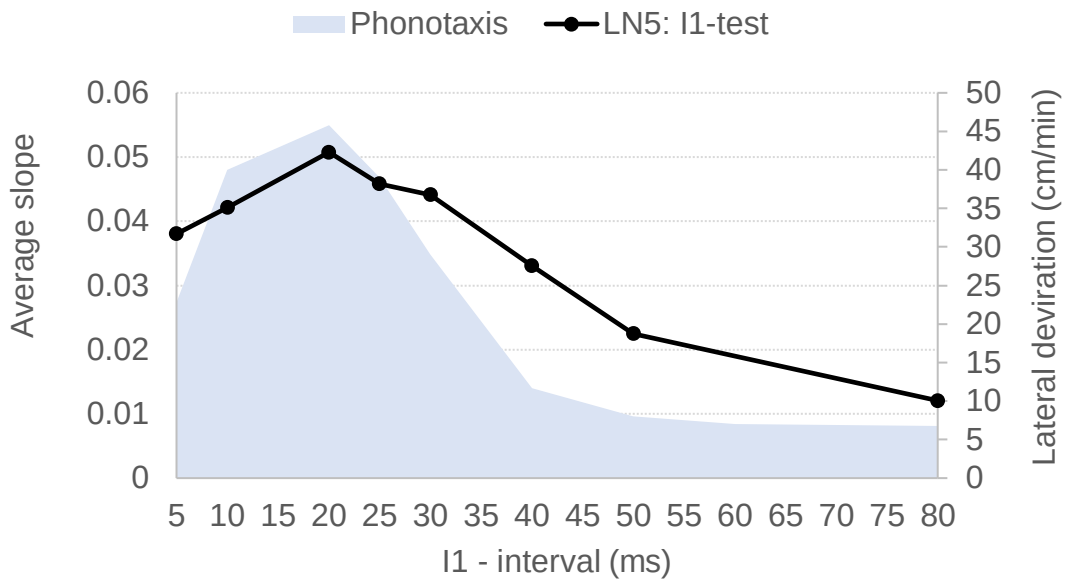

Fig. 19 The tuning of the mean 'slope' of LN5 in the I1-test. The tuning curve is averaged from slope1, slope2 and slope3 in response to each chirp of the I1-test (N=4, n=18). Phonotactic response is in blue shade.

The average slope of the PIRs in response to different I1-chirps is plotted in Fig. 19. The curve increases from short I1 and exhibits a peak at I1-20, it then gradually decreases as I1 reaches 80 ms. This tuning curve of LN5 activity reflects the band-pass property of the phonotactic tuning and provides the best match from all parameters analysed. This may indicate a gradual increase of an underlying slow depolarising conductance, which triggered by inhibition may drive the post-inhibitory membrane depolarisation of LN5 over the time course of a chirp. The effect of this may be relevant for the phonotactic tuning.

The coincidence detector – LN3

Neuron LN3 functions as the coincidence detector in the network and is driven by a direct input from AN1 spikes and a delayed graded input from LN5 rebound potentials (Fig. 20A), an example recording shows its activity pattern (Fig. 20B).

LN3 response to a single 20 ms sound pulse

LN3 responded with a depolarisation to a 20 ms sound pulse (and all I1-chirps) with a latency of 23.2±0.2 ms by summation of EPSPs followed by spikes occurring with a latency of 34.1±0.8 ms (Table. 1). Without subsequent sound pulses following, the LN3 response towards a 20 ms sound pulse was a prominent supra-threshold depolarisation lasting for 54.0±0.3 ms (measured from the I1-80), which outlasted the sound pulse. Therefore, a 20 ms interval between adjacent two responses of LN3 is too short for the repolarisation to complete.

LN3 response to the normal chirp

For the normal chirp (I1-20), the depolarisation and spikes evoked by the second sound pulse occurred with a latency of 23.4±0.4 ms and 27.3±0.4 ms, respectively. The depolarisation elicited by the first sound pulse (P1) lasted for 33.8±0.3 ms and the spiking activity lasted 6.7±0.6 ms. The depolarisation elicited by the second sound pulse lasted for 33.7±1.3 ms whereas the spiking activity in the second burst lasted 16.7±1.3 ms, which is longer than in the first burst ($p=0.005$, t-test, $n=10$) (Table. 1). The third sound pulse (P3) elicited a depolarisation which occurred with a latency of 24.0±0.2 and spikes at 29.8±0.5 ms, respectively. Without subsequent stimuli, the third sound pulse gave a longer depolarisation as 41.5±2.1 ms and spiking activity of 14.2±0.8 ms. A subthreshold excitatory activity followed the last spiking activity, this however is not always very clear in the example shown (Fig. 20B, blue arrows). This excitation is considered to be an input from the post-inhibitory rebound PIR3 of LN5.

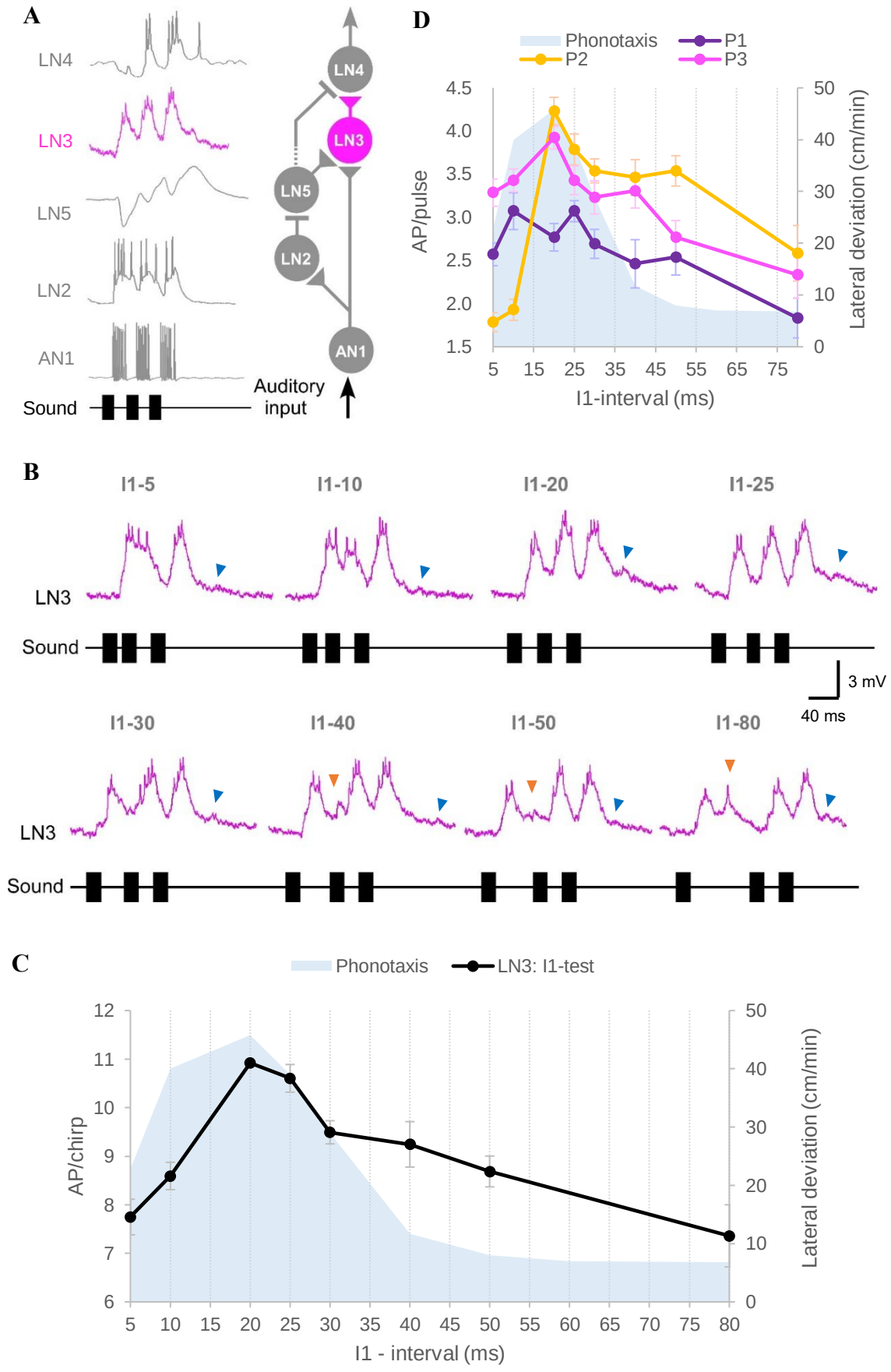

Fig. 20 Response of the coincidence detector neuron LN3 to I1-test.

Fig. 20 Response of the coincidence detector neuron LN3 to I1-test. A. Characteristic response of LN3 to the normal chirp and its role in the pattern recognition circuit. **B.** Activity of LN3 in response to chirps with interval (I1) varied. The activity of LN3 is coloured in pink, the tested chirps are labeled above each response. Blue arrowheads indicate a lagging depolarization after the end of the third burst of spikes. Orange arrowheads represent a depolarization following the first burst of spikes. **C.** AP/chirp elicited by LN3 in response to the I1-test (N=5, n=13), and the phonotactic response indicated by blue shade. **D.** AP/pulse elicited in LN3 by each pulse within a chirp in I1-test (N=5, n=13). The number of spikes was averaged from 5 animals, 13 repeats. Error bars represent standard error means (SEM). Phonotactic response is in blue shade.

LN3 response to the I1-chirps

When exposed to short I1 (I1-5 and I1-10) neuron LN3 responded with a prolonged plateau-like depolarisation generating 4.4±0.2 APs, as the interval between the pulses was so short that the second excitatory input arrived before the first depolarisation had declined (Fig. 20B, I1-5 and I1-10). The response to the third sound pulse (P3) was a separate depolarisation and 3.3±0.2 AP, followed by a small subthreshold depolarisation (Fig. 20B, I1-5 blue arrow); the overall activity was 7.7±0.4 AP/chirp. For I1-10, the first sound pulse (P1) elicited 3.1±0.2 APs, the first depolarisation had not yet declined, when the second excitatory input arrived, which joined the first depolarisation and elicited a burst of 1.9±0.1 APs. The third sound pulse (P3) caused a separate depolarisation and a burst of 3.4±0.1 APs; overall the chirp I1-10 resulted in 8.6±0.3 AP. Two features characterise the responses to short I1: 1. The responses to the first two sound pulses (P1 and P2) are not completely separated and merged. 2. The response to the first sound pulse (P1) of I1-10 was stronger than that to the second sound pulse (P2).

In response to chirps with medium I1, LN3 generated three separated supra-threshold depolarisations leading to bursts of spikes, and due to their duration also generated a maintained depolarisation over the time course of the chirp. The first sound pulse (P1) elicited about three spikes in LN3 (I1-20: 2.8±0.2 AP/pulse; I1-25: 3.1±0.1 AP/pulse; I1-30: 2.7±0.2 AP/pulse). The second pulse (P2) elicited 4.2±0.2, 3.8±0.2 and 3.5±0.1 AP/pulse, respectively, and the response was significantly stronger than the first response ($P<0.0001$, paired t-test). The third response was slightly lower as compared to the second response with 3.9±0.1, 3.4±0.2 and 3.2±0.2 AP/pulse respectively ($P=0.00163$, paired t-test). The overall spike activity elicited by these chirps was very similar and 10.9±0.0, 10.6±0.3 and 9.5±0.2 AP/chirp, respectively. Two features are typical for these LN3 responses: 1. LN3 responded with three clearly separated bursts of spikes. 2. The second burst of spikes was stronger than the first and the third bursts of spikes. 3. The neuron showed a maintained depolarisation over the time course of the chirps.

When exposed to I1-40 and I1-50 the first sound pulse (P1) elicited a depolarisation with 2.5±0.3 AP/pulse. With the long intervals, a depolarisation occurred following the first burst (orange arrows), and the overall depolarisation of the membrane potential decreased. The second sound pulse again elicited a greater number of spikes than the first pulse (I1-40: 3.5±0.6 AP/pulse; I1-50: 3.5±0.2 AP/pulse). For both I1-chirps the response to the third pulse was slightly lower with 3.3±0.2 and 2.8±0.2 AP/pulse, respectively. The overall number of spikes generated by each chirp was 9.2±0.5 and 8.7±0.3 AP/chirp, respectively. In response to I1-80

the first pulse (P1) resulted in 1.8±0.2 AP, which in this recording was followed by a supra-threshold depolarisation (Fig. 20B I1-80, orange arrow). P2 elicited 2.6±0.3 AP and the third response was 2.3±0.3 AP, the total number of spikes per chirp was 7.4±0.6 AP. Two features characterised the responses: 1. An depolarisation followed the first - and last - burst of spikes. 2. For long I1 the second burst of spikes was weaker than the first and the third response.

For a quantitative analysis I compared the LN3 activity with the tuning of phonotaxis (Fig. 20C). LN3 activity significantly increased from 7.7±0.4 to 10.9±0.0 AP/chirp as I1 increased from 5 ms to 20 ms (I1-5 vs I1-20: $p<0.0001$; I1-10 vs I1-20: $p=0.0007$, Friedman test, N=5, n=13), corresponding to the increase of the phonotactic tuning. The activity slightly decreased to 10.6±0.3 AP/chirp when the interval was 25 ms, and decreased further to 9.5±0.2 AP/chirp as I1 was 30 ms, this decrease corresponds to the reduction in the phonotactic responses when I1 increased from 20 to 30 ms (Fig. 20C). The activity of LN3 then only gradually decreased from 9.2±0.5 (I1-40) to 7.4±0.6 AP/chirp at I1-80 ms; while the behavioural tuning sharply dropped from I1-30 to I1-40 and then stayed at a very low level. Qualitatively the gradual decrease in LN3 activity reflected the behavioural tuning in this test range. The overall changes in LN3 activity matched the behavioural tuning, the increase in activity from I1-5 to I1-20 was steeper than the decrease from I1-20 to I1-80. At long I1, the activity of LN3 was significant lower when compared to the response to a 'normal chirp' (I1-40: 9.2±0.5 AP/chirp; I1-50: 8.7±0.3 AP/chirp and I1-80: 7.3±1.0 AP/chirp. I1-40 vs I1-20: $p=0.0243$; I1-50 vs I1-20: $p=0.0016$; I1-80 vs I1-20: $p<0.0001$, Friedman test, N=5, n=13). The average activity of LN3 in response to the I1-chirps was 57.51% lower than the activity of AN1 (AN1: 21.3±0.1 AP/chirp vs LN3: 9.1±0.4 AP/chirp).

To explore whether the tuning of LN3 differs for the different sound pulses, I separately plotted the number of spikes for each pulse (P1-P3) over the I1-chirps (Fig. 20D).The response to the first pulse (P1) was around a mean of 2.7±0.1 AP/pulse, it dropped towards I1-80but overall did not show any signs of matched tuning across the I1-test ($p=0.0665$, Friedman test, N=5, N=13), (Fig. 20D). The response to the second pulse (P2) sharply increased from 1.8±0.1 to 4.2±0.2 AP/pulse when I1 increased from 5 to 20 ms and reflects the increase in phonotactic tuning. The peak response at I1-20 was significantly higher than that elicited by chirps containing short or long I1 (I1-5 vs I1-20: $p<0.0001$; I1-10 vs I1-20: $p<0.0001$; I1-80 vs I1-20: $p=0.001$, Friedman test, N=5, n=13). The response to P2 then gradually declined to 3.5±0.1 AP/pulse at I1-30 and then further to 2.6±0.3 at I1-80; qualitatively matching the decline of the

behaviour (Fig. 20C). The overall response to the second pulse P2 was 37.5±4.4% stronger than that to the first pulse P1, at least between I1-20 to I1-50 (P1: 2.7±0.1 AP and P2: 3.7±0.1 AP, p=0.0029, One-way ANOVA with repeated measures, Tuckey, N=5, n=13). This is in accordance with the function of the delay-line and coincidence detector mechanism, P2 elicits stronger activity due to the coincidence of the LN5 post-inhibitory rebound triggered by P1 and the AN1 activity elicited by P2.

The spike response to the third pulse (P3) showed an increase from 3.3±0.2 to its maximum of 3.9±0.1 AP when I1 changed from 5 to 20 ms. At longer I1 the activity gradually decreased from 3.4±0.2 AP/pulse (I1-25) to 2.3±0.3 AP/pulse (I1-80). Thus the tuning of LN3 activity overall also reflected the phonotactic tuning, however in a more moderate form. The mean response of LN3 to P3 (3.2±0.2 AP/pulse) was stronger than that to P1 (2.8±0.2 AP/pulse) and to P2 (3.1±0.2 AP/pulse) (P3 vs P2: p=0.0459; P3 vs P1: p=0.04, One-way ANOVA with repeated measures, Tuckey). Based on these three tuning curves the overall tuning of LN3 (Fig. 20C) is likely determined by the additive effect of the responses to P2 and P3. This also indicates that varying the first interval effects the response to P2 and also has a carry-on effect on the P3 response.

The feature detector – LN4

The response of the feature detector neuron LN4 is driven by an inhibitory input from LN2 and an excitatory input from LN3 (Fig. 21A). An LN4 recording is presented containing some background activity, which may have been caused by injury of the cell by the microelectrode; the corresponding spikes are marked by grey arrows in Fig. 21B.

LN4 response to a single 20 ms sound pulse and the normal chirp

LN4 responded with an inhibition to single sound pulses. The latency of the inhibition was 24.9±0.3 ms and it lasted for 75.6±1.2ms when evoked by a 20 ms pulse. Spike activity for a normal chirp occurred with a latency of 96.9±2.9 ms with reference to the first pulse; such a very long latency to the start of a chirp for LN4 was also reported by Kostarakos and Hedwig (2012), and is due to the initial inhibition. When compared to the second sound pulse P2, the latency of the first burst of spikes was 30.3±0.5 ms, and was very similar to that caused by the third pulse as 29.1±0.2 ms. It is noteworthy that the duration of the depolarisations elicited by P2 and P3 turned out to be different. For example, in response to the normal chirp, the depolarisation caused by P2 lasted for 19.3±0.5 ms, while it lasted for 30.6±2.0 ms in response

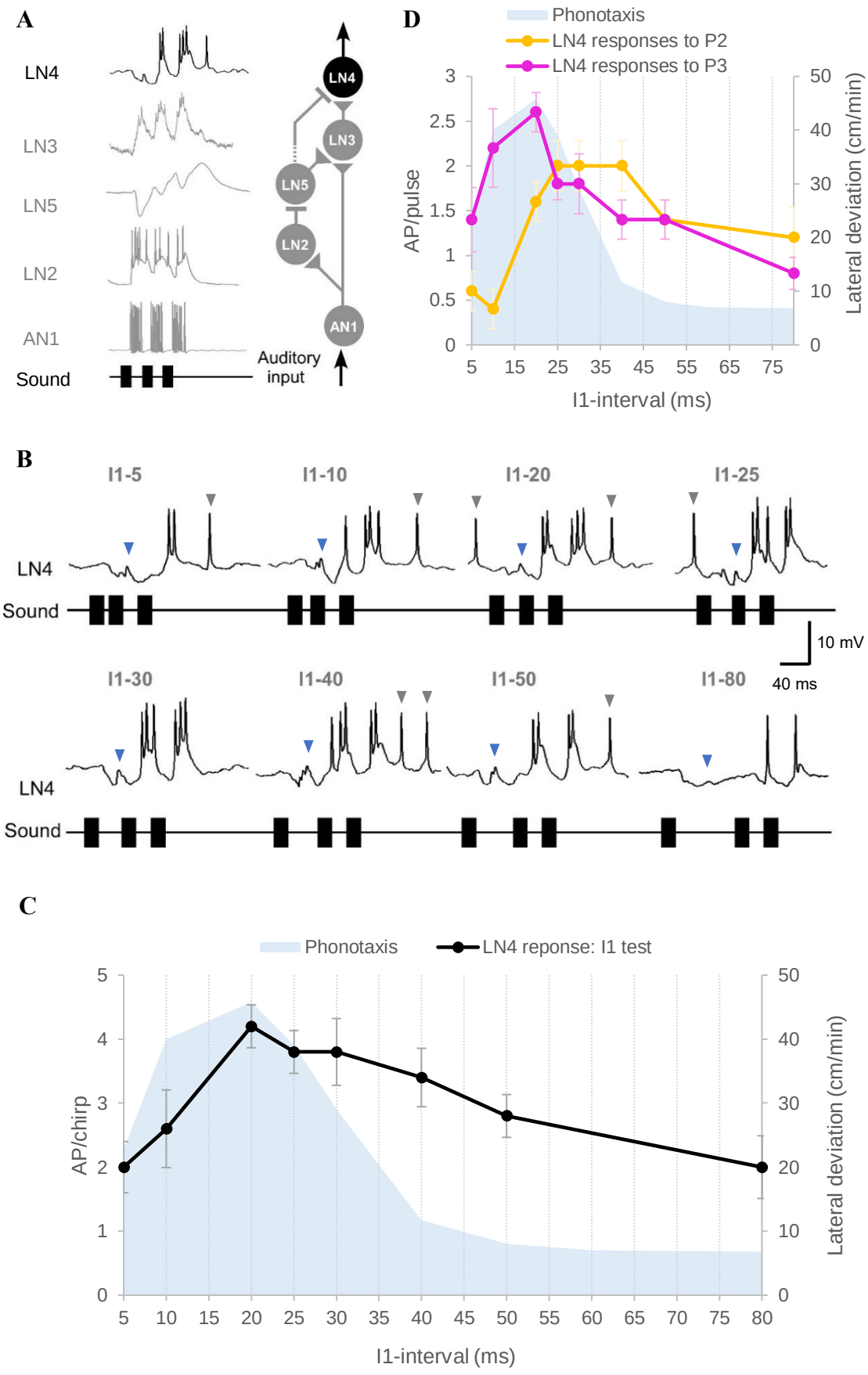

Fig. 21 Response of the coincidence detector neuron LN4 to I1-test.

Fig. 21 Response of the coincidence detector neuron LN4 to I1-test. A. Characteristic response of LN4 to the normal chirp and its role in the pattern recognition circuit. **B.** Activity of LN4 in response to chirps with interval (I1) varied. The neuronal activity of LN4 is coloured in black, the tested chirps are labeled above each response. Blue arrowheads indicate EPSPs occurring during the initial inhibition, grey arrowheads represent the spontaneous spikes. **C.** AP/chirp elicited in LN4 in response to the I1-test, and the phonotactic response indicated by blue shade. **D.** AP/pulse elicited in LN4 by each pulse within a chirp in I1-test. The number of spikes was averaged from 5 animals, 5 repeats. Error bars represent standard error means (SEM). Phonotactic response is in blue shade.

to P3 (p=0.015, n=5, t-test). The spiking activity lasted even shorter as 9.7±1.4 ms for P2 and 16.5±1.1 ms for P3 (p=0.031, n=5, t-test).

LN4 response to the I1-chirps

The initial response of LN4 to chirps with I1-5 was dominated by a pronounced inhibition, in which the response to P1 and P2 merged. For I1-5 a subthreshold depolarisation and occasionally a spike occurred after P2, and for I1-10 the second sound pulse (P2) initiated a depolarisation and a single spike (Fig. 21B, I1-5 and 1-10). The response to the third pulse (P3) was a pronounced depolarisation with a burst of 2-3 spikes. The mean response of LN4 to P2 was 0.4±0.2 and 0.6±0.2 AP, while P3 elicited 1.4±0.4 and 2.2±0.4 AP for I1-5 and I1-10, respectively. These properties are typical for the response to short I1: 1. The initial inhibition caused by P1 and P2 can merge. 2. Only a single spike, if any, occurred in response to the second sound pulse (P2).

Also the chirps that cover medium I1 (I1-20 to I1-30) elicited an inhibition following P1 (Fig. 21B). Now the response to P2 was a burst of spikes with 1.6±0.2 (I1-20), 2.0±0.3 (I1-25) and 2.0±0.3 (I1-30) AP/pulse. The response to P3 was a separate burst of spikes reaching 2.6±0.2 (I1-20), 1.8±0.2 (I1-25) and 1.8±0.3 (I1-30) AP/pulse. Thus, for medium I1 the LN4 response starts with an inhibition and is followed by two pronounced depolarisations with 2-3 spikes. When stimulated with chirps with long I1 (I1-40 to I1-80), which are outside the phonotactic tuning, the full time course of the inhibition became obvious (I1-80) and the initial inhibitory response also revealed a subthreshold depolarization embedded in the inhibition (Fig. 21B, blue arrowheads), which was less obvious at shorter I1, and matched the timing of the additional depolarisations in LN3 (Fig. 20B). As the membrane potential recovered to the resting level the response elicited by P2 was 2±0.3 (I1-40) and 1.4±0.2 (I1-50) AP/pulse, while the burst of spikes elicited by P3 reached 1.4±0.2 AP/pulse for both I1-40 and I1-50. Interestingly, the pattern of these LN4 responses was not substantially different to the response to a normal chirp. When stimulated with I1-80 the initial inhibition dominated the response, the inhibition fully recovered to the resting potential, and P2 and P3 each elicited only a single spike (P2: 1.2±0.3 AP, P3: 0.8±0.2 AP).

Overall, the LN4 responses to the different I1-chirps showed two typical features: 1. All responses started with an inhibition mixed with some subthreshold EPSPs. The inhibition occurred after a latency of 25.1±0.6 ms. 2. Spiking activity with a burst of 2-3 spikes started

only with the second sound pulse (P2), and with reference to the chirp after a long latency of 96.9±2.9 ms.

In LN4 a reduction in the number of spikes occurred by 66.66%, as compared to LN3, and of 85.63% when compared to AN1 (LN4: 3.1±0.3 AP/chirp; LN3: 9.1±0.4 AP/chirp; AN1: 21.3±0.1 AP/chirp).

Plotting the LN4 activity over the I1-test, shows a steep increase from I1-5 to its peak at I1-20 (I1-5: 2±0.4 AP/chirp; I1-10: 2.6±0.1 AP/chirp I1-20: 4.2±0.3 AP/chirp, I1-5 vs I1-20: p=0.0109, Friedman test, Tuckey, N=5, n=5)(Fig. 21C). This increase in LN4 activity matches the increase of the behavioural tuning within this range. Both the behavioural and the neuronal tuning showed a peak at I1-20, however the neuronal activity in response to I1-10 was relatively lower compared to the behaviour tuning (Fig. 21C). The neuronal activity gradually declined from I1-25 to I1-80 (I1-80 vs I1-20: p=0.0169, Friedman test, N=5, n=5). This decrease in activity was more gradual than the decline of the behavioural responses. The quantitative analysis of LN4 responses showed a band-pass like shape in the tuning of its activity, matching the behavioural tuning (Fig. 21C). A peak occurred at I1-20 (4.2±0.3 AP/chirp), while the response to chirps containing very short or very long I1 turned out to be considerably lower (I1-5: 2±0.4 AP/chirp; I1-80: 2±0.5 AP/chirp). The short I1 and long I1 resulted in very similar level of activity in LN4 (I1-5: 0.476±0.4; I1-80: 0.476±0.5). This may be due to the fact that the first two pulses of I1-5 act as a prolonged sound pulse and LN4 responded to this chirp as a two-pulse chirp. This response is supposed to be lower than that evoked by a reference chirp containing two 20 ms sound pulses since the first two sound pulses resulted in a more pronounced inhibition than a single 20 ms pulse. For I1-80, the first inhibition, although far from the other two pulses, still had an effect on the subsequent responses. Even though with two 20 ms pulses at the end, I1-80 only elicited a lower response than a reference chirp. Therefore, the neuronal background is different even though I1-5 and I1-80 gave the same level of activity in LN4.

I also conducted a more detailed analysis into the response of LN4 towards each sound pulse within the I1-chirps (Fig. 21D). The first pulse (P1) always elicited an inhibition and is not included. The response to P2 increased from 0.6±0.2 AP to 1.6±0.2 AP as interval I1 increased from 5 ms to 20 ms, which shows a delayed increase in activity as compared to the tuning of the phonotactic behaviour. When the I1-interval was between 25 ms to 40 ms, LN4 responded to P2 with the same number of spikes i.e. 2.0±0.3 AP/pulse for all three chirps,

different to the decline of the behaviour. Its response to P2 then decreased to 1.4±0.2 AP for I1-50 and 1.2±0.3 AP for I1-80 (Fig. 21D), in line with a decrease of phonotaxis.

Considering the third pulse (P3) LN4 activity increased from 1.4±0.4 to 2.6±0.2 AP/pulse from I1-5 to I1-20 (Fig. 21D) and the tuning curve between I1-5 and I1-20 perfectly matched the behavioural tuning. Same to the behavioural tuning, the peak neuronal response occurred at I1-20 and then dropped towards I1-25 with 1.8±0.2 AP/pulse. With increasing I1 the LN4 activity decreased to 1.4±0.2 (I1-40) AP/pulse and then gradually declined to 0.8±0.2 AP/pulse at I1-80. Overall, the LN4 response to P3 gave a very good match to the behaviour; the activity peak was more salient and the decrease of activity for longer intervals was more pronounced as for the tuning curve from P2 (Fig. 21D). These results indicate that the overall tuning of the feature detector LN4 came mostly from the response elicited by P3, while the response to P2 rather may blur the overall tuning.

The consequences of changing the I1 interval in the pattern recognition process

The response patterns of the individual neurons allow a more comprehensive understanding of the processing within the circuit. Here I compare the tuning curves of the five neurons and I align the responses of all the neurons for the I1-test to analyse the flow of information. I want to point out that these recordings have been obtained in different experiments.

For the comparison of the tuning curves, I normalized the activity of each neuron to its activity elicited by a 'normal chirp' and plotted the curves as in Fig. 22A. AN1 and LN2 did not show any filtering property to changes in I1, whereas both LN3 and LN4 exhibited band-pass filtering with a peak response at I1-20. Both the tuning of LN3 and LN4 overall fit the phonotactic behaviour, while LN4 showed a slightly sharper tuning to changing I1 compared to LN3, which becomes obvious when I1 was smaller than 20 ms and larger than 40 ms. In summary, in response to changes of the first interval I1 the activity of AN1 and LN2 just copy the pattern, while the responses of LN3 and LN4 become sharper and better tuned, which was also reported by Schöneich et al. (2015) for tests of pulse periods.

The aligned I1-test responses of the five neurons are shown in Fig. 22B and provide evidence, how the auditory activity is subsequently processed within the delay-line and coincidence detector circuit. I will focus on the short, medium and long I1, as they correspond to critical parts of the phonotactic tuning. For short I1, the response of AN1 to P1 and P2 is not clearly separated (Fig. 22B). This prolonged AN1 response is forwarded to LN2 and LN3

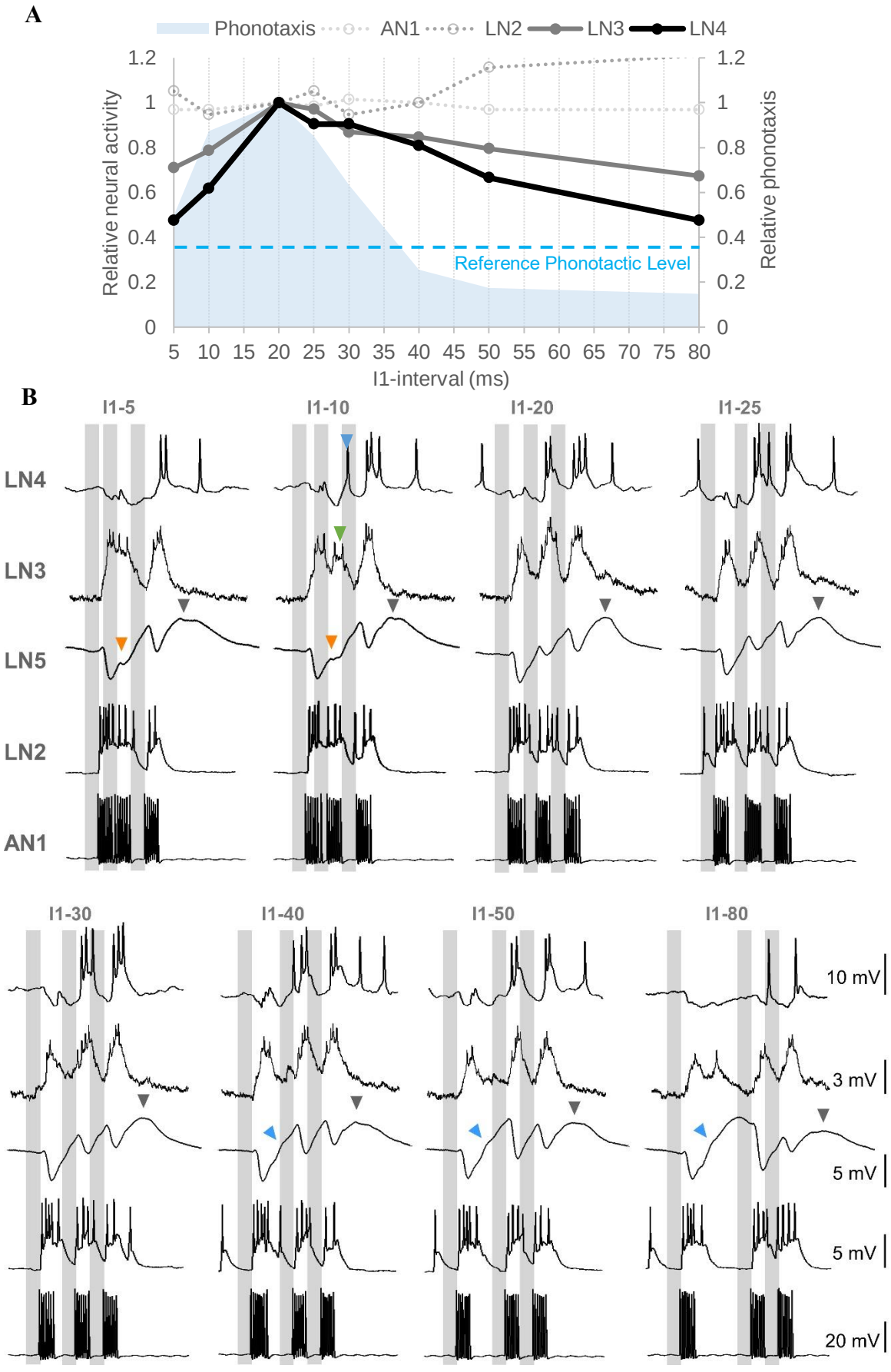

Fig. 22 Sequential filtering to varied 1st interval (I1 test) by the pattern recognition circuit.

Fig. 22 Sequential filtering to the I1-interval by the pattern recognition circuit. A. The tuning curves of the spiking neurons (AN1, LN2, LN3 and LN4) in the pattern recognition circuit and the phonotactic response. The responses elicited by the normal chirp in the neurons and for phonotaxis were set as 1 and activity evoked by other chirps is calculated as the relative change compared to 1. The tuning curves of AN1 and LN2 are in dotted lines, they do not show any temporal selectivity. The tuning curve of LN3 is given in grey and of LN4 in black. The reference level indicates the phonotactic response elicited by a 2-pulses chirp. **B.** The recordings of LN4, LN3, LN5, LN2 and AN1 are aligned vertically to the sound pulses, sound pulses are shown as grey bars. The names of different chirps are given on top of each column. For LN4, LN3, LN2 and AN1, only one example recording is shown, for LN5, the traces are averaged from 14 recordings. Green arrowhead indicates the second burst of spikes in LN3 elicited by I1-10. Orange arrowheads indicate the premature rebound elicited by short I1. Blue arrowheads shown in I1-40, I1-50 and I1-80 tests indicate the deflection in the first rebound. Grey arrowheads indicate the peak of PIR3, the only completed rebound depolarization.

resulting in prolonged depolarisations and a burst of spikes in both neurons. The pronounced spiking activity in LN2 matches the pronounced inhibition in LN5, which starts the rebound although LN2 continues to spike. LN2 activity also matches the extended inhibition of LN4. In case of I1-5 the LN2 activity causes an inhibitory response of LN4 to P1 and P2, and the excitation from LN3 did not overcome this inhibition resulting in subthreshold compound EPSPs only. Only when the third response of AN1 coincides with the LN5 rebound following P2, is the overall excitatory input to LN4 strong enough to make it spike. As a consequence of short I1-intervals the feature detector LN4 responds mainly with inhibition and only with one clear burst of spikes to the third sound pulse (P3); this changes with increasing I1.

For medium I1 in the range from I1-20 to I1-30, AN1, LN2 and LN3 responded with clearly separated bursts of spikes to each sound pulse. LN5 showed a coupled oscillation of its membrane potential, which gradually build up over the time course of a chirp, as did the membrane potential of LN3. In response to P1, the excitation forwarded from LN3 to LN4 does not overcome the inhibition that LN4 receives from LN2, for P1 there is no coincidence of excitatory inputs from AN1 and LN5 at the level of LN3. Then the first and the second PIR of LN5 coincide with the second and the third response of AN1, respectively, which leads to a stronger spiking activity in LN3 to P2 and P3. At the level of LN4, these excitatory inputs from LN3 overcome the now weaker inhibition elicited by lower LN2 activity and result in two pronounced depolarisations and bursts of spikes. These two bursts of spikes seem to be the characteristic features of the LN4 response, correlated with the best phonotactic tuning.

As I1 increased from 40 to 80 ms, AN1 and LN2 still mirrored the sound pulses. The graded response of LN5 however decreased over a chirp, it became less regular and was dominated by the inhibition and rebound to the first pulse (Fig. 22B, I1-40 to I1-80). The depolarisation and spiking activity in LN3 decreased, which may be due to the coincidence between AN1 activity and the LN5 rebound, now occurring at different phases of the rebound. The decrease in the LN3 spiking response resulted in a reduction of the LN4 activity, and two smaller bursts of spikes occurred for I1-40 and I1-50. Finally, at I1-80, the first rebound in LN5 starts to repolarise before the second inhibition kicks in, and the second PIR has a low amplitude. The coincidence between AN1 and LN5 activity occurs on the falling phase of the first rebound. As the coincidence is out of phase LN3 activity is reduced, and the LN4 activity is dominated by the initial inhibition, followed by a minor spiking response. The substantial change in the LN5 response and the lack of pronounced activity in the feature detector LN4 are in line with

the low phonotactic response at long I1-intervals.

Response of the pattern recognition network neurons to chirps with different second intervals: I2-test

In this test paradigm the duration of the second interval (I2) was systematically varied, while the first interval (I1) and the duration of all pulses (P1-P3) was kept constant at 20 ms (Fig. 11). The behavioural data for systematic changes of I2, are similar to the responses obtained by changes of I1 (Fig. 9C). For long I2-intervals the phonotactic response however, is higher than for the I1-intervals and corresponds to the reference value of a 2-pulse chirp (Hedwig and Sarmiento-Ponce 2017). As in the description of the results for I1, particular focus will be given to short, medium and long I2-intervals, which represent different sections of the phonotactic behaviour during the test.

The number of recordings of the neurons are: 10 repeats of AN1 (N=5, n=10), 10 repeats of LN2 (N=2, n=10), 10 repeats of LN5 (N=4, n=10), 10 repeats of LN3 (N=5, n=10) and 5 repeats of LN4 (N=5, n=5) for the characteristic responses of the neurons elicited by 20-ms pulses and normal chirps, and 5 repeats of AN1 (N=5, n=5), 2 repeats of LN2 (N=2, n=2), 18 repeats of LN5 (N=4, n=18), 13 repeats of LN3 (N=5, n=13) and 5 repeats of LN4 (N=5, n=5) for the I2-test.

The ascending neuron – AN1

The ascending neuron AN1 forwards auditory information to the inhibitory neuron LN2 and the coincidence detector LN3 (Fig. 23A). Also, in the I2-test the activity of AN1 reliably copied the pulse pattern (Fig. 233B). The neuron responded to the 20 ms pulses with a consistent activity of 6.5±0.0 AP/pulse, spike activity lasted for 22.1±0.2 ms (n=10). Responses to the chirps had a latency of 18.9±0.1msand all chirps led to a very similar number of spikes ranging from 20.7±0.5 to 21.7±0.5 AP/chirp (Fig. 23C), which did not significantly differ across the I2-test (p=0.2918, Friedman test, N=5, n=5). All of the chirps elicited three clear bursts of spikes, even for I2-5 the second and third burst of spikes were separated by a short interval. Again, the tuning curve of AN1 did not match the behavioural tuning, indicating a lack of temporal filtering of sound patterns at this stage (Fig. 23C).

The inhibitory neuron – LN2

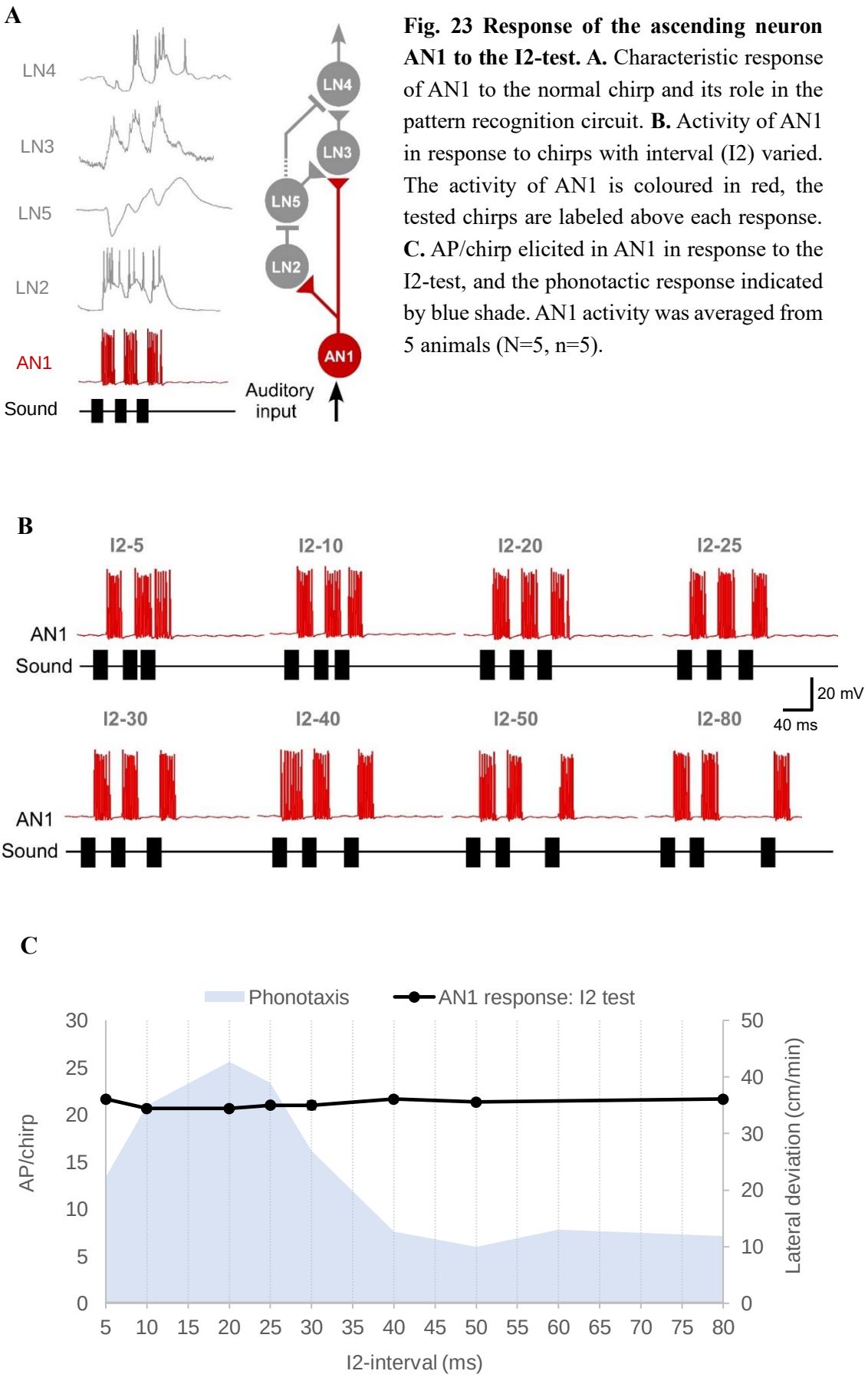

Fig. 23 Response of the ascending neuron AN1 to the I2-test. A. Characteristic response of AN1 to the normal chirp and its role in the pattern recognition circuit. **B.** Activity of AN1 in response to chirps with interval (I2) varied. The activity of AN1 is coloured in red, the tested chirps are labeled above each response. **C.** AP/chirp elicited in AN1 in response to the I2-test, and the phonotactic response indicated by blue shade. AN1 activity was averaged from 5 animals (N=5, n=5).

The inhibitory neuron LN2 is driven by AN1 and inhibits the non-spiking neuron LN5 and the feature detector LN4 (Fig. 24A). The general features of the LN2 response are highly similar to the I1-test. For all chirps the response to the first sound pulse (P1) was a pronounced depolarisation, which elicited 4.4±0.2 AP/pulse. The depolarisation only gradually decayed and always merged with the depolarisation elicited by the second pulse (P2).

In response to short I2-intervals (I2-5 or I2-10) and for I2-20 the response to P1, P2 and P3 fused, and formed an extended excitatory activity, spikes occurred on this maintained depolarization (Fig. 24B). Also, when stimulated with chirps from I2-25 to I2-80 the response to P1 and P2 merged to a pronounced depolarisation and spike activity, due to the prolonged excitatory response elicited by the first sound pulse. While I2 was increased over 25 ms, P2 elicited 2.6±0.2 AP/pulse and the depolarisation elicited by P2 returned to the resting potential before the response to the third sound pulse (P3) occurred. The response to P3 became a separated pronounced depolarisation, with a burst of 3.0±0.4spikes (Fig. 24B, I2-50 and I2-80).

The number of spikes in LN2 caused by the I2-chirps remained very similar across the test and did not correspond to the tuning of the behaviour. The minimum occurred at I2-5 with 7.48 AP/chirp while the maximum was at I2-80 with 9.68 AP/chirp (Fig. 24C). Overall, LN2 responded to I2-chirps with only 60.05±1.04% of the number of spikes elicited in AN1 (AN1: 21.2±0.1 AP/chirp; LN2: 8.5±0.2 AP/chirp). In summary in these recordings, LN2activity transformed the well-timed excitatory input from AN1 to a rather broad excitatory response, but it did not match the behavioural tuning for the I2-test (Fig. 24C).

The non-spiking neuron – LN5

The non-spiking delay-line neuron LN5 forwards a delayed excitation to the LN3 interneuron (Fig. 25A). Its characteristic response to the normal chirp has been described before (Fig. 16), and the corresponding diagram is shown in Fig. 25B.

There are some general features in the responses to the I2-test: 1. All three PIRs (Fig. 25C) elicited by each chirp reached above the resting potential. 2. Same as in I1-test, the third rebound (PIR3) of LN5 was completed without a cut-off from inhibition. Therefore, the peak of PIR3 (Fig. 25C, grey arrows) comes from intrinsic LN5 properties rather than being determined by an inhibition as for PIR1 and PIR2. 3. The timing of the first 2 sound pulses is identical for all chirps of the I2-test. Therefore, the first two inhibitory responses (INH1 and INH2) and two post-inhibitory rebounds (PIR1 and PIR2) were identical across the I2-test. In

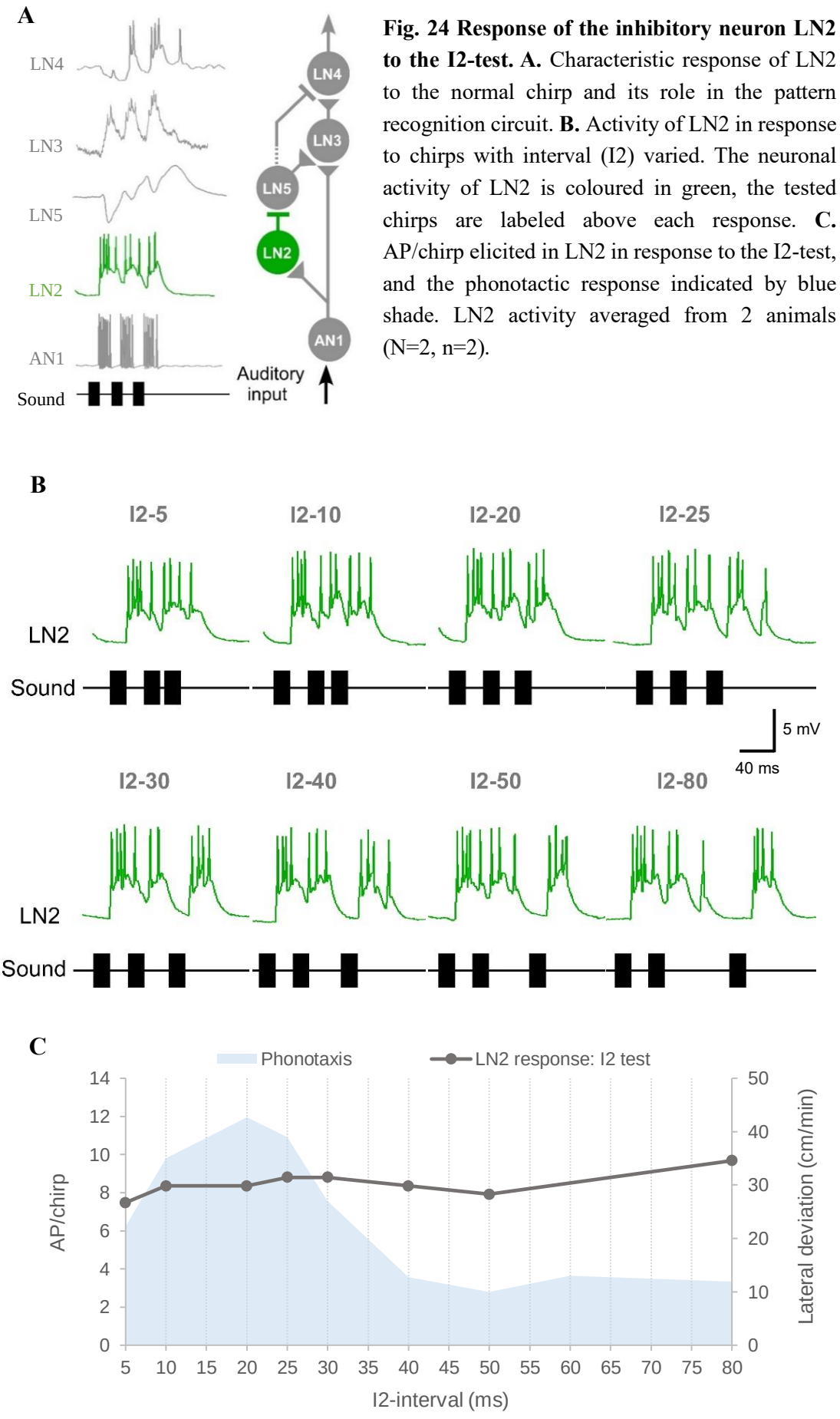

Fig. 24 Response of the inhibitory neuron LN2 to the I2-test. A. Characteristic response of LN2 to the normal chirp and its role in the pattern recognition circuit. **B.** Activity of LN2 in response to chirps with interval (I2) varied. The neuronal activity of LN2 is coloured in green, the tested chirps are labeled above each response. **C.** AP/chirp elicited in LN2 in response to the I2-test, and the phonotactic response indicated by blue shade. LN2 activity averaged from 2 animals (N=2, n=2).

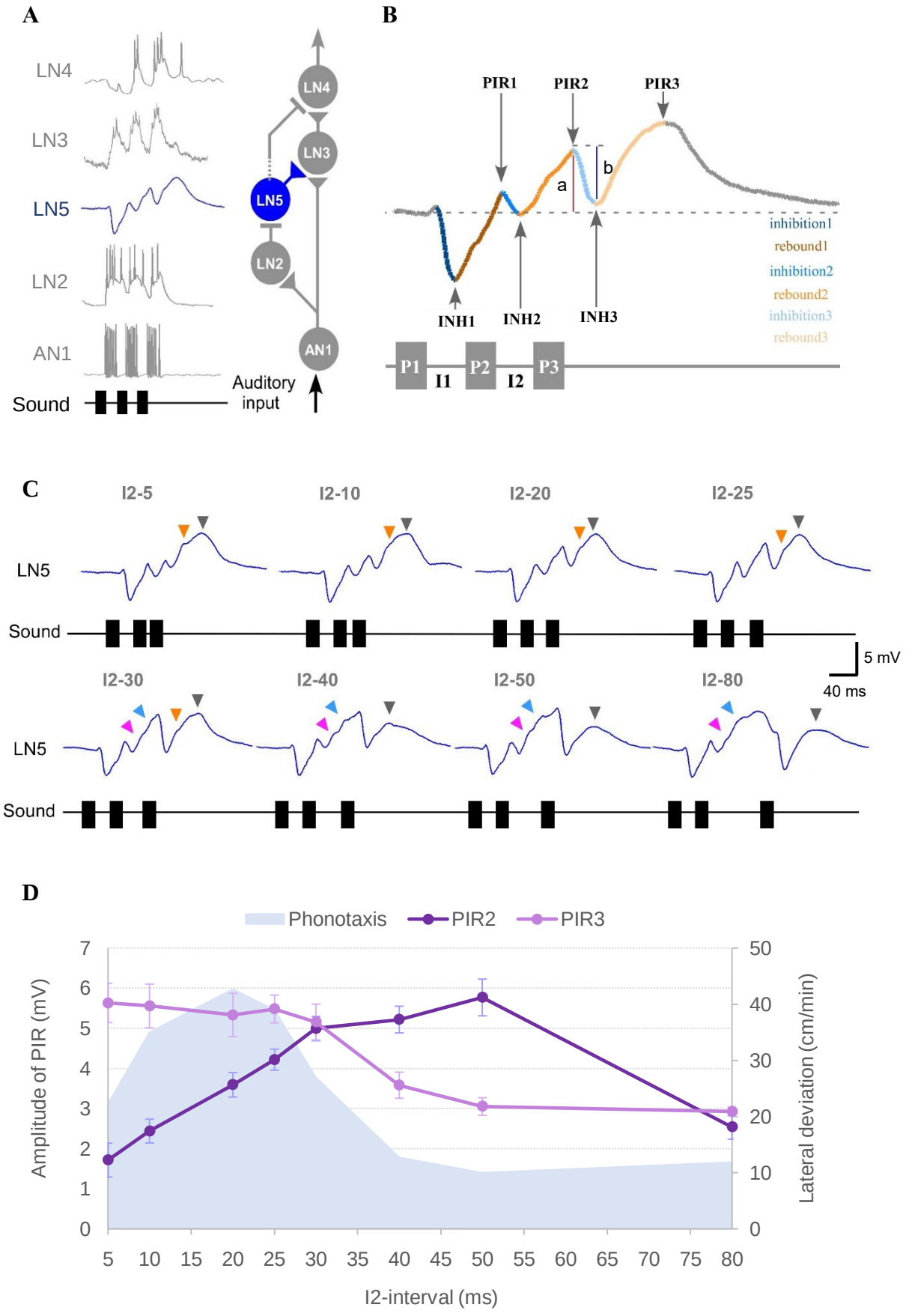

Fig. 25 Activity of LN5 elicited by I2-test and the tuning of the amplitude of PIRs.

Fig. 25 Activity of LN5 elicited by the I2-test and the tuning of the amplitude of PIRs. **A.** Diagram showing characteristic activity of LN5 to the normal chirp and its role in the pattern recognition circuit. **B.** Activity elicited in LN5 in response to a normal chirp. P1, P2 and P3 represent the three sound pulses, I1 and I2 refer to the two intervals. LN5 responds to the three pulses with three inhibitions (inhibition1, inhibition2 and inhibition3) and three rebounds (rebound1, rebound2 and rebound3). The maximum amplitudes of the inhibitions are labelled as INH1, INH2 and INH3. The highest membrane potential of rebound1 (brown) and rebound2 (orange) is reached at the start of the following inhibition (blue and light blue) and marked as PIR1 and PIR2. The peak amplitude of rebound3 (light yellow) is labelled as PIR3. **C.** Average responses of LN5 to the I2-test (N=4, n=18). The activity of LN5 is colored in blue, the names of the chirps are given above each recording. Orange arrowheads represent a deflection generated in rebound3 in response to I2-5, I2-10, I2-20 and I2-30. Blue and pink arrowheads represent the change in the dynamics during rebound1 in response to I2-30, I2-40, I1-50 and I1-80. Grey arrowheads indicate the peak of the last post-inhibitory rebound (PIR3), which is the only complete rebound. **D.** Maximum amplitude of the rebounds over the I2-test. The PIR2 and PIR3 are colored in dark to light purple. The data are averaged from 10 recordings. Error bar indicates the standard error mean (SEM). Phonotactic response is in blue shade.

response to P1 the latency of the start of the inhibition was 26.4±0.2 ms. The membrane potential then decreased and reached its minimum of -6.5±0.1 mV for INH1 at 36.4±0.5 ms after the onset of the sound pulse P1. In the subsequent rebound the membrane potential depolarised and reached a peak amplitude of 1.9±0.2 mV at PIR1 with a latency of 25.7±0.5 ms after P2 (Fig. 25C). The subsequent responses of LN5 depended on the duration of the I2-interval between P2 and P3.

For I2-5 the rebound PIR2 was rather weak and reached a peak of 1.7±0.4 mV above the resting potential at 23.8±0.4 ms after the onset of the third sound pulse (Fig. 25C), whereas for I2-10 the amplitude increased to 2.4±0.3 mV. The subsequent third inhibition (INH3) reached an amplitude of 1.0±0.4 mV (I2-5) and 1.8±0.3 mV (I2-10) and did not go below the resting potential. For both I2-5 and I2-10 the final third rebound (PIR3) reached a maximum of 5.6±0.5 mV at 63.5±2.5 ms after the onset of the third sound pulse and then gradually decayed over 115.4 ms (I2-5) and 107.5 ms (I2-10). During the rising phase of the third rebound a slight deflection in the membrane potential occurred, which may indicate an additional input to LN5 involved in generating the rebound (Fig. 25, I2-5, I2-10, orange arrowheads). Two features are relevant for these responses: 1. For short I2 the PIR2 was not well expressed and its peak was lower than PIR1. 2. A deflection in the membrane potential occurred during the generation of the third rebound (PIR3).

Over medium I2 (I2-20 - I2-30)the PIR2 increased to 3.6±0.3 (I2-20), 4.2±0.3 (I2-25) and 5.0±0.3 (I2-30) mV and was always higher than PIR1 (Fig. 25C). Also, INH3 was more pronounced and reached 2.8±0.3, 3.6±0.3 and 5.5±0.3 mV, respectively. PIR3 then climbed to an even higher amplitude than PIR2 and peaked at 5.3±0.5 (I2-20), 5.5±0.3 (I2-25) and 5.0±0.3 (I2-30) mV. These high amplitudes of INH3 and PIR3 resulted from a continuous build-up of the LN5 membrane potential over the course of the chirps, although the amplitude of PIR3 (5.2±0.5 mV) was only slightly higher than PIR2 (5.0±0.3 mV). The main feature of the LN5 response to medium I2 is the continuous build up in membrane potential over the three successive PIRs.

Some substantial changes in the activity of LN5 occurred in response to long I2 (I2-40 to I2-80). With increasing I2 the PIR2 increased in amplitude and reached 5.2±0.3 (I2-40), 5.8±0.5 (I2-50) and 5.67 (I2-80) mV. Especially PIR2 for I2-80 was well pronounced, it reached its maximum at 96.0±1.0 ms after the onset of the second sound pulse and started to decline before the subsequent inhibition INH3 kicked in. Some deflections of the membrane potential,

which are not directly linked to the timing of the sound pulses, occurred during the second rebound at 47.0±0.7 and 76.9±1.0 ms after the onset of P2 (Fig. 25C, I2-40 and I2-50, pink and blue arrowheads). For long I2, INH3 reached an amplitude of 5.2±0.3, 6.8±0.5 mV, and 5.3±0.3 mV, respectively. Over the course of the chirps the three PIRs did not increase in amplitude, and the highest amplitude occurred for PIR2.The subsequent PIR3 was considerably lower and reached 3.6±0.3, 3.1±0.2, and 2.9±0.1mV, respectively. The response of LN5 to long I2 shows 3 features: 1. PIR2 had the highest rebound amplitude. 2. There was no continuous build-up of the membrane depolarisation over a chirp. 3. Deflections in the membrane potential occurred during the build-up of the second rebound (PIR2).

Over the whole I2-test two characteristics of the LN5 activity may be noteworthy: At the normal chirp pattern (I2-20) the membrane potential showed a very regular oscillation and build up in the rebound response. This activity pattern, however, became strongly distorted for short (I2-5) and long (I2-80) I2-intervals.

For a quantitative analysis I plotted the amplitudes of PIR2 and PIR3 over the I2-test (Fig. 25D). As INH1, PIR1, and INH2 were not affected by changing I2 these are not considered. As I2 increased from 5 to 30 ms, the amplitude of PIR2 steeply increased from 1.7±0.4 to 5.0 ±0.3 mV with a slope of m=0.1276 mV/ms (R^2=0.99975) (Fig. 25D). For I2 increasing further from 30 ms to 50 ms PIR2 increased gradually from 5.0±0.3 to 5.8±0.56 mV with a lower rate (m=0.0388 mV/ms, R^2=0.9422) and with I2 reaching 80 ms it levelled off at 2.5±0.3 mV (Fig. 25D). The initial steep increase in PIR2 may be in line with the increase of the behavioural response, but for longer I2 the LN5 activity rather shows an opposite effect.

The amplitude of PIR3 was at a high level for short I2, it slightly decreased from 5.5 mV at I2-5 to 5.2±0.4 mV at I2-25 ms. It then fell to 3.1±0.2 mV when I2 was 50 ms and remained at this level with 2.93±0.12 mV at I2-80 (Fig. 25D). Over the whole I2-test the PIR3 amplitude thus qualitatively matched the phonotactic tuning, it was high for I2-5 to I2-25 and low for long I2, corresponding to phonotactic response (Fig. 25D).

The detailed effect of changing I2 on the inhibitory and post-inhibitory response of LN5 can be demonstrated by superimposing the membrane potential changes in respect to the first or last sound pulse (Fig. 26A, B). When aligned to the beginning of the I2-chirps, the highly similar response to P1 and P2 becomes obvious, as INH1, PIR1 and INH2 all have a very similar time course (Fig. 26A). With increasing I2 the amplitude of the second post-inhibitory rebound

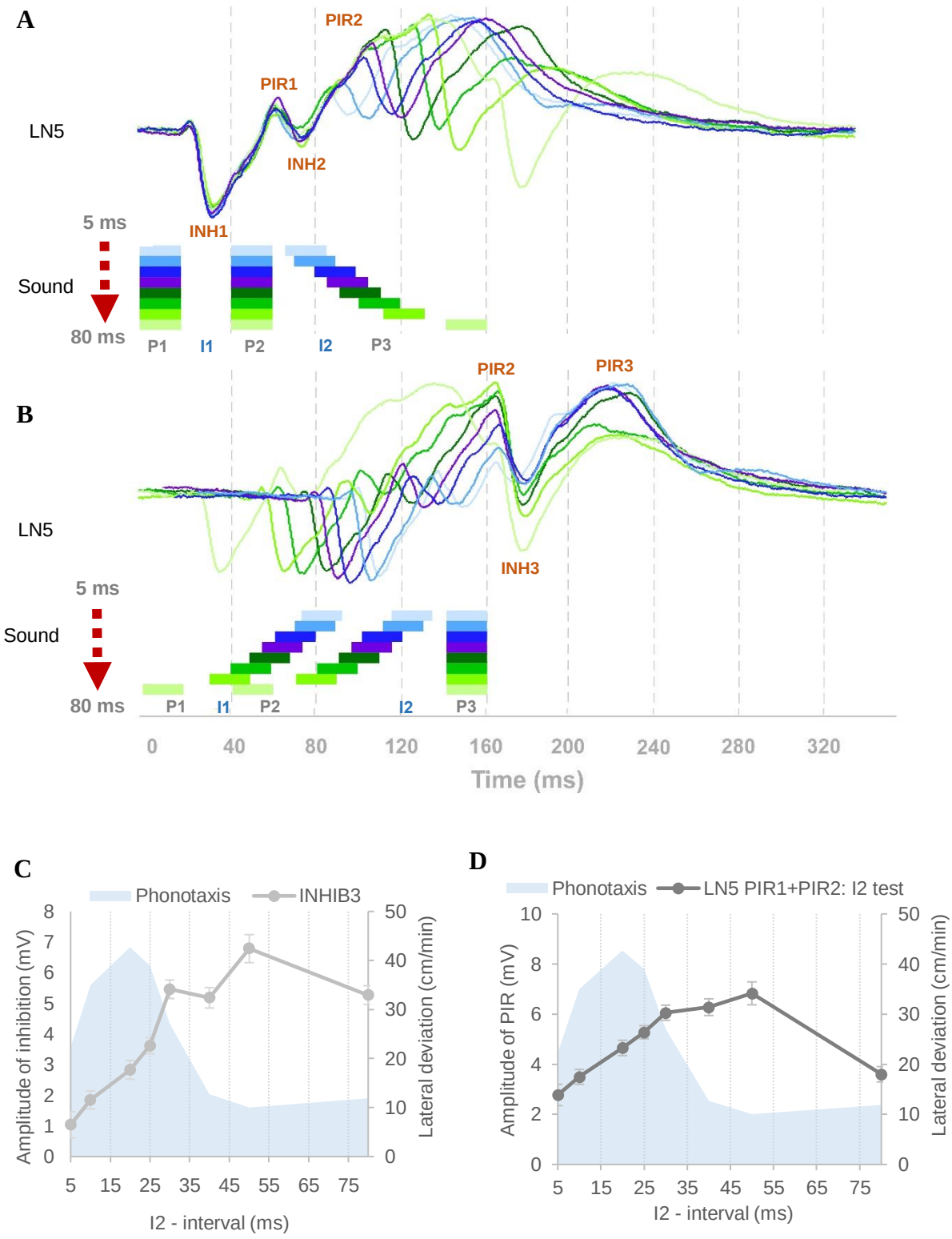

Fig. 26 LN5 activity elicited by I2-test aligned to the first or the last sound pulses and the tuning curves of inhibitions and summed PIRs.

Fig. 26 LN5 activity elicited by I2-test aligned to the first or the last sound pulse and the tuning curves of inhibitions and summed PIRs. A. Averaged LN5 activity in response to I2-chirps aligned to the onset of P1. **B.** Averaged LN5 activity in response to the I2-chirps aligned to the onset of P3. When interval I2 is smaller than 30 ms, the chirps and LN5 responses (I2-5, I2-10, I2-20 and I2-25) are colored as light to dark blue and purple, respectively. For I2 equal to or larger than 30 ms, chirps and LN5 (I2-30, I2-40, I2-50 and I2-80) are colored as dark to light green, respectively. Responses in dark blue and purple are to chirps I2-20 and I2-25 that elicit the best phonotactic behavior. Each response is averaged from 14 recordings. **C.** Maximum of INH3 over the I2-test, colored in grey. **D.** Sum of PIR1 and PIR2 over the I2-test. The data are averaged from 10 recordings. Error bar indicates the standard error mean (SEM). Phonotactic response is in blue shade.

(PIR2) becomes larger and extended, as it is cut off by the subsequent INH3 at a later time. It also shows deviations in its rising phase. The amplitude of INH3 also increases, while the amplitude of PIR3 declines with increasing I2, although its time course remains very similar (Fig. 26B, C). The summed amplitude of PIR1 and PIR2 shows an increase over the I2-interval from 5 to 50 ms, and when I2 further increased to 80 ms the summed amplitude drops (Fig. 26D). Neither INH3 nor the summed PIR amplitudes however, reveal a coupling to the behavioural tuning.

The change in the peak amplitude of the PIRs over the course of the I2-chirps was strongly affected by the duration of I2 and four chirps were chosen for comparison to highlight the effect (Fig. 27). In response to I2-5, the increase in amplitude from PIR1 to PIR2 was low, and the increase from PIR2 then stronger to PIR3 (Fig. 27A). In response to the normal chirp, the amplitude of the three PIRs continuously increased (Fig. 27B). For I2-50, the amplitude of the rebounds increased from PIR1 to PIR2 and then dropped with PIR3. Finally, for I2-80, the increase from PIR1 to PIR2 was similar to I2-50, however the decrease to PIR3 was even more pronounced (Fig. 27C, D). Additionally, from I2-5 to I2-80 the PIR2 became more and more pronounced and finally dominated the LN5 response. These results demonstrate that chirps containing long I2 elicit a very different membrane potential dynamic when compared to the normal chirp. Whereas chirps with short I2 exhibited more similar oscillations of the membrane potential to that generated by the normal chirp. These features of LN5 activity may be linked to the different phonotactic responses, which were close to the maximum for I2-5 but were low and corresponded to the reference level for long I2.

The trend of the change in the peak amplitude of the three PIRs in response to the chirps of the I2-test was quantitatively analysed using the same approach described for the I1-test (see I1-test). The average slope of the PIRs (Fig. 28) remained at a similar level when I2 was between 5 and 25 ms, it then decreased as I2 increased from 25 to 50 ms and stayed at a low level until I2-80. The result reveals that the gradual increase of the underlying depolarisation that drives the membrane depolarisation of LN5 over the I2-test overall matches the behavioural tuning curve, besides the response to very short I2-intervals (Fig. 28). This result also indicates that this tuning of LN5 is based on an accumulating effect of the three sound pulses.

The coincidence detector – LN3

The coincidence detector neuron LN3 is driven by a direct input from AN1 and the delayed

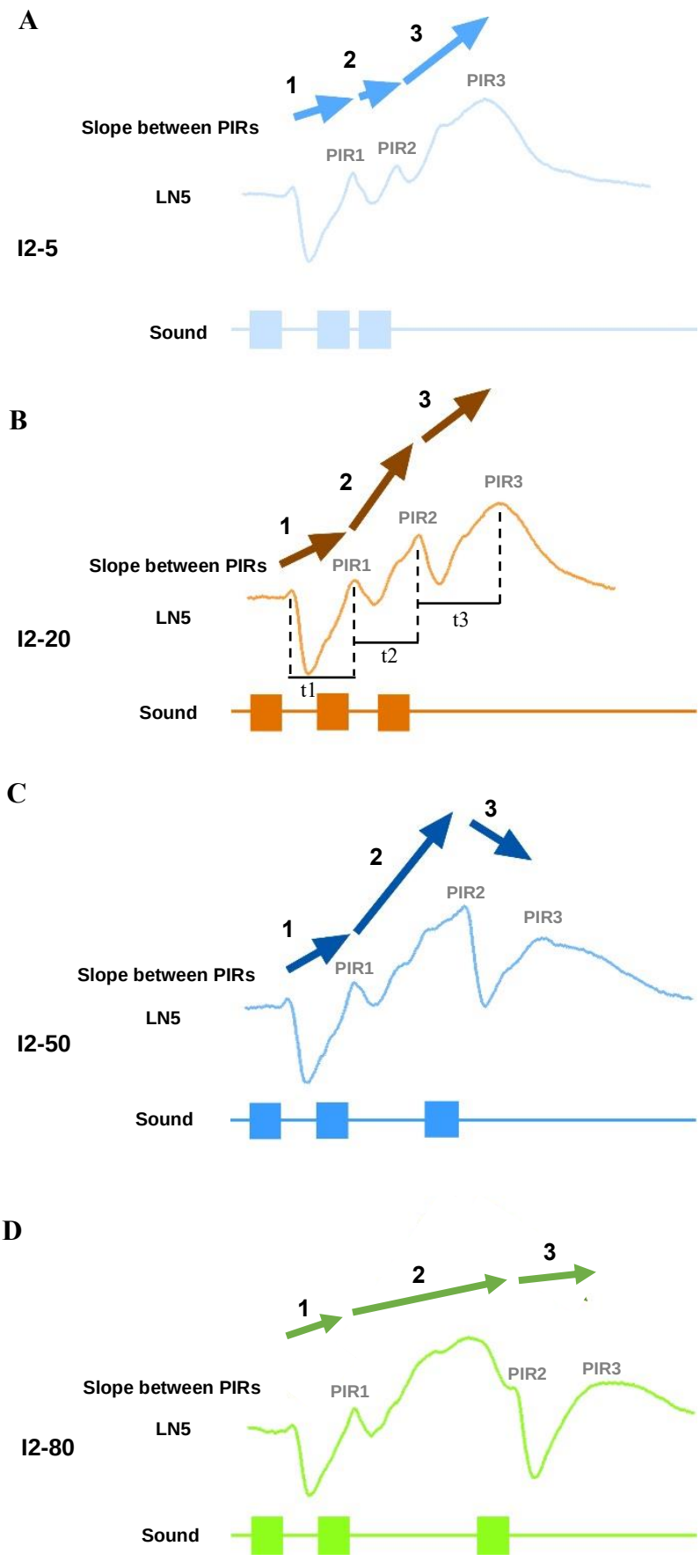

Fig. 27 The changes in the amplitude of adjacent PIRs over time (slope between PIRs) in I2-test.

Fig. 27 The changes in the amplitude of adjacent PIRs over time (slope between PIRs) in I2-test. The changes in the maximum amplitude of adjacent rebounds over time in response to four example chirps (I2-5, I2-20, I2-50 and I2-80) of the I2-test. The arrows indicate the changes between two adjacent peaks of the rebounds over time between the two PIRs (t1, t2 and t3) which is referred to as slope1, slope2 and slope3. The slope1 and slope2 elicited by each chirp were directly influenced by varying interval I2. Data are averaged from 10 recordings.

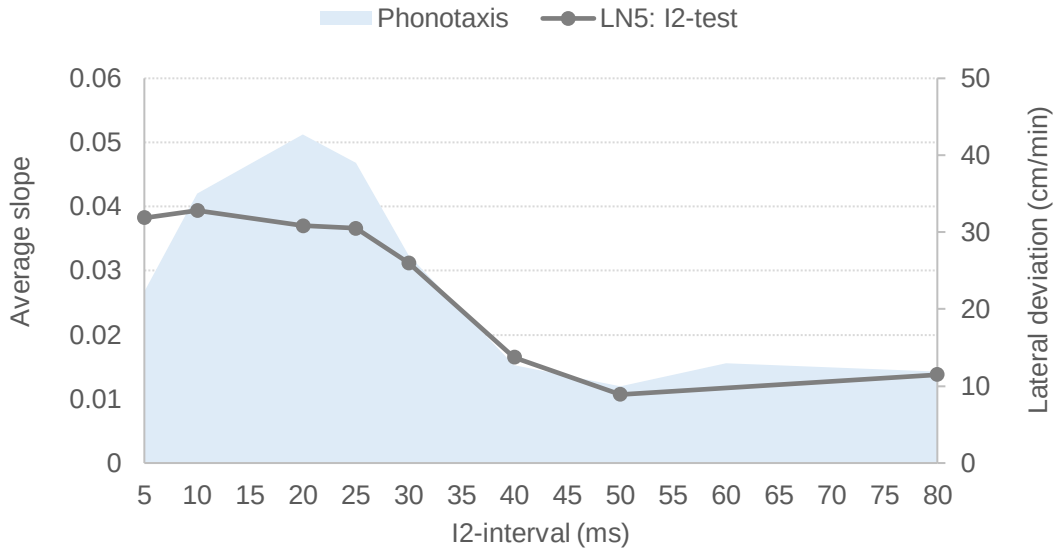

Fig. 28 The tuning of the average 'slope' of LN5 in the I2-test. The curve is based on averages of slope1, slope2 and slope3 in response to each chirp of the I2-test. Data are averaged from 10 recordings. The phonotactic response is in blue shade.

input from LN5 (Fig. 29A).The first two sound pulses (P1, P2) and the first interval (I1) were identical across the I2-test, therefore the response to P1 was similar with 2.9±0.0 AP/pulse for all I2-chirps, whereas P2 always elicited a stronger response with 3.8±0.1 AP/pulse (Fig. 29B). LN3 responded to the I2-chirps with9.4±0.4 AP/chirp after a latency of 23.2±0.4ms. Following the bursts of spikes, LN3 sometimes showed a graded depolarisation as a consequence of the input derived from PIR3 of the LN5 responses (Fig. 29, blue arrowheads). Also when the I2-interval was longer than 40 ms, a graded potential emerged following the second burst of spikes as a consequence of PIR2 (Fig. 29, orange arrowheads). Overall the average spike activity to all chirps in I2-test of LN3 was 55.70±2.11 % lower than the activity in AN1 (AN1: 21.2±0.1 AP/chirp vs LN3: 9.4±0.4 AP/chirp). The detailed characteristic responses of LN3 to the normal chirp was already described in the I1-test.

When stimulated with short I2 (I2-5) LN3 activity showed only two pronounced depolarisations and two bursts of spikes, as the response to the second (P2) and the third (P3) sound pulses merged to one suprathreshold depolarisation with 5.0±0.3 APs (Fig. 29B). In response to I2-10 the neuron generated separated depolarisations to P2 and P3, with P2 eliciting 4.0±0.0 AP and P3 a lower response of 2.2±0.4 AP. For both chirps the membrane depolarisation did not repolarise between the stimuli and outlasted the stimulus.

Also, in response to medium I2 (I2-20 to I2-30) did the membrane potential maintain a depolarised state over the whole chirp (Fig. 29B) and did not return to the resting level between the responses. The spike activity elicited by the second pulse (I2-20: 4.2±0.2 AP; I2-25: 3.8±0.2 AP; I2-30: 3.4±0.5 AP) was similar to the activity by the third sound pulse (I2-20: 4.0±0.0 AP; I2-25: 4.2±0.2 AP; I2-30: 3.8±0.3 AP).Only for long I2 (I2-40 to I2-80) did the membrane potential after the response to P2 gradually return to the resting potential. Spike activity elicited by P2 (I2-40: 3.6±0.2 AP, I2-50: 3.6±0.2 AP; I2-80: 3.4±0.5 AP) was in the mean slightly higher than activity by P3 (I2-40: 3.6±0.4 AP; I2-50: 3.2±0.3 AP; I2-80: 3.0±0.3 AP), although at I2-50 and I2-80 also P3 elicited a pronounced depolarisation following the first two responses.

The activity elicited by the different I2-chirps ranged from 8.0±0.6 AP/chirp (I2-80) to 11.0±0.0 AP/chirp (I2-20) and was significantly different between all chirps ($p<0.0001$, Friedman test, Tuckey, N=5, n=13).I plotted the LN3 activity (AP/chirp) over the I2-test to compare with the behavioural response (Fig. 29C). LN3 activity significantly increased from 8.1±0.3 to 11±0.0 AP/chirp as I2 was extended from 5 to 20 ms (I2-5 vs I2-20: $p<0.0001$; I2-10 vs I2-20: $p=0.0285$, Friedman test, Tuckey, N=5, n=13) (Fig. 29C). The increase was more

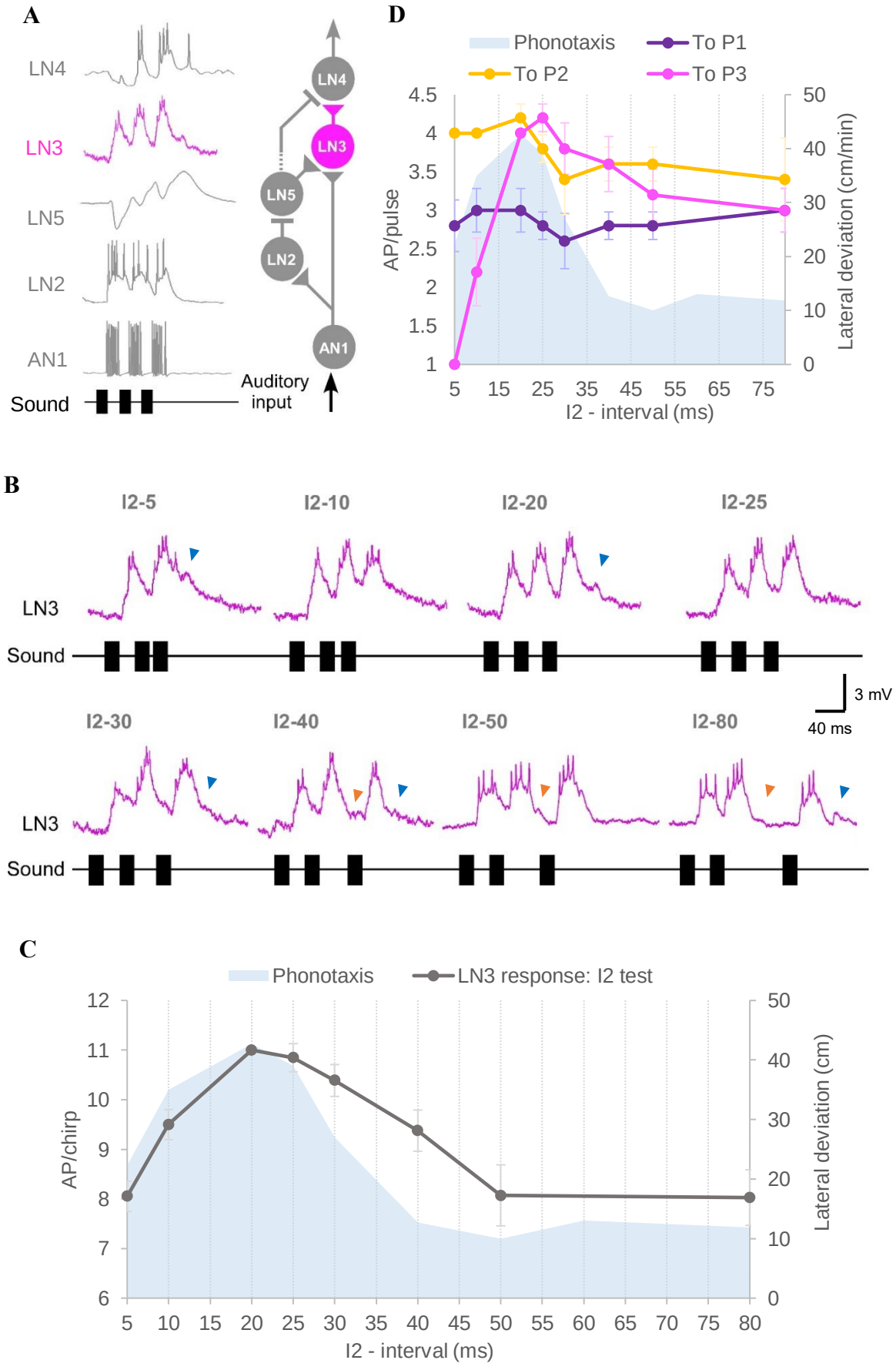

Fig. 29 Response of the coincidence detector neuron LN3 to I2-test.

Fig. 29 Response of the coincidence detector neuron LN3 to the I2-test. A. Characteristic response of LN3 to the normal chirp and its role in the pattern recognition circuit. **B.** Activity of LN3 in response to chirps with interval (I2) varied. The neuronal activity of LN3 is coloured in pink, the tested chirps are labeled above each response. Blue arrowheads indicate the lagging depolarization at the end of the third burst of spikes. Orange arrowheads indicate the depolarization following the second burst of spikes. **C.** AP/chirp elicited in LN3 in response to the I2-test (N=5, n=13), and the phonotactic response indicated by blue shade. **D.** AP/pulse elicited in LN3 by each pulse within a chirp of the I2-test (N=5, n=13). The number of spikes was averaged from 5 animals, 13 repeats. Error bars represent standard error means (SEM). Phonotactic response is in blue shade.

pronounced from I2-5 to I2-10 than from I2-10 to I2-20 and perfectly matched the phonotactic tuning to the I2-chirps within this range. LN3 activity was maximum at I2-20 and followed by a slight decrease to I2-25 ms, which again reflects the behavioural response (Fig. 29C). Activity then decreased to 8.1±0.6 AP/chirp at I2-50 ms, again qualitatively similar to the behavioural tuning, but with a slower rate. LN3 activity from I2-50 to I2-80 remained at its lowest level, closely matching the behavioural tuning. The response at I2-80 was significantly less than that elicited by the normal chirp (I2-80: 8.0±0.6 AP/chirp; I2-50 VS I2-20: p=0.0009; I2-80 vs I2-20: p=0.0003, Friedman test, Tuckey, N=5, n=13). Overall, the responses of LN3 to the I2-test showed band-pass shape and reflected the phonotactic tuning. The increase in LN3 activity from I2-5 to I2-20 was steeper with a slope of m=0.19 mV/ms (R^2=0.9684, Pearson correlation coefficient) than the decrease from I2-20 to I2-50 with a slope of m=-0.1002 (R^2=0.977, Pearson correlation coefficient). Only between I2-30 and I2-50 ms did the tuning of LN3 show a slightly slower decrease than the behavioural tuning. In summary, the LN3 tuning curve matched the behavioural tuning, however showed a slightly broader peak (Fig. 29C).

I explored whether the tuning of LN3 is based on an accumulating effect of the three sound pulses, and calculated the number of spikes in response to each pulse (P1-P3) and plotted this over the duration of I2 (Fig. 29D).The response to P1 ranged from 2.6±0.4 AP to 3.0±0.3 AP and did not show any significant difference across I2-tests (p=0.6059, Friedman test, N=5, N=13).The response to P2 was also similar across the I2-test, it slightly decreased from 4.2±0.2 AP at I2-5 to 3.4±0.5 AP at I2-80 (p =0.5121, Friedman test, N=5, n=13).The average response elicited by P2 was 31.64±3.0% stronger than the response evoked by P1 (P1: 2.9±0.0 AP and P2: 3.8±0.1 AP, p=0.0029, One-way ANOVA with repeated measures, Tuckey, N=5, n=13), and it was 15.7±9.9%stronger than the response to P3, while the response to P3 was 10.2±13% stronger than the response to P1. In comparison to the P1 and P2 tuning curves, the response to P3 showed a band-pass tuning qualitatively reflecting the phonotactic tuning (Fig. 29D). When I2 increased from 5 to 25 ms, activity increased from 1.0±0.0 AP/pulse to 4.1±0.1 AP/pulse, respectively, followed by a gradual decrease to 3.1±0.3 AP/pulse at I2-80 (p<0.0001, Friedman test, N=5, n=13). For short I2 of 5 to 10 ms, LN3 responded to P3 significantly weaker as compared to a ‘normal chirp’ when I2 was 20 ms (I1-5 vs I1-20: p=0.0012; I1-10 vs I1-20: p=0.0268, Friedman test, Tuckey, N=5, n=13). In summary the tuning curves for the different pulses (P1-P3) indicate that the overall tuning of LN3 (Fig. 29C) is mainly shaped by the response to the third sound pulse (P3), while the response to P1 may give the lowest contribution.

The feature detector – LN4

The feature detector neuron LN4 is driven by an inhibitory input from LN2 and an excitatory input from LN3 (Fig. 30A). During the recording some spontaneous spikes occurred not related to the acoustic stimuli (Fig. 30, grey arrowheads). The characteristics of LN4 sparse coding is reflected in its spiking response, which was 66.24±0.94% lower as compared to the activity of LN3, and 84.99±0.95% lower when compared to the activity in AN1 (LN4: 3.2±0.2 AP/chirp; LN3: 9.4±0.4 AP/chirp; AN1: 21.2±0.1 AP/chirp).

LN4 responded to the first two pulses (P1, P2) of all I2-test patterns in a very similar way; after P1 it generated an initial inhibition with a latency of 24.9±0.3ms, mixed with subthreshold EPSPs. This response was followed by a pronounced depolarisation and a burst of 2 spikes induced by P2 after a latency of 95.2±2.9 ms to the start of the chirp and 30.3±0.5 ms latency to the second sound pulse (Fig. 30B). Differences in LN4 activity emerged from the responses to the third sound pulse.

When LN4 responded to chirps with short I2 (I2-5 and I2-10) the depolarisation to the last two sound pulses P2 and P3 merged and the neuron generated one burst of spikes (I2-5: 2.8±0.4 AP/chirp; I2-10: 3.6±0.2 AP/chirp) followed by the fast repolarisation of the membrane (Fig. 30B). The duration of the depolarisation however was only 22.0±0.7 ms and did not represent the duration of both sound pulses. When stimulated with medium I2 (I2-20 to I2-30), P2 and P3 elicited two bursts of spikes, and activity elicited by P2 (I2-20: 1.8±0.2 AP, I2-25: 1.4±0.2 AP; I2-30: 1.4±0.2 AP) was lower than the activity elicited by P3 (I2-20: 2.2±0.2 AP; I2-25: 2.2±0.2 AP; I2-30: 2.0±0.0 AP). The duration of the depolarisation elicited by the second P2 or the third sound pulse P3 remained similar from I2-20 to I2-30. The third sound pulse, however, always elicited a longer depolarisation than the second sound pulse (P2: 18.6±0.7 ms; P3: 29.8±0.5 ms). In response to long I2-intervals (I2-40 to I2-80) the third pulse (P3) mainly failed to elicit a pronounced depolarisation, and rather caused an inhibitory response (see I2-80). As a consequence, for long I2-intervals neuron LN4 overall generated only one burst of spikes occurring in response to the second pulse P2.

I compared the LN4 activity (AP/chirp) and the phonotactic behaviour for the I2-test (Fig. 30C). The number of spikes elicited in LN4 increased from 2.8±0.4 to 4.0±0.3 AP/chirp as I2 increased from 5 ms to 20 ms, and activity increased with a slope of m=0.743 mV/ms(R^2=0.8622, Pearson Correlation Coefficient), matching the phonotactic tuning. From

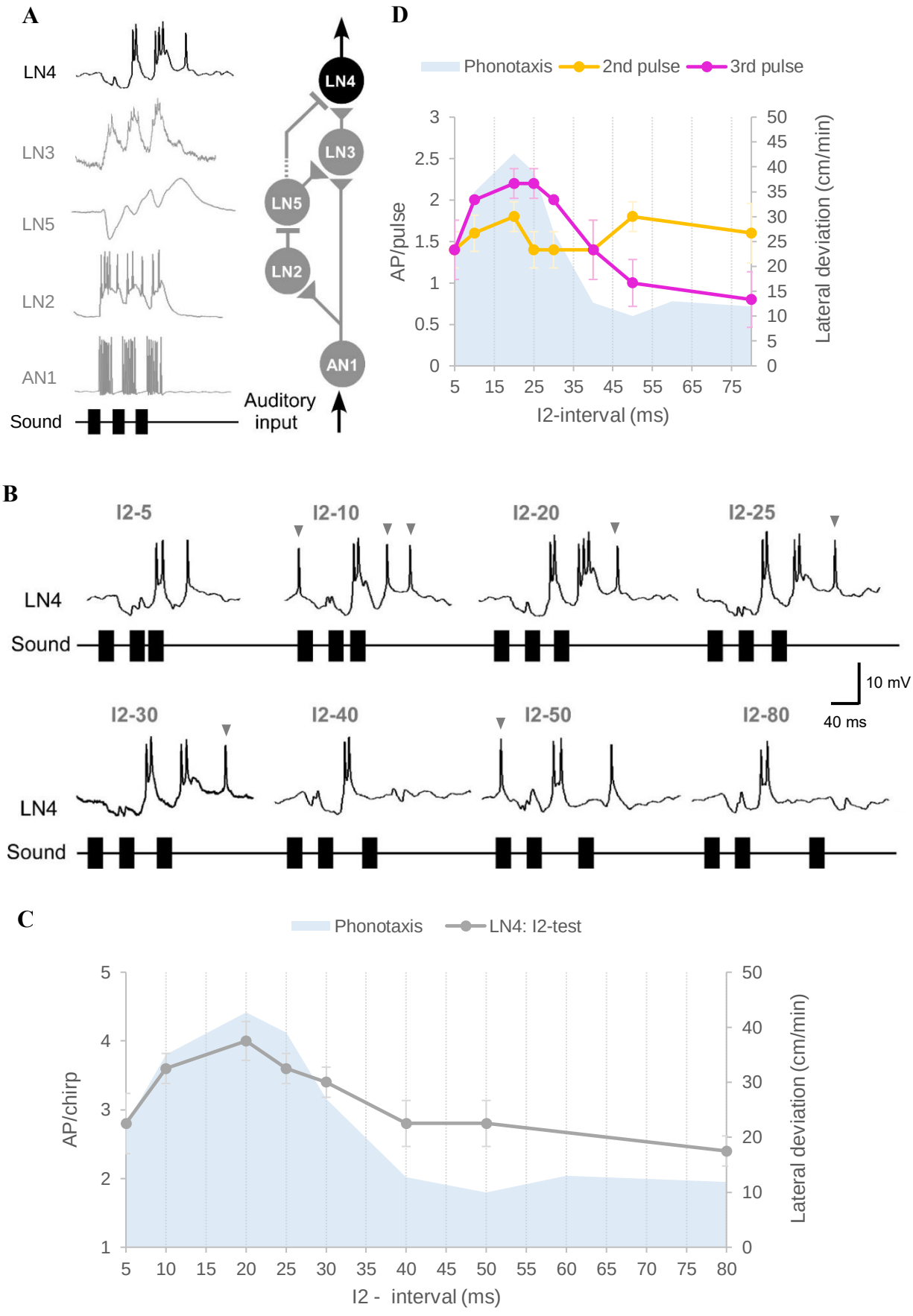

Fig. 30 Response of the coincidence detector neuron LN4 to I2-test.

Fig. 30 Response of the coincidence detector neuron LN4 to the I2-test. A. Characteristic response of LN4 to the normal chirp and its role in the pattern recognition circuit. **B.** Activity of LN4 in response to chirps with interval (I2) varied. The neuronal activity of LN4 is coloured in black, the tested chirps are labeled above each response. Grey arrowheads represent the spontaneous spikes. **C.** AP/chirp generated in LN4 in response to the I2-test, and the phonotactic response indicated by blue shade. **D.** AP/pulse elicited in LN4 by each pulse within a chirp in the I2-test. The number of spikes was averaged from 5 animals, 5 repeats. Error bars represent standard error means (SEM). Phonotactic response is in blue shade.

the peak at I2-20 to I2-40 the response gradually decreased to 2.8±0.3 AP/chirp with a slope of m=-0.38 mV/ms (R^2=0.9627, Pearson Correlation Coefficient), showing a slower rate compared to the reduction of the phonotactic response. Activity further decreased to its minimum with a slope of m=-0.2 mV/ms (R^2=0.75, Pearson Correlation Coefficient) to I2-80 ms with 2.4±0.2 AP/chirp, which was significantly lower that the response to I2-20 (I2-20 vs I2-80: p=0.016, Friedman test, Tuckey, N=5, n=5). The phonotactic response was flat and just at the reference level over this range (Fig. 30C). The phonotactic response to chirps with short I2 (5 ms) was stronger than to chirps with long I2 (80 ms). Similarly, the LN4 response to chirps containing short I2 was stronger than to chirps containing long I2 (I2-5: 1.4±0.4 AP/chirp; I2-80: 0.8±0.3 AP/chirp). Due to the sparse spiking activity of LN4, the maximum difference in the mean number of spikes elicited by chirps of the I2-test was only 1.6 spikes, but may be of functional significance. In summary, the tuning curve of LN4 for the I2-testshowed a band-pass tuning and matched the phonotactic response.

I conducted a more detailed analysis to reveal if the responses to P2 and P3 showed a similar tuning (Fig. 30D). In response to P2 neuron LN4 showed a very constant level of activity ranging from 1.4±0.2 AP to 1.8±0.2 AP over all tested I2-intervals, which did not match the phonotactic tuning. LN4 activity in response to P3 was more dynamic, the number of spikes increased from 1.4±0.4 to 2.2±0.2 AP/pulse as I2 increased from 5 to 25 ms (Fig. 30D), generally reflecting the increase in the phonotactic response. Spike activity reached a broad peak at I2-20 and I2-25 and then gradually decreased to 0.8±0.3 AP/pulse at I2-80. The decrease of the neuronal response reflected well the reduced phonotactic response occurring for long I2. In summary, the tuning curves for P2 and P3 indicate that the overall spike activity of LN4 in response to I2-chirps (Fig. 30C)is mainly determined by the response to the third sound pulse (P3), which depends on the preceding interval and elicits a burst of spikes only in the range of the normal interval durations.

The consequences of changing I2 in the pattern recognition process

The results above allow insight into the characteristic responses to the I2-test of each neuron and how this affects subsequent processing within the circuit. To compare the responses of the five neurons, I normalized their responses to the activity elicited by a ‘normal chirp’ and plotted the curves (Fig. 31A). AN1 and LN2 did not show any filter properties to the I2-test pattern, whereas both LN3 and LN4 exhibited band-pass filtering with peak response at I2-20. The tuning curves of LN3 and LN4 when I2 was equal to or smaller than 20 ms were very similar,

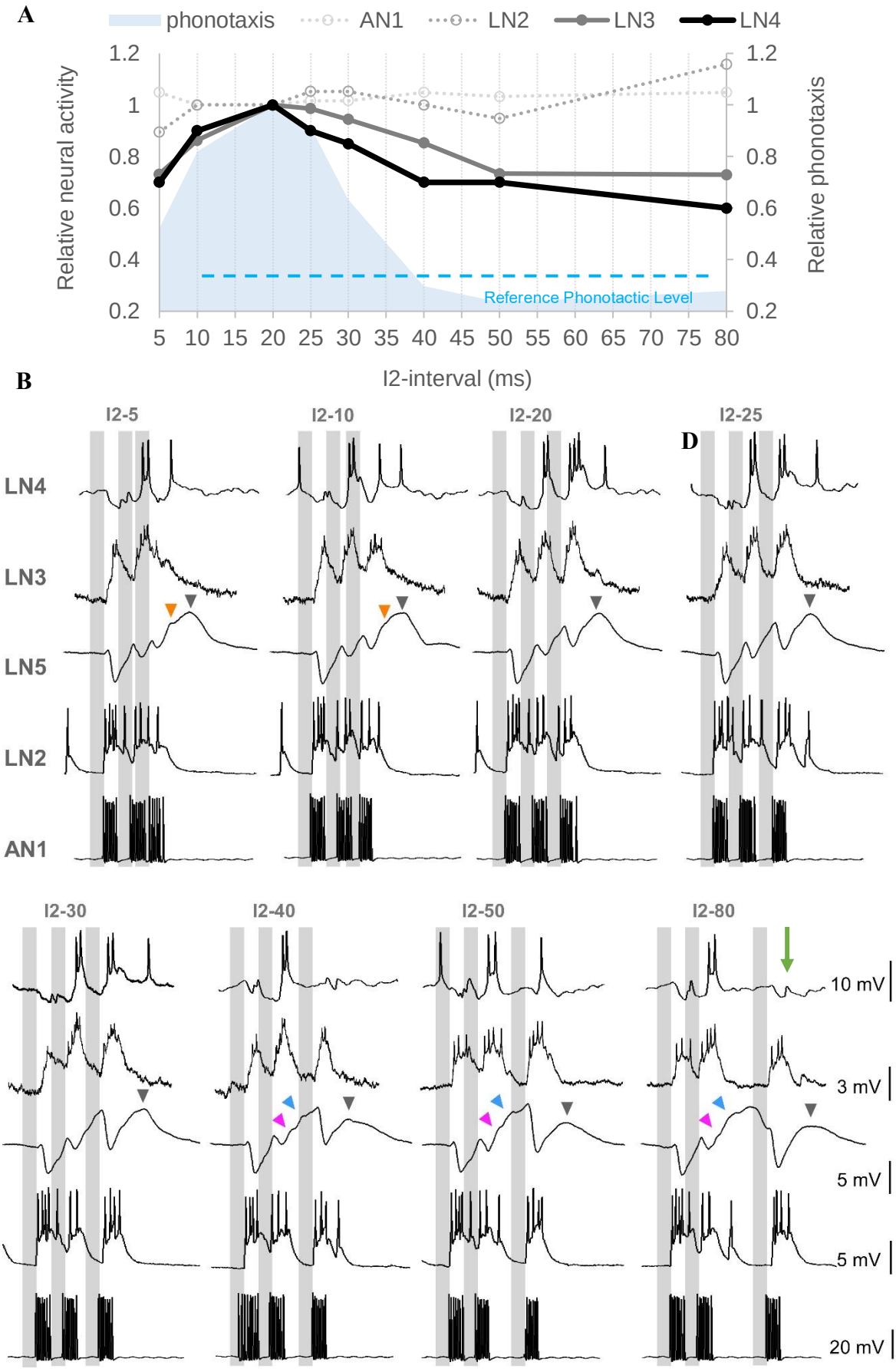

Fig. 31 Sequential filtering to varied 2nd interval (I2-test) by the pattern recognition circuit.

Fig. 31 Sequential filtering of the I2-interval by the pattern recognition circuit. A. The relative tuning curves of the spiking neurons (AN1, LN2, LN3 and LN4) in the pattern recognition circuit and the phonotactic response. The responses elicited by the normal chirp in the neurons and for phonotaxis were set as 1, and activity evoked by other chirps was calculated as the relative change compared to 1. The tuning curves of AN1 and LN2 are in dotted lines, they do not show any temporal selectivity. The tuning curve of LN3 is given in grey and of LN4 in black. The reference level indicates the phonotactic response elicited by a 2-pulses chirp. **B.** The recordings of LN4, LN3, LN5, LN2 and AN1 are aligned vertically in a column aligned to the sound pulses, sound pulses are shown as grey bars. The names of different chirps are given on top of each column. For LN4, LN3, LN2 and AN1, only one example recording is shown, for LN5, the traces are averaged from 14 recordings. The green arrow indicates the inhibition and EPSPs elicited by P3 in I2-80. Orange arrowheads indicate the additional deflection in rebound3 for short I2. Blue and pink arrowheads shown in I2-40, I2-50 and I2-80 chirps indicate the changes in the membrane dynamics observed in the second rebound. Grey arrowheads indicate PIR3, the peak of only completed rebound.

but for larger I2 the relative activity of LN4 was lower than that of LN3. The decrease rate in LN4 when I2 was increased from 20 to 40 ms was higher than that in LN3 (LN4: m=-0.38 mV/ms; LN3: m=-0.1009 mV/ms), indicating a narrower tuning in LN4 than in LN3.Overall, the tuning of LN3 and LN4 quantitatively and qualitatively matched the phonotactic behaviour very well. Especially for LN4 activity, both the level of its increase when I2 increased from 5 to 20 ms and its decrease when I2 changed from 20 to 80 ms matched the changes in phonotactic behaviour, indicating a tight coupling between the activity of LN4 and the behavior or at least a good representation of the behaviour at the level of LN4 activity.

To reveal the flow of information in the circuit, I aligned the responses of the five neurons to the I2-chirps, which are indicated as vertical grey bars (Fig. 31B). For short I2 (I2-5, I2-10) the response of AN1 to the second (P2) and the third pulse (P3) either merged (I2-5) or had only a short interval (I2-10) (Fig. 31B). This resulted in a merged maintained depolarisation and spiking in LN2, which however was not tightly coupled to the sound pulses and did not mirror the temporal pattern. The short interval between the response to the second and the third pulses (P2 and P3) in LN2 may be reflected in the rather small PIR2 in LN5. Comparing the almost tonic spike activity of LN2 and the well-timed inhibitions of LN5, may indicate a discrepancy between the LN2 activity and LN5 activity. Although a more quantitative analysis would be required, besides the first inhibition (INH1) in LN5 also the subsequent ones (INH2 and INH3) are not clearly matched by the pattern of LN2 spikes; indicating that LN5 may receive further inputs. For short I2, the coincidence detector LN3 appears to be mainly driven by the AN1 activity, as the PIR2 of LN5 is not well expressed, although the LN5 depolarisation increases. At the level of the feature detector LN4, the initial activity is dominated by the inhibition from LN2, and subsequently only one pronounced depolarisation and burst of spikes is generated, when the depolarising input from LN3 in response to P2 kicks in.

For medium I2-intervals (I2-20 to I2-30) AN1 and LN3 responded with excitation (Fig. 31B), coupled to the sound pulses. Although spike activity in LN2 was again quite variable, the three post-inhibitory rebounds in LN5 were well pronounced, and increased over the time course of the chirps. The coincidence between AN1 activity and LN5 rebounds leads to a stronger activation of LN3, which also showed an increase of its membrane potential over the course of the chirps. At the level of LN4 the input from LN3 overcomes the inhibitory input from LN2 and results in two pronounced depolarisations and bursts of spikes. The fact that the

LN4 depolarisation in response to P3 is broader and declines more gradually than the pronounced depolarisation response to P2 correlates with the weaker spike activity of LN2 in response to P3, imposing a weaker inhibition on LN4. Occasionally the peak of the last PIR of the LN5 neuron was followed by a single spike in LN4.

With long I2 (40-80ms) activity of AN1 and LN3 remained tightly coupled to the sound pulses, and in LN2 the response to the third sound pulse became more distinct. Activity of LN5 became dominated by the post-inhibitory rebound to the second sound pulse (P2). This also revealed some deflections in the rebound potential, indicating additional inputs or conductance driving LN5 activity (Fig. 31; I2-40 to I2-80, blue and pink arrowheads). The response of LN2 to the third sound pulse forwarded an inhibitory input to LN4, which was so strong that the excitatory input from LN3 could not compensate, with the consequence that LN4 responded to the third sound pulse with a mixed inhibition and excitation (Fig. 31. I2-80, green arrowhead). At the level of LN4 the long I2-intervals caused only one suprathreshold depolarisation.

When compared to the behavioural tuning, two features of the network response seem to be linked to phonotaxis. At the best phonotactic response LN5 showed a regular and increasing membrane potential oscillation, while LN4 generated two pronounced depolarisations with spiking activity. At short and long I2, LN5 activity in response to P2 was either very low (I2-5) or extremely pronounced (I2-80), but at the level of LN4 still one depolarisation with one burst of spikes was generated in both cases. The activity of LN4 elicited by I2-40, I2-50 and I2-80 should be the same as that elicited by a reference chirp composed of two 20-ms pulses, since only the first two sound pulses were effective. Otherwise, comparing the timing of inhibitory LN2 spike activity and LN5 inhibition there appears a discrepancy, which will need further analysis.

Comparing the neuronal and behavioural responses to the I1 and I2-test pattern

The phonotaxis of *G. bimaculatus* to the I1- and I2-tests both showed a very similar band-pass tuning with a peak response when the varied interval was 20 ms (Fig. 32A). With increasing short intervals, the phonotactic response steeply increased and for intervals between 50 to 100 ms the response in both tests gradually declined. Nevertheless, the behavioural response to long I1 was lower than that to long I2, which was at the same level as the response to a reference chirp with 2 pulses.

The tuning of LN3 to I1- and I2-tests exhibited a similar shape (Fig. 32B). Since each

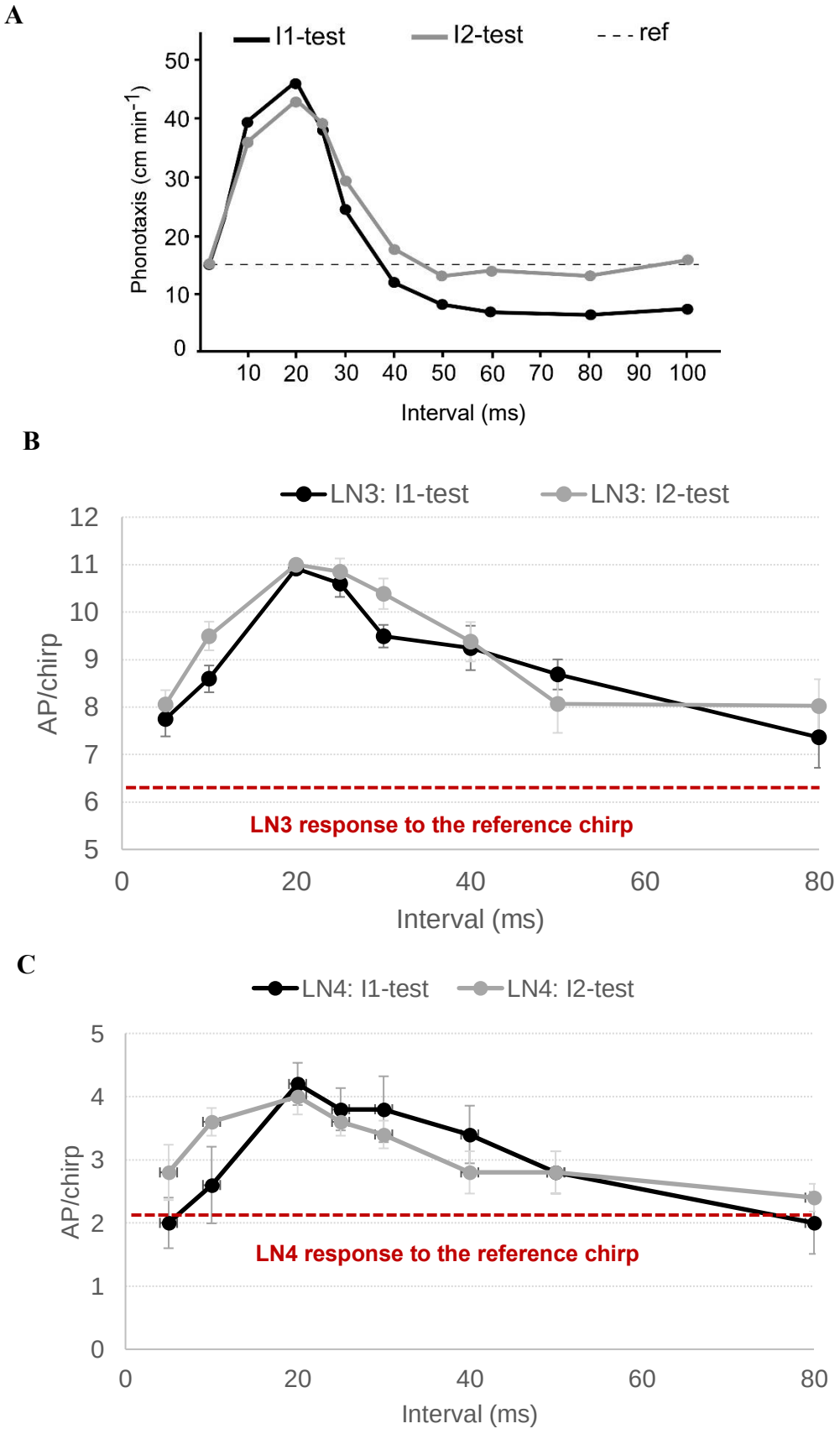

Fig. 32 Comparison of the tuning of phonotaxis, LN3 and LN4 for the I1-and I2-tests.

Fig. 32 Comparison of the tuning of phonotaxis, of LN3 and LN4 activity for the I1- and I2-tests. A. Diagram modified from Hedwig and Sarmiento-Ponce 2017. The level of the phonotactic response to the reference chirp (2-pulses chirp) is shown as a dotted line. **B.** Comparison of the LN3 tuning between I1- and I2-tests. The tuning of LN3 to I1-chirps is in black and for I2-chirps in grey. The activity elicited by the reference chirp is indicated by a red dotted line. The number of spikes was averaged from 5 animals, 13 repeats. Error bars represent standard error means (SEM). **C.** Comparison of the LN4 tuning between I1- and I2-tests. The tuning of LN4 to I1-chirps is in black and for I2-chirps in grey. The activity elicited by the reference chirp indicated by red dotted line. The number of spikes was averaged from 5 animals, 5 repeats. Error bars represent standard error means (SEM).

sound pulse elicited a burst of spikes in LN3, the response to the 2-pulse reference chirp is lower than both tuning curves. The activity of LN4 elicited by a 2-pulse reference chirp was 2.4± AP/chirp (Fig. 32C, red dotted line, data not shown). The overall tuning of LN4 to the I1- and I2-tests was very similar (Fig. 32C): The number of spikes generated by short I1 and I2 were very similar to that caused by a 2-pulse reference chirp, with short I2 may be able to elicit slightly more spikes than I1 in LN4 (Fig. 32C). In the range of medium I1 or I2, LN4 always generated two bursts of spikes, which correlate with the best phonotactic response (see Fig. 21 and 30). The tuning of LN4 to these chirps was very similar, with slightly less spikes generated by medium I2 than I1 (Fig. 32C). Both the activity of LN4 elicited by I1-80 and I2-80 gave very similar response as the reference chirp (Fig. 32C). This may explain why the behavioural response to long I2-intervals is closer to the reference level and higher than the corresponding response to the I1-intervals. In contradiction to this LN4 generated two bursts of spikes at I1-40 and I1-50 (see Fig. 21), which corresponding to this reasoning also would indicate a strong phonotactic response, which however did not occur in the behavioural test. Other parameters, which are not obvious in these recordings, may therefore contribute to the behavioural response to long I1- and I2-intervals.

The timing of LN5 and AN1 activity

As proposed by Schöneich et al. (2015), the tuning of the coincidence detector LN3 depends on the well-timed overlap of the spike activity forwarded directly by AN1and the graded rebound depolarisation by delay-line neuron LN5 (Fig. 1). In response to chirps with short pulse periods AN1 does not resolve the intervals and LN5 generates one extended inhibition and no post-inhibitory rebound. For pulse periods between 34 and 42 ms, the LN5 rebound and AN1 activity coincide, whereas the two excitatory inputs to LN3 drift out of phase for long pulse period. It was concluded that the direct and delayed input are only effective when they coincide at the detector LN3.To illustrate whether this reasoning applies to the I1- and I2-tests, I aligned the averaged LN5 activity and an example AN1 recording for all I1- and I2-chirps (Fig. 33), being aware that these recordings were not obtained in the same specimen.

The rising phases of the post-inhibitory rebound of LN5 are marked in dark blue and the falling phases in green (Fig. 33). In response to chirps with I1 or I2 in the range of 5 to 50 ms, the peaks of PIR1 and PIR2are determined by the start of the subsequent inhibition, which always occurs in the rising phase of the rebound and transiently interrupts the rebound. In case of PIR1, for I1-5 to I1-30, the AN1 spike activity elicited by the second sound pulse P2 mainly

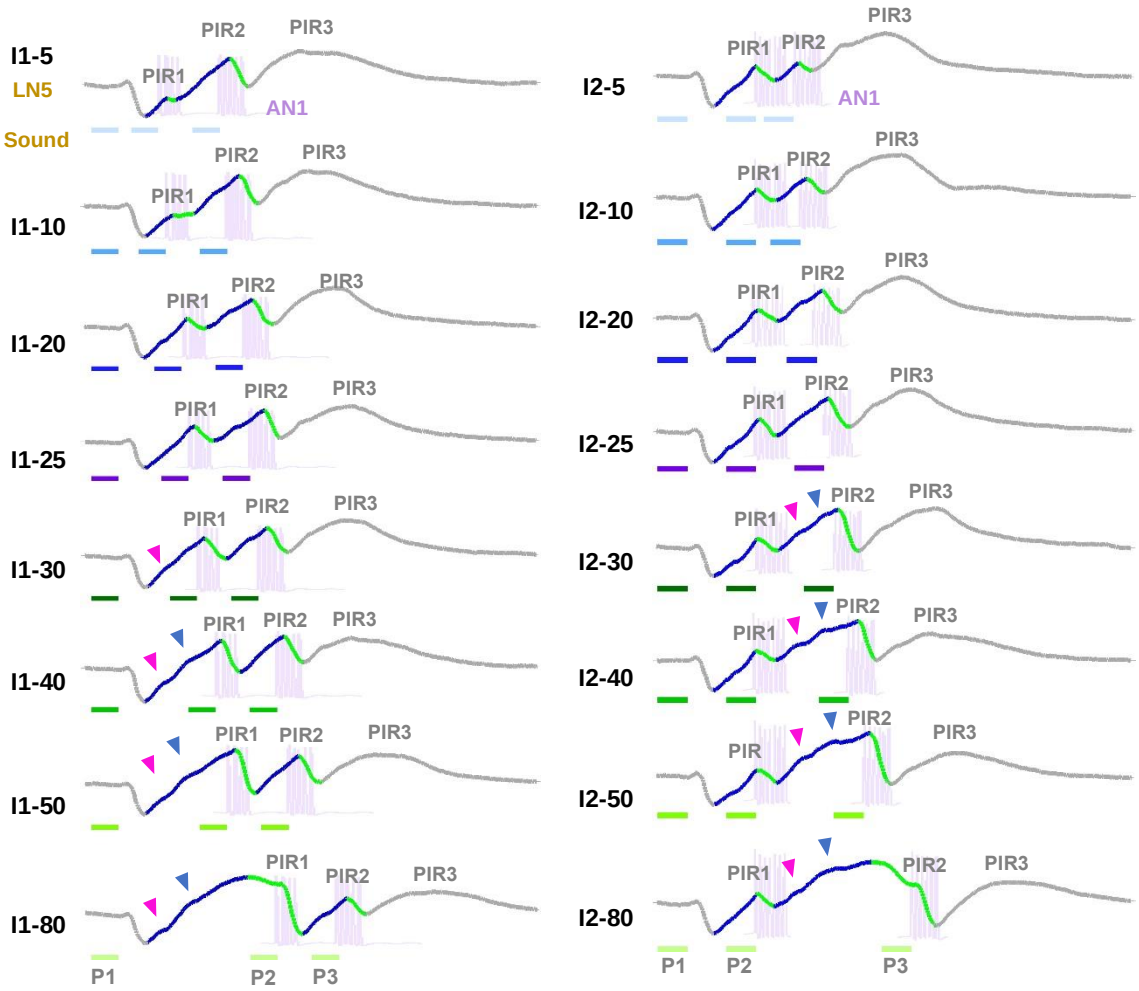

Fig. 33 The coincidence between AN1 and different phases of the post-inhibitory rebound in LN5. Coincidence of AN1 and LN5 in different phases of the post-inhibitory rebound in response to the I1- and I2-tests. Sound patterns are given below the LN5 recordings. AN1 activity to the last two pulses in each chirp are in purple. The first two rebounds are colored since these are the parts coinciding with AN1 activity while other parts of the LN5 activity are in grey. The rising phases of the rebounds are in blue and the falling phases are in green. The falling phase may be naturally occurring, or the falling phase initiated by the subsequent inhibition. The blue and pink arrow heads indicate the deflections in the rebound during the I1-test and the I2-test. The name of each chirp is listed to the left of each test pattern. The LN5 activity is averaged from 18 recordings.

overlapped with the primary rising phase of the rebound (before the blue arrowhead). This also happened in the coincidence between the AN1 activity elicited by the third sound pulse and the PIR2 for I2-5 to I2-20. However, with an increasing I1 interval (I1-30 to I1-50) the first rebound became longer and the overlap of the AN1 activity shifted to the secondary phase of the PIR1 (Fig. 33, after the blue arrowheads). For the I2-test, the coincidence between the third AN1 activity and the later phase of the PIR2 occurred for I2-25 to I2-50. At 80 ms intervals, both the first rebound in the I1-test and the second rebound in the I2-test passed their peaks and started to depolarize before the subsequent inhibition; the AN1 activity (elicited by P2 in the I1-test and by P3 in the I2-test) completely occurred during the falling phase of the prolonged rebound (PIR1 in the I1-test and PIR2 in the I2-test).Thus a similar shift in timing of the activity of AN1 and LN5 as reported by Schöneich et al. (2015) occurred in response to the I1- and I2-chirp patterns, and the coincidence between AN1 spike activity and LN5 rebound activity at the level of the coincidence detector LN3 occurred at different phases of the rebound.

The latency of the post-inhibitory rebound and the AN1 activity recorded in the I1- and I2-tests clearly support this hypothesis. For example, the peak of the rebound elicited by a single 20 ms sound pulse occurred with a latency of 89.4±2.2 ms. Any second AN1 activity elicited by I1-chirps occurred with a latency of only about 18.4 ms and initially coincided with the rising phase of the rebound before this reached its peak, whereas when the interval was 80 ms, the coincidence happened at the falling phase of the rebound. In summary, the coincidence of AN1 and LN5 activity occurring at different phases of the post-inhibitory rebound appears to contribute to different levels of activity in the coincidence detector LN3, thus affecting the activity of the feature detector LN4 and the phonotactic behaviour. Since the latency of AN1 activity to each sound pulse was constant at about 19 ms (Table.1), and the latency of each inhibition elicited by each sound pulse was about 26 ms (Table.1), there is always about 7 ms overlap between the AN1 activity and the post-inhibitory rebound, which allows approximately 3 spikes of AN1.

The above results show that changes in a single interval of a chirp pattern can cause very different responses at the level of the feature detector LN4, which depend on the altered interval. When the long interval occurred at an earlier position (I1) of a chirp, the activity of LN4 was more reduced than when the long interval occurred at later position (I2) in the chirp. This difference between the tuning curves of LN4 to long I1 and I2 may be related to the preceding different LN5 responses that subsequently lead to different upstream responses in the

circuit. It may form the basis for the corresponding different behavioural responses towards the I1- and I2-test patterns.

Response of the pattern recognition network neurons to chirps with all intervals varied: PI-test

The results above demonstrate that varying a single interval in a chirp pattern changes the phonotaxis response and the activity of higher-level neurons in the pattern recognition circuit in a characteristic way. Both the tuning curves of the LN4 activity elicited by the sound pulses P2 or P3 showed selectivity to different chirps to some extent (Fig. 21D and 30D). This indicates that the specific duration of an interval affects not only the subsequent response to a sound pulse but also the following responses. This implies that changing all intervals over the time course of a chirp may cause an accumulative stronger effect, which should be more obvious in the response of the feature detector LN4. To follow this reasoning in the Pulse Interval test (Fig. 12 PI-test, Fig. 34), I also tested sound patterns with all the intervals within a chirp systematically varied following the paradigm of Kostarakos and Hedwig (2012).When tested with different PI-chirps, the phonotactic response revealed a narrowly tuned optimum curve with a best response at PI-15 ms, and the activity of LN4 matched the tuning of the phonotactic behavior (Kostarakos and Hedwig, 2012). To include the chirps with very short intervals like 2 ms, and to compare the neuronal response to the behavioural response obtained by Adam Bent (not published), I tested these chirps on AN1 and LN4. For these tests each chirp contained four sound pulses. The duration of all pulses was kept at 20 ms; all intervals were systematically changed to 2, 5, 10, 15, 20, 25, 30, 35, 40, 50, 60, 80 and 100 ms (Fig. 12).

Recordings of the ascending interneuron AN1 and the local interneuron LN4 were obtained in different crickets (Fig. 34), AN1 was recorded 8 times in 8 specimen and LN4 was recorded 5 times in 4 specimens. The ascending neuron AN1 always copied the pulse patterns when the interval was between 10 to 100 ms; when challenged with PI-2 and PI-5 chirps with short intervals it did not resolve the individual sound pulses. A modulation of its spike pattern by the sound pattern became stronger for PI-10 and more obvious with increasing intervals, so that AN1 responded to each sound pulse with a burst of spikes.

In its typical way, LN4 responded to the chirps with an initial inhibition (Fig. 34). As the neuron did not resolve the short intervals between sound pulses, AN1 and LN4 responded

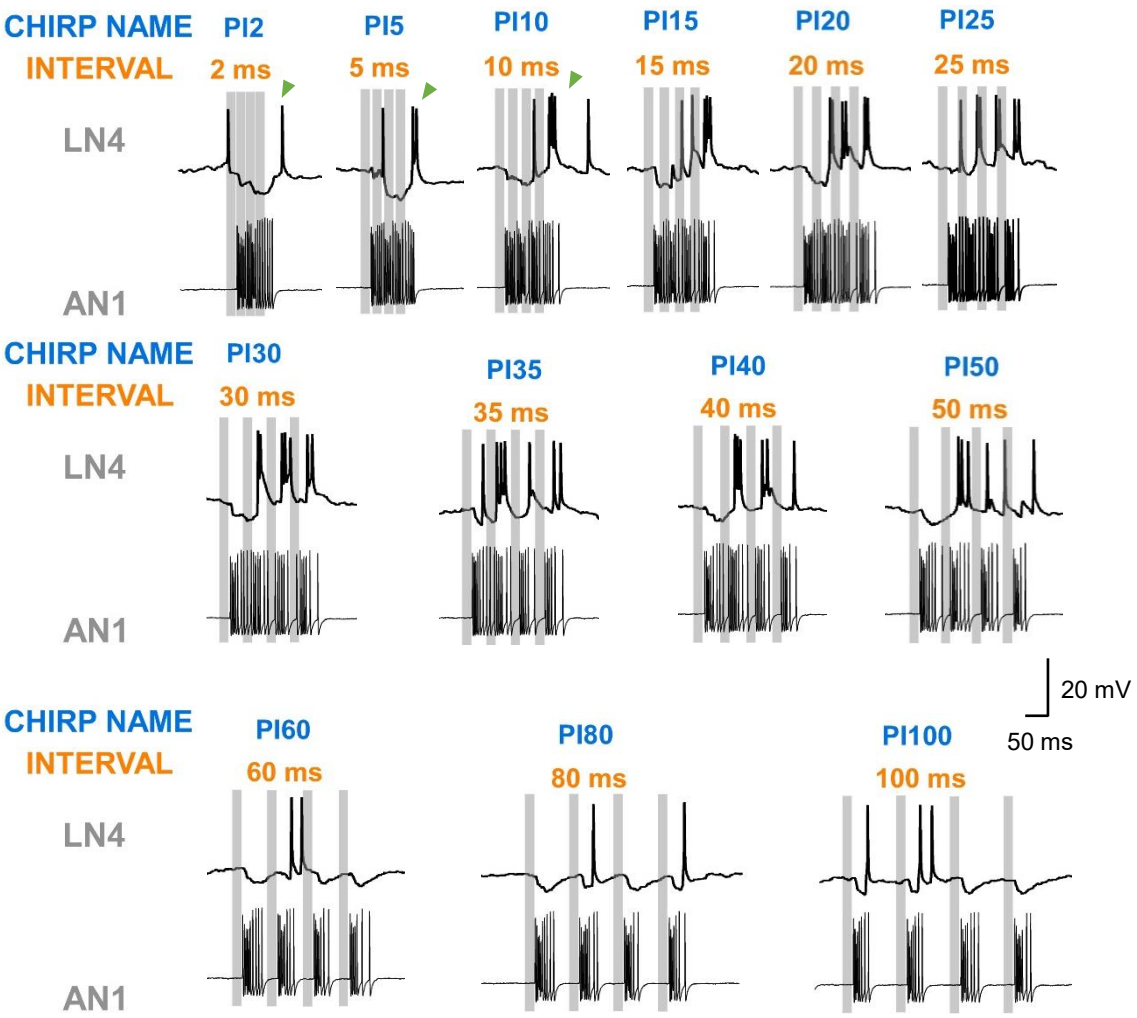

Fig. 34 Response of AN1 and LN4 to the chirps in the PI-test. Example activity of AN1 and LN4 in response to chirps with all intervals varied (PI-test). The chirps were composed of four 20-ms pulses with pulse intervals of 2, 5, 10, 15, 20, 25, 30, 35, 40, 50, 60, 80 and 100 ms which are labelled as PI2, PI5, PI10, PI20, PI25, PI30, PI35, PI40, PI50, PI60, PI80 and PI100. The names of the tested chirps are given above each chirp. For chirps with short intervals the green arrow heads indicate the burst of spikes elicited at the end of each chirp.

to PI-2 as a continuous long sound pulse. LN4 showed an initial pronounced inhibition followed by a single burst of spikes (1.6±0.5 AP/chirp). Also, PI-5, PI-10 and PI-15 caused an initial prolonged inhibition superimposed by some EPSPs, and occasionally single spikes coupled to the third pulse (0.4-0.6 AP). Activity ended with a suprathreshold depolarisation with a burst of 1-3 spikes (Fig. 34, green arrowheads). This response to the last sound pulse reached 1.6±0.0 AP/pulse (PI-5), 2.8±0.3 AP/pulse (PI-10) and 2.2±0.2 AP/pulse for PI-15 and was always the strongest response.

To medium PI-intervals (PI-20 to PI-30) LN4 responded to the first sound pulse with an inhibition and then generated a burst of 2-3 spikes for each of the subsequent three sound pulses. For the second pulse the activity was PI-20: 2.4±0.2 AP; PI-25: 2.2±0.2 AP; PI-30: 2.6±0.2 AP and for the third sound pulse it was PI-20: 2.6±0.2 AP; PI-25: 2.6±0.2 AP; PI-30: 2.2±0.2 AP. The last pulse caused slightly less activity, with PI-20: 1.8±0.2 AP; PI-25: 1.6±0.2 AP and PI-30: 1.8±0.2 AP. Thus, the pronounced depolarisations in LN4 were particular prominent for the PI-patterns that also elicited strong phonotactic behaviour. Towards chirps with longer intervals (PI-35 to PI-50) the initial hyperpolarisation already had waned, when the response to the second sound pulse started, which elicited a prominent depolarisation and a burst of 2-3 spikes (PI-35: 2.4±0.2 AP; PI-40: 2.2±0.2 AP; PI-50: 2.6±0.2 AP). This response was followed by relative lower spike activity in response to the third and the fourth pulse. The response to the third sound pulse was at PI-35: 1.8±0.2 AP; PI-40: 2.0±0.2 AP; and PI-50: 1.2±0.3 AP. The fourth sound pulse gradually became less effective and elicited only a single spike or a depolarisation with PI-35: 1.2±0.3 AP; PI-40: 1.2±0.2 AP and PI-50: 0.4±0.2 AP.

The LN4 response pattern changed substantially towards chirps with long intervals (PI-60 to PI-100). Its activity was now dominated by the inhibition triggered by the individual sound pulses. After an initial inhibition in response to the first pulse, the membrane potential recovered to baseline before the subsequent sound pulse elicited the next IPSP mixed with an EPSP or very few spikes. The second sound pulse elicited 1-2 spikes PI-60: 1.8±0.3 AP; PI-80: 0.8±0.2 AP; PI-100: 0.8±0.3 AP. With increasing interval duration the third and the fourth sound pulses mainly elicited IPSPs and very little spiking activity occurred (pulse three: PI-60: 0.2±0.2 AP; PI-80: 0.2±0.2 AP; PI-100: 0.8±0.4 AP) and for the fourth pulse (PI-60: 0.4±0.2 AP; PI-80: 0.4±0.2 AP; PI-100: 0.8±0.3 AP). As a consequence, LN4 spike activity was substantially reduced and the prominent depolarisations and burst of spikes, typical for the normal intervals (PI-20) were abolished.

To quantify the response of LN4 to the PI-test pattern, I measured the number of spikes per chirp (N=4, n=5). The phonotactic response of *G. bimaculatus* to chirps with different PIs (orange curve) and the average number of LN4 spikes elicited per chirp (purple curve) are pooled over all animals (Fig. 35A).

The LN4 response shows a band-pass tuning. As the PI increased from 2 ms to 15 ms, LN4activity increased from 1.6±0.5 to4.8±0.2 AP/chirp, which reflects the sharp increases of the phonotactic behaviour towards its maximum at PI-15. The broad maximum response of LN4 activity started at PI-20 with 6.8±0.2 AP/chirp and was significantly higher than to chirps with intervals of 2, 5, 60, 80 and 100 ms (PI-20 vs. PI-2: 6.8±0.2 vs. 1.6±0.5, p=0.0213; PI-20 vs. PI-5: 6.8±0.2 vs. 2.0±0.7, p=0.0036; PI-20 vs. PI-60: 6.8±0.2 vs. 3±1.8, p=0.0121; PI-20 vs. PI-80: 6.8±0.2 vs. 2.5±1.1, p=0.0007; PI-20 vs. PI-100: 6.8±0.2 vs. 2.6±1.6, p=0.0161; Friedman test, n=5). The LN4 activity peak however, was rather broad as the activity elicited by chirps with PI-20 to PI-30 was statistically not different (PI-20: 6.8±0.2 AP; PI-25: 6.4±0.2 AP; PI-30: 6.6±0.2 AP, p=0.8090). In contrast to the LN4 activity, the phonotactic response strongly decreased when the interval increased from 20 to 30 ms. As PI increased further from 35 to 50 ms, the phonotactic response decreased to 14.89% of the maximum response and LN4 activity decreased from 5.4±0.4 AP/chirp to 4.2±0.5 AP/chirp (62.86% of the maximum response). For long intervals from 50 to 100 ms, phonotactic response even fell further and was very low overall. Over the same range LN4 activity decreased from 4.2±0.5 to about 2.4±0.6 AP/chirp and stayed at this low level. In summary, the increase of LN4 activity matches the behaviour, the best tuning is shifted towards longer intervals and occurs over a wider range, while at long intervals the low activity corresponds to the low phonotactic response.

Tuning of LN4 activity towards individual pulses of the PI chirps

The AP/chirp reflect the excitatory response of LN4 to a complete chirp (Fig. 35A). I also asked if the band-pass tuning is reflected in the LN4 responses to the different sound pulses within a chirp. Since the first sound pulse of a chirp always elicited an inhibition, I focused on the response to the last three sound pulses (P2 - P4) (Fig. 35B).

The neuron did not respond to the second sound pulse (P2) if the PI interval was 5 or 10 ms (Fig. 35B, blue line). LN4 activity sharply increased as the interval increased to 20 ms, and then reached a broad maximum between PI-20 and PI-50 (PI-20: 2.4±0.2 AP, PI-25: 2.2±0.2 AP; PI-30: 2.6±0.2 AP; PI-35: 2.4±0.2 AP; PI-40: 2.2±0.2 AP; PI-50: 2.6±0.2 AP), (Fig. 35B).

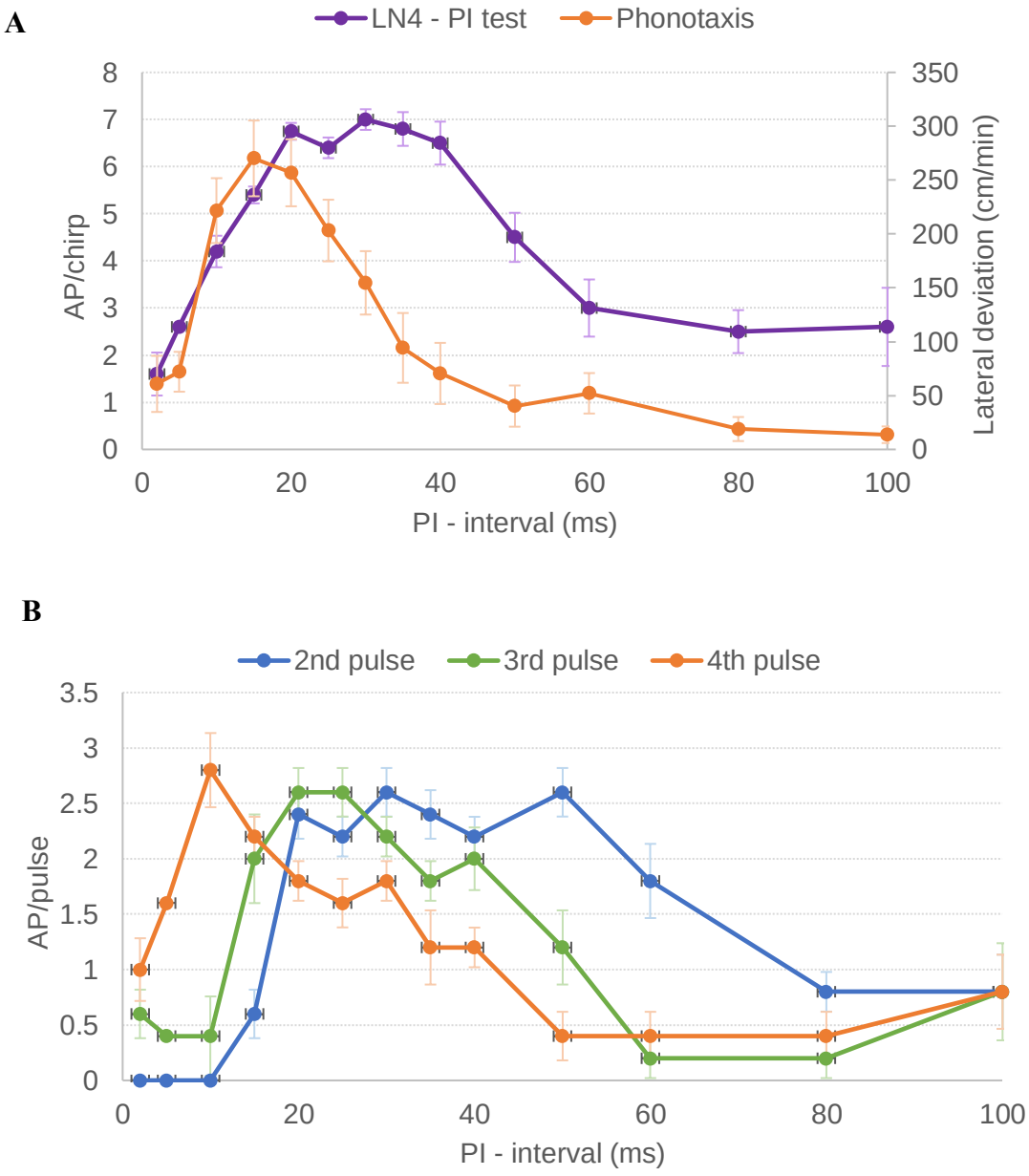

Fig. 35 The tuning curves of LN4 to the PI-chirps and to individual pulses of the PI-chirps. A. Tuning curve of LN4 in response to PI-chirps, the number of spikes generated in LN4 is colored in purple. The data is averaged from 4 animals and 5 repeats. The phonotactic response is in orange and derived from experiment by Adam Bent (unpublished). Error bars indicated the standard error mean (SEM). **B**. Tuning curve of LN4 in response to the last three sound pulses of the PI chirps. The activity elicited by the second sound pulse is in blue, the third sound pulse is in green and the last sound pulse is in orange. The data is averaged from 4 animals and 5 repeats. The error bars indicate the standard error mean (SEM).

The response then dropped to 1.8±0.3 AP/pulse (PI-60) and further to 0.8±0.3 AP/pulse when PI increased to 80 and 100 ms.

The LN4 response to the third pulse (P3) revealed no activity for short intervals of 2 or 5 ms (Fig. 35B, green line). LN4 activity then steeply increased as the intervals increased to 20 ms and gave a peak response for PI-20 (2.6±0.2 AP/pulse) and PI-25 (2.6±0.2 AP/pulse). LN4 activity then sharply decreased to 0.2 AP/pulse (PI-60) and remained at a low level. The response to the chirps with the 'normal' 20-ms intervals was significantly higher than the responses to chirps with 2, 5, 10, 60 and 80 ms intervals (20ms vs. 2ms: 2.4±0.2 vs. 0±0, p=0.0024; 20ms vs. 5ms: 2.4±0.2 vs. 0±0, p=0.0024; 20ms vs. 10ms: 2.4±0.2 vs. 0.4±0.4, p=0.0169; 20ms vs. 60ms: 2.4±0.2 vs. 0.2±0.2, p=0.0006; 20ms vs. 80ms: 2.4±0.2 vs. 0.2±0.2, p=0.0006, Dunnett's multiple comparison, n=5).

Analysing the LN4 response to the fourth pulse (Fig. 35B, orange line) demonstrates a further shift of the peak response towards shorter intervals. LN4 activity steeply increased towards the peak response at PI-15 (2.8±0.3 AP/pulse). It then almost continuously decreased towards a level of 0.8 AP/chirp at PI-50 and then remained at a similar low level for longer intervals. The response at PI-20 was significantly higher than the responses to long intervals (20ms vs. 50ms: 1.8±0.2 vs. 0.4±0.2, p=0.0168; 20ms vs. 60ms: 1.8±0.2 vs. 0.4±0.2, p=0.0168; 20ms vs. 80ms: 1.8±0.2 vs. 0.4±0.2, p=0.0168, Dunnett's multiple comparison, n=5).

In summary, three tuning curves showed a band-pass shape, the maximum LN4 response however became narrower from the P2 to P4 and shifted towards shorter intervals. Whereas the tuning curve to P2 demonstrates a broad maximum, the tuning curve for P4 matches the behavioural tuning very well, while the tuning curve shown in Fig. 35A shows a mismatch and shift in comparison to the behavioural response. This is may indicate that the responses to the different pulses may have a different weight, when contributing to pattern recognition underlying the phonotactic behaviour, or it may be an effect of the different test regimes used in the behavioural and neurophysiological experiments (see Discussion).The tuning of LN4 reported here is broader than the tuning described by Kostarakos and Hedwig (2012).

Major conclusions

1. The recordings of the five neurons of the pattern recognition circuit confirm and extend the neurophysiological response properties described before (Kostarakos and Hedwig 2012;

Schöneich et al. 2015)

2. The pattern recognition circuit filters and sharpens the response to the sound pulses progressively along the ascending neuron (AN1), the inhibitory neuron (LN2), the non-spiking neuron (LN5), the coincidence detector (LN3) and the feature detector (LN4).

3. AN1 and LN2 do not show any selectivity in the interval paradigms, they rather copy the duration of the sound pulses. LN2 responds with a prolonged EPSP, which is longer than the actual duration of the sound pulses.

4. The tuning curves of LN3 in response to I1- and I2-tests exhibit a band-pass filtering property with a peak at 20 ms as in the phonotactic tuning supporting its role as a coincidence detector.

5. All the tuning curves of LN4 in response to I1-test, I2-test and the PI-test show a narrower tuning curve as compared to LN3 and match the corresponding phonotactic tuning. The peak response to the normal chirp (PI-20) supports its role as a feature detector for phonotaxis. All the conclusions above support that one single long interval is sufficient for a reduced activity in LN4 compared to the normal chirp.

6. The varied interval at different positions (I1, I2) within a chirp can result in slightly different levels of responses along processing in the circuit. This is an indication that the response of the pattern recognition circuit to a sound pulse depends on the preceding processing.

7. The effect of changing intervals may be linked to the decrease of the postinhibitory rebound and the timing of the interaction of the direct and indirect inputs to coincidence detector.

8. The effect of the varied intervals is accumulative within a chirp.

DISCUSSION

My experiments compared the tuning of auditory pattern recognition neurons with the tuning of phonotactic behaviour for chirp patterns in which one individual interval was varied in otherwise identical chirps. My recordings reveal activity patterns corresponding to all 5 elements of the pattern recognition network proposed by Schöneich et al. (2015), and provide further insight into the pattern recognition process at the level of the network and the individual neurons in the brain of *G. bimaculatus.*

Acoustic Stimulation

Intracellular recordings of the local auditory brain neurons were obtained in the frontal protocerebrum, while crickets were standing and moving on a trackball. Phonotactic walking of the females could occur but was rare. However, any walking motor activity caused neuronal background activity and made some of the recordings noisy, likely due to the mechanical activation of the hearing organ (Schildberger et al. 1988). Recordings of the local interneurons are difficult to obtain and may last for short periods of time only. Different to the behavioural experiments, where the same chirp pattern is presented for at least 1min with about 150 repeats, my emphasis was to obtain neuronal responses to a variety of chirp patterns. I therefore looped the chirp stimuli presenting all the different chirps of a test in one sequence, in which each chirp type was presented only once. This allowed to test the responses to a range of chirp patterns, although with a low number of repeats, but the organisation of the test patterns may have a substantially effect on the pattern recognition system. Ongoing presentation of the normal calling song pattern induces some form of a modulatory component in the nervous system (Poulet and Hedwig 2005), and immediately after listening to a calling song, females will also orient to non-attractive patterns. The build-up of this component may have been prevented by the looped presentation of the chirp patterns, as the normal chirp was presented only once in a sequence of different chirps. The possible impact that this had on the neuronal responses is however difficult to judge.

AN1 copies the pulse pattern and does not exhibit temporal filtering properties

The thoracic interneuron AN1 is one of the best characterized neurons in the cricket auditory pathway (Schildberger et al. 1989, Wohlers and Huber 1982). The crucial role of AN1 is to forward the temporal pattern of the sound pulses with high reliability to the auditory brain neurons. This is reflected in the AN1 activity patterns during the interval tests as the neuron copied the pulse pattern in its spike activity. Only the patterns with very short intervals (I1-5, I2-5) and pulses (PI-2 and PI-5) were not reliably resolved and sound pulses separated by such small intervals rather were processed as a single pulse. AN1 activity was uniform across all interval tests and did not reveal any filter properties or pattern preferences. This is in line with previous studies on AN1 filter properties (Wohlers and Huber 1982, Schildberger 1984, Kostarakos and Hedwig 2012).

LN2 activity follows AN1 activity and does not show temporal selectivity

The structure and activity of LN2 has been characterized in few recordings by Kostarakos and Hedwig (2012) and by Schöneich et al. (2015). LN2 followed the pulse pattern with pronounced suprathreshold depolarizations. Spiking activity of LN2 showed a phasic-tonic response, the first sound pulse always gave the strongest spike response, activity then dropped for the second and third pulse. As the spiking activity elicited by a single 20 ms pulse lasted about 25 ms but the membrane potential only gradually decayed over 40-55ms, the pattern of pulses separated by 10 ms intervals (I1-10 and I2-10) was reflected in two groups of spikes but not clearly separated depolarizations. The long decay in the LN2 membrane potential has not been reported before. Like AN1, the tuning of LN2 spike activity did not reveal any filter properties during the I1- and I2- test, as also described by Kostarakos and Hedwig (2012) for chirp patterns with different intervals. LN2 spike activity followed AN1 activity by 3.3 ms and the start of the depolarization only showed a delay of 1 ms, indicating that LN2 is driven by AN1 activity, as *proposed by Schöneich et al. (2015).*

LN5 shows complex membrane potential changes due to consecutive inhibitions and post-inhibitory rebounds

The non-spiking neuron LN5 is the delay-line in the pattern recognition network and shows complex auditory responses (Schöneich et al. 2015). LN5 responds to a sound pulse with an inhibition; which is supposed to be driven by LN2 spike activity; and a subsequent rebound depolarization (Kandel and Spencer, 1961; Kandel. et al. 1969; Anderson and Eccles, 1962). The inhibitory response to the first sound pulse of a chirp was always the strongest, which may be due to the pronounced phasic onset activity of LN2; a phasic onset activity is a general feature of the auditory pathway (Givois and Pollack 2000). With reference to the sound pulse the post-inhibitory rebound reached a broad maximum with a latency of about 89.4 ms which is in the range of the latency reported by Schöneich et al. (2015) (~80 ms). If no second pulse was presented the rebound developed over 53 ms starting from the peak of the inhibition.

Interestingly, in response to a sound pulse the rebound always started to build up from the maximum inhibition, although the inhibitory LN2 spike activity was still ongoing. For a 20 ms sound pulse the inhibition of LN5 always peaked with a latency of 36.4 ms, independent of the subsequent pulse interval. After the onset of the inhibition at 26.4 ms, it took about 10 ms for the peak inhibition to develop and the rebound to start, while the spiking activity in LN2 started at 22.2 ms and lasted for 25 ms, and therefore overlapped with the development of the rebound. It is noteworthy that the activity of LN2 is in a phasic-tonic form in response to a

single sound pulse, i.e. the first sound pulse of a chirp. The firing rate of the initial 3 spikes reached 236.15±6.48 Hz and this transient phasic activity lasted for 10.3 ms, while inhibition in LN5 starts 4 ms after the first spike in LN2 (Table 1). This indicates that the LN5 conductance driving the rebound overcomes the inhibition mediated by LN2 and that just the start of LN2 activity in response to a sound pulse is sufficient to trigger the LN5 inhibition.

In response to a sequence of sound pulses the build-up of a rebound is cut short by each subsequent sound pulse triggering a new inhibition and leading to a new rebound activity. At short pulse intervals of 5-10 ms, the inhibition of LN5 was not or only weakly expressed, corresponding to the LN2 activity, which did not represent short intervals. The longer the interval - in the range up to 60 ms - the larger was the amplitude of the rebound depolarisation when the inhibition kicked in. This should have functional consequences for the coincidence detection at the next level of processing. For long intervals, the LN5 responses revealed a more complex rebound pattern, as deviations occurred in the rising phase of the rebound after about 40 ms, matching the pulse period of a normal chirp although no stimulus was present. This might imply additional inputs to LN5 or may reflect the ongoing inhibitory inputs from LN2 that interact with the rebound depolarization.

Over the time course of a chirp the recordings revealed a build-up of the rebound amplitudes, which had been observed (K. Kostarakos, personal communication), but have not yet been reported. This build-up in the LN5 membrane potential was strongest, for intervals in the normal range, it declined when long intervals were introduced into the chirp pattern. When comparing parameters of LN5 activity with the phonotactic tuning towards the I1- or I2-test, it was the slope of the overall increase in the LN5 membrane potential that matched best. The rebound activity of LN5 is thought to contribute to the coincidence detection at the level of LN3 via graded transmission (Schöneich et al 2015); however also the overall increase of the LN5 membrane potential may be a contributing factor driving LN3 activity via graded synaptic transmission (Pearson and Fourtner 1975, Siegler 1984, Burrows and Siegler 1976).

LN3 as coincidence-detector for AN1 and LN5 activity

The coincidence detector LN3 integrates excitatory activity from the spike activity of AN1 and a delayed graded excitatory input from the rebounds of the non-spiking neuron LN5 (Schöneich et al. 2015).

The neuronal response of LN3 did not resolve pulses separated by short intervals of 5

ms, which appears to be a common response property throughout the network. When a sequence of two sound pulses was presented with an interval of 20 ms, LN3 responded to the second sound pulse with a stronger burst of spikes than to the first one. This is due to the coincidence of the delayed post-inhibitory rebound (PIR1) initiated by the first sound pulse and the AN1 spike activity caused by the second sound pulse (P2). For corresponding pulse patterns, my results show a stronger LN3 response to the second pulse, which is in accordance to the delay-line and coincidence-detector mechanism Schöneich et al. (2015). For long intervals and at the end of a response to a chirp, I also observed subthreshold depolarizations of LN3 following its previous response to a sound pulse, as reported by Schöneich et al. (2015). These may have been driven just by the LN5 rebound potential when it did not coincide with AN1 activity. The depolarizations are in line with the coincidence detector mechanism; however they were not always clearly discernible. The third burst of spikes in response to P3 was at similar strength as the second burst, although the membrane potential of LN5 was continuously increasing and therefore would have provided a stronger graded input. This may be because LN3 may have reached its limit of depolarisation and could not generate stronger spike activity.

The proposed synaptic connection between the non-spiking LN5 and LN3 implies that not only the LN5 rebounds will depolarize LN3, but that a graded release of transmitter by LN5 might act on LN3, as described for non-spiking interneurons in the locust sensory-motor system (Burrows 1978). Comparing the membrane potential changes of LN3 over the time course of a chirp shows a build-up of its depolarization in a similar way like the LN5 membrane potential increases over the time course of a chirp and supports this assumption. The depolarisation of LN3 evoked by a 20-ms sound pulse lasted for 40-55ms, which is 20-34 ms longer than the 20 ms spiking activity of AN1 and may be due to the graded input from LN5.

LN3 spike activity per chirp matched the behavioral tuning of the phonotactic response to the interval test patterns. A more detailed analysis at the level of the responses to the sound pulses showed, that the tuning of LN3 was driven by its responses to the second and third pulse, as the response to the first pulse was not affected by coincidence detection and remained quite stable. This assigns a different relevance to the neuronal activity elicited by the different pulses in a chirp and is in line with the flow of information through the pattern recognition network by a delay-line and coincidence detection mechanism(Schöneich et al. 2015, Hedwig and Sarmiento-Ponce 2017).

Reconsidering the timing of the coincidence between the post-inhibitory rebound in LN5

and the AN1 activity

According to the delay-line and coincidence detector mechanism proposed by Schöneich et al. (2015), the non-spiking neuron LN5 serves as the key element in the circuit for processing the temporal pattern of the calling song. This is achieved at the level of the coincidence detector LN3 by the temporal overlap between the peak of the delayed post-inhibitory rebound of LN5 - elicited by a (first) sound pulse - and the AN1 spike activity elicited by the subsequent pulse. When the pulse period is in the range of the normal calling song (30-42 ms) both inputs overlap and boost the response of the coincidence-detector, but outside this range of pulse periods the two excitatory inputs shift away from each other, the coincidence detector is activated to a lower extend. However, in my experiment the inhibition reached maximum with a latency of 36 ms and the post-inhibitory rebound reached its maximum at 89.4 ms, which means it builds up over a time course of approximately 53.4 ms and an overlap between the still increasing post-inhibitory rebound and the AN1 activity always occurred, besides for very long intervals of 80 ms. The duration of the coincidence depends on the latency of AN1 activity and the latency by which the LN5 inhibition starts after a sound pulse. Based on the latency of inhibition in LN5 (~26 ms) and the latency of spiking activity of AN1 (~19 ms), the AN1 activity and the post-inhibitory rebound overlapped for about 7.5ms, allowing about 3-4 spikes of AN1 to coincide with the post-inhibitory rebound. A temporal shift between AN1 activity and the peak of the rebound as described by Schöneich et al. (2015) (Fig. 1) was not observed, AN1 activity rather coincided with different states of the post-inhibitory rebound in LN5. This different state can be reflected as the different phases of the post-inhibitory rebound or different ‘slope’ of the changes in amplitude of the PIRs (see Fig. 18 and 27).Only when the interval was 80 ms did the rebound decline and the previously proposed shift mechanism would work. The crucial point is that the peaks of the LN5 rebounds (PIR1 and PIR2) that overlap with the AN1 activity were formed due to the cut-off of the rebound by the subsequent inhibition, rather than by the actual maximum of the post-inhibitory rebound as determined by the intrinsic properties of the LN5 neuron for PIR3, which does not contribute to coincidence with AN1.

My experimental data therefore do not support the proposal in its current form that the temporal overlap between AN1 and the post-inhibitory rebound of LN5 determines the basis of the filter mechanism (Schöneich et al. 2015). Especially one factor may be linked to this discrepancy. My recordings always showed a gradual build-up of the LN5 membrane potential over the time course of a chirp, this has not been reported before but had been observed by K.

Kostarakos (pers. communication). The LN5 recordings by Schöneich et al. (2015) may have been obtained in branches, which do not fully represent the neuron's membrane potential changes, or were subject to a high-pass filter, which removed the slow membrane potential changes. Furthermore, different neurons may belong to a group of LN5 neurons that exhibit different membrane and conductance properties. These factors could affect the time course of the recorded LN5 rebound potential, however the details of this discrepancy cannot yet be resolved.

Response properties of the feature detector LN4

The spike activity of the feature LN4 closely matches the tuning of the phonotactic behavior. Its overall activity pattern depends on the processing of an inhibitory input from LN2 and an excitatory input from LN3, and is characterized by an inhibitory response to the first pulse of a chirp and an overall sparse spike coding pattern (Kostarakos and Hedwig 2012; Schöneich et al. 2015). These features of the LN4 activity consistently occurred in my recordings.

The response of LN4 to the first sound pulse of a chirp was always an inhibition, while the activity of LN3 may have caused subthreshold EPSPs during the ongoing inhibition. The excitation forwarded by LN3 to LN4 depends on the coincidence between AN1 and LN5 activity and therefore was stronger for the second sound pulse; while the inhibitory spike activity of LN2 gradually decreased and was lower for the second sound pulse. As a consequence, it was not the first, but the second sound pulse that caused a strong enough excitation of LN4 to overcome its inhibition. This leads to a very long latency for the LN4 spike activity relative to the start of a chirp which I observed, and which is in line with the recordings by Kostarakos and Hedwig (2012). The spike activity of LN4 in response to the 2nd and the 3rd sound pulse lasted only for about 9.7 and 16.5 ms and the underlying depolarization rapidly decayed, even when the pulse interval was very short. A reason for this could be that inhibition mediated by LN2 activity may terminate the suprathreshold responses in LN4, and while the LN4 response to the third pulse in normal chirps is broader than the response to the second sound pulse, the corresponding LN2 activity is also weaker (Table 1). The inhibitory effect of LN2 points to a pulse duration filter and should be more pronounced when longer sound pulses are presented as in the pulse duration tests.

In response to the second or third sound pulse LN4 generated a pronounced suprathreshold depolarization, which were strongest for the normal pulse pattern, and depended

on the preceding time interval. Inhibition dominated the LN4 response for very short and very long intervals in the I1-test. In the I2-test the response to the third pulse decreased with increasing I2-interval, however the response to the first two pulses always elicited pronounced suprathreshold depolarization. Besides the sparse spike activity of LN4, it may be the occurrence and the timing of these short suprathreshold depolarizations with brief bursts of spikes that are relevant for the pattern recognition process, in a similar way as proposed by Nabatiyan et al. (2003). The relevance for high frequency spike bursts at a lower level of sensory processing has been highlighted by Marsat and Pollack (2006) and Hartbauer et al. (2010) but it may also be relevant for these higher stages of auditory processing.

When analyzing the AP/chirp the tuning of LN4 activity showed a good agreement to the behavioral tuning to both test paradigms. A close similarity between LN4 activity and behavioral responses had been demonstrated before (Kostarakos and Hedwig 2012, Schöneich et al. 2015), and led to the suggestion that LN4 functions a feature detector, which responds to the species-specific pulse pattern. My more detailed analysis revealed that for both the I1- and the I2-test specifically the spike response to the third sound pulse shaped the overall tuning curve. A two-pulse chirp pattern may be sufficient to detect the pulse rate, but it is not efficient to drive phonotaxis, this rather requires the processing of the third sound pulse in a normal chirp. This also demonstrates that the specificity of the response builds up over the time course of the pulse pattern. As in a delay-line coincidence-detection network the processing of each sound pulse has a knock-on effect on the processing of the subsequent one, while the effect depends on the pulse interval.

Sequential effects of auditory processing

The results obtained from the I1- and I2-tests reveal how the system deals with chirps containing only one ‘abnormal’ interval. Increasing the first or second interval beyond the normal level, clearly diminishes the phonotactic response to the level of a two-pulse reference chirp, or even below. The results of the PI-test show how the feature detector LN4 responds when all three intervals in a chirp are systematically modified. When all three intervals were shorter than 15 ms, the initial inhibitory response of LN4 is pronounced, and only single spike or burst of spikes might be generated at the end of the chirp. In the range of normal pulse intervals LN4 generates sequences of pronounced suprathreshold depolarization. However, when the intervals increase beyond 40 ms the inhibition, which is triggered by each sound pulse, starts to dominate the response and consistently diminishes the neuron’s excitatory activity.

The situation is highly similar to the response properties of the AN4 interneuron in the locust and grasshopper auditory pathway, in which a leading inhibition triggered at the start of a sound suppresses spike activity when the auditory system is exposed to song patterns interrupted by small silent intervals (Ronacher and Stumpner 1988; Stumpner and Ronacher 1994). This balance of inhibition and excitation together with the different time courses of the activity points to the crucial filter mechanism at the level of the feature detector.

In the PI-test the activity of LN4 gradually decreased along the second, the third and the fourth sound pulse when the pulse interval was equal to or longer than 30 ms. This suggests that the reduction in the overall activity elicited by the chirps with long PIs is progressively emerging. The gradually shifted peak of the tuning curves and the progressively narrower tuning along the second, the third and the fourth pulses (Fig. 35B) all point towards an accumulative effect of changing successive pulse intervals. It may also be concluded that every pulse interval within a chirp contributes to the activity of the feature detector LN4.This is in accordance with the conclusions from the previous I1 and I2 experiments. The specific tuning curves of the last three sound pulses which elicit spiking activity in LN4 (P2, P3 and P4) showed a different shape and strength. The tuning curves to P3 and P4 exhibit a narrower shape and reflect the tuning curve to the whole chirp better than the response to P2. This indicates that the activity elicited by each sound pulse contributes with a different weight to the overall response of LN4 to a chirp. This could mean that the system, when exposed to chirps with 4 pulses, may tolerate if a single interval is distorted; and also that the phonotactic tuning may become more narrow when more pulses can be analysed. Behavioral experiments could easily test this assumption.

For a single sound pulse the post-inhibitory rebound in LN5 will reach a peak with a latency of about 89 ms, which is about 63 ms after the maximum of the inhibition. Therefore the coincidence between AN1 activity and the post-inhibitory rebound always occurred at the rising phase, as long as the pulse intervals was shorter than 63 ms. However, both the activity of LN4 and the phonotaxis did not show a similar level of response for chirps containing intervals of 50 ms as to the normal chirp. Therefore, the system is recognizing sound patterns not simply by coincidence detection as proposed by Schöneich et al. (2015). Based on the results obtained from the interval tests here, one of the possible mechanisms underlying pattern recognition when pulse intervals are changing may be as follows: the different strength of input received by the coincidence detector LN3 comes from the activity of AN1 (direct line)

coinciding with different state of the post-inhibitory rebound in LN5 (delayed line) at different phases of the post-inhibitory rebound or a different ‘slope’ of the changes in amplitude of the PIRs. Then the interplay between the strength of inhibitory input coming from LN2 and the excitatory input from LN3 determines the number of bursts and spikes at the level of the feature detector LN4. The number of bursts can be integrated to different degrees in the descending pathway based on the intervals between two adjacent bursts. The very sharp phasic spiking activity generated in LN4 may imply a coding mechanism based on the instantaneous spike rate as described by Nabatiyan et al. (2003). Moreover, unlike proposed by Schöneich et al. (2015) that two sound pulses can be the minimal number for pattern recognition, the results here also demonstrated the importance of the third sound pulse in pattern recognition because the tuning curve of LN4 to the third sound pulse exhibited a closer similarity to the tuning of the phonotactic behaviour and phonotactic responses are very low, when only 2 pulses are presented (Hedwig and Sarmiento-Ponce 2017).

In summary, the best phonotactic response occurred in response to chirps containing 20 ms intervals, which was reflected in the tuning curve of the feature detector LN4 and the coincidence detector LN3. The selectivity to chirps containing 20 ms intervals may be a result of the strongest level of coincidence between AN1 and the post-inhibitory rebound of LN5. The possible explanation might be that 20 ms intervals lead to a result that the coincidence between AN1 and LN5 occurred in the rising phase of the rebound and at a membrane state of LN5,which may possess a higher conductance that drives the membrane potential of LN5.

CHAPTER 4: THE EFFECTS OF CHANGING PULSE DURATIONS WITHIN A CHIRP ON PROCESSING BY THE PATTERN RECOGNITION CIRCUIT

INTRODUCTION

According to the delay-line coincidence detector concept (Schöneich et al. 2015) each sound pulse in a chirp will have a knock-on effect on the processing of the subsequent pulse, with the exception of the last pulse. Based on this prediction Hedwig and Sarmiento-Ponce (2017) tested the phonotactic behaviour of female *G. bimaculatus* to chirps with systematic changes in the duration of each pulse of a three-pulse chirp (Fig. 36A). Different to previous test paradigms in which the duration of all pulses in a chirp was changed at one time, here only the duration of the first (P1), second (P2) or the third pulse (P3) was systematically altered between 5 and 100 ms. These tests revealed different characteristic tuning curves of the phonotactic behaviour (Fig. 36B). Testing the effect of changes of P1 demonstrated that the phonotaxis response was already strong at a P1 duration of 5 ms. Phonotaxis showed its maximum at P1-15 to P1-20 and then gradually declined towards P1-50. For longer P1 durations the response fell below the response to a 2-pulse reference chirp. The characteristic curve for P2-chirps was similar, besides P2-5 was less effective, and the response increased strongly at P2-10 ms and stayed close to the reference response for long P2. The tuning to P3 was however substantially different. The phonotactic response increased more gradually towards its broad maximum at P3-25 and – although slightly declining – it then stayed at a high level even at long P3.

Based on these tuning curves, an attractive 3-pulse chirp pattern with increasing pulse durations was designed with a 5-ms pulse played first, followed by a 20-ms pulse and a 50-ms pulse at the end, which combines the very strong response of the different tuning curves (Fig. 36B, C) (Hedwig and Sarmiento-Ponce 2017). It gives a non-attractive pattern, when it is played in reversed order with decreasing pulse durations (50-20-5 ms) as P1-50 and P3-5 only elicited weak phonotaxis (Fig. 36B, C). These patterns were tested in behavioural experiments along with a normal pattern (20-20-20 ms) and a reference pattern with chirps composed of two 20 ms pulses. The results show the attractive pattern and the normal pattern elicit similar levels of phonotaxis, which is significantly higher than the level of phonotaxis caused by the non-attractive pattern (Fig. 36D).

It can be expected that the outcome of these different behavioural tests, will be mirrored

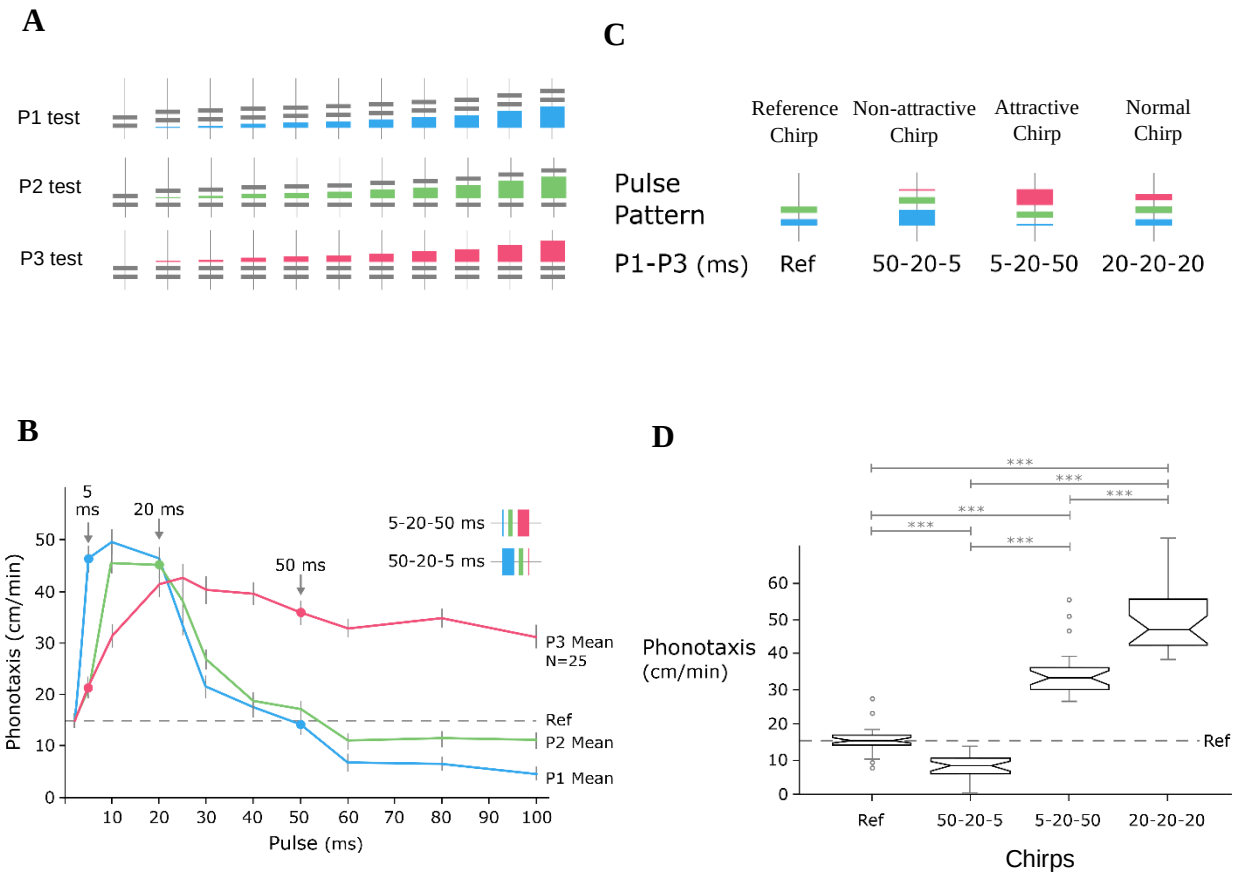

Fig. 36 Effect of changing the duration of sound pulses on phonotaxis. A. Chirp patterns with increasing duration of P1 (blue pulse), P2 (green pulse) and P3 (red pulse). The duration of the sound pulses varied from 5, 10, 20, 25, 30, 40, 50,60, 80 and 100 ms. The other two pulses and all pulse intervals were 20 ms. **B.** Characteristic tuning curves for changes of P1 (blue), P2 (green) and P3 (red). The tuning curves for P1, P2 and P3 indicate that chirps composed of 5, 20 and 50 ms pulses will be efficient to elicit phonotaxis; a lower response is expected if the chirps are played in reverse order. Selected pulses of the tuning curves are indicated and the chirp patterns with 5-20-50 ms and 50-20-5 ms pulses are given in the inset **C.** Chirp patterns of the attractive and non-attractive patterns. The reference chirp was with 20-20 ms pulses, the non-attractive chirp was with 50-20-5 ms pulses, the attractive chirp was with 5-20-50 ms pulses and the normal chirp was with 20-20-20 ms pulses. **D.** Phonotactic responses of 25 females towards the reference chirp, to the non-attractive chirp, to the attractive chirp and to the normal chirp.The phonotactic scores are presented as box-and-whisker plots; whiskers represent the 25th and 75th percentile (lower and upper quartiles, respectively), the band in the middle of the box is the 50th percentile (the median) and open circles indicate outliers (from Hedwig and Sarmiento-Ponce, 2017).

in the neuronal activity of the pattern recognition network. The responses of the spiking and the non-spiking neurons in the pattern recognition network should be different when tested with the different sound patterns. Recording the neurons of the pattern recognition network while presenting the different sound patterns should reveal to what degree the specific changes in pulse duration affect the subsequent neuronal response to a pulse.

METHODS

Details of the dissection, recording and stimulation procedures have been described in Chapter 2. The number of recordings of each neuron was also given in Chapter 2.

Acoustic stimulation paradigms

Five acoustic paradigms were designed to analyse the temporal selectivity of the auditory neurons: P1-test, P2-test, P3-test, PD-test and attractive and nonattractive tests. The patterns are explained below. As the duration of the sound pulses are changed, the intervals in all chirps are kept at 20 ms. The normal chirp in P1, P2 and P3 tests corresponds to chirps containing three 20 ms pulses separated by 20 ms intervals and four 20 ms pulses separated by 20 ms intervals in PD test. The inter-chirp interval in these tests was set as 400 ms.

P1-test: Each chirp in this test consisted of three sound pulses. The duration of the first pulse (P1) was systematically changed between 5, 10, 20, 25, 30, 40, 50 and 80 ms. The duration of the other two pulses (P2 and P3) and the two intervals (I1 and I2) were set as 20 ms (Fig. 37A).

P2-test: The duration of P2 among three sound pulses in the P2-chirps was systematically changed between 5, 10, 20, 25, 30, 40, 50 and 80 ms while keeping the other parameters constant. For example, in P2-50, P2 was 50 ms, whereas P1, P3, I1 and I2 were kept at 20 ms (Fig. 37A).

P3-test: In this test, the duration of P3 was systematically changed as described for P1 and P2 (Fig. 37A).

Pulse duration test (PD-test): The chirps in this test consisted of four sound pulses and three intervals. All four pulses of one chirp were together changed in duration from 5, 10, 15, 20, 25, 30, 40, 50, 60, 80 to 100 ms, while the intervals were kept as 20 ms. For example, in PD-5 four

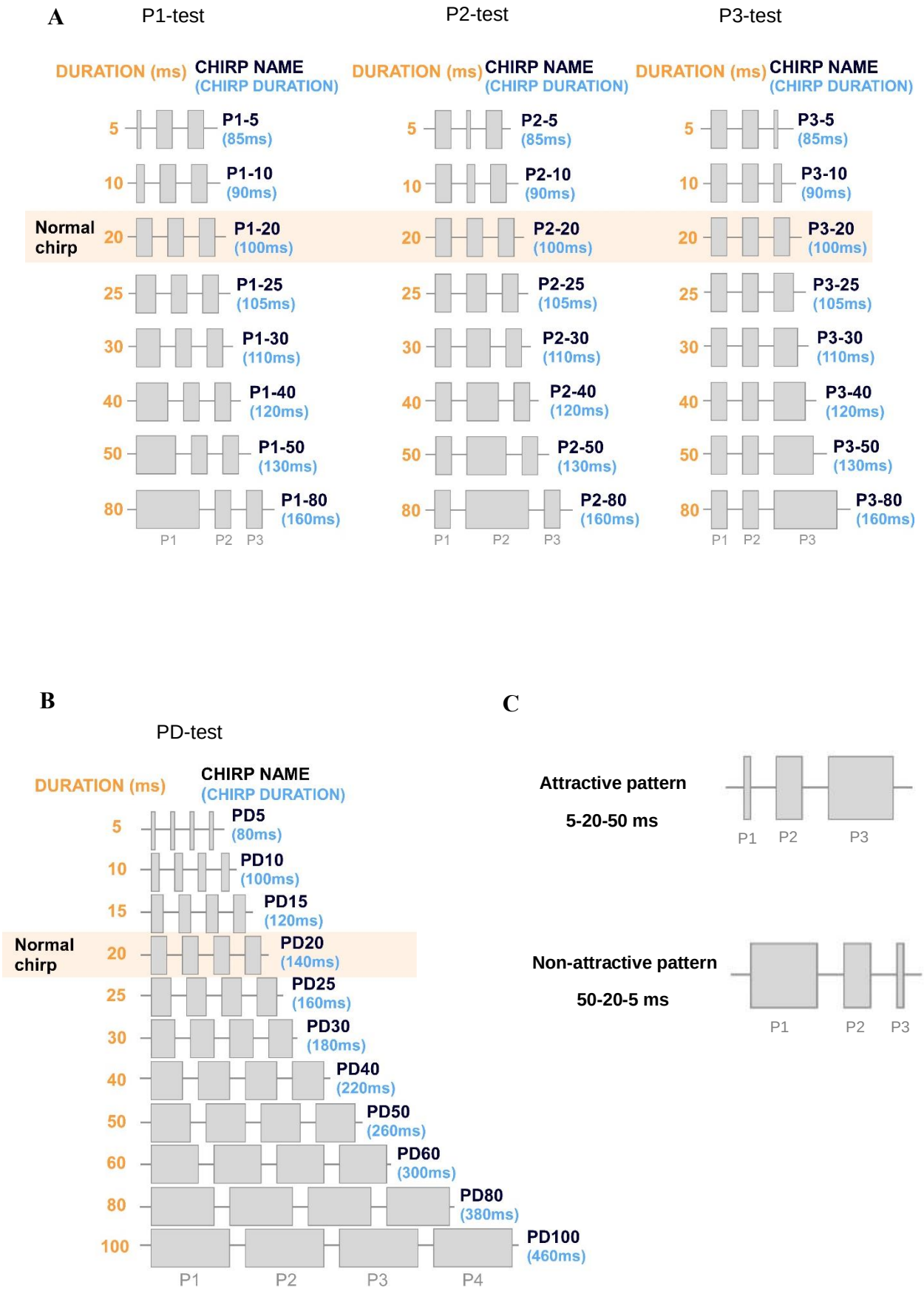

Fig. 37 Sound patterns with the duration of individual pulses (P1-, P2- and P3-tests) and all pulses varied (PD-test) within a chirp.

Fig. 37 Sound patterns with the duration of individual pulses (P1-, P2- and P3-tests) and all pulses varied (PD-test) within a chirp. A. All chirps with 3 pulses, the duration of the varied pulse ranged from 5, 10, 20, 25, 30, 40, 50 to 80 ms, leading to 8 different chirps. Other pulses and pulse intervals were kept at 20 ms. **P1-test:** Chirps with varied duration of the first sound pulse **P2-test:** Chirps with the duration of the second pulse varied. **P3-test:** Chirps with the duration of the third sound pulse altered. **B. PD-test:** Chirps with the duration of all pulses of a 4-pulse chirp were simultaneously varied from 5, 10, 15, 20, 25, 30, 40, 50, 60, 80 to 100 ms. Pulse intervals were set at 20 ms. The normal chirp indicates a chirp with 20-ms pulses separated by 20-ms intervals, designed based on the calling song of *Gryllus bimaculatus*. **C.** The attractive and non-attractive patterns. The attractive pattern is composed of three pulses of 5, 20 and 50 ms, respectively, the non-attractive pattern is composed of 50, 20 and 5 ms pulses, all separated by 20 ms intervals. The carrier frequency was 4.8 kHz and sound intensity was calibrated to 70dB SPL

5 ms pulses were separated by three 20 ms intervals (Fig. 37B). The inter-chirp interval was set to 400 ms.

Attractive and non-attractive test: The attractive chirp contains three sound pulses with a duration of 5 ms (P1), 20 ms (P2) and 50 ms (P3). The non-attractive pattern is consisted of the identical sound pulses however in reversed order as P1 is 50 ms, P2 is 20 ms and P3 is 5 ms (Fig. 37C). All intervals are kept at 20 ms and the inter-chirp interval at 400 ms.

In all paradigms, the rising and falling ramps for sound pulses were 2 ms. Sound stimuli were designed with Cool Edit Pro 2000 software (Syntrillium, Phoenix, AZ, USA). Sound signals were presented by two speakers (Sinus live NEO 13s, Conrad Electronics, Hirschau, Germany) placed frontal to the cricket at an angle of 45º from the left and the right to the animal's long axis. Sound intensity was calibrated to 75 dB SPL relative to 20 µPa at the location of the cricket using a Brüel&Kjær measuring amplifier and a 1/2-inch free field microphone (models 2610 and 4939, respectively; Nærum, Denmark).

For all tests, the chirps were played in a looped mode rather than the repeated mode used in the behavioural test conducted by Hedwig and Sarmiento-Ponce (2017). For example, in my experiments each of the eight chirps in the P1-test (P1-5 to P1-80) was played once in the sequence as shown in Fig. 37A. The sequence of P1-chirps (P1-5 to P1-80) was repeated and in each sequence every of the chirps was played one time, an interval of 1s separated sequences.

RESULTS

In the following I first will present the five neurons of the pattern recognition circuit and their responses to the P1-test, P2-test and the P3-test. At the end of each part I will compare the tuning curves and the responses to elucidate the flow of auditory processing. General features of the neurons e.g. latency of the responses, which are identical for all tests, will only be given for the P1-test. Then the responses of AN1 and LN4 to the PD-test will be presented and compared to the behavioural tuning. Last, the activity of the five neurons elicited by the attractive and non-attractive patterns will be described and compared.

For description of the neuronal responses to the P1-, P2- and P3-tests, I used categories

of short, medium and long chirps. The chirps in short category contain sound pulses shorter than those in the normal chirp (20 ms) (P1-5 to P1-10; P2-5 to P2-10; P3-5 to P3-10). The medium chirps contain pulses between 20 to 30 ms (P1-20 to P1-30; P2-20 to P2-30; P3-20-P3-30) since the phonotactic response exhibited the sharpest decline from the normal chirp in both P1 and P2 tests. The long chirps refer to those containing longer pulses (P1-40 to P1-80; P2-40 to P2-80; P3-40 to P3-80) as the phonotactic responses elicited by these chirps in both P1- and P2-tests were either close to or below the reference level.

Response of the pattern recognition network neurons to chirps with first pulses of different duration: P1- test

The mechanism underlying pattern recognition proposed by Schöneich et al. (2015) indicated that the post-inhibitory rebound generated by LN5 is coupled to the end of the sound pulses. This implicated that changing the duration of the first pulse in a chirp pattern, should not have a strong effect on phonotaxis. Behavioural experiments (Hedwig and Sarmiento-Ponce, 2017) however, revealed that the response to chirps with long first pulses is considerably reduced. My neurophysiological experiments therefore aimed to provide insight into the underlying processing.

The number of recordings of the neurons are: 10 repeats of AN1 (N=5, n=10), 10 repeats of LN2 (N=2, n=10), 10 repeats of LN5 (N=4, n=10), 10 repeats of LN3 (N=5, n=10) and 5 repeats of LN4 (N=5, n=5) for the characteristic responses of the neurons elicited by 20-ms pulses and normal chirps, and 5 repeats of AN1 (N=5, n=5), 2 repeats of LN2 (N=2, n=2), 18 repeats of LN5 (N=4, n=18), 13 repeats of LN3 (N=5, n=13) and 5 repeats of LN4 (N=5, n=5) for the P1-test.

The ascending neuron – AN1

AN1 forwards information to the inhibitory neuron LN2 *and* the coincidence detector LN3 (Fig. 38A), its activity reflects the duration of the sound pulses (Fig. 38B).

<u>AN1 response to a single 20 ms sound pulse and the normal chirp</u>

The neuron responded to 20 ms pulses with a consistent activity of 6.5±0.0 AP/pulse and to the normal chirp with 19.5±0.6 AP/chirp. The duration of the spiking activity elicited by a single 20 ms sound pulse was 22.1±0.2 ms (n=10). The latency of AN1 in response to the normal chirp

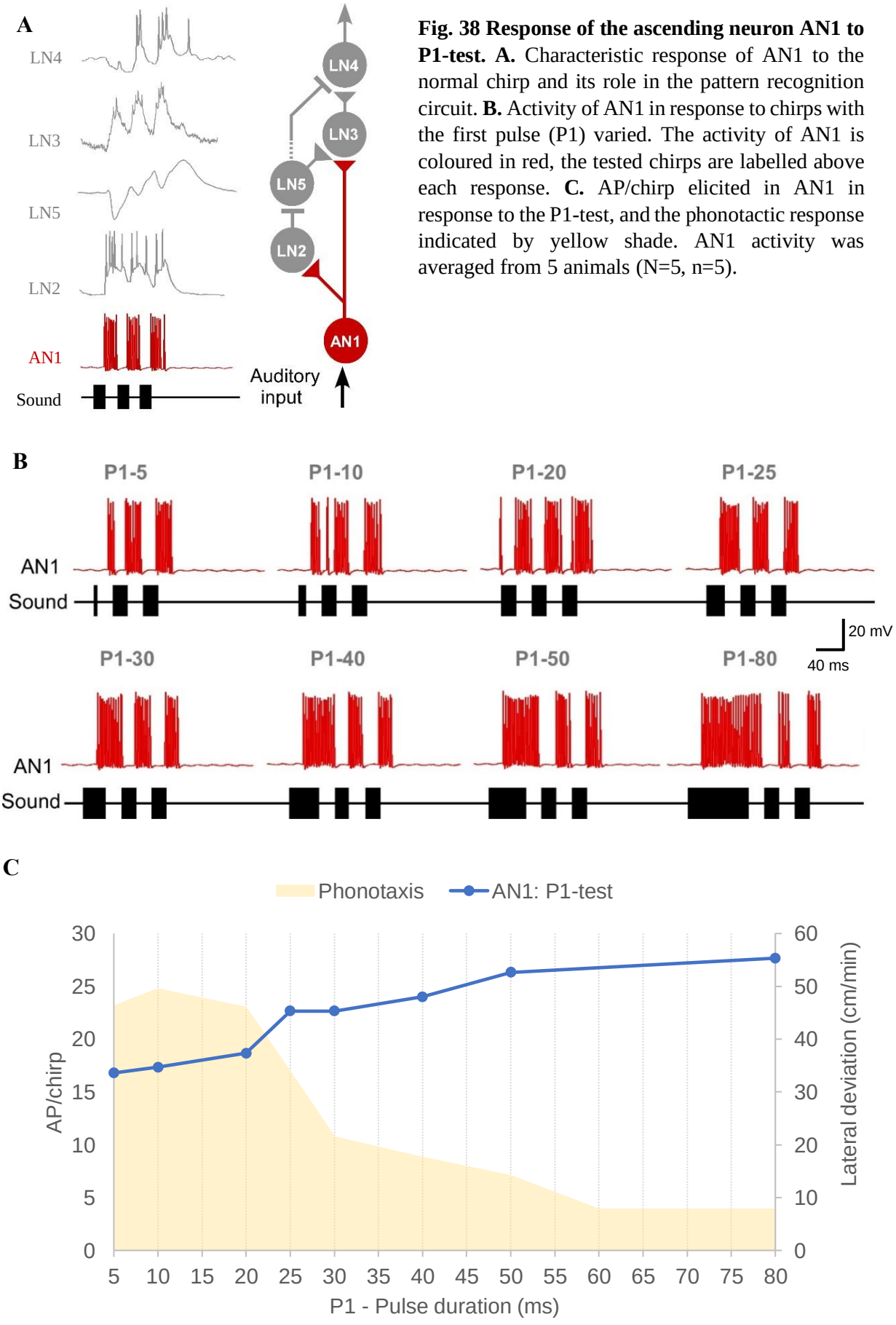

Fig. 38 Response of the ascending neuron AN1 to P1-test. A. Characteristic response of AN1 to the normal chirp and its role in the pattern recognition circuit. **B.** Activity of AN1 in response to chirps with the first pulse (P1) varied. The activity of AN1 is coloured in red, the tested chirps are labelled above each response. **C.** AP/chirp elicited in AN1 in response to the P1-test, and the phonotactic response indicated by yellow shade. AN1 activity was averaged from 5 animals (N=5, n=5).

was 18.9±0.1 ms to the first sound pulse, 18.4±0.2 ms to the second and 19.6±0.1 ms to the third sound pulse (n=10).

AN1 response to P1-chirps

Since AN1 reflects the duration of the pulses the number of spikes elicited by the various P1-chirps was different from each other (p=0.0049, Friedman test, N=5, n=5). As the duration of P1 increased from 5 to 80 ms, the number of spikes of AN1 increased from 21.3±0.3 to 27.7±0.3 AP/chirp, nearly linearly with a slope of m=0.1264 (R^2=0.7585, correlation coefficient), (Fig. 38B, C). When P1 was longer than 25 ms, AN1 responded to the chirps with a significantly greater number of spikes than to the normal chirp (P1-30 vs. P1-20: p<0.0001, P1-40 vs. P1-20 p=0.0424, P1-50 vs. P1-20 p=0.0053, P1-80 vs. P1-20 p=0.0115, Friedman test, N=5, n=5), (Fig. 38C). The tuning curve of AN1 activity did not match the behavioural tuning for varying the duration of P1 (Fig. 38C).

The inhibitory neuron – LN2

Neuron LN2 is driven by AN1 and inhibits both the non-spiking neuron LN5 and the feature detector LN4 (Fig. 39A).

LN2 response to a single 20 ms sound pulse and the normal chirp

The depolarisation evoked by a single 20 ms sound pulse always slowly declined and gave a duration of 58.4±3.8 ms, while the spiking activity lasted for 25.0±1.9 ms. In response to the normal chirp LN2 generated 8.4±0.1 AP (Fig. 39B, P1-20). Its change in membrane potential in response to the first pulse occurred with a latency of 19.9±0.2 ms and its spiking with a latency of 22.2±0.2 ms (Fig. 39B, P1-20). The first sound pulse elicited 5-6 spikes. The initial phasic response with 3-4 spikes reached a spike rate of 236.2±6.5 Hz and lasted 10.3±0.2 ms, while the overall spiking activity lasted 25.0±1.9 ms. The underlying depolarization was shorter than that elicited by a single 20 ms pulse and lasted 39.2±0.7 ms which remained the same level when elicited by the second sound pulse 40.6±0.6 ms. The latencies of the second depolarisation and the spiking event to the second sound pulse were 21.7±0.5 and 24.5±0.5 ms. The duration of the second spiking activity was 20.5±1.7 ms, and 4.5 ms shorter than the first one (25.0±1.0 ms) (p=0.018, t-test, n=10). The spiking activity further decreased in duration in response to the third sound pulse P3, which lasted only 10.0±0.7 ms (P2 vs. P3: p=0.001, t-test, n=10) (Fig. 39B, P1-20, Table. 1). The latencies of the depolarisation and the spikes elicited by the third

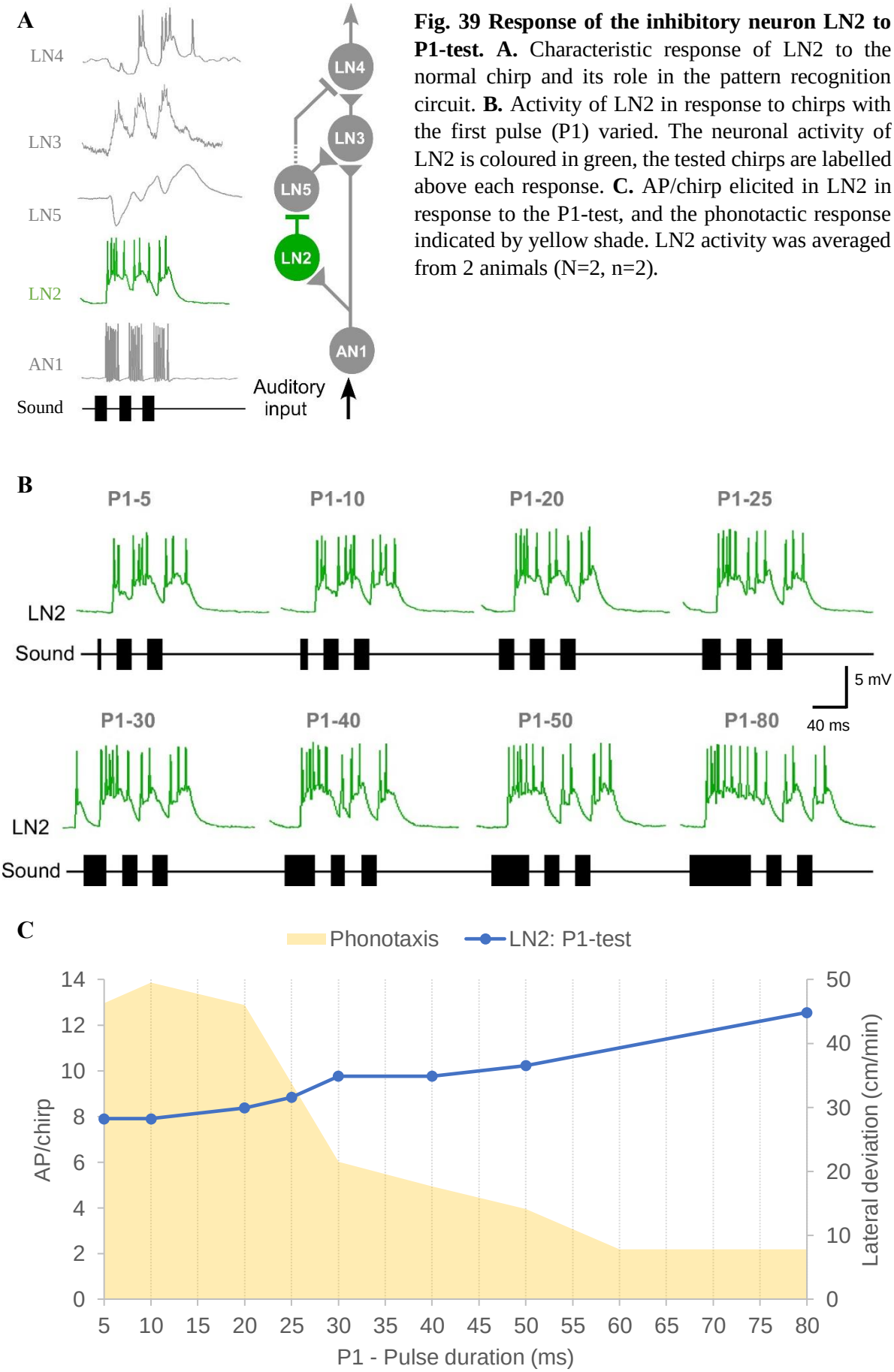

Fig. 39 Response of the inhibitory neuron LN2 to P1-test. A. Characteristic response of LN2 to the normal chirp and its role in the pattern recognition circuit. **B.** Activity of LN2 in response to chirps with the first pulse (P1) varied. The neuronal activity of LN2 is coloured in green, the tested chirps are labelled above each response. **C.** AP/chirp elicited in LN2 in response to the P1-test, and the phonotactic response indicated by yellow shade. LN2 activity was averaged from 2 animals (N=2, n=2).

sound pulse were 22.5±0.5 and 26.4±0.5 ms. For the last response the depolarisation was 54.9±1.9 ms and declined to the resting potential, thus lasting longer than the first two responses. The spiking activity elicited by the first, the second and the third sound pulse follow AN1 by about 3.3, 6.1 and 6.8 ms, respectively, while the depolarisation of LN2 always occurred with a latency of only 1 ms after AN1 spikes activity. Compared to AN1, LN2 responded to single 20 ms pulse with a longer spiking activity (AN1: 22.1±0.2 ms; LN2: 25.0±1.9 ms, both n=10). As the intervals were constant at 20 ms, the rather long depolarisations elicited by the first two sound pulses merged and did not decline to the resting potential (Fig. 39B, P1-20).

LN2 response to P1-chirps

Across all chirps in the P1-test, each pulse elicited a suprathreshold depolarisation with several spikes, and the increase of P1 led to linearly increased activity of LN2 with a slope of m=0.0629 (AP/chirp)/ms (R^2=0.9694, correlation coefficient); activity started from 7.9 AP/chirp at P1-5 and reached a maximum of 12.6 AP/chirp at P1-80 (Fig. 39C). Similar to AN1 the LN2 tuning did not fit the behavioural tuning to the P1-test, while its overall spike activity based on all eight chirps in the P1-test was 58.19±1.11% less than the AN1 activity (Fig. 39C).

The non-spiking neuron – LN5

The non-spiking neuron LN5 is inhibited by LN2 and generates a delayed post-inhibitory rebound (PIR), which drives the coincidence detector LN3 (Fig. 40A).

LN5 response to 20 ms sound pulse and the normal chirp

Its typical response pattern has been described before (see Chapter 1, LN5). The peak of the post-inhibitory rebound elicited by a single 20 ms sound pulse occurred at a latency of 89.4±2.2 ms, as measured from I1-80. In response to a normal chirp, the response of LN5 can be characterised by three consecutive inhibitory responses INH1, INH2 and INH3, each of which leads to a subsequent post-inhibitory rebound depolarisation i.e. PIR1, PIR2 and PIR3 (Fig. 40B). It is noteworthy that although P1 initiates the first inhibition which starts the subsequent rebound, the latency and amplitude of the peak of the first rebound (PIR1) is defined by P2, as the start of the second inhibition cuts off the first rebound, i.e. PIR1 occurs after P2 (Fig. 40B). Besides, both PIR2 and PIR3 occur after the third sound pulse. Therefore, the latency of PIR1 will be given in relation to the onset of the second sound pulse (P2). Similarly, the latency of PIR2 and PIR3 will be measured from the start of the third sound pulse (P3).

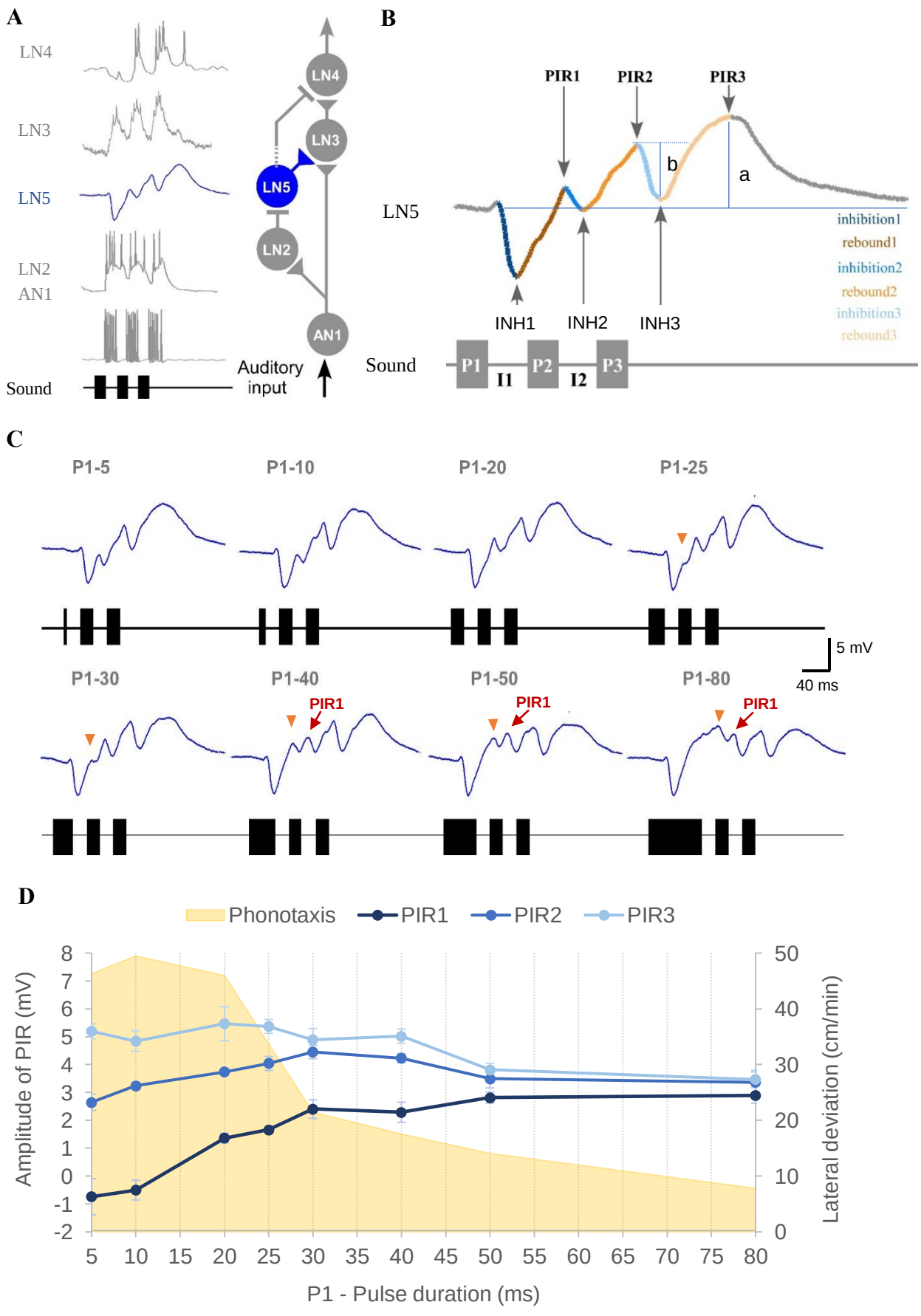

Fig. 40 Activity of LN5 elicited by the P1-test and the tuning of the amplitude of PIRs.

Fig. 40 Activity of LN5 elicited by the P1-test and the tuning of the amplitude of PIRs. A. Diagram showing characteristic activity of LN5 to the normal chirp and its role in the pattern recognition circuit. **B.** Activity elicited in LN5 in response to a normal chirp. P1, P2 and P3 represent the three sound pulses, I1 and I2 refer to the two intervals. LN5 responds to the three pulses with three inhibitions (inhibition1, inhibition2 and inhibition3) and three rebounds (rebound1, rebound2 and rebound3). The maximum amplitudes of the inhibitions are labelled as INH1, INH2 and INH3. The highest membrane potential of rebound1 (brown) and rebound2 (orange) are marked as PIR1 and PIR2, they occur at the start of the following inhibition (blue and light blue). The peak amplitude of rebound3 (light yellow) is labelled as PIR3, this rebound is not interrupted by an inhibition. **C.** Average responses of LN5 to the P1 test (N=4, n=18). The activity of LN5 is coloured in blue, the tested chirps are labeled above each recording. Orange arrowheads represent the additional peak formed in rebound1 in response to P1-25 to P1-80. Red arrows indicate the peak of the first rebound (PIR1) generated by P1-40 to P1-80 for the purpose of discriminating from the additional peak. **D.** Maximum amplitude of the rebounds over the P1-test. The PIR1, PIR2 and PIR3 are coloured in dark to light blue. Error bar indicate the standard error of the mean (SEM). Phonotactic response is indicated by yellow shade.

The latency of LN5 activity to each sound pulse were very similar (Table. 1, LN5 LAT_{inh}). The three inhibitory responses (INH1-INH3) reached a maximum amplitude all with a latency of around 36.2 ms (INH1: 36.4±0.5 ms to P1; INH2: 35.4±1.0 ms to P2; INH3: 36.9±0.3 ms to P3), which is about 10 ms after the start of each inhibition (Table. 1, LN5 $LAT_{max\ inh}$). This may be related to the onset spiking activity in LN2.

Due to the post-inhibitory rebound activity, each inhibition was followed by a rebound depolarisation, which was transiently interrupted by the subsequent inhibition. Therefore, the peak of each PIRs in response to the normal chirp is defined by the start of subsequent inhibition. The PIR1 reached a maximum amplitude of 1.1±0.2 mV at 25.7±0.5 ms after the second sound pulse, PIR2 reached 3.6±0.1 mV with a latency of 26.2±0.4 ms to the third sound pulse and maximum amplitude of PIR3 was 5.4±0.3 mV at 79.9±3.1 ms after the onset of the third sound pulse. The amplitude of the PIRs was measured between the resting potential and the peak of the PIR, as indicated for the amplitude of PIR2 (Fig. 40B, a). The amplitude of the inhibition was measured from the starting point of the inhibition (i.e. resting potential for INH1; or the peak of the previous PIR for INH2 and INH3) to the lowest point as shown for the amplitude of INH3 (Fig. 40B, b).

LN5 responses to P1-chirps

The LN5 responses reveal that even P1-5 elicited a pronounced inhibition, followed by a post-inhibitory rebound. Aligning the LN5 activity to the start of the first sound pulse (Fig. 41A) reveals that the first inhibition generated by LN5 was not affected by the duration of P1. INH1 always started with a latency of 26.4±0.2 ms and reached an amplitude of -3.3±0.0 mV with a latency of 36.4±0.5 ms which is 10.0±0.1 ms after the onset of the inhibition. Thus, INH1 is not maintained for the duration of the sound pulse, this is different to previous reports (Schöneich et al. 2015). The start of the post-inhibitory rebound depolarisation leading to PIR1 is not coupled to the end of the sound pulses, it rather starts from the peak of INH1, and for all P1 pulse durations initially follows a very similar time course (Fig. 41A). Although starting from different membrane potentials, the strength of the other two inhibitions were constant across the P1-test, with a mean amplitude of 1.8±0.2 mV (INH2) and 3.2±0.1 mV (INH3). Therefore, I will focus on describing the time course of the PIRs in the following paragraphs.

For short P1 (P1-5 and P1-10), the first sound pulse was too short for the first rebound to develop an amplitude reaching above the resting potential, PIR1 reached an amplitude of -

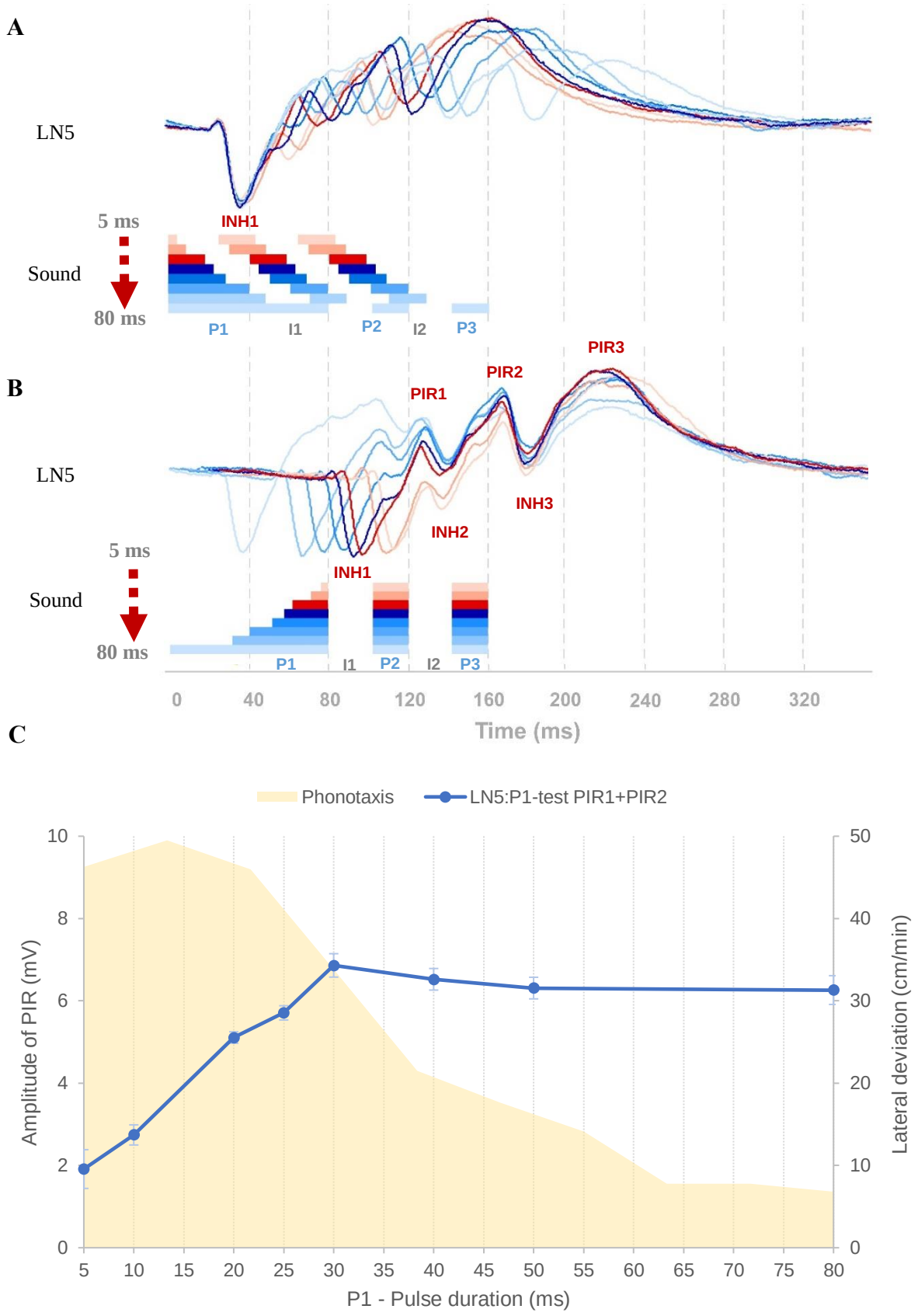

Fig. 41 LN5 activity elicited by P1-test aligned to the first or the last sound pulses and the tuning curves of summed PIRs.

Fig. 41 LN5 activity elicited by the P1-test aligned to the first or the last sound pulse and the tuning curves of summed PIRs. A. Averaged LN5 activity in response to the P1-test aligned to the onset of P1 (N=4, n=18). **B.** Averaged LN5 activity aligned to the onset of P2. When P1 is smaller than 25 ms, the chirps and LN5 responses (P1-5, P1-10, P1-20 and P1-25) are coloured as light to dark red, respectively. For P1 equal to or larger than 25 ms, chirps and LN5 responses are coloured as dark to light blue, respectively. Responses in dark red and blue are to chirps P1-20 and P1-25 that elicit the best phonotactic behaviour. **C.** Sum of PIR1 and PIR2 over the P1-test. Error bar indicates the standard error of the mean (SEM). Phonotactic response is in yellow shade.

0.7±0.6 mV (P1-5) with a latency of 29.1±0.3 ms. and -0.5±0.4 mV (P1-10) at 28.8±0.2 ms. Since the peak of the PIRs were formed from the interruption by the subsequent inhibition, the latency of the PIR1 was tightly coupled to the start of the second sound pulse (Fig. 41B). The second rebound then overshot the resting potential with an amplitude of 2.7±0.3 mV (P1-5) and 3.2±0.1 mV (P1-10). Similar to PIR1, the peak of PIR2 was tightly coupled to the start of the third sound pulse, resulting in identical latencies (28.9±0.1 ms to the onset of the third sound pulse) across the P1-test. The third rebound then developed to a higher membrane potential. With a completed peak, PIR3 reached an amplitude of 5.2±0.3 mV at 94.6±0.6 ms (P1-5) and 4.8±0.3 mV at 82.3±0.4 ms (P1-10) after the onset of the third sound pulse. It took another 110.1 ms (P1-5) and 126.2 ms (P1-10) for the third rebound to fully decline and return to the resting potential.

For medium P1 (P1-20 to P1-30), all three PIRs elicited by a chirp occurred above the resting potential. As P1-20 has described in the '*normal chirp*' section, I will not describe it again here. During the first rebound, a deflection of the membrane potential emerged which formed small 'bump' and can be recognised for P1-25 and P1-30 (Fig. 40C, P1-25 and P1-30, orange arrowheads). The 'bump' occurred with a latency of 56.6 ms to the onset of the first sound pulse for P1-25, and 60.2 ms for P1-30, which are 31.6 and 30.2 ms after the start of the first inhibition, respectively. The PIR1 in response to these chirps reached an amplitude of 1.7±0.1 mV (P1-25) and 2.4±0.3 mV (P1-30), its latency was 27.8 and 28.8 ms after the onset of the second sound pulse, respectively. The second PIR2 reached an amplitude of 4.0±0.3 (P1-25) and 4.5±0.2 mV (P1-30) and was higher than PIR1. The amplitude of PIR3 elicited by P1-25 and P1-30 was 5.4±0.2 and 4.9±0.4 mV, respectively. Even though the absolute amplitude of PIR3 here was still greater than PIR2, the difference between PIR2 and PIR3 became less prominent compared to that for the short P1.

For long P1 (P1-40, P1-50 and P1-80), the deflection during the first rebound became more prominent and formed an extra peak during the rebound (Fig. 40C, P1-40, P1-50 and P1-80, orange arrowheads), it even exceeded the PIR1 as P1 increased in duration to P1-80. The peaks of PIR1 for P1-40 to P1-80 are pointed out (Fig. 40C, red arrows) as the extra rebound peak (Fig. 40C, orange arrowheads) became more pronounced. The extra peak occurred with a latency of 69.9±0.3 (P1-40), 79.4±0.4 (P1-50) and 108.2±2.0 ms (P1-80) to the onset of the first sound pulse. These latency gave very similar delay to the offset of P1 about 29.9 ms (P1-25: 31.6 ms; P1-30: 30.2 ms; P1-40: 29.9 ms; P1-50: 29.4 ms; P1-80: 28.2 ms). As the rebound had

more time to develop, the amplitude of PIR1 elicited by long P1 was larger than those elicited by short and medium P1, giving 2.3±0.4 mV for P1-40, 2.8±0.2 mV for P1-50 and 2.9±0.3 mV for P1-80. The difference between the peaks of the first and the second rebound (PIR1 and PIR2) for long P1 was less prominent and they gradually converged in amplitude as P1 increased from 40 to 80 ms (Fig. 40C). The amplitude of PIR2 was 4.2±0.2 for P1-40, 3.5±0.3 for P1-50 and 3.4±0.4 mV for P1-80. The peak of the last rebound (PIR3) was still larger in amplitude (5.0±0.3 mV) than PIR1 and PIR2 in response to P1-40, whereas in response to P1-50 and P1-80 the amplitude of PIR3 decreased to almost the same level as the PIR1 and PIR2 (P1-50: 3.8±0.2 mV; P1-80: 3.4±0.3 mV).

The typical membrane potential oscillations of the three rebounds in LN5 as driven by the normal pattern also occurred for the short P1-chirps (P1-5 to P1-20). The peak amplitudes of the three rebounds clearly increased over a chirp when P1 was in a range of 5 to 20 ms (Fig. 40C), indicating an underlying enhanced depolarisation of LN5. For medium and long P1 (PI-25 to P1-80), this effect became less prominent, and when P1 was 80 ms the peak amplitudes of the rebounds rather decreased over the duration of the chirps. This less pronounced trend in the overall increase of the PIRs may be linked to the extra deflection in the membrane potential during the first rebound (Fig. 40C, 41B, orange arrowheads), which emerged for medium P1 and became more pronounced and formed an additional peak for long P1. This extra deflection could result from additional excitatory inputs that transiently drive the rebound, or may be caused by an extra inhibition, that is not directly linked to the sound pattern and that interrupts the build-up of the rebound. Compared to the regular membrane potential oscillations elicited by the normal pattern (P1-20) the rebounds became irregular and distorted at long P1. The duration of P1 should therefore be relevant for the subsequent processing in the pattern recognition circuitry. Since PIR1 and PIR2 are determined by the second and the third inhibition, the latency of PIR1 and PIR2 to the second and the third sound pulses was not affected by the increase of the P1 sound pulses. Also, PIR3, the only completed rebound that was not affected by a subsequent inhibition, occurred with a quite constant latency of 98.9±0.9 ms after the start of last sound pulse (Fig. 41B).

For a quantitative analysis of LN5 activity I plotted the amplitudes of PIR1 to PIR3 (Fig. 40D). The amplitude of PIR1 increased linearly from -0.7±0.7 to 2.4±0.3 mV with a slope of m=0.1322 (R^2=0.9768, correlation coefficient) when P1 increased from 5 to 30 ms (Fig. 40D), it then increased more slightly from 2.4±0.3 to 2.9±0.3 mV (m=0.0113, R^2=0.6686, correlation

coefficient) for P1-30 to PI-80. The amplitude of PIR2 increased from 2.7±0.3 to 4.5±0.2 mV when P1 increased from 5 to 30 ms (Fig. 40D), it then decreased to 3.5±0.3 mV when the P1 duration was 50 ms, and it remained at a level of 3.4±0.4 mV up to P1-80. The amplitude of PIR3 was at 5.1±0.1 mV when P1 was between 5 ms and 40 ms, it then gradually decreased to 3.5±0.3 mV when P1 increased to 80 ms (Fig. 40D). The different amplitudes of PIR2 and PIR3 are also illustrated by aligning the LN5 activity by P2, as shown in Fig. 41B.

In response to a 3-pulse chirp, the peak of the last rebound does not contribute to the coincidence detection; only PIR1 and PIR2 can contribute to the input to the coincidence detector LN3. I therefore summed the amplitudes of PIR1 and PIR2 and plotted these as in Fig. 41C. When P1 increased from 5 to 30 ms the summed amplitude increased from 1.9±0.5 mV to 6.9±0.3 mV with a slope of m=1.2864 (R^2=0.9629, Pearson Correlation Coefficient), then the amplitude slightly decreased to 6.3±0.3 mV when P1 was 80 ms.

Overall, the strong phonotactic responses elicited by P1-5 and P1-10 and the sharp reduction in response to P1-30 and longer P1-chirps were not reflected in any of these LN5 parameters evaluated.

I also analysed the velocity of the change in the peak amplitude of the three PIRs over the time course of the chirps (Fig. 42, illustrated for 4 chirps by arrows 1 to 3; see Interval Chapter). For example, for the normal chirp the slopes are revealed from the start of the resting membrane potential to the peak of PIR1 (1) over t1, from the peak of PIR1 to the peak of PIR2 (2) over t2, and from the peak of PIR2 to the peak of PIR3 (3) over t3. In response to P1-5 (Fig. 42, P1-5) the first PIR has a low amplitude and the initial slope is slightly negative (arrow 1), however PIR2 and PIR3 are both increasing revealing a subsequent increase in the response (Fig. 42, P1-5, arrows 2,3). In response to the normal chirp, the amplitude of the PIRs continuously increased over the chirp exhibiting three positive slopes (Fig. 42, P1-20). For P1 of 50 ms (Fig. 42, P1-50), an additional peak occurred during PIR1, which slightly reduced the slope of arrow 1 compared to that in P1-20. PIR2 reached a higher amplitude than PIR1 (arrow 2), whereas PIR3 only slightly increased in amplitude compared to PIR2 (arrow 3). In case of P1-80 (Fig. 42, P1-80), the additional peak became more pronounced than in P1-50, and the amplitude of PIR1 became smaller than that of the additional peak. The steepness of slope 1 became smaller than that in P1-50, and PIR2 reached an amplitude similar to PIR1 (arrow 2). PIR3 remained at the similar level as PIR2, resulting in a flat slope (arrow 3). The development of the PIR maxima over the time course of the chirps demonstrates that for P1 shorter than 20

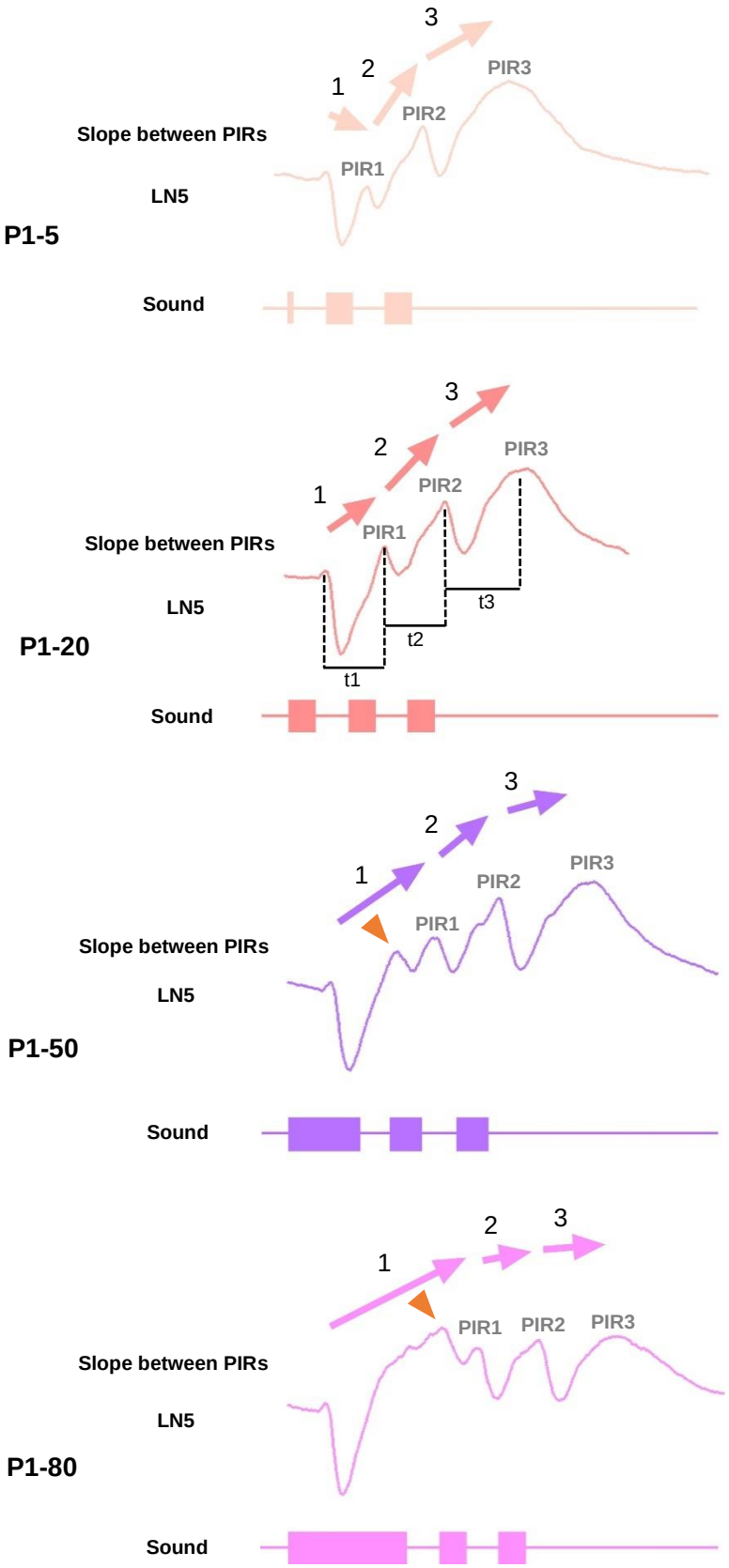

Fig. 42 The changes in the amplitude of adjacent PIRs over time (slope between PIRs) in P1-test.

Fig. 42 Changes in the amplitude of adjacent PIRs (slope between PIRs) over different chirps in the P1-test. The changes in the maximum amplitude of adjacent rebounds over time in response to four example chirps (P1-5, P1-20, P1-50 and P1-80) of the P1-test (N=4, n=18). The arrows indicate the change and slope between two adjacent PIRSs over the time interval between the PIRs (t1, t2 and t3), which are named as slope1, slope2 and slope3. Slope1 and slope2 were directly influenced by varying P1. Orange arrowheads indicate the extra peak generated in the first rebound.

ms, the PIR amplitudes did not exhibit a continuous increase as seen in response to the normal chirp, which revealed the strongest increase. When P1 was longer than 20 ms, a pronounced increase of the PIRs no longer occurred, the amplitudes became rather flat.

This overall trend of the change in the peak amplitude of the three PIRs was quantified by averaging the three slopes. For example, the slope1 of LN5 in response to P1-20 is the differences in the membrane potential between the resting potential and PIR1 over the duration of t1. For the P1-chirps the overall slope is averaged from slope 1, 2 and 3 (Fig. 42) and is plotted in Fig. 43. Overall the tuning of the slopes is in good agreement with the phonotactic tuning and shows a better match than any of the other LN5 activity parameters. The LN5 activity is high for the range of P1-5 to P1-20 when also the phonotactic response is high, and it declined like the behavioural response with longer P1 durations. Although not fully coupling to the behavioural tuning in all scales, the relatively high level of phonotactic response for short P1 and the declining trend of the phonotactic response when P1 was longer than 20 ms were reflected in the tuning curve of the averaged slopes (Fig. 43). This indicates that the peak amplitude of the three PIRs over the time course of the chirps may be relevant for the phonotactic tuning.

Three features of the PIRs of LN5 elicited in the P1-test are noteworthy. 1. The post-inhibitory rebounds start from the peak of the inhibition elicited by the sound pulses. The peaks of PIR1 and PIR2 are defined by the start of the inhibition triggered by P2 and P3, respectively. 2. Pulses longer than 20 ms lead to an additional peak in the first rebound, which increased in amplitude and was coupled to the end of the sound pulse. 3. The three PIRs elicited by a normal chirp successively increased in amplitude. The overall change in the PIR peak amplitudes (average slope) corresponded well with the phonotactic tuning.

The coincidence detector – LN3

Neuron LN3 functions as the coincidence detector in the network and is driven by a direct input from AN1 and a delayed graded input from LN5 (Fig. 44A).

LN3 response to a single 20 ms sound pulse and the normal chirp

In response to a single 20 ms sound pulse, LN3 generated a prolonged depolarisation which lasted for 34.1±0.8 ms (Table. 1). The latency of the beginning of the depolarisation and the first spike were 23.2±0.2 and 34.1±0.8 ms, respectively (Table 1). As the intervals were set to

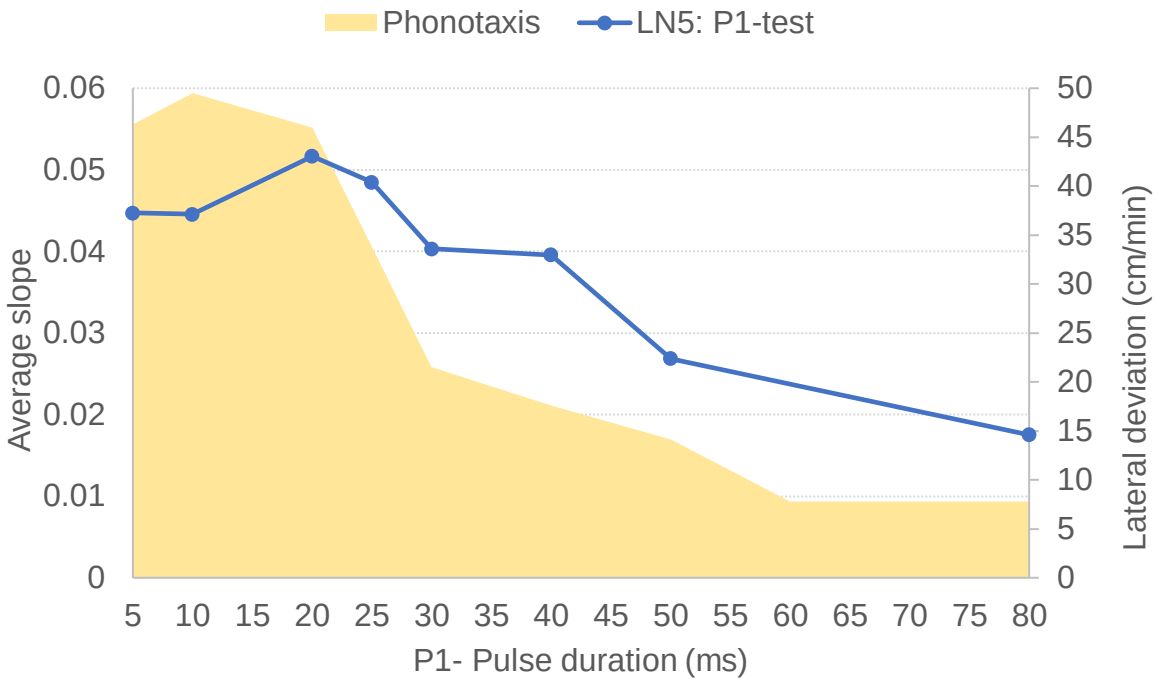

Fig. 43 Tuning of the mean 'slope' of LN5 in the P1-test. The tuning curve is averaged from slope1, slope2 and slope3 in response to each chirp of the P1-test (N=4, n=18). Phonotactic response is in yellow shade.

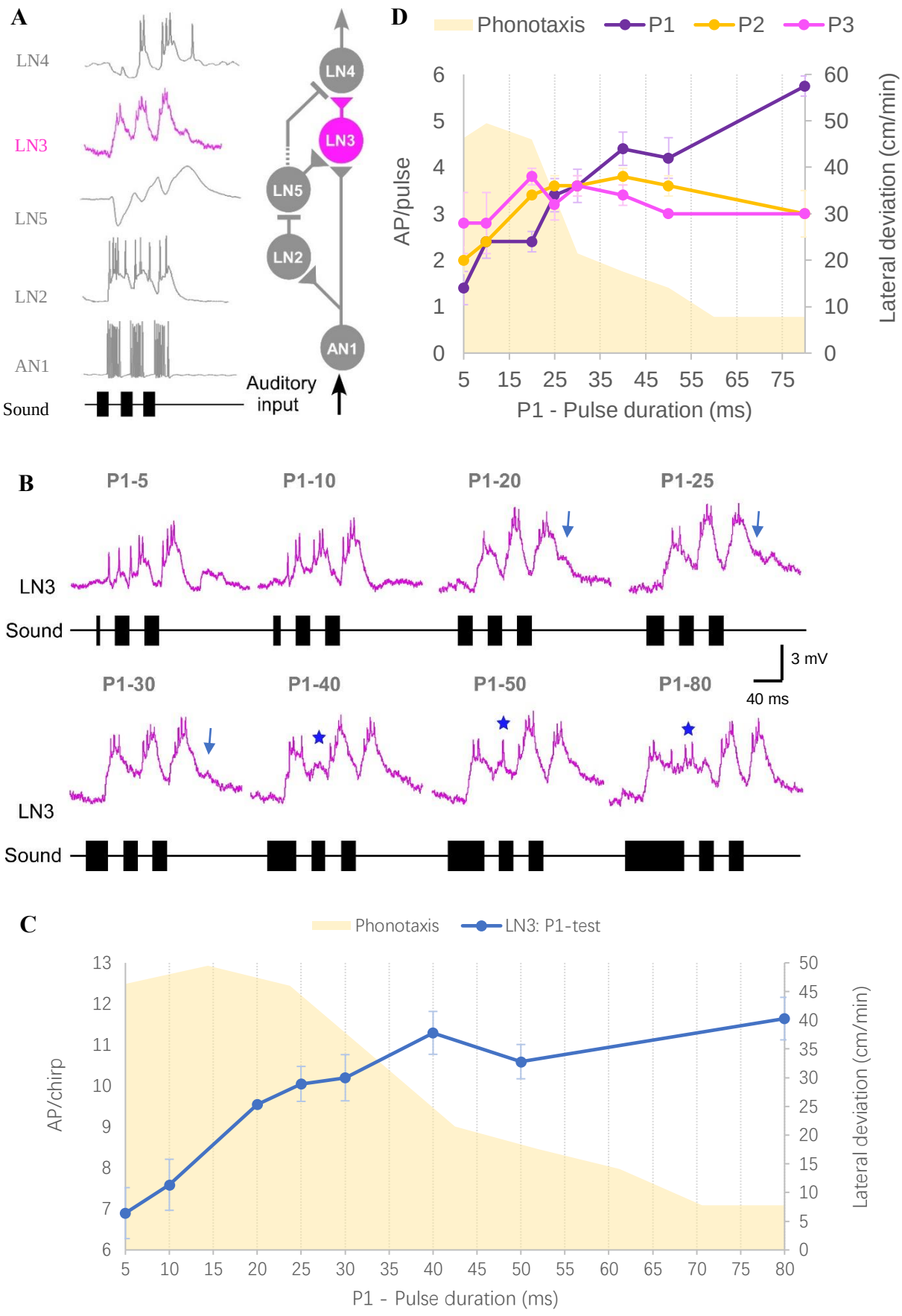

Fig. 44 Response of the coincidence detector neuron LN3 to P1-test.

Fig. 44 Response of the coincidence detector neuron LN3 to P1-test. A. Characteristic response of LN3 to the normal chirp and its role in the pattern recognition circuit. **B.** Activity of LN3 in response to the P1-test. Activity of LN3 is coloured in pink, the chirp label is given above each response. Blue arrows indicate a delayed depolarization after the end of the third burst of spikes. LN3 shows a biphasic response to long P2. For long P1 blue stars represent a biphasic depolarization with extra spikes following the initial suprathreshold depolarisation. **C.** AP/chirp elicited in LN3 in response to the P1-test (N=5, n=13), and the phonotactic response indicated by yellow shade. **D.** AP/pulse elicited in LN3 by each pulse within a chirp (N=5, n=13). Error bars represent standard error of the mean (SEM). Phonotactic response is in yellow shade.

20 ms in this test, the depolarisation evoked by a sound pulse did not return to the resting potential before the next depolarisation was elicited. The latency of the depolarisation and spikes evoked by the second sound pulse P2 were 23.4±0.4 ms and 27.3±0.4 ms, and for the activity elicited by the third sound pulse P3, the latency was 24.0±0.2 (depolarisation) and 29.8±0.5 ms (spikes), respectively. The duration of the depolarisations evoked by P1 and P2 were similar (P1: 33.8±0.3 ms and P2: 33.7±1.3 ms). Without subsequent stimuli, the third sound pulse gave a longer depolarisation of 41.5±2.1 ms. The spiking activity, however, was more transient and lasted only 6.7±0.6 (P1), 16.7±1.3 (P2) and 14.2±0.8 ms (P2) (Table 1). Following the last burst of spikes, a subthreshold excitatory activity sometimes occurred with a latency of 68.6±0.9 ms to P3, which may be an input from the post-inhibitory rebound of LN5 (Fig. 44B, blue arrows).

LN3 response to P1-chirps

For short P1 (P1-5 and P1-10), LN3 did not show a clear response coupled to the pulses. The 5 ms sound pulse did not elicit a clear depolarisation and only 1.4±0.4 APs, and the 10 ms sound pulse in P1-10 only evoked a low amplitude depolarisation with 2.4±0.4 APs. However, for medium and long P1, LN3 gave a good representation of the sound pattern, each pulse elicited a separate suprathreshold depolarisation causing several spikes (Fig. 44B). For medium P1 (P1-25 and P1-30), the responses of LN3 were similar to that evoked by the *normal* chirp: the second and the third bursts of spikes were stronger than the first one. Therefore, when P1 was equal to or shorter than 30 ms, the second pulse (P2) always elicited a stronger response than P1.

For long P1 (P1-40, P1-50 and P1-80), the initial burst of spikes elicited by the first sound pulse did not increase with the duration of the sound pulse, rather an additional depolarisation emerged following the first burst of LN3 spikes. The additional depolarisation eventually initiated spikes, when P1 was 50 and 80 ms (Fig. 44B, blue stars). This demonstrates a form of intrinsic network oscillations that was not described before, which may be linked to a pulse duration filter. This additional excitatory activity did not affect the following activity elicited by P2 and P3, which gave a similar number of spikes as for the *normal* and medium P1. Although not obvious in every response in Fig. 44B, an EPSP was observed regularly following the three responses elicited by the sound pulses (Fig. 44B, blue arrows). Both the additional depolarisation (Fig. 44B, blue stars) and the EPSP at the end (Fig. 44B, blue arrows) may be linked to the PIRs of LN5, which are an input to LN3. The dendritic recordings demonstrated that over the time course of a chirp, the membrane potential of LN3 did not completely

repolarise in the pulse intervals. The neuron rather generated a maintained depolarisation with the responses to the sound pulses superimposed. The spike activity to all P1-chirps of LN3 was 56.75±1.83 % lower than the activity in AN1, which indicates a more sparse coding for the sound patterns.

Quantitative analysis revealed that the LN3 activity showed a significant difference between all P1-chirps (p<0.0001, Friedman test, N=5, n=13) ranging from 6.9±0.6 AP/chirp (P1-5) to 11.6±0.5 AP/chirp (P1-80). As P1 increased from 5 ms to 40 ms LN3 activity linearly increased from 6.9±0.6 to 11.3±0.5 AP/chirp with a slope of m=0.8656 (AP/chirp)/ms (R^2=0.9309, correlation coefficient, P1-5 vs P1-20: p=0.0428, Friedman test, N=5, n=13). Its activity then stayed at a similar level giving 10.6±0.4 AP/chirp at P1-50 and 11.6±0.5 AP/chirp at P1-80 (P1-80 vs P1-20: p=0.0248, Friedman test, N=5, n=13). The tuning curve of LN3 was basically linear (R^2=0.723), but the slope of increasing (m=0.0591) was smaller than that in LN2 (m=0.0629) and AN1 (m=0.1264). This is another indication for a further filtering property of LN3 to the long pulse duration. The resulting tuning curve reveals a gradual increase in activity over the P1-test and does not match the behavioural tuning (Fig. 44C).

To explore whether the responses to the different pulses contribute differently to the response property of LN3, I calculated the number of spikes for each pulse (P1 to P3) within a chirp and plotted the data over the P1 duration (Fig. 44D). The response of LN3 to P1 linearly increased with a slope of m=0.0543 (R^2=0.9167, correlation coefficient, p<0.0001, Friedman test, N=5, N=13). The response elicited by P1-80 was significantly stronger compared to the activity elicited by P1-20 (P1-20: 2.4±0.2 AP/pulse; P1-80: 5.8±0.2 AP/pulse, p=0.0027, Friedman test, N=5, n=13). This tuning curve (Fig. 44D, P1) contributes the most to the overall tuning curve in Fig. 44C.

The response of LN3 to P2 did not show strong differences over the test. It slightly increased from 2.0±0.3 AP/pulse to 3.4 AP/pulse when P1 increased from 5 to 20 ms, the activity then showed a plateau for P1-25 to P1-50 (P1-25: 3.6±0.2 AP/pulse; P1-30: 3.6±0.2 AP/pulse; P1-40: 3.8±0.2 AP/pulse; P1-50: 3.6±0.2 AP/pulse) and finally decreased to 3±0.5 AP/pulse at P1-80. According to the delay-line and coincidence detector mechanism, the time course of the post-inhibitory rebound of LN5 always coupled to offset of a sound pulse, that is to say, the level of overlap between AN1 and the post-inhibitory rebound mainly depends on the duration of the interval following the sound pulse. The direct outcome would be the second response of LN3 is believed to be stronger than the first response, for pulses of the same

duration when the intervals are 20 ms. Here in response to the chirps of the P1-test, this phenomenon occurred for P1-5 to P1-20, which elicited LN3 activity 28.18±11.5% stronger by P2 than P1 (P1: 2.1±0.3 AP; P2: 2.6±0.3 AP). Although the intervals were still 20 ms, when P1 was between 25 and 30 ms the activity elicited by the second pulse (P2) was (P1-25: 3.6±0.2 AP; P1-30: 3.6±0.2 AP) at the same level as the response to P1 (P1-25: 3.4±0.4 AP; P1-30: 3.6±0.4 AP). For P1 between 40 and 80 ms, the response of LN3 to P2 was even 26.25±9.2% weaker than to P1. This suggests that the delay-line and coincidence detector mechanism proposed by Schöneich (2015) may only explain part of the responses in this P1-test. The response to P3 was 3.2±0.1 AP/pulse on average and did not show significant differences across the test (p=0.2686, Friedman test, N=5, n=13), it gave a minor peak at 20 ms with 3.8±0.2 AP/pulse (Fig. 44D). For P1-5 to P1-20 the response of LN3 to P3 was 22.81±7.11% stronger than P2 and 58.33±19.64% stronger than to P1. For P1-25 and P1-30 it was similar to the P1 and P2 response and for long P1 (40-80 ms) the response to P3 was similar to the response to P2, and 33.05±6. It was 19% weaker than the response to P1 (Fig. 44D). These suggest that the activity elicited by P3 was not always the strongest among the three bursts, but overall similar to the P2 response.

The above results indicate that: 1. For P1 between 5 and 25 ms, the number of spikes elicited by all three pulses (AP/chirp) increased as P1 increased. 2. When P1 was longer than 25 ms, it did not alter the responses elicited by P2 and P3. 3. The increase in the overall tuning of LN3 (Fig. 44C) is due to the increase in the number of spikes caused by the first pulse P1.

The feature detector – LN4

The activity of the feature detector LN4 is driven by an inhibitory input from LN2 and an excitatory input from LN3 (Fig. 45A).

LN4 response to a single 20 ms sound pulse and the normal chirp

In response to a 20 ms pulse LN4 with a latency of 24.9±0.3 ms consistently generated an inhibition, which lasted for 75.6±1.2 ms. Spike activity for a normal chirp started at 96.9±2.9 ms after the onset of the first sound pulse (i.e. a latency of 30.3±0.5 ms after the second sound pulse). The latency of the response to the third sound pulse P3 was 29.1±0.2 ms, and very similar to that caused by the second pulse P2. The depolarisation elicited by P2 lasted for 19.3±0.5 ms, while it lasted for 30.6±2.0 ms in response to P3 (p=0.015, n=5, t-test); the spiking activity lasted even shorter with 9.7±1.4 ms for P2 and 16.5±1.1 ms for P3 (p=0.031, n=5, t-

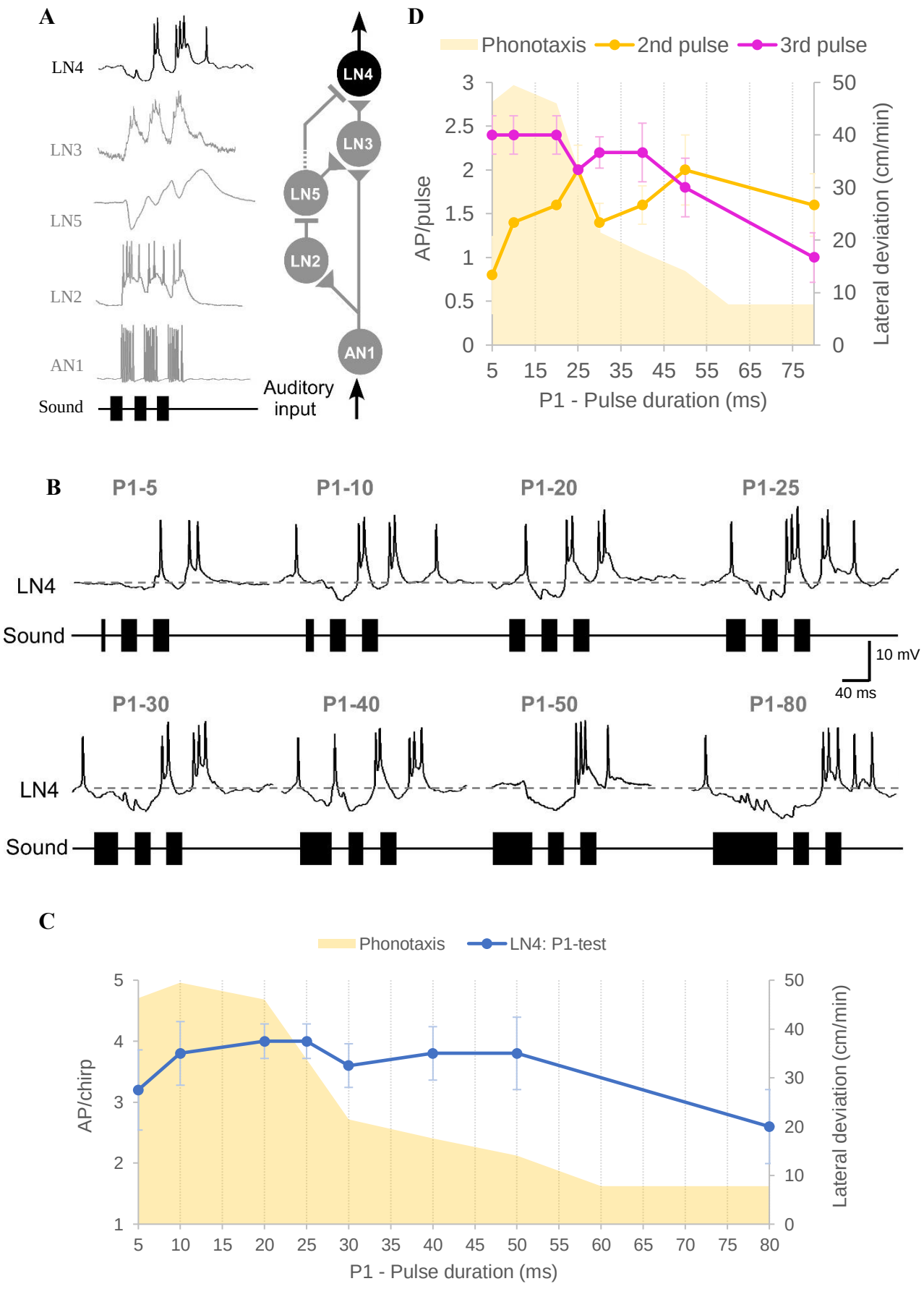

Fig. 45 Response of the feature detector neuron LN4 to P1-test.

Fig. 45 Response of the coincidence detector neuron LN4 to P1-test. A. Characteristic response of LN4 to the normal chirp and its role in the pattern recognition circuit. **B.** Activity of LN4 in response to chirps with P1 varied. The activity of LN4 is coloured in black, tested chirp are labelled above each response. Dotted lines indicate the resting potential. **C.** AP/chirp elicited in LN4 in response to the P1-test (N=5, n=5), and the phonotactic response indicated by yellow shade. **D.** AP/pulse elicited in LN4 by pulse P2 and P3 (N=5, n=5). Error bars represent standard error of the means (SEM). Phonotactic response is in yellow shade.

test). Overall the typical response to the normal chirp was an initial inhibition followed by two pronounced depolarizations with short burst of spikes elicited by P2 and P3.

LN4 response to P1-chirps

When the P1-5 chirp was presented, LN4 generated a very weak inhibition in response to the first sound pulse (P1), and the second sound pulse failed to reliably elicit spikes with only 0.8±0.4 APs generated. P1-10, however, caused a prominent inhibition followed by two bursts of spikes. The inhibition occurred with a latency of 25.1±0.6 ms, it was mixed with some subthreshold EPSPs. For the medium P1, the initial inhibition became longer and the EPSPs during the inhibition turned out to be stronger than those generated in short P1. The second and third sound pulse P2 and P3 elicited pronounced suprathreshold depolarisations with bursts of 2-3 spikes. For long P1, the inhibition became more pronounced as P1 increased. When P1 was 40 ms, the response of LN4 was still similar to that evoked by the normal chirp. Therefore, the excitatory response to P1-20 is not different to the response to P1-30 or P1-40, although the phonotaxis responses to these chirps is considerably lower. When P1 was 50 and 80 ms, the burst of spikes in response to P2 was still quite strong while the spiking activity in response to P3 did not form a burst, which may be a result of the pronounced inhibition elicited by the extended first sound pulse.

The mean spiking activity of LN4 was low and only 3.6±0.2 AP/chirp and reflected the sparse coding properties of the neuron. Overall the LN4 number of spikes to each chirp was reduced by 61.84±2.82%, as compared to the activity in LN3, and of 83.56±1.33% when compared to the activity in AN1 (LN4: 3.6±0.2 AP/chirp; LN3: 9.7±0.6 AP/chirp; AN1: 22.6±1.2 AP/chirp).

The summed number of spikes elicited by P2 and P3 is given in Fig. 45C. The LN4 activity does not show pronounced differences across the P1-test. When P1 was between 5 and 50 ms, LN4 responded to the chirps with 3.7±0.1 AP/chirp, and when P1 increased to 80 ms, activity decreased to 2.6±0.6 AP/chirp. The resulting LN4 tuning curve does not match the phonotactic tuning (Fig. 45C).

A more detailed analysis into the response of LN4 towards each sound pulse within the P1-chirps is given in Fig. 45D and shows different trends for P2 and P3, while the response to P2 increased up to P1-25 the response to P3 decreased. As the duration of P1 increased from 5 ms to 25 ms the response to the second pulse (P2) increased from 0.8±0.4 AP to 2±0.3 AP. LN4

activity then showed no clear pattern, it decreased to 1.4±0.2 AP/pulse at P1-30 and increased again towards 2±0.4 AP/pulse at P1-50. In comparison the response to P3 had a level of 2.4±0.2 to 2.2±0.3 AP/pulse for P1-5 to P1-40, and as P1 increased to 80 ms activity gradually declined to 1.0±0.3 AP/pulse.

In summary, the spike activity of LN4 for the P1-test did not show a clear pattern in line with the behavioural tuning and it did not exhibit a band-pass shape filter property.

The sequential filtering in the pattern recognition circuit as revealed by the P1-test

To compare the tuning curves of the five neurons, I normalized the activity elicited in the P1-test to the activity caused by the 'normal chirp' and plotted the curves over the corresponding phonotactic response (Fig. 46A). AN1 and LN2 showed a similar level of increase in their activity as P1 increased, and overall, the response of LN3 also showed a similar trend. However, as P1 increased from 40 to 80 ms, the increase in LN3 spike activity was not as high as in AN1 and LN2, which may indicate a filtering property of LN3 to long P1s. Differently in LN4, the number of spikes climbed to a broad maximum for P1 at 20 and 25 ms and then – with a dip at P1-30 – activity gradually declined towards long P1 pulses, thus, the LN4 tuning may show some general match with the behaviour. However, none of the 4 tuning curves closely represented the phonotactic tuning.

Processing of the P1-chirps by the delay-line and coincidence-detection circuit

In order to reveal the flow of neuronal activity, I aligned the responses of all neurons in respect to the P1-chirps (Fig. 46B). In my comparative description I will especially consider the short (P1-5 to P1-10), medium (P1-20 to P1-30) and long pulse durations (P1-40 to P1-80).

For all chirps, since the rising phase of the post-inhibitory rebound was interrupted by the second and the third inhibition, the AN1 activity and the post-inhibitory rebound overlapped for about 7 ms before the inhibition kicked in (latencies of PIR1 in LN5 and the second AN1 response: 26.4±0.2 vs. 18.4±0.2 ms; PIR2 in LN5 and the third AN1: 25.7±0.5 vs. 19.6±0.1 ms) (Table. 1). This allows about 3-4 spikes of AN1 to coincide with the post-inhibitory rebound.

Even for short P1, neurons AN1, LN2 and LN3 copied the pattern of the sound pulses, with AN1 being more precise than LN2 and LN3. Also neuron LN5 already showed rhythmic changes in its membrane potential, very similar to the pattern obtained by the normal chirp; and

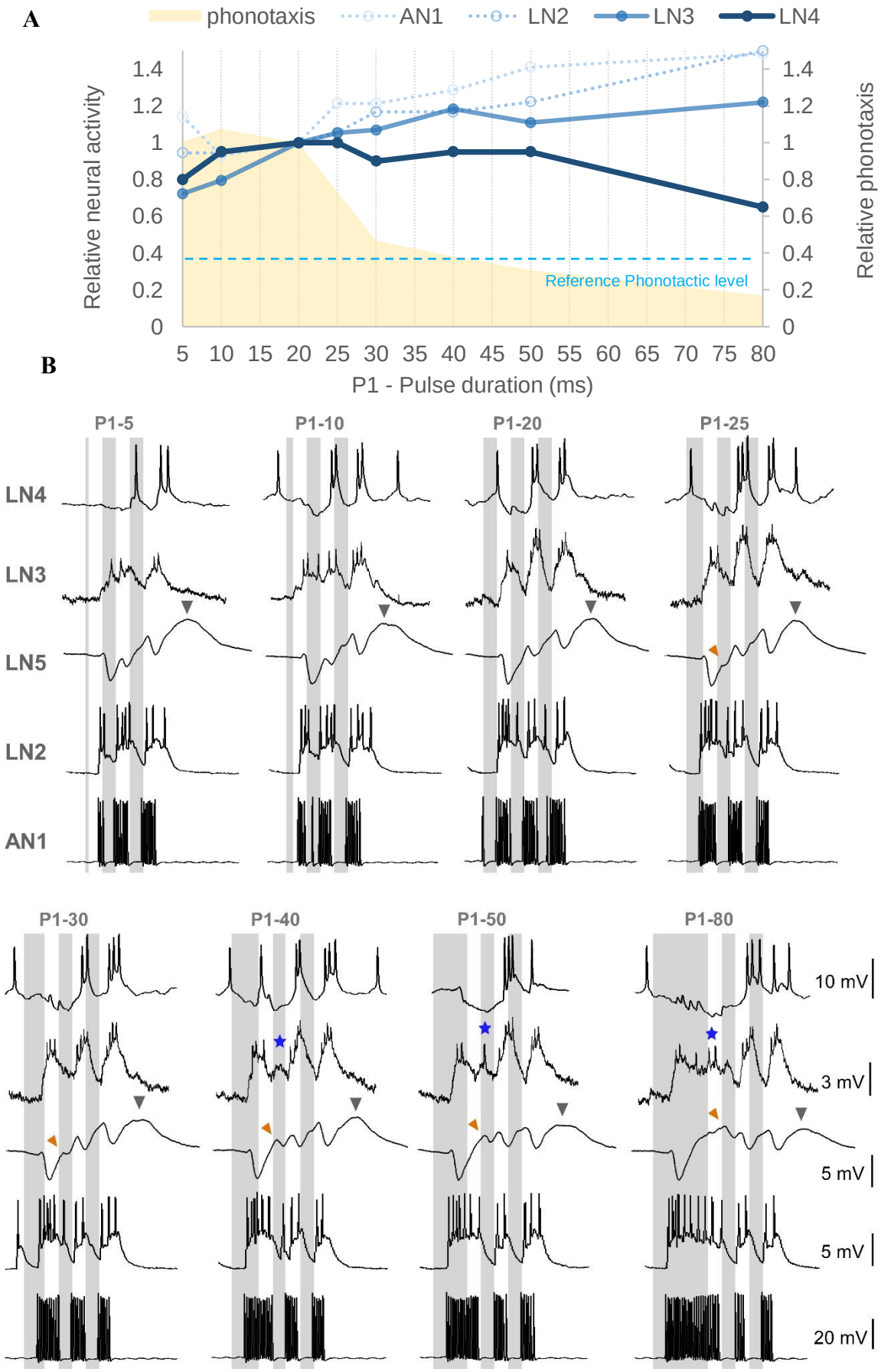

Fig. 46 Sequential filtering to varied 1st pulse (P1-test) by the pattern recognition circuit.

Fig. 46 Sequential processing of P1-chirps by the pattern recognition circuit. A. Tuning curves of the spiking neurons AN1, LN2, LN3 and LN4 in the pattern recognition circuit and the phonotactic response to P1-chirps. The response elicited by the normal chirp in the neurons and for phonotaxis was set as 1, activity was calculated as the relative change. The tuning curves of AN1 and LN2 are in dotted lines, they do not show any temporal selectivity. The tuning curve of LN3 is given in light blue and of LN4 in dark blue. The reference level indicates the phonotactic response elicited by a 2-pulse chirp. **B.** Recordings of LN4, LN3, LN5, LN2 and AN1 are aligned vertically to the sound pulses shown as grey bars. Chirp labels are given on top of each column. For LN4, LN3, LN2 and AN1, one example recording is shown, for LN5, the traces are averaged from 18 recordings. For LN5, orange arrowheads indicate the additional rebound occurring for medium and long P1. Grey arrowheads indicate PIR3, the only completed rebound. For LN3, blue stars indicate the extra EPSP/burst of spikes apart from the onset activity elicited by long P1.

LN4 showed a response pattern for P1-5 and P1-10, which was very similar to the pattern elicited by the normal chirp. This activity of LN5 and LN4 may be in line with the strong phonotaxis response for P1-5 and P1-10.

At medium P1 durations the pulse pattern was again copied by AN1 and LN2. The postinhibitory rebounds in LN5 and the representations of the pulse pattern in LN3 became more pronounced. The feature detector neuron LN4 showed the typical activity pattern with an initial inhibition, followed by two pronounced suprathreshold depolarisations accompanied by bursts of spikes. These depolarisations elicited by P2 and P3 are very similar for the range of P1-10 to P1-40, although the phonotaxis response dropped over the same range by about 60%. This may be linked to the initial inhibition in the LN4 response, which became more prominent with increasing P1 duration.

For long P1-pulses the rhythmic oscillation pattern in LN5 became strongly distorted; an extra inhibition and rebound peak occurred during the first rebound (orange arrowhead) and the amplitudes of PIR2 and PIR3 started to decrease over the time course of the chirps. The LN3 activity in response to a long P1 was extended, it generated an initial short burst of spikes followed by another suprathreshold EPSP (blue stars). In line with the LN2 activity, the LN4 response became dominated by a strong initial inhibition; this was followed by one pronounced depolarisation and a burst of spikes. As a consequence, for long P1 the activity pattern of LN5 and LN4 was substantially different when compared to the response to a normal P-20 chirp. Moreover, it indicates that the duration of the first sound pulse has a substantial effect on neuronal processing, and it may indicate a filter process for pulse durations, which previously was not described for the circuit properties.

Response of the pattern recognition network neurons to chirps with the second pulse of different duration: P2- test

In the P2-test the duration of the second sound pulse (P2) was changed (Fig. 37A). This should not affect processing of the first pulse (P1) and only have an impact on processing of the second (P2) and the third pulse (P3).

The number of recordings of the neurons are: 10 repeats of AN1 (N=5, n=10), 10 repeats of LN2 (N=2, n=10), 10 repeats of LN5 (N=4, n=10), 10 repeats of LN3 (N=5, n=10) and 5

repeats of LN4 (N=5, n=5) for the characteristic responses of the neurons elicited by 20-ms pulses and normal chirps, and 5 repeats of AN1 (N=5, n=5), 2 repeats of LN2 (N=2, n=2), 18 repeats of LN5 (N=4, n=18), 13 repeats of LN3 (N=5, n=13) and 5 repeats of LN4 (N=5, n=5) for the P2-test.

The ascending neuron – AN1

AN1 forwards auditory activity to the inhibitory neuron LN2 and the coincidence detector LN3 (Fig. 47A). Its activity copies the duration of the sound pulses (Fig. 47B). Its typical- response properties to the normal chirp were given before (see P1-test).

AN1 response to P2-chirps

As the duration of P2 increased from 5 to 80 ms, the number of AN1 spikes increased linearly from 17.0±0.0 to 28.7±0.3 AP/chirp with a slope of m=0.1722 (R^2=0.9356, correlation coefficient), (Fig. 47B, C). When P2 was longer than 25 ms, AN1 responded to the chirps with a greater number of spikes than to the normal chirp corresponding to P2-20 (P2-30 vs. P2-20: p=0.0164, P2-40 vs. P2-20 p=0.0364, P2-50 vs. P2-20 p=0.0361, P2-80 vs. P2-20 p=0.0116, Friedman test, N=5, n=5) (Fig. 47C), correspondingly AN1 activity increased over the P2-test. The tuning curve of AN1 did not match the behavioural tuning for varying the P2 duration (Fig. 47C).

The inhibitory neuron – LN2

Neuron LN2 is driven by AN1 activity and inhibits both the non-spiking neuron LN5 and the feature detector LN4 (Fig. 48A). Its fundamental response properties were given before (see P1-test).

LN2 response to P2-chirps

The response of LN2 to the P2-test was obtained with two stimulus repeats. Across all chirps in the P2-test, each pulse elicited a suprathreshold EPSP with several spikes, P1 elicited a high frequency burst with 4-5 spikes, while the response to P3 was only 2-3 AP. The duration of the EPSP and the number of spikes elicited by P2 increased with the pulse duration. (Fig. 48B), it started from 6.5 AP/chirp at P2-5 and reached a maximum of 11.2 AP/chirp at P2-80. At P2-5 the second pulse was not reflected in the LN2 activity, but at P2-80, it caused a pronounced plateau-like depolarisation with 8AP. The increase of P2 led to a linearly increasing activity of

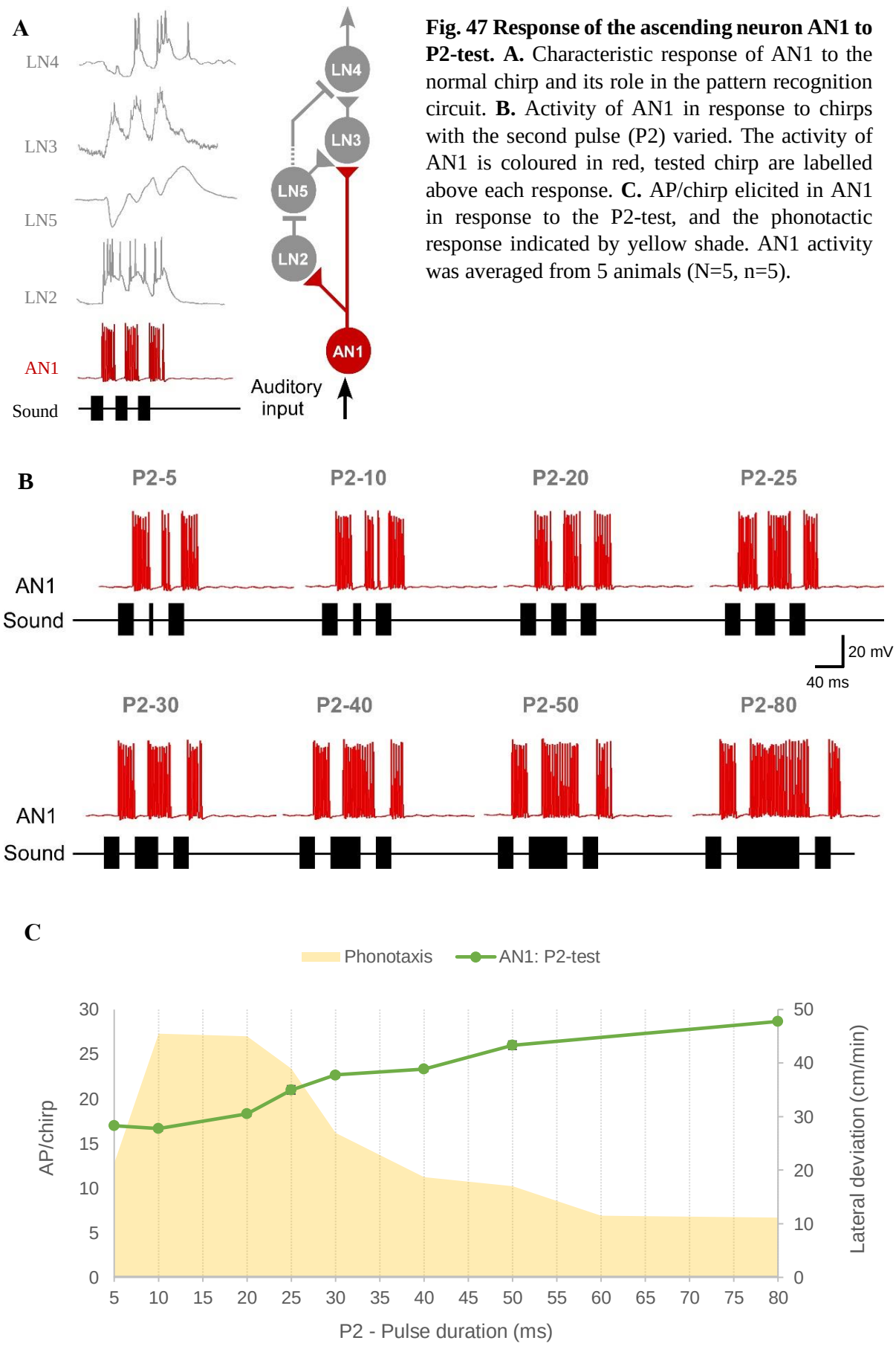

Fig. 47 Response of the ascending neuron AN1 to P2-test. A. Characteristic response of AN1 to the normal chirp and its role in the pattern recognition circuit. **B.** Activity of AN1 in response to chirps with the second pulse (P2) varied. The activity of AN1 is coloured in red, tested chirp are labelled above each response. **C.** AP/chirp elicited in AN1 in response to the P2-test, and the phonotactic response indicated by yellow shade. AN1 activity was averaged from 5 animals (N=5, n=5).

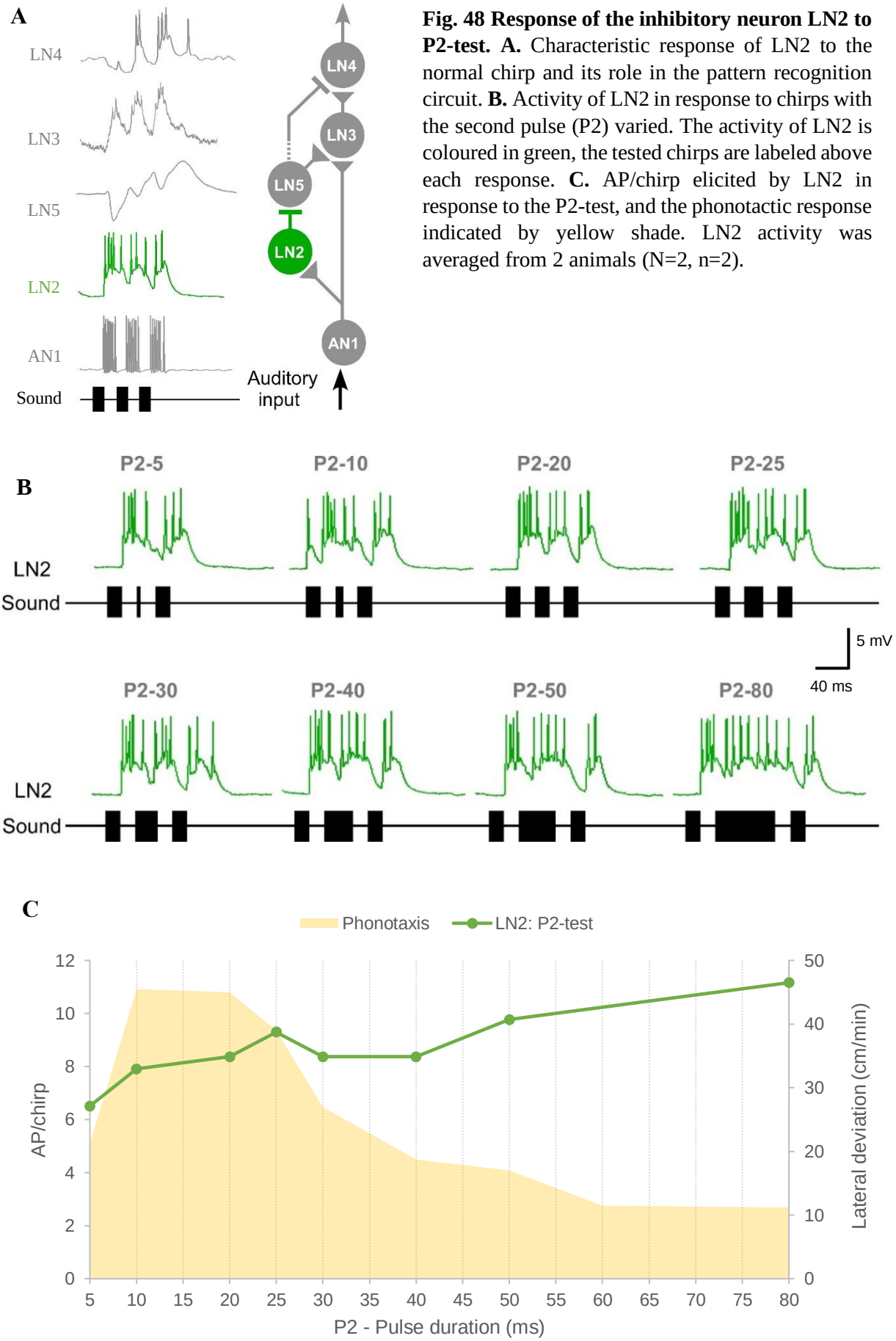

Fig. 48 Response of the inhibitory neuron LN2 to P2-test. A. Characteristic response of LN2 to the normal chirp and its role in the pattern recognition circuit. **B.** Activity of LN2 in response to chirps with the second pulse (P2) varied. The activity of LN2 is coloured in green, the tested chirps are labeled above each response. **C.** AP/chirp elicited by LN2 in response to the P2-test, and the phonotactic response indicated by yellow shade. LN2 activity was averaged from 2 animals (N=2, n=2).

LN2 with a slope of m=0.0516 (R^2=0.821, correlation coefficient). The tuning of LN2 is similar to AN1 and did not match the behavioural tuning (Fig. 48C); its overall activity in response to the P2-test was 59.38±1.47% less than the AN1 activity.

The non-spiking neuron – LN5

The non-spiking neuron LN5 is a key element in the circuit, it is inhibited by LN2 and generates a delayed post-inhibitory rebound (PIR), which is forwarded to the coincidence detector LN3 (Fig. 49A). The typical response pattern of LN5 to a normal chirp has been described before (see P1-test). The activity of LN5 was averaged from 4 animals with 18 repeats.

LN5 responses to P2-chirps

As expected from the stimulus design, the first inhibition (INH1), the first rebound (PIR1) and the second inhibition (INH2) were not affected by the changes in P2 duration (Fig. 49B, C). This also becomes obvious in the superimposed activity of LN5 aligned to the first sound pulse (Fig. 50A). Inhibition started with a latency of 29.9±0.3 ms, it increased over 11.4 ms and reached its peak INH1 with -3.99±0.07 mV at 41.4±0.2 ms after the onset of P1. The following PIR1 reached 1.3±0.1 mV and occurred at 28.3±0.3 ms after the start of P2. The shape and the amplitude of INH2, which is driven by P2, remained very similar throughout the test, despite the changes in P2 duration (Fig. 50A). The peak of INH2 was 1.4±0.1 mV, it occurred 41.2±0.7 ms after the start of P2, and 12.8 ms after the onset of the second inhibition.

The amplitude of PIR2 however, changed substantially as the duration of P2 increased (Fig. 49B, 50A). For short P2 (P2-5 and P2-10), the dynamics of the membrane oscillation were very similar to that caused by the normal chirp (P2-20). The three peaks of the rebounds (PIR1, PIR2 and PIR3) all reached above the resting potential and continuously increased in amplitude. PIR2 reached an amplitude of 3.7±0.1 mV (P2-5) at 27.5±0.3 ms and of 3.2±0.1 mV (P2-10) at 26.7±0.2 ms after the start of the P3, respectively. The third rebound reached its broad maximum (PIR3) of 5.3±0.2 mV (P2-5) at 78.8 ms and 5.6±0.1 mV (P2-10) at 75.0 ms after the start of P3. It then took about 146.3 (P2-5) and 150.5 ms (P2-10) for the third rebound to fully recover to the resting potential.

The response to P2-20 was already introduced in the *LN5 response to the normal chirp,* see P1-test, LN5. For medium P2 (P2-25 and P2-30), a deflection of the membrane potential during the second rebound emerged, as seen in the P1-test for P2-25 and P2-30 for the first

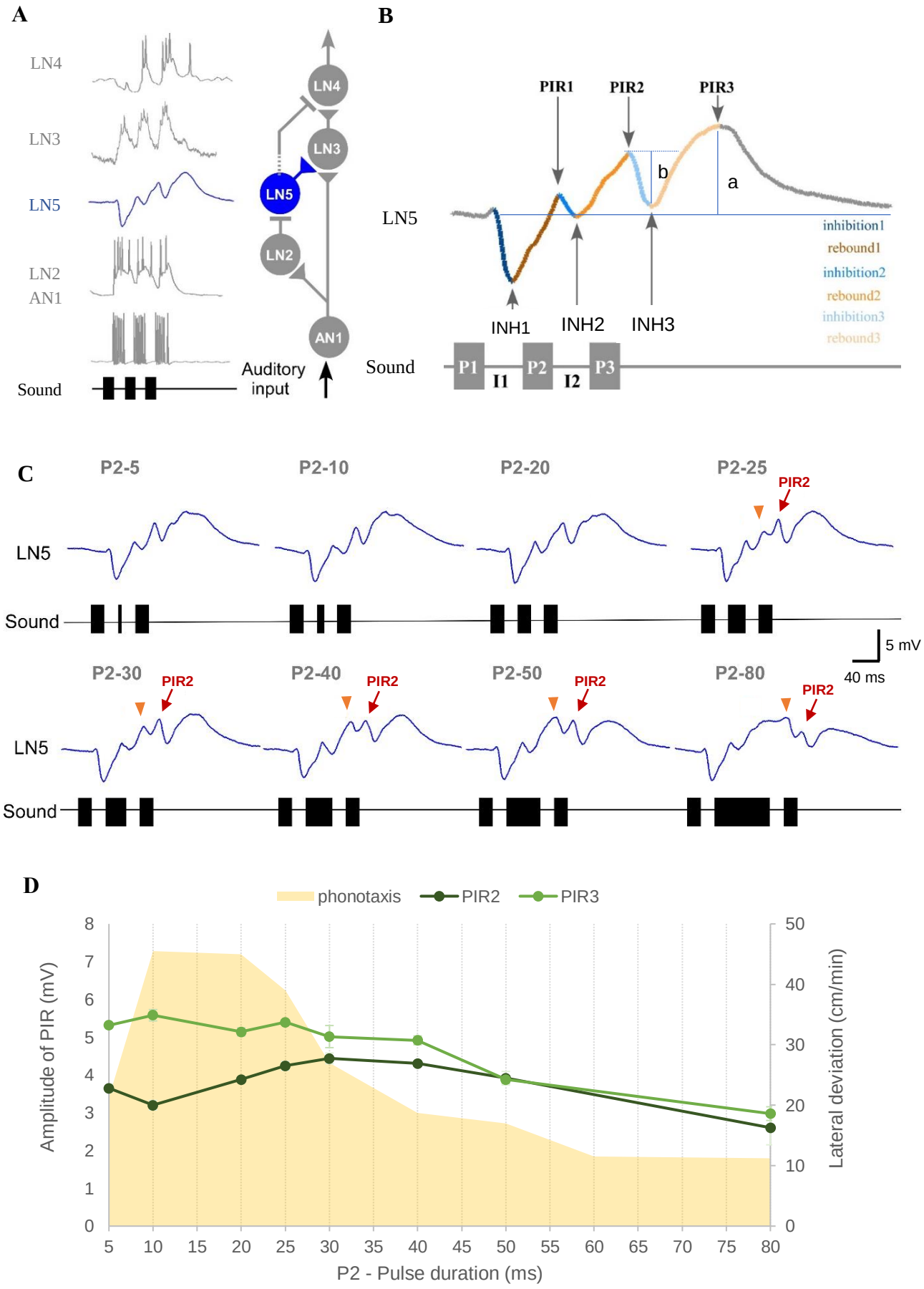

Fig. 49 Activity of LN5 elicited by the P2-test and the tuning of the amplitude of PIRs.

Fig. 49 Activity of LN5 elicited by the P2-test and the tuning of the amplitude of PIRs. A. Diagram showing characteristic activity of LN5 to the normal chirp and its role in the pattern recognition circuit. **B.** LN5 activity in response to a normal chirp. P1, P2 and P3 represent the three sound pulses, I1 and I2 refer to the two intervals. LN5 responds to the three pulses with three inhibitions (inhibition1, inhibition2 and inhibition3) and three rebounds (rebound1, rebound2 and rebound3). The maximum amplitudes of the inhibitions are labelled as INH1, INH2 and INH3. The highest membrane potential of rebound1 (brown) and rebound2 (orange) are marked as PIR1 and PIR2, they occur at the start of the following inhibition (blue and light blue). The peak amplitude of rebound3 (light yellow) is labelled as PIR3, this rebound is not interrupted by an inhibition. **C.** Average responses of LN5 to the P2-test (N=4, n=18). The neuronal activity of LN5 is coloured in blue. Tested chirps are labelled above each recording. Orange arrowheads represent the additional rebound peak formed in response to P2-25 to P2-80, red arrows indicate the second rebound (PIR2) for the purpose of discriminating from the additional peak. **D.** Amplitude of PIR2 and PIR3 over the P2-test, PIR2 is given in dark green and the PIR3 in light green. Error bar indicates the standard error of the mean (SEM). Phonotactic response is in yellow shade.

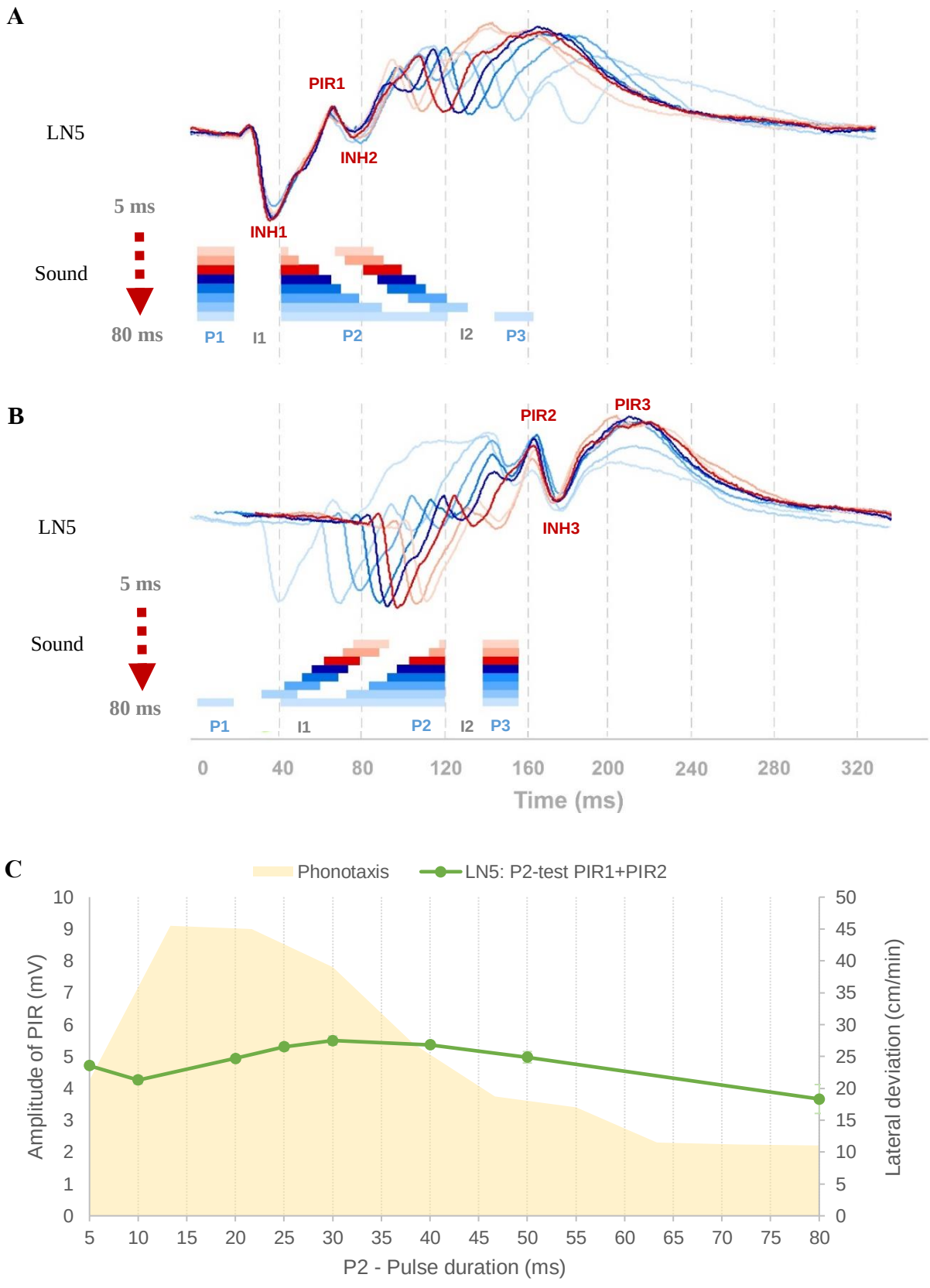

Fig. 50 LN5 activity elicited by P2-test aligned to the first or the last sound pulses and the tuning curves of summed PIRs.

Fig. 50 LN5 activity elicited by the P2-test aligned to the first or the last sound pulse and the tuning curves of summed PIRs. A. Averaged LN5 activity in response to the P2-test aligned to the onset of P1 (N=4, n=18). **B.** Averaged LN5 activity aligned to the onset of P3. When P2 is smaller than 25 ms, the chirps and LN5 responses (P2-5, P2-10, P2-20 and P2-25) are coloured as light to dark red, respectively. For P2 equal to or larger than 25 ms, chirps and LN5 responses are coloured as dark to light blue, respectively. Responses in dark red and blue are to chirps P2-20 and P2-25 that elicit the best phonotactic behaviour. **C.** Sum of PIR1 and PIR2 over the P2-test. Error bar at P2-50 indicates the standard error of the mean (SEM). Phonotactic response is in yellow shade.

rebound (Fig. 49C, P2-25 and P2-30, orange arrowheads). The deflection formed a small 'bump' in the second rebound in P2-25 which preceded PIR2 with a latency of 53.2±1.1 ms to P2. In response to P2-30, the deflection of the membrane potential developed into an extra peak with a latency of 58.5±0.3 ms to the onset of P2. These extra peaks may be caused by additional excitatory or inhibitory inputs from the network. In 3 of 10 recordings, LN5 responded to the 'normal chirp' with this extra peak. When P2 was 5 and 10 ms, the percentage of recordings showing this extra peak was 50% and 70% respectively. The amplitude of PIR2 reached 4.2±0.1 (P2-25) and 4.4±0.1 mV (P2-30) at 29.6 and 31.1 ms after the onset of P3, respectively. When calculating the time course between the extra peak and the offset of P2, it turned out the occurrence of the extra peak was coupled to the end of the second sound pulse (P2-25: 28.2 ms; P2-30: 28.5 ms). The peak of the third rebound (PIR3) reached a similar amplitude for these two chirps of 5.4±0.0 (P2-25) and 5.1±0.3 mV (P2-30) with a latency of 80.5 and 79.6 ms to P3. In response to these chirps the difference in the amplitude of PIR2 and PIR3 became smaller, as compared to the normal chirp.

For long P2 (P2-40, P2-50 and P2-80), the extra peak in the second rebound further became more prominent (Fig. 49, P2-40, P2-50 and P2-80, orange arrowheads). The peaks of PIR1 for P1-40 to P1-80 are pointed out (Fig. 49C, red arrows) as the extra rebound peak (Fig. 49C, orange arrowheads) became more pronounced. The extra peak elicited by P2-40 achieved a similar amplitude as PIR2 (extra peak: 4.1±0.2 mV; PIR2: 4.3±0.1 mV) at 67.9 ms after the onset of P2. For longer P2, this peak reached an amplitude of 4.6±0.6 (P2-50) and 4.8±0.4 mV (P2-80) at 77.8 and 108.9 ms, respectively, which was higher than PIR2. The extra peak occurred with a quite constant delay to the offset of P2 in all medium and long P2 (P2-25: 28.2 ms; P2-30: 28.5 ms; P2-40: 27.9 ms; P2-50: 27.8 ms and P2-80: 28.9 ms after the end of P2). As this extra peak developed, the amplitude of PIR2 decreased (P2-40: 4.3±0.1 mV; P2-50: 3.9±0.2 mV; P2-80: 2.6±0.5 mV). Therefore, although the absolute amplitude of PIR2 elicited by long P2 was still larger than PIR1, the relative difference in the amplitude between PIR1 and PIR2 was much smaller than seen for short and medium P2; especially for P2-80, the difference was as small as 1.6 mV. The last rebound was also affected by the long P2, it resulted in an amplitude of PIR3 of 4.9±0.1 (P2-40), 3.9±0.1 (P2-50) and 3.0±0.2 mV (P2-80), which was similar to the amplitude of PIR2. The PIR3 elicited by these chirps were with a latency of 78.6, 79.4 and 68.4 ms to P3, respectively.

When considering the complete P2-test, the depolarisation underlying LN5 activity was

enhanced along the three sound pulses in one chirp for P2-5 to P2-40. This resulted in the successive increase of the amplitude of PIR1, PIR2 and PIR3 in these chirps as seen in the normal chirp (Fig. 49C). This trend was then weakened at long P2 when the extra peak in the second rebound became dominant and exceeded the amplitude of PIR2. It implies a possible influence of the input causing the extra peak on the depolarising drive underlying the build-up of the membrane potential of LN5. The peak of the first and the second rebound were determined by the onset of the sound pulses and the subsequent inhibition. Therefore, the latency of PIR1 and PIR2 was quite constant across the test (PIR1: 28.3±0.3 ms to P2; PIR2: 27.4±0.2 ms to P3). As the only competed post-inhibitory rebound among the three, the rebound3 reached its peak with no interference from a subsequent inhibition and may be a reflection of the influence of changing P2 on the cell conductance after processing the whole chirp. For P2-5 to P2-40, both the amplitude and the latency of PIR3 turned out to be constant with an averaged latency of 78.8±0.6 ms and averaged amplitude of 5.2±0.1 mV. The amplitude of PIR3 were reduced in when P2 was 50 ms. Despite of different amplitudes, the latency of PIR3 was still very similar to that in P2-5 to P2-40 as 79.4 ms. However, for P2-80 both the latency and the amplitude of PIR3 were affected. The PIR3 occurred a little earlier at 67.4 ms and the amplitude was only 3.0±0.2 mV. This may be an indication that the conductance of LN5 after processing the whole chirp was not affected by changing P2 when it lies in the range between 5 to 40 ms while the P2 longer than 40 ms may influence the cell conductance after processing the sequence of pulses, which led to a smaller amplitude and a shorter latency of PIR3.

For a quantitative analysis of the LN5 activity I plotted the amplitudes of PIR2 and PIR3 over the duration of P2 (Fig. 49D). Because it is the PIR2 that coincides with the third AN1 activity rather than the extra peak even though it may be more pronounced, I did not plot the amplitude of the extra peak here.

The amplitude of PIR2 slightly increased from 3.65±0.11 mV to 4.44±0.14 mV when P2 increased from 5 to 30 ms, and it then decreased to 2.61±0.45 mV as P2 reached 80 ms (Fig. 49D). The amplitude of PIR3 was constant at about 5.2±0.1 mV when P2 was between 5-40 ms. When P2 was 50 and 80 ms, the extra peak exceeded the PIR2 and the amplitude of PIR3 decreased to 3.9±0.1 and 3.0±0.2 mV (Fig. 49D). The difference in the amplitude of PIR2 and PIR3 is also shown by aligning the activity of LN5 to P2-chirps by the start of P3 (Fig. 50B).

Since the first two PIRs elicited by a 3-pulses chirp contribute to the coincidence

detection according to the delay-line and coincidence detector mechanism, I calculated the overall outcome of PIRs to LN3 by summing the amplitude of PIR1 and PIR2 up. The summed amplitude (Fig. 50D) gradually increased from 4.7±0.1 to 5.5±0.1 mV when P2 increased from 5 to 30 ms then gradually decreased to 3.7±0.5 mV for P2-80, which was not tuned like the behavior.

To conclude, neither the tuning of the individual nor the summed amplitude of the PIRs reflected the phonotactic tuning in P2-test. The peak response at P2-10 to P2-20 shown in phonotaxis was missing in the tuning of the PIR amplitude in LN5. Only the reduction of responses for P2-80 was observed for both tuning of phonotaxis and the PIR amplitudes.

Two features of the LN5 activity are noteworthy.1. The three PIRs successively increased in amplitude, when P2 was between 5 and 40 ms, but not for P2-50 and P2-80. 2. P2-pulses longer than 25 ms caused an extra peak in the rebound during PIR2. The timing of the additional peak was coupled to the end of the second sound pulse. The peak amplitudes of the three rebounds clearly increased over a chirp across the whole P2-test (Fig. 49C), indicating an underlying enhanced depolarisation of LN5. Therefore, beside of the parameters above, I analysed the velocity of the change in the peak amplitude of the three PIRs over the time course of the chirps, i.e. the slope as illustrated by three arrows 1 to 3 (Fig. 51), see also P1-test and Interval Chapter. In general, all the slopes were positive and exhibited a continuous increase of the peak amplitude. The slope1 was not affected across the test. In response to P2-5 and P2-20 (Fig. 51), the amplitudes of the PIRs continuously increased over the chirp. When P2 was longer than 20 ms, the slope2 and slope3 became less steep, For P2 of 50 and 80 ms (Fig. 51), the additional rebound peak became more dominant during second rebound, and slope2 and slope3 decreased in steepness, and became almost flat for slope3 in P2-80.

The trend of the change in the peak amplitude of the three PIRs in response to the P2-chirps was analyzed by averaging the slopes (Fig. 52, see also P1-test). The average slope continuously decreased from the strongest response at P2-5 to its lowest level at P2-80. The average slope did not reflect the phonotactic response for P2 shorter than 30 ms, but rather for P2 equal to and longer than 30 ms. This indicates that the average slope is in line with the behavioural tuning to medium and long P2.

The coincidence detector – LN3

Neuron LN3 functions as the coincidence detector in the network and is driven by a direct input

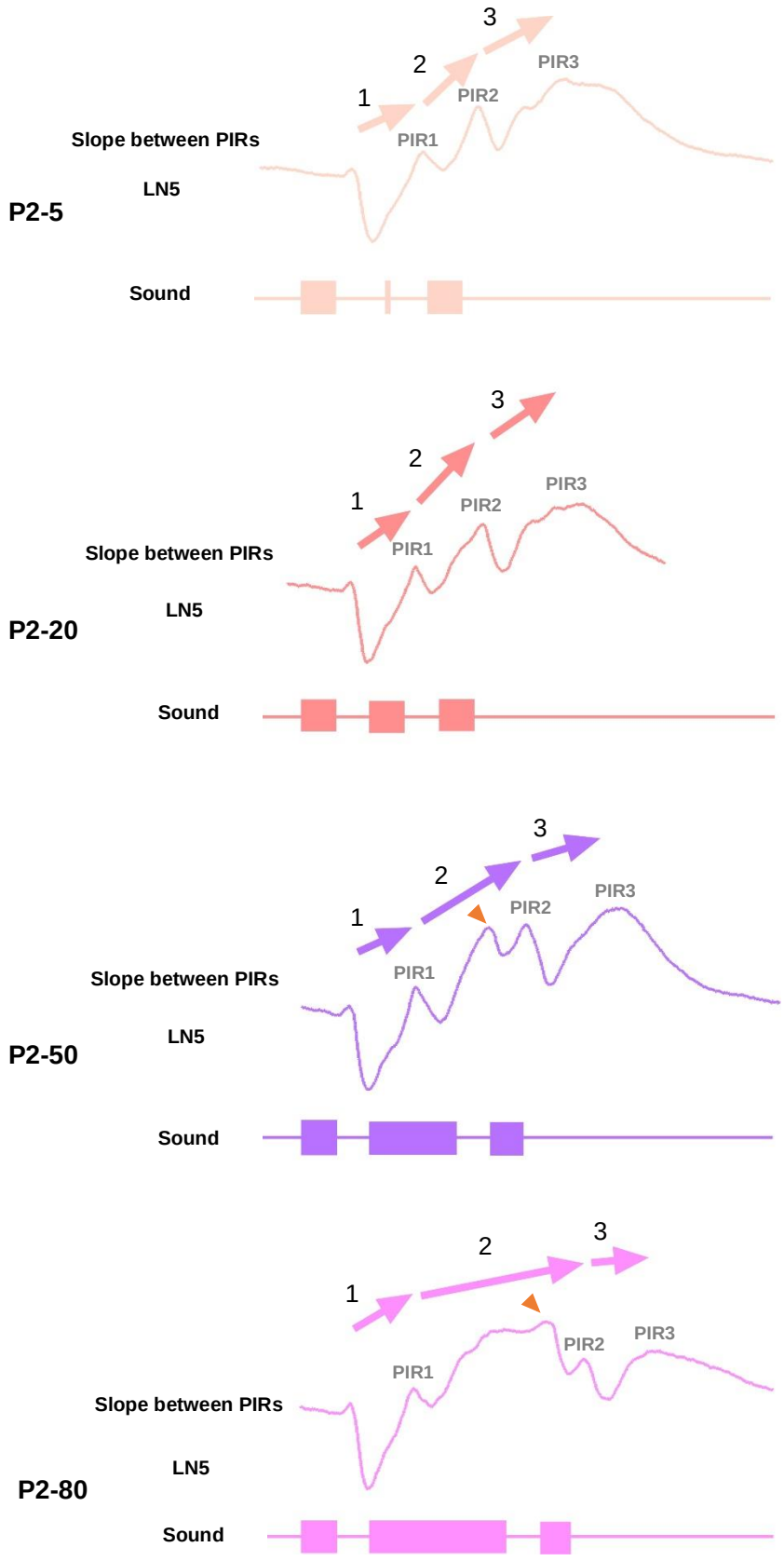

Fig. 51 The changes in the amplitude of adjacent PIRs over time (slope between PIRs) in P2-test

Fig. 51 Changes in the amplitude of adjacent PIRs (slope between PIRs) over different chirps in the P2-test. The changes in the amplitude of adjacent PIRS over time in response to four example chirps (P2-5. P2-20, P2-50 and P2-80) of the P2-test (N=4, n=18). The arrows indicate the change and slope between two adjacent PIRS over the time interval between the PIRs (t1, t2 and t3), which are named as slope1, slope2 and slope3. The slope2 and slope3 were directly influenced by varying P2. Orange arrowheads indicate the extra peak in the second rebound in P2-50 and P2-80.

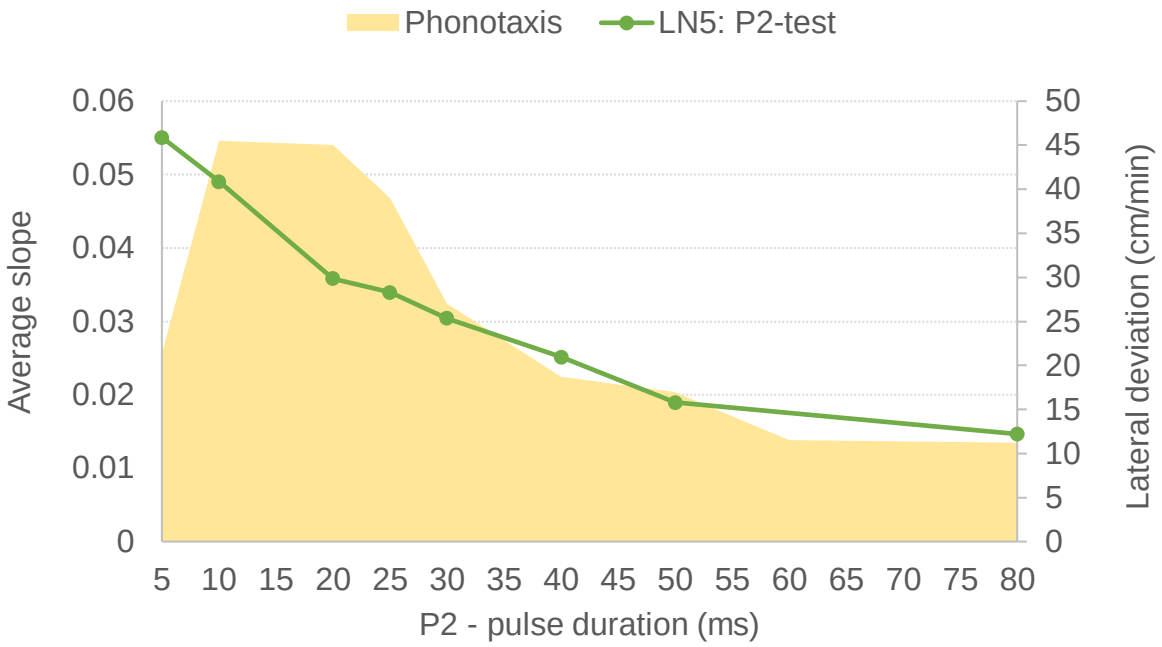

Fig. 52 Tuning of the mean 'slope' of LN5 in the P2-test. The tuning curve is averaged from slope1, slope2 and slope3 in response to each chirp of the P2-test (N=4, n=18). Phonotactic response is in yellow shade.

from AN1 spikes and a delayed graded input from LN5 (Fig. 53A).

LN3 response to P2-chirps

LN3 responded with a constant latency of 30.2±0.5 ms to all chirps in the P2-test. The number of spikes elicited by the P2-chirps increased from 8.3±0.3 to 12.4±0.4 AP/chirp, when P2 increased from 5 to 80 ms (Fig. 53B). The activity elicited by the first sound pulse was identical across the test with 2.1±0.1 AP/pulse. The activity of LN3 exhibited a good representation of each sound pulses in the P2-test with separate suprathreshold depolarisations. Nevertheless, the second burst of spikes elicited by P2-5 was weaker than the first burst due to the very short duration of P2 (first burst: 2.5±0.2 AP/pulse; second burst: 1.6±0.2 AP/pulse). Starting from P2-10, the second response of LN3 became stronger than the first burst of spikes (P1:2.0±0.0 AP/pulse; P2: 3.0±0.8 AP/pulse). For P2-10 and the medium P2 (P2-20 to P2-30), the activity elicited by P2 and P3 was quite similar with 3.4±0.1 AP (P2) and 3.1±0.2 AP (P3). For long P2 (P2-40, P2-50 and P2-80), LN3 did not copy the duration of the second sound pulse with continuous spiking activity, but rather showed a rhythmic oscillatory response. LN3 generated an initial depolarization (lasting for 38.7±0.5 ms) and burst of spikes (lasting for 18.6±0.3 ms) (Fig. 53B, red arrows); it then repolarized and an additional subthreshold depolarisation occurred when P2 was 40 ms. When P2 was 50 and 80 ms the depolarization became suprathreshold leading to a burst of spikes (Fig. 53B, blue stars). This additional depolarisation occurred with similar latency in P2-40, P2-50 and P2-90 of 65.3±0.3 ms to the onset of P2. These the additional depolarisations of LN3 (Fig. 53B, blue stars) appear to be linked to the extra rebound in LN5, providing an input to LN3.

The final last bursts of spikes elicited by medium and long P2 was not affected and showed a very similar number of spikes (averaged from P2-20 to P2-80: 2.9±0.1 AP/pulse) which was less than that elicited by short P2 (P2-5: 3.3±0.2 AP/pulse; P2-10: 3.7±0.3 AP/pulse). A subthreshold EPSP following the three responses was not very obvious and only rarely occurred (Fig. 53B, green arrows). The EPSP at the end (Fig. 53B, green arrows) may be linked to the PIRs of LN5 as an input to LN3. Overall, the activity of LN3 in response to each chirp was 46.87±1.52 % lower than the AN1activity, which, similar to in the P1-test, supports the conclusion of a more sparse coding property of LN3.

Quantitative analysis showed that the LN3 activity showed a significant difference between all chirps (p<0.0001, Friedman test, N=5, n=13) ranging from 8.0±0.6 AP/chirp (P2-

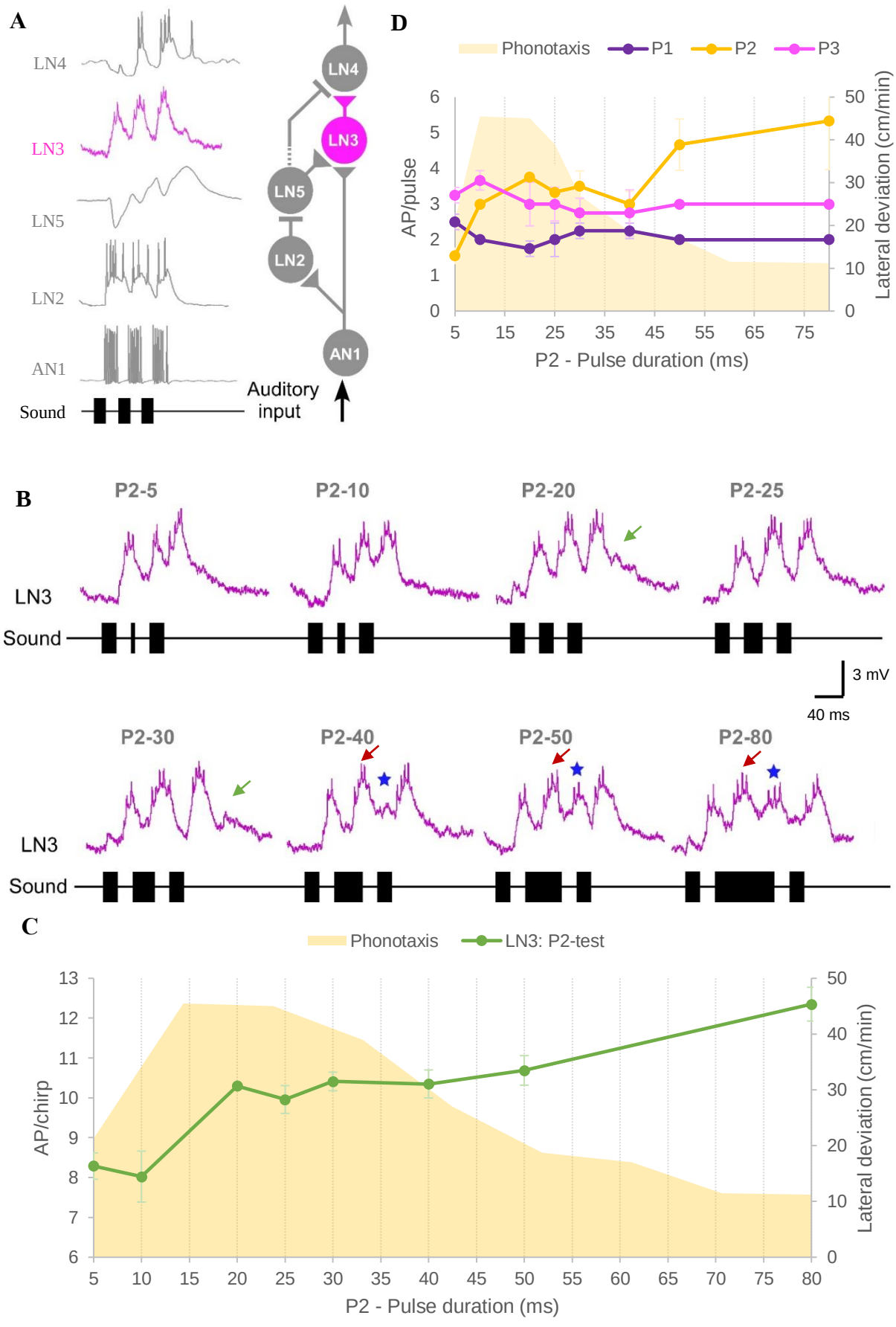

Fig. 53 Response of the coincidence detector neuron LN3 to P2-test.

Fig. 53 Response of the coincidence detector neuron LN3 to P2-test. A. Characteristic response of LN3 to the normal chirp and its role in the pattern recognition circuit. **B.** Activity of LN3 in response to the P2-test. Activity of LN3 is coloured in pink, tested chirps are labelled above each response. Green arrows indicate a delayed depolarization after the end of the third burst of spikes. LN3 shows a biphasic response to long P2, red arrows indicate the first part of the response and blue stars indicate a depolarization/extra spikes following the initial burst of spikes. **C.** AP/chirp elicited in LN3 in response to the P2-test (N=5, n=13), and the phonotactic response indicated by yellow shade. **D.** AP/pulse elicited in LN3 by each pulse within a chirp (N=5, n=13). Error bars represent standard error of the mean (SEM). Phonotactic response is in yellow shade.

10) to 12.4±0.4 AP/chirp (P2-80) (Fig. 53C). The tuning curve exhibits a rising trend as P2 increased. The number of spikes increased from 8.3±0.3 to 12.4±0.4 AP/chirp with a slope of m=0.1475 as P2 increased from 5 ms to 20 ms (R^2=0.8189, correlation coefficient, P2-5 vs P2-20: p=0.0181, Friedman test, N=5, n=13). LN3 activity then stayed at a similar level of 10.3±0.1 AP/chirp when P2 was between 20 and 50 ms (p>0.9999, Friedman test, N=5, n=13). The activity then increased to 12.4±0.4 AP/chirp at P2-80 (P2-80 vs P2-20: p=0.0326, Friedman test, N=5, n=13). The gradual increase in LN3 activity over the P2-test gives the strongest neuronal activity at long pulses and does not match the behavioural tuning (Fig. 53C).

To explore whether the filtering property in LN3 is based on an additive effect, I calculated the number of spikes for each pulse within a chirp and plotted this over the P2-test (Fig. 53D). The spiking response of LN3 to the first pulse (P1) did not show a significant difference across the test (p=0.1718, Friedman test, N=5, n=13). The response to the second pulse (P2) increased from 1.8±0.2 AP to 3.8±0.2 AP when P2 increased from 5 to 20 ms, activity then decreased to 3.0±0.4 AP/pulse at P2-40. With the occurrence of the extra burst of spikes at P2-50 and P2-80, LN3 activity increased to 4.7±0.7 and 5.3±1.4, respectively. In comparison P2 - which increased in duration - elicited 1.4±0.3 APs more than P1 (p=0.009, Paired t-test, n=8). The number of spikes elicited by P3 was similar across the test at 3.1±0.1 AP/pulse (p=0.9704, Friedman test, N=5, n=13), and was 0.9±0.1 AP higher than the response to P1 (p=0.0002, Paired t-test, n=8).

None of the three tuning curves (Fig. 53C, D) to individual pulses showed a close match to the behavioural response. Their summed activity indicates that the overall tuning for LN3 (Fig. 53C) was shaped by the response to P2. Increasing the duration of P2, however does not affect the number of spikes elicited by P3.

The feature detector – LN4

The response of the feature detector neuron LN4 is driven by an inhibitory input via LN2 and an excitatory input via LN3 (Fig. 54A).

LN4 response to P2-chirps

For all the P2-chirps the first sound pulse P1 always elicited an inhibitory response, with a latency of 25.1±0.6 ms mixed with subthreshold EPSPs, while the second and third pulse (P2, P3) each elicited a depolarisation and a burst of spikes (Fig. 54B). The depolarisation elicited

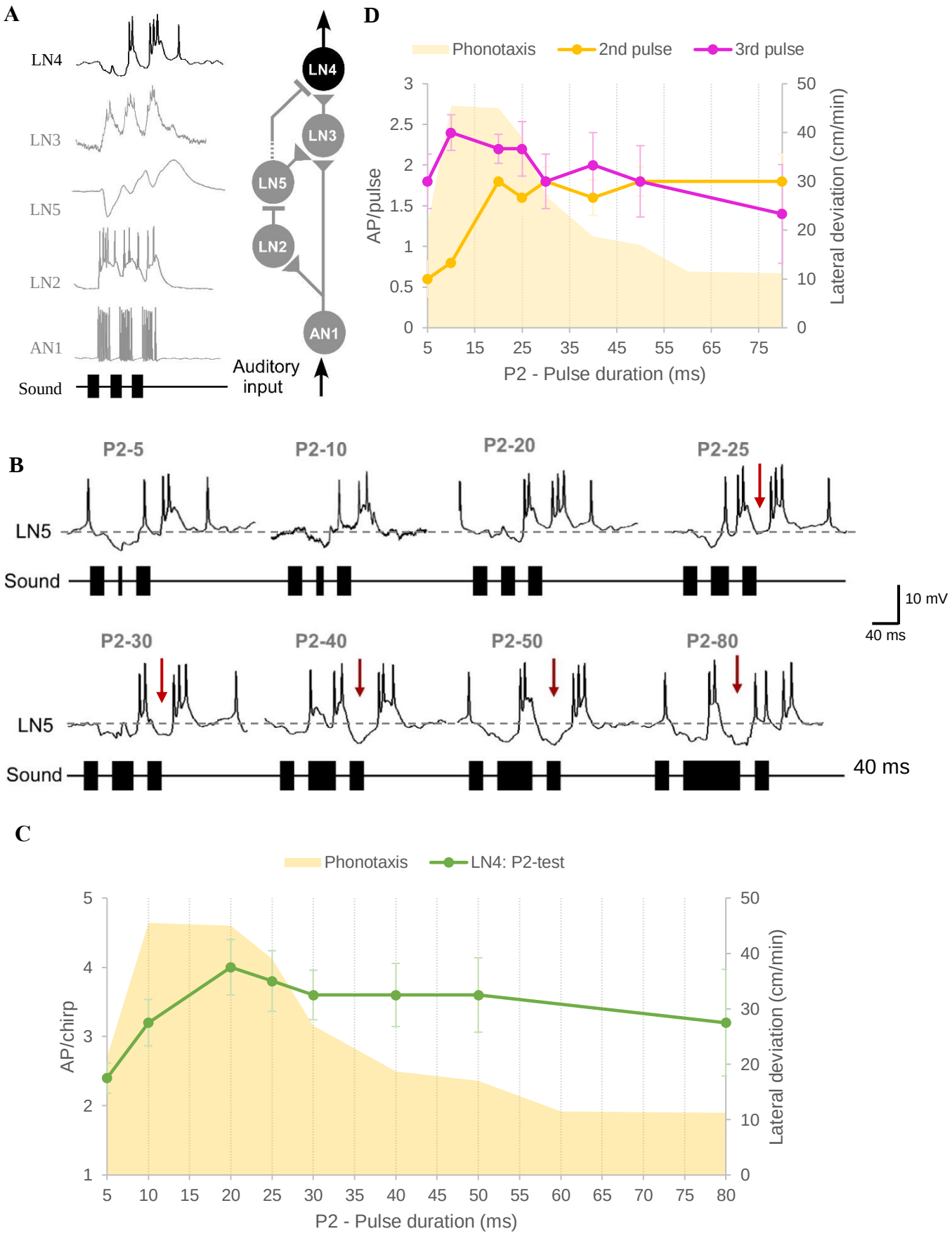

Fig. 54 Response of the coincidence detector neuron LN4 to P2-test.

Fig. 54 Response of the coincidence detector neuron LN4 to P2-test. A. Characteristic response of LN4 to the normal chirp and its role in the pattern recognition circuit. **B.** Activity of LN4 in response to chirps with P2 varied. The activity of LN4 is coloured in black, tested chirps are labelled above each response. Dotted lines indicate the resting potential. For medium and long P2 red arrows indicate the inhibition following the spiking activity elicited by the second sound pulse (P2). **C.** AP/chirp elicited in LN4 in response to the P2-test (N=5, n=5), and the phonotactic response indicated by yellow shade. **D.** AP/pulse elicited by P2 and P3 (N=5, n=5). Error bars represent standard error of the mean (SEM). Phonotactic response is in yellow shade.

by P2 had a latency of 32.8±0.8 ms from the start of P2.

For short P2 (P2-5 and P2-10), the response to P2 was not strong with spiking activity only giving 0.6±0.2 (P2-5) and 0.8±0.3 AP/pulse (P2-10), while the third sound pulse (P3) elicited a burst of spikes of 1.6±0.2 AP/pulse to both short P2 chirps. For medium P2 (P2-20, P2-25 and P2-30), a typical pronounced depolarisation with a burst of 2 spikes occurred (P2-20: 1.8±0.3 AP/pulse; P2-25: 1.6±0.2 AP/pulse; P2-30: 1.8±0.2 AP/pulse). As the duration of P2 exceeded 20 ms, an inhibition gradually emerged following the burst of spikes elicited by P2 which made the membrane recover to the resting potential (Fig. 54B, P2-25, red arrow). For P2-25, the membrane potential of LN4 recovered to the resting potential after the depolarisation caused by P2, indicating the interference of the inhibition. The inhibition further pushed the membrane potential below the resting potential when P2 was 30 ms (Fig. 54B, red arrows). For medium P2 chirps the activity elicited by the third sound pulse of the medium was quite constant with about 2 spikes (P2-20: 2.2±0.2 AP/pulse; P2-25: 2.2±0.3 AP/pulse; P2-30: 1.8±0.3 AP/pulse). The LN4 response changed substantially with longer P2 pulses. The inhibition following the first burst of spikes became more prominent as P2 increased (Fig. 54B, P2-40, P2-50 and P2-80, red arrows). The long duration of P2, however was not matched, by a correspondingly long depolarisation of LN4 which rather was cut short to a duration of 22.0±1.0 ms. This depolarisation at P2-80 is very similar to the depolarisation elicited by a normal 20 ms pulse and implicates that the effective pulse duration processed in the circuit may be limited. The short depolarisation also gave about 2 spikes as in the medium and long P2 (P2-40: 1.6±0.2 AP/pulse; P2-50: 1.8±0.2 AP/pulse; P2-80; 1.8±0.3 AP/pulse). Despite the cut-off effect on the burst of spikes and the inhibition elicited by medium and long P2, the number of spikes elicited by P3 in these chirps was also about 2.0±0.1AP/pulse which was similar to that elicited by short P2 (P2-5: ; P2-10:). Due to the build-up of the inhibition, LN4 was the only neuron responding to chirps containing longer P2 with less spikes compared to the normal chirp. Overall, LN4 showed characteristics of sparse coding, its activity to each chirp was lower by 65.66±1.61% when compared to the LN3 activity (6.6±0.4 AP/chirp), and lower by 83.81±1.11% when compared to the AN1 activity (18.3±1.4 AP/chirp).

The number of spikes elicited by each chirp was plotted in Fig. 54C. Over the P2-test, LN4 activity increased from 2.4±0.2 to 4.0±0.4 AP/chirp as P2 increased from 5 to 20 ms followed by a marginal decrease to 3.2±0.8 AP/chirp at P2-80 (Fig. 54C). The tuning curve of LN4 activity partially fits the phonotactic tuning; for P2 from 5 to 20 ms it steeply increases to

a maximum and then gradually declines towards P2-80. This decline, however, does not reflect the more pronounced reduction in phonotaxis. Although the activity of the feature detector did not perfectly match the phonotactic tuning, LN4 exhibited indications of band-pass tuning to the P2-test with a peak at P2-20.

An analysis into the response of LN4 towards the pulses P2 and P3 within the P2-test is presented in Fig. 54D. The response to pulse P2 increased from 0.6±0.2 AP/pulse at P2-5 to 1.8±0.3 AP/pulse at P2-20. Then the number of spikes remained at the same level of 1.7±0.0 AP/pulse for all P2 pulses up to 80 ms. LN4 activity elicited by pulse P3 peaked at P2-10 with 2.4±0.2 AP and then gradually decreased to 1.4±0.6 AP/pulse when P2 was 80 ms. When compared, both tuning curves exhibit different tendencies for short and medium P2; whereas the response to P2 showed an increase up to 20 ms, the response to P3 overall decreased over this range, both however stayed at a similar level for long P2. In summary, in the P2-test the spike activity of LN4 elicited by P3 showed some similarities, as it was strongest for small and declined towards long P2 durations, the response dominated the overall tuning of the neuron (Fig. 54C).

The sequential filtering in the pattern recognition circuit as revealed by the P2-test

For comparison, I normalized the spiking activity of the neurons to the activity caused by the 'normal chirp' (Fig. 55A). The relative increase in spike activity is similar in all the neurons for P2-5 to P2-20. In response to chirps with longer P2 the activity of AN1, LN2, and LN3 continues to increase linearly until P2-80. None of these 3 neurons shows a response maximum matching the behaviour. Only the tuning of LN4 qualitatively matches the tuning of phonotaxis with a broad and shallow maximum at P2-20, i.e. the normal chirp pattern.

Processing of the P2-chirps by the delay-line and coincidence-detector circuit

In Fig. 55B typical responses of the 5 neurons have been aligned to the start of the P2-chirps to reveal the flow of auditory activity in the pattern recognition circuit. Throughout the P2-test the spike activity of AN1 precisely copied the temporal pattern of the sound pulses. LN2 spike activity followed the sound pattern, but with less accuracy and underlying rather broad depolarisations.

Even for short P2, the LN5 activity showed a sequence of inhibitions and post-inhibitory rebounds, and LN3 generated 3 bursts of spikes, while LN4 responded with a typical initial

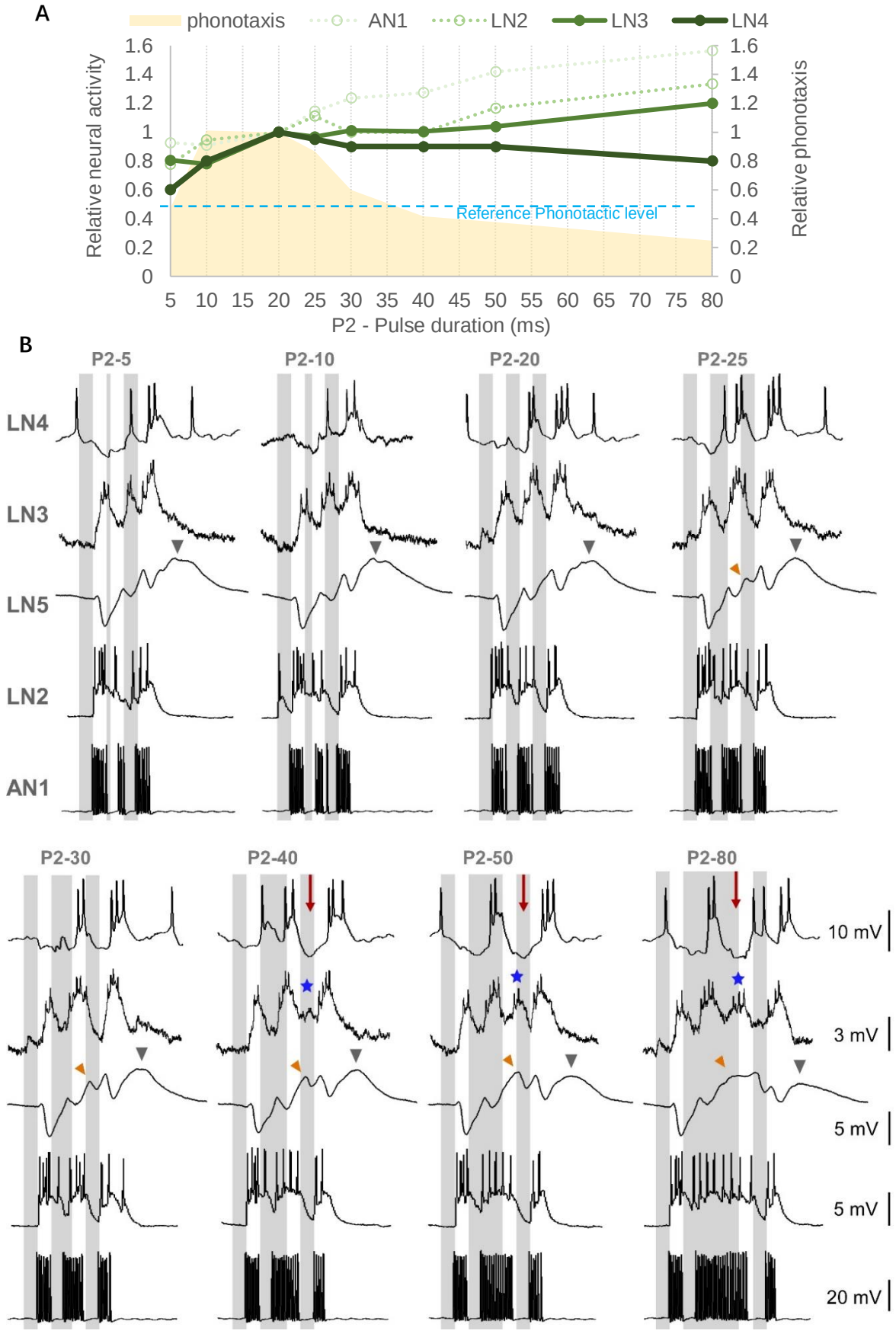

Fig. 55 Sequential filtering to varied 2nd pulse (P2) by the pattern recognition circuit.

Fig. 55 Sequential processing of P2-chirps by the pattern recognition circuit. A. Tuning curves of the spiking neurons AN1, LN2, LN3 and LN4 in the pattern recognition circuit and the phonotactic response to P2-chirps. The response elicited by the normal chirp in the neurons and for phonotaxis was set as 1, activity was calculated as the relative change compared to 1. The tuning curves of AN1 and LN2 (dotted lines) and of LN3 (light green) do not show any temporal selectivity. The tuning curve of LN4 (dark green) shows a weak match. The reference level indicates the phonotactic response elicited by a 2-pulses chirp. **B.** The recordings of LN4, LN3, LN5, LN2 and AN1 are aligned to the sound pulses, indicated by grey bars, chirps are labelled at top of each column. For LN4, LN3, LN2 and AN1, one example recording is shown, for LN5, the traces are averaged from 18 recordings. For LN5, orange arrowheads indicate the additional rebound for medium and long P2. Grey arrowheads indicate PIR3, of the only completed rebound. For LN3, blue stars indicate the extra EPSP/spikes elicited by long P2. For LN4, red arrows indicate the inhibition following the excitatory response to the second sound pulse (P2).

inhibition followed by two suprathreshold depolarisations. Thus, the responses of these 3 neurons were very similar to their response to a normal chirp, a fact that may be linked to the strong phonotactic behaviour occurring at short P2.

For medium P2, LN5 showed its typical rhythmic changes in membrane potential, coupled to the sound pattern. The coincidence between PIR1 of LN5 and the second burst of spikes in AN1, and the coincidence between PIR2 and the third spike burst in AN1 always elicited strong responses in LN3. The spiking activity in LN3, subsequently led to a pronounced depolarisation with burst of spikes in LN4. For these chirps i.e. the chirps with a good phonotaxis response, the feature detector LN4 generated 2 pronounced suprathreshold depolarisations. Similar to the gradual increase in the LN5 depolarisation, also the membrane potential of LN3 showed an increase in its depolarization.

For long P2 a pronounced extended and extra rebound activity in the LN5 activity became more prominent (orange arrowhead). This may be related to the development of an additional depolarisation in LN3, following the initial activity elicited by P2 (blue stars). When P2 increased to 50 and 80 ms, the extra rebound became stronger and the depolarisation in LN3 became suprathreshold and resulted in a burst of spikes. At the level of LN4 however, the excitatory input from the extra spikes of LN3 is not reflected. Due to the extended inhibitory input from LN2, for long P2 pulses a pronounced inhibition followed the first burst of spikes (red arrow), which likely cancelled the excitatory input from LN3. The short response of LN4 towards an ongoing sound stimulus indicates a network and cellular processing mechanisms that is sensitive to pulse duration. A similar response, however, was not observed for the processing of P1 pulses of different duration since P1 only elicit an inhibition in LN4.

Response of the pattern recognition network neurons to chirps with the third pulse of different duration: P3- test

In behavioural experiments with the P3-test females tolerated substantial changes in the duration of the third pulse P3 and responded with strong phonotactic activity even to chirps with long pulses (Fig. 36B). In this test the first two sound pulses and both intervals remained constant at 20 ms. Therefore, only the processing of the third sound pulse (P3) was affected.

The number of recordings of the neurons are: 10 repeats of AN1 (N=5, n=10), 10 repeats of LN2 (N=2, n=10), 10 repeats of LN5 (N=4, n=10), 10 repeats of LN3 (N=5, n=10) and 5 repeats of LN4 (N=5, n=5) for the characteristic responses of the neurons elicited by 20-ms

pulses and normal chirps, and 5 repeats of AN1 (N=5, n=5), 2 repeats of LN2 (N=2, n=2), 18 repeats of LN5 (N=4, n=18), 13 repeats of LN3 (N=5, n=13) and 5 repeats of LN4 (N=5, n=5) for the P3-test.

The ascending neuron – AN1

AN1 forwards the auditory information to neuron LN2 and the coincidence-detector LN3 (Fig. 56A). Its fundamental response properties to the normal chirp were given before (see P1-test).

AN1 response to P3-chirps

The spike pattern of AN1 reflected the duration of the pulses (Fig. 56B), it responded to P3-5 with a short burst of spikes, and the duration of its response then increased with increasing duration of P3. Overall AN1 activity gradually increased from 15.0±0.0 to 29.0±0.0 AP/chirp as the duration of P3 increased from 5 to 80 ms (Fig. 56B, C). Each chirp, except for P3-30, elicited a significantly different number of spikes when compared to the normal chirp (P3-5 vs. P3-20: p=0.0275, P3-10 vs. P3-20: p=0.0424, P3-25 vs. P3-20: P=0.0424, P3-40 vs. P3-20: p=0.0304, P3-50 vs. P3-20: p=0.0177, P3-80 vs. P3-20: p=0.0027, Friedman test, N=5, n=5). The increase of the AN1 activity over the P3-test was linear (slope of m=0.2004, R^2=0.914, correlation coefficient), its response did not match the behavioural tuning (Fig. 56C).

The inhibitory neuron – LN2

Neuron LN2 is driven by AN1 activity and inhibits the non-spiking neuron LN5 and the feature detector neuron LN4 (Fig. 57A). Its fundamental response properties were given before (see P1-test).

LN2 response to P3-chirps

Across all chirps each sound pulse elicited a suprathreshold EPSP, which only gradually decayed; the depolarisation elicited by the first sound pulse (P1) did not return to the resting potential in the interval between P1 and P2 (Fig. 57B). The increase of P3 led to almost linearly increased activity of LN2 over the P3-test with a slope of m=0.0777 (R^2=0.9506, correlation coefficient) (Fig. 57C). LN2 activity started at 6.9 AP/chirp at P3-5 and reached maximum of 12.9 AP/chirp at P3-80; at P3-5 the neuron generated an EPSP with just one spike and P3-80 caused a maintained depolarisation with 7 AP. LN2 activity in the P3 test was 55.17±0.95% less than the AN1 activity. The increase of LN2 activity over the P3-test did not match the

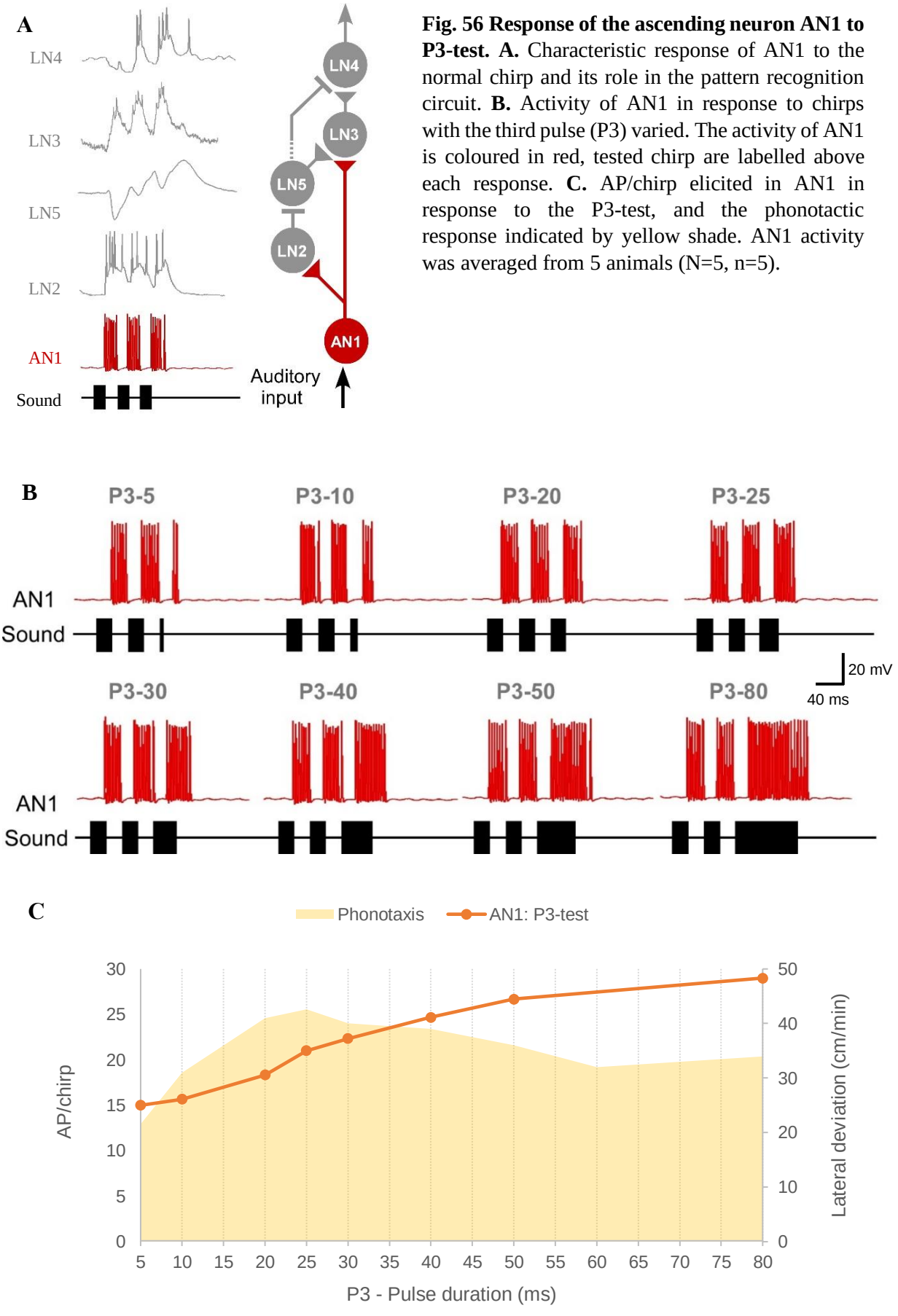

Fig. 56 Response of the ascending neuron AN1 to P3-test. A. Characteristic response of AN1 to the normal chirp and its role in the pattern recognition circuit. **B.** Activity of AN1 in response to chirps with the third pulse (P3) varied. The activity of AN1 is coloured in red, tested chirp are labelled above each response. **C.** AP/chirp elicited in AN1 in response to the P3-test, and the phonotactic response indicated by yellow shade. AN1 activity was averaged from 5 animals (N=5, n=5).

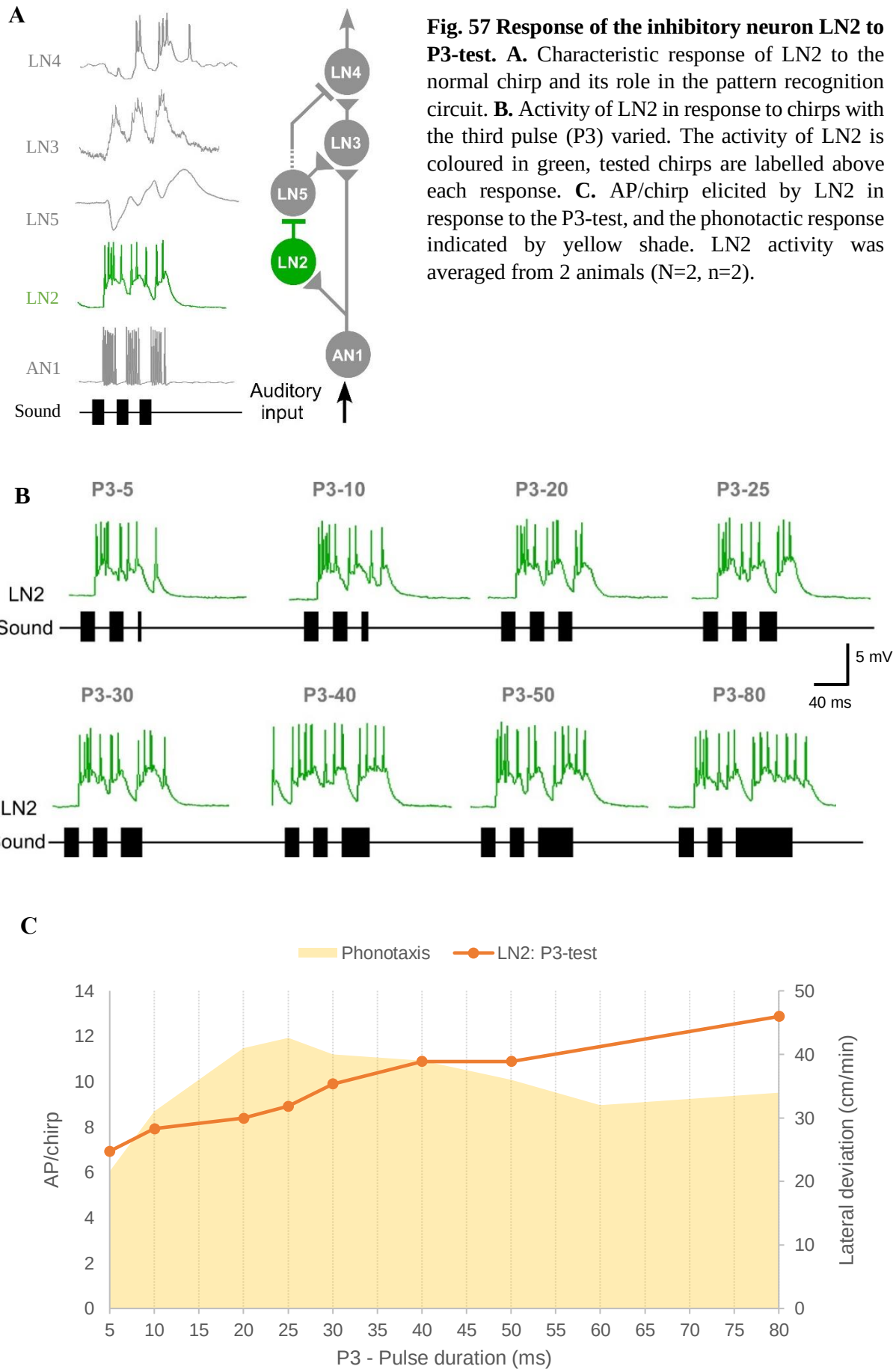

Fig. 57 Response of the inhibitory neuron LN2 to P3-test. A. Characteristic response of LN2 to the normal chirp and its role in the pattern recognition circuit. **B.** Activity of LN2 in response to chirps with the third pulse (P3) varied. The activity of LN2 is coloured in green, tested chirps are labelled above each response. **C.** AP/chirp elicited by LN2 in response to the P3-test, and the phonotactic response indicated by yellow shade. LN2 activity was averaged from 2 animals (N=2, n=2).

behavioural tuning (Fig. 57C).

The non-spiking neuron – LN5

The non-spiking neuron LN5 is inhibited by LN2 and generates a post-inhibitory rebound; it forwards its activity to the coincidence detector LN3 (Fig. 58A). The typical response pattern of LN5 to a normal chirp has been described before (Fig. 58B and see P1-test).

LN5 responses to P3-chirps

In this test, INH1, PIR1, INH2, PIR2 and INH3 were not affected by varying P3, chirps elicited the typical response of LN5 with its rhythmic oscillations driven by the pulse pattern (Fig. 59). The responses of LN5 started with an inhibition with a latency of 27.28 ms, INH1 reached a peak amplitude of -3.75±0.06 mV at 36.4±0.5 ms after the onset of the P1. PIR1 then reached a maximum of 1.5±0.1 mV at 25.7±0.5 ms after the onset of P2. The second inhibition had a maximum amplitude (INH2) of -1.5±0.1 mV at 35.4±1.0 ms after the start of P2 and the peak of the following PIR2 was 4.3±0.1 mV at 26.2±0.4 ms after the start of P3. The response to the first two sound pulses was almost identical for all P3-chirps, the only parameters that could have been affected by varying the duration of P3 were the third inhibition INH3 and the last rebound PIR3 (Fig. 58C, 59). The INH3 occurred with a very similar time course, it reached a maximum of -3.2±0.1 mV, which consistently occurred at 36.9±0.3 ms after the start of P3. There was no evidence that the duration of the third inhibition was driven by the duration of P3, as the initial recovery from INH3 was identical over all P3-pulses (Fig. 59).

For short P3 (P3-5 and P3-10), the membrane potential oscillation of LN5 was very similar to that in the normal chirp. The third rebound PIR3 (Fig. 58C, grey arrowheads) of LN5 occurred with a large amplitude (P3-5: 5.8±0.2 mV; P3-10: 5.6±0.3 mV) and a similar time course of the peak (P3-5: 84.2±1.3 ms; P3-10: 89.3±3.2 ms). For medium P3 (P3-20, P3-25 and P3-30), the amplitude of PIR3 decreased to a similar level as PIR2 (4.4±0.3 mV) when P3 was 30 ms (4.7±0.4 mV). The peak of PIR3 elicited by P3-20 occurred at 88.5±1.1 ms after the onset of P3. An extra peak similar as in the P1- and P2-tests emerged in the third rebound of LN5 for P3-25 and P3-30 (Fig. 58C, orange arrowheads). These extra peaks occurred at 60.6 (P3-25) and 64.8 ms (P3-30) after the onset of P3. At the same time, the peak of PIR3 (grey arrowheads) for these two chirps occurred at a later time after the onset of P3 compared to that elicited by P3-20 (P3-20: 88.5±1.1 ms, P3-25: 100.3±2.2 ms; P3-30: 109.1±3.5 ms). For long P3 (P3-40, P3-50 and P3-80), the amplitude of PIR3 was even lower than PIR2, giving 3.7±0.3

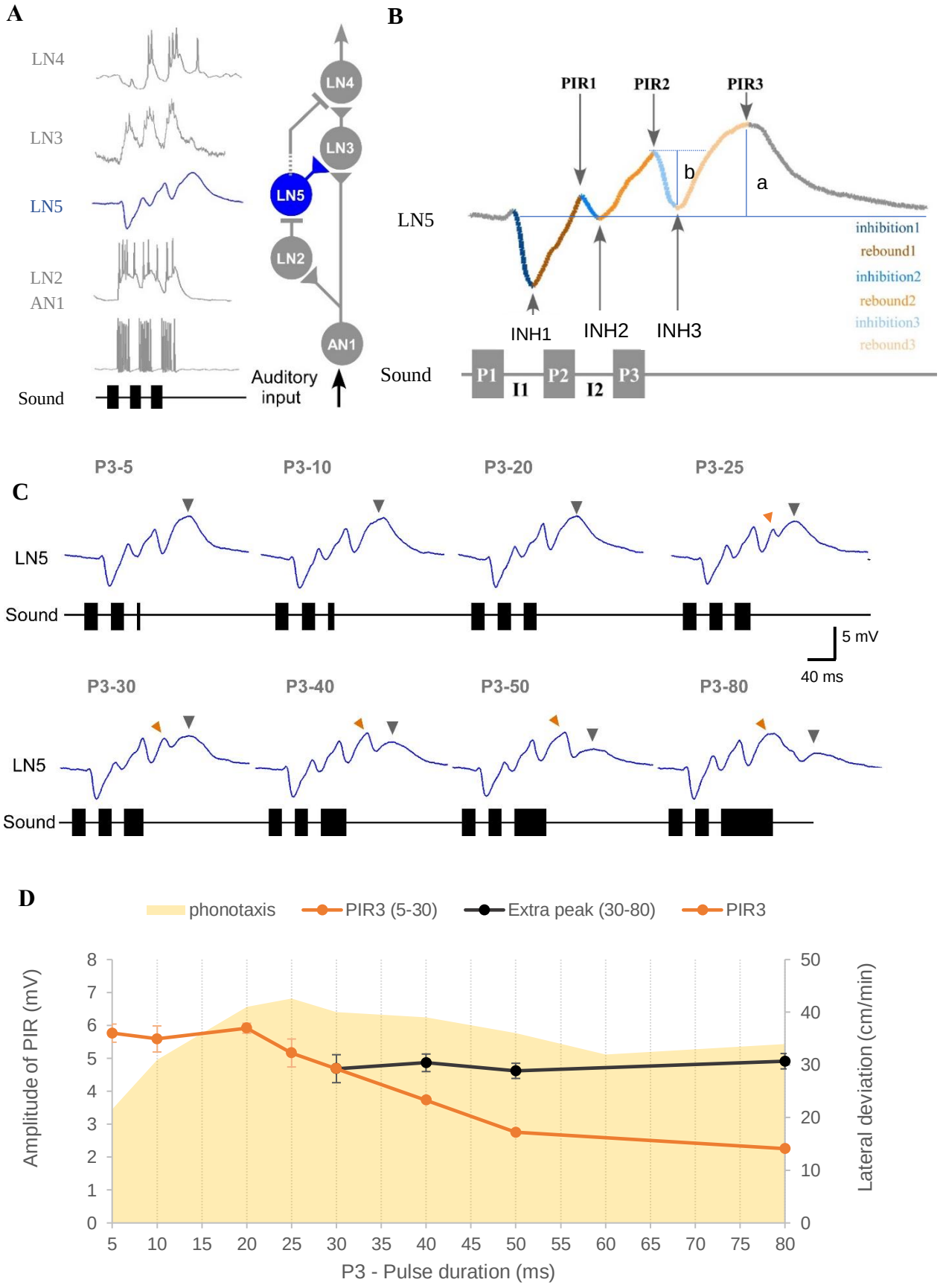

Fig. 58 Activity of LN5 elicited by the P3-test and the tuning of the amplitude of PIRs.

Fig. 58 Activity of LN5 elicited by the P3-test and the tuning of the amplitude of PIRs. A. Diagram showing characteristic activity of LN5 to the normal chirp and its role in the pattern recognition circuit. **B.** LN5 activity in response to a normal chirp. P1, P2 and P3 represent the three sound pulses, I1 and I2 refer to the two intervals. LN5 responds to the three pulses with three inhibitions (inhibition1, inhibition2 and inhibition3) and three rebounds (rebound1, rebound2 and rebound3). The maximum amplitudes of the inhibitions are labelled as INH1, INH2 and INH3. The highest membrane potential of rebound1 (brown) and rebound2 (orange) are marked as PIR1 and PIR2, they occur at the start of the following inhibition (blue and light blue). The peak amplitude of rebound3 (light yellow) is labelled as PIR3, this rebound is not interrupted by an inhibition. **C.** Average responses of LN5 to the P3-test (N=4, n=18), activity of LN5 coloured in blue. Tested chirps are labelled above each recording. Orange arrowheads represent the additional rebound peak formed in response to medium and long P3, grey arrowheads indicate the peak of the third rebound (PIR3). D. The tuning of the maximum membrane potential in the third post-inhibition rebound (N=4, n=18). The amplitude of PIR3 over P3-5 to P3-30 (orange line) and the extra peak over P3-30 to P3-80 (black line) (N=4, n=18). Error bars indicate the standard error of the mean (SEM). Phonotactic response is in yellow shade.

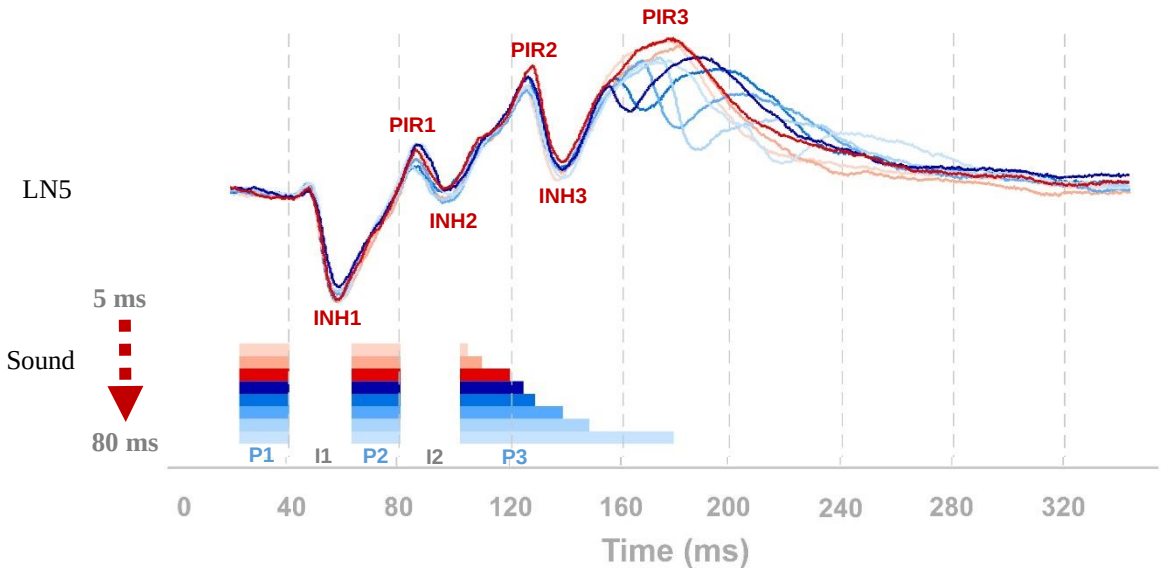

Fig. 59 LN5 activity elicited by the P3-test aligned to the first sound pulses. Averaged LN5 activity in response to the P3-chirps is aligned to the onset of P1 (N=4, n=18). When P3 is smaller than 25 ms, the chirps and LN5 responses are coloured as light to dark red, respectively. For P3 equal to or larger than 25 ms, chirps and LN5 responses are coloured as dark to light blue, respectively. Responses in dark red and blue are to chirps P3-20 and P3-25 that elicited the best phonotactic behaviour.

mV for P3-40, 2.8±3.7 mV for P3-50 and 2.3±0.2 mV for P3-80. Meanwhile, the latency of PIR3 increased compared to the latency for medium P3, to 118.8±4.1 ms, 132.6±6.0 ms and 158.8 ms, respectively. The extra peak (Fig. 58C, orange arrowheads), became more pronounced and reached an amplitude higher than both PIR2 and PIR3 (grey arrowheads) and occurred at 75.8 ms (P3-40), 84.4 ms (P3-50) and 87.1 ms (P3-80) after the onset of P3. For P3-25 to P3-50, the extra peak always occurred with a delay of about 35.2 ms after the offset of P3 (P3-25: 35.6 ms; P3-30: 34.8 ms; P3-40: 35.8 ms; P3-50: 34.4 ms). This delay was a little longer than the one in P1 (29.9 ms to the offset of P1) and P2 (28.4 ms to the offset of P2) tests.

For the P3-test the amplitude of PIR3 was plotted in Fig. 58D. When P3 increased from 5 to 20 ms PIR3 showed a similar amplitude of 5.8±0.1ms. For P3-25 to P3-80 the amplitude decreased gradually to 3.62±0.23 mV (Fig. 58D), while the extra peak increased in amplitude (P3-25: 4.15±0.15 mV; P3-30: 4.36±0.42 mV; P3-40: 4.60±0.27 mV; P3-50: 4.62±0.23 mV and P3-80: 4.99±0.23 mV). It is noteworthy that the extra peak (Fig. 58C, orange arrowheads) exceeded the PIR3 in amplitude when P3 was equal to or longer than 40 ms. To illustrate the tuning of the extra peak in P3 test, I plotted the amplitude of the extra peak for P3-30 to P3-80 in Fig. 58D (black line). The tuning of the extra peak was flat (Fig 23D black line) which better represented the tuning of phonotaxis than the tuning of PIR3 within the range of P3-30 to P3-80 (Fig. 58D orange line). Since both the amplitude of PIR1 and PIR2 were identical across the P3-test, the summed amplitude of PIR1+PIR2 as in P1- and P2- tests was not different among each chirp in P3-test.

In terms of INH3, with the increase in P3 duration from P3-25 to P3-80, the INH3 occurred with a very similar time course, and did not follow the duration of P3 (Fig. 59). An extra rebound peak occurred during the last rebound (Fig. 58C, orange arrowheads), indicating that LN5 received an additional inhibitory input, that was not directly driven by a sound pulse.

In terms of the average slope of the PIRs in the P3-test, it was basically determined by the amplitude of PIR3 as shown in Fig. 60 (for calculation, see P1-test). Only slope3 was variable in response to each of these four chirps while slope1 and slope2 are identical in response to all chirps in P3-test. Thus the tuning curve of the average slope (Fig. 61, orange line) showed similar declining trend as the tuning of PIR3. I also plotted the average slope for the extra peak when P3 was between 30 to 80 ms (Fig. 61, black line) because its amplitude surpassed that of the PIR3 in this range. Similar to what was seen in the tuning of the amplitude, the average slope based on the extra peak (Fig. 61, black line) was more constant and reflected

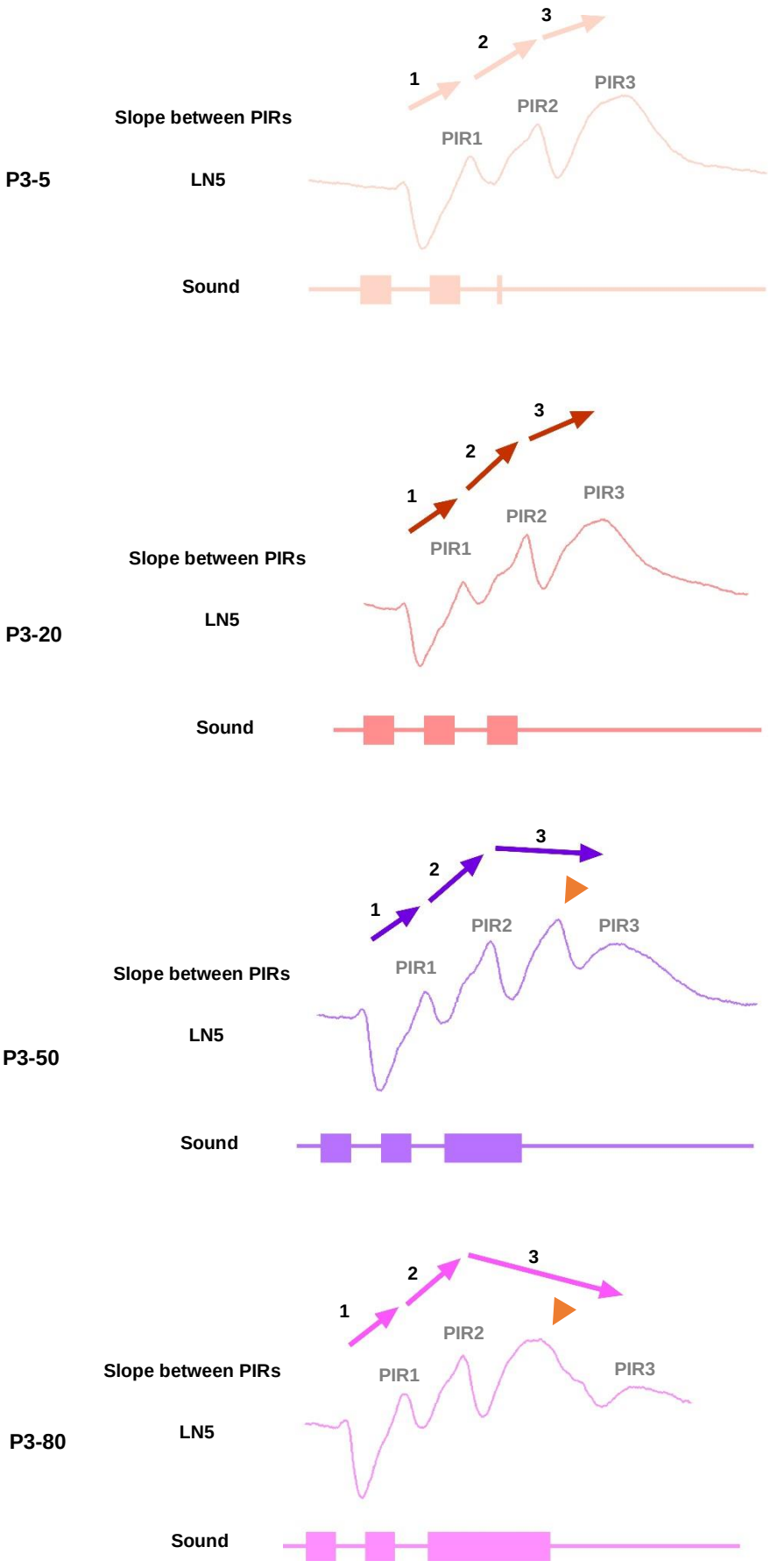

Fig. 60 The changes in the amplitude of adjacent PIRs over time (slope between PIRs) in P3-test

Fig. 60 Changes in the amplitude of adjacent PIRs (slope between PIRs) over different chirps in the P3-test. The changes in the amplitude of adjacent PIRS over time in response to four example chirps (P3-5. P3-20, P3-50 and P3-80) of the P3-test (N=4, n=18). The arrows indicate the change and slope between two adjacent PIRs over the time interval between the PIRs (t1, t2 and t3), which are named as slope1, slope2 and slope3. The slope2 and slope3 were directly influenced by varying P3. Orange arrowheads indicate the extra peak in P3-50 and P3-80.

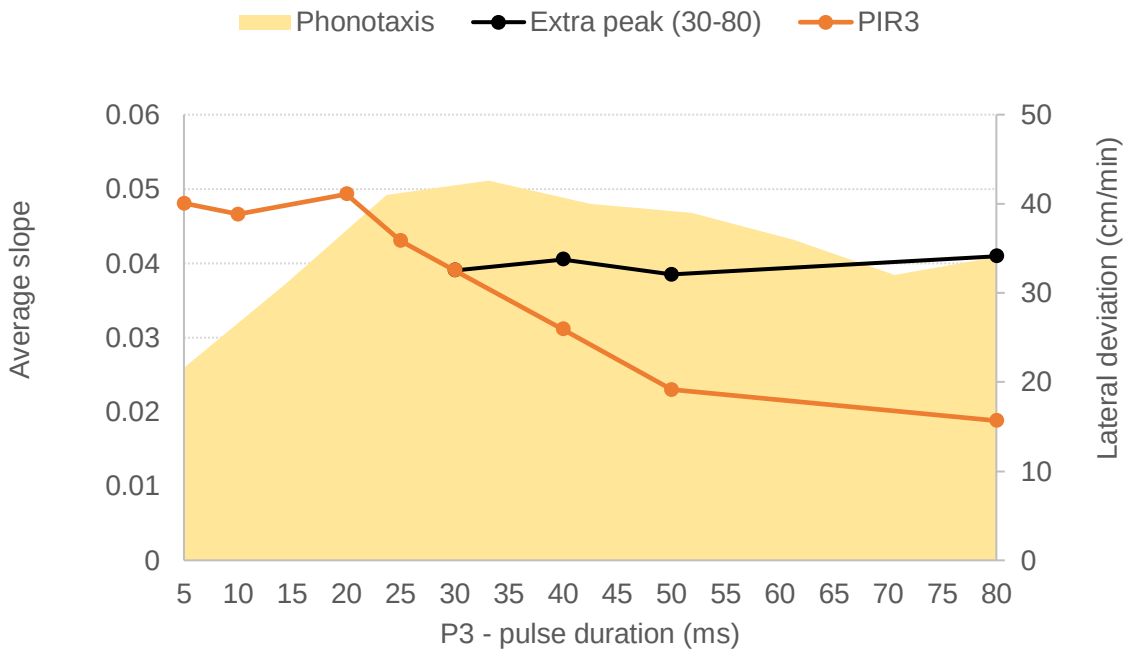

Fig. 61 Tuning of the mean 'slope' of LN5 in the P3-test. The tuning curve is averaged from slope1, slope2 and slope3 in response to each chirp of the P3-test (N=4, n=18). Average slope when slope3 was measured with PIR3 is given in orange. Average slope when slope3 was measured with the extra peak for P3-30 to P3-80 is indicated in black. Phonotactic response is in yellow shade.

the tuning of the phonotaxis better than that of the PIR3 (Fig. 61, orange line).

In summary, the amplitudes of PIR1, PIR2 and PIR3 successively increased over the time course of a chirp for P3-5 to P3-20 (Fig. 58C, 59), and at P3-20 the rebound PIR3 reached its highest amplitude, indicating an underlying enhanced depolarisation of LN5. When P3 increased from 25 to 80 ms the situation became more complex, due to an extra rebound and inhibition. When comparing the LN5 responses over the P3-test pattern, the membrane potential oscillations were overall very similar to the response to a normal chirp: Even when P3 was short a pronounced PIR3 was generated, and at very long P3 the additional rebound peak occurred at a similar time, as when PIR3 was generated in response to the normal chirp. Thus, changing the P3 duration overall did not substantially affect the LN5 response.

Three features of the LN5 response during the P3-test are noteworthy. 1. The initial activity pattern of LN5 was highly similar for all P3-chirps. 2. The time course of the inhibition caused by P3 did not depend on the duration of the pulse. 3. For P3 pulses longer than 25 ms LN5 generated an extra peak during the third rebound.

Despite of the changes and features described above, in a 3-pulse chirp the PIR3 may not contribute to pattern recognition according on the delay-line and coincidence detector mechanism.

The coincidence detector – LN3

Neuron LN3 is driven by a direct input from AN1 and a delayed graded input from LN5 and is the coincidence detector in the network (Fig. 62A).

LN3 response to P3-chirps

When tested with the P3 pattern, neuron LN3 responded with a latency of 30.2±0.5 ms, and each pulse within a chirp elicited a separate suprathreshold depolarisation, which gradually built up over a chirp and elicited 2-4 AP/pulse (Fig. 62B). LN3 activity was 52.38±2.42 % lower than the activity in AN1. The response to P1 was 2.4±0.1 AP (p=0.2296, Friedman test, N=5, n=13), while the response to P2 was 4.1±0.1 AP and 74.31±4.37% higher than the response to P1.

As P3 changed in duration the response of LN3 became more complex. For short P3 (P3-5 and P3-10), the number of spikes elicited (P3-5: 1.5±0.3 AP; P3-10: 3.3±0.2 AP) was less

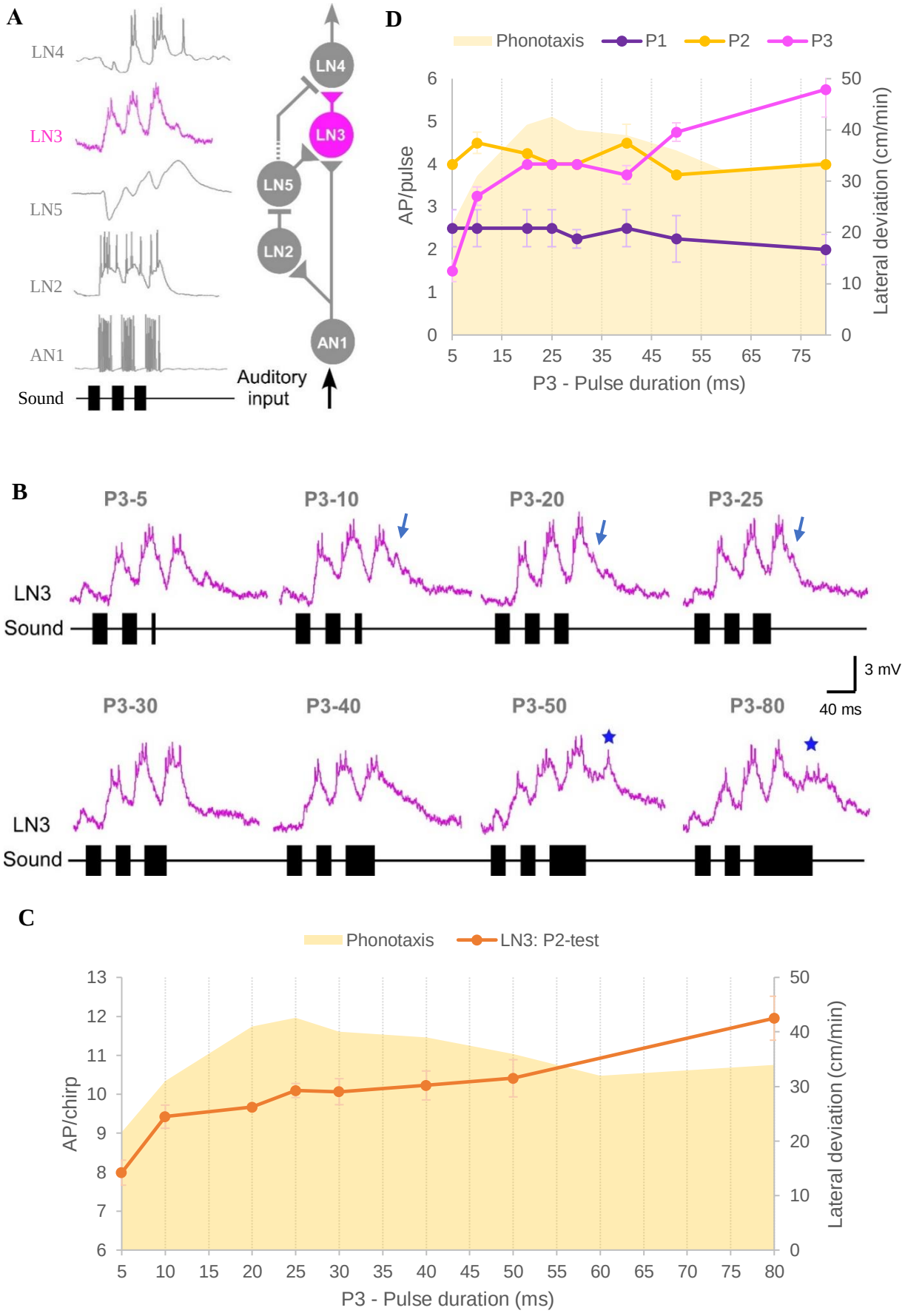

Fig. 62 Response of the coincidence detector neuron LN3 to P3-test.

Fig. 62 Response of the coincidence detector neuron LN3 to the P3-test. A. Characteristic response of LN3 to the normal chirp and its role in the pattern recognition circuit. **B.** Activity of LN3 in response to chirps with P3 varied. LN3 recording coloured in pink, chirps are labelled above each response. Blue arrows indicate a delayed depolarization after the end of the third burst of spikes. For long P3 blue stars indicate a depolarization/extra spikes following the third burst of spikes. **C.** AP/chirp elicited in LN3 in response to the P3-test (N=5, n=13), and the phonotactic response indicated by yellow shade. **D.** AP/pulse elicited in LN3 by each pulse (N=5, n=13). Error bars represent standard error of the mean (SEM). Phonotactic response is in yellow shade.

than that elicited by P2 (4.1±0.1 AP). For medium P3 (P3-20, P3-25 and P3-30), the depolarisation elicited by P3 became stronger and elicited a similar number of spikes than P2 (P3-20: 4.0±0.1 AP; P3-25: 4.0±0.1 AP; P3-30: 4.0±0.2 AP). For long P3 (P3-40, P3-50 and P3-80), the initial suprathreshold depolarisation caused by P3 lasted for 39.9±0.6 ms and the spikes lasted for 19.3±1.0 ms. An additional subsequent depolarisation with spikes occurred at 74.7±1.3 ms after the onset of P3 for P3-50 and P3-80 (Fig. 62B, blue stars), and may be linked to the rebound pattern in LN5. Therefore, the number of spikes elicited by the third pulse of P3-50 and P3-80 was greater than that caused by second pulse (P3-50: 4.8±0.2 AP; P3-80: 5.8±0.6 AP).

Plotting the activity of LN3 over the P3-test showed a gradual increase from 8.0±0.3 AP/chirp at P3-5 to 12.0±0.6 AP/chirp at P3-80 (Fig. 62C). P3-80 elicited significantly more spikes than P3-20 (P3-80: 12.0±0.6 AP/chirp; P3-20: 9.7±0.0 AP/chirp, p=0.0108, Friedman test, N=5, n=13). The tuning curve shows a high level of activity over the P3-test, which is in line with the phonotactic behaviour, but the particular strong response to long P3 does not match the behavioural tuning (Fig. 62C).

To explore whether the response property of LN3 is different for the individual sound pulses, I calculated for P1 to P3 the AP/pulse and plotted this over the P3-test (Fig. 62D). The number of spikes elicited by P1 was identical across the test at 2.4±0.1 AP (p=0.2296, Friedman test, N=5, n=13) and was the lowest response to the three pulses. Also, the activity elicited by P2 remained at a stable level of 4.1±0.1 AP and was not different across the test (p=0.2038, Friedman test, N=5, n=13). The activity elicited by P3 increased from 1.5±0.3 AP to 4±0.0 AP when P3 increased from 5 to 20 ms (slope of m=0.15 AP/pulse/ms, R^2=0.8359, correlation coefficient), the response then remained at a level of 4.0±0.0 AP/pulse for P3 between 20 and 30 ms. As P3 further increased activity increased from 3.8±0.2 AP/pulse (P3-40) to 5.8±0.6 AP/pulse (P3-80) with a slope of m=0.046 AP/pulse/ms (R^2=0.9231, Pearson correlation coefficient). The response to P3 matches the behaviour, as it increases from P3-5 to P3-20 and stays at a high level until P3-50, its only deviation occurs at the very long P3 pulses. The response to P1 and P2 were very stable across the P3-test and for medium and long P3 pulses similar to the behavioural tuning. The data indicate that the LN3 tuning curve for the whole test (Fig. 62C) is mainly shaped by the response to P3.

The feature detector – LN4

The response of the feature detector neuron LN4 is driven by an inhibitory input from LN2 and an excitatory input from LN3 (Fig. 63A). The characteristic sparse coding of LN4 was reflected in its mean low spike activity, which was 62.4±1.6% lower compared to the activity in LN3, and 82.1±1.1% lower when compared to the activity in AN1 (LN4: 3.8±0.2 AP/chirp; LN3: 10.0±0.4 AP/chirp; AN1: 21.6±1.7 AP/chirp).

As the first two pulses P1 and P2 of the test pattern were identical, an initial inhibitory response occurring with a latency of 25.1±0.6 ms mixed with subthreshold EPSPs was typical for all P3-chirps (Fig. 63B). The response to the second sound pulse P2 however, showed some variability related to the strength of these EPSPs, and the strength of the suprathreshold depolarisation elicited by. This could be pronounced with a high discharge rate burst of 3 spikes as for P3-20 (blue arrowhead), or a rather weak depolarisation with just 1 spike as for P3-80 (blue arrowhead), although the acoustic stimulus was identical (Fig. 63B).

For short P3 (P3-5 and P3-10), the depolarisation elicited by P3 was weaker than the one caused by P2. Even when P3 was only 5 ms in duration, the pulse elicited a spike in LN4. For medium P3 (P3-20, P3-25 and P3-30), each P3 elicited a pronounced depolarisation with a burst of 2-3 spikes (Fig. 63B). When P3 was 30 ms, an inhibition occurred following the second burst of spikes (Fig. 63B, red arrow). At long P3 the inhibition at the end of the LN4 spike activity became more prominent, like for P3-50 (red arrows). The depolarisation response of the neuron was 21.2±0.7 ms and shorter than the duration of the long sound pulses. A similar response of LN4 occurred in the P2-test for the response to the P2-80 chirp (Fig. 54B), indicating a filter for pulse duration.

The LN4 spike activity over the P3-test is plotted in Fig. 63C. Activity increased from 2.8±0.2 AP/chirp at P3-5 to its peak of 4.4±0.5 AP/chirp at P3-20, it then gradually decreased to a level of 4.0±0.1 AP/chirp for P3-80. Only when P3 was shorter than the normal 20 ms pulse, should the change in its duration affect the responses of LN4. The activity elicited in LN4 should be at a similar level for chirps with a P3 duration longer than 20 ms, as only the initial part of the P3 pulse can be effective in the coincidence-detection. This is what is revealed by the tuning curve of the feature detector LN4, which showed an increase of its response for short P3, it matched the phonotactic with a broad maximum in the range of the best phonotactic response and subsequently showed a very slight gradual decline towards long P3-pulses. The resulting tuning curve matches the behavioural tuning very well, and this may support the assumption of a close link between LN4 activity and phonotactic behaviour.

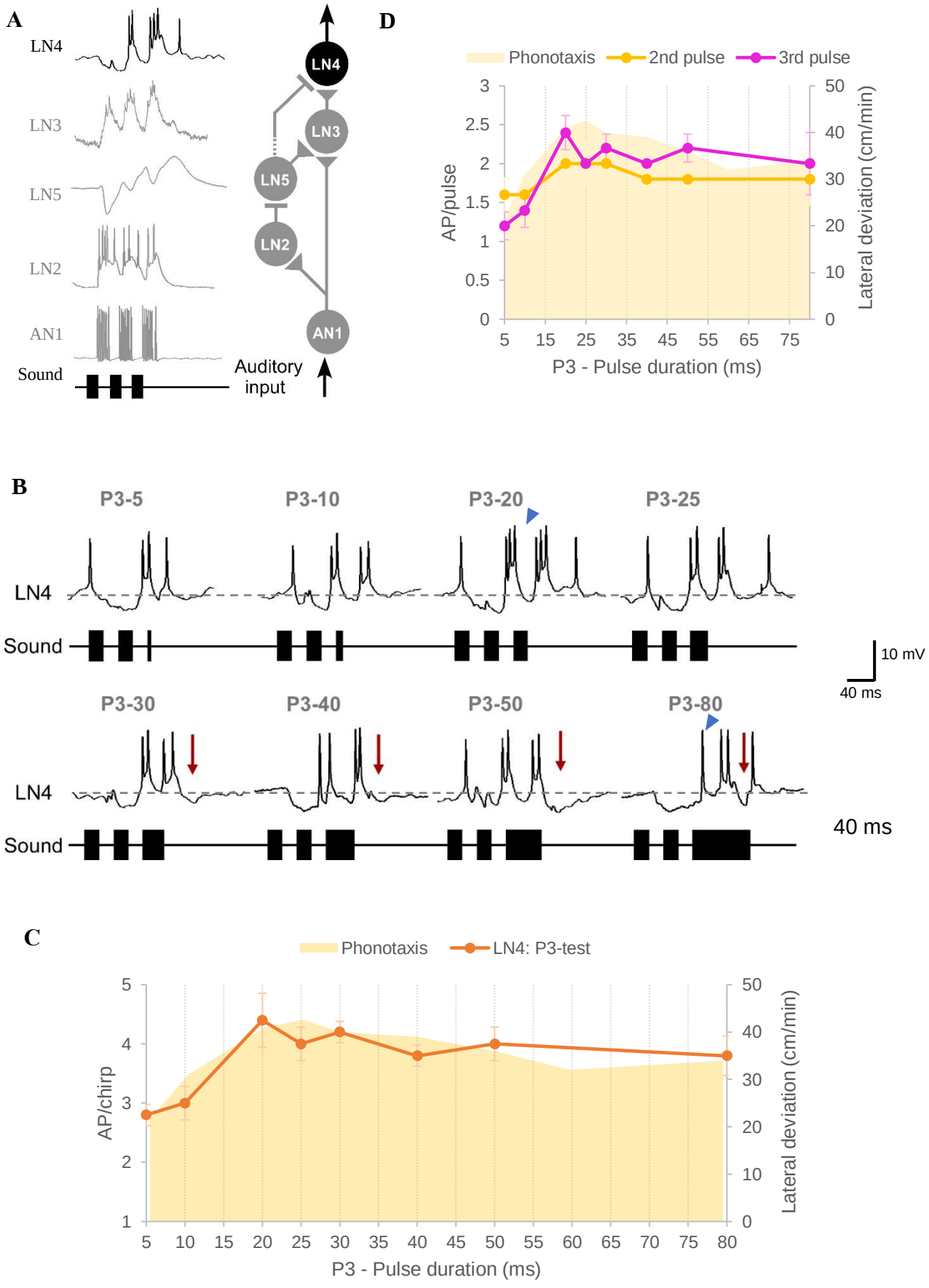

Fig. 63 Response of the coincidence detector neuron LN4 to P3-test.

Fig. 63 Response of the coincidence detector neuron LN4 to the P3-test. A. Characteristic response of LN4 to the normal chirp and its role in the pattern recognition circuit. **B.** Activity of LN4 in response to P3-chirps (coloured in black), tested chirps are labelled above each response. Dotted lines indicate the resting potential. Blue arrowheads indicate the spiking activity elicited by the second sound pulse (P2) in P3-20 and P3-80. Red arrows indicate the inhibition following the last burst of spikes. **C.** AP/chirp elicited by LN4 in response to the P3-test (N=5, n=5), and the phonotactic response indicated by yellow shade. Error bars represent standard error of the mean (SEM). Phonotactic response is in yellow shade.

An analysis into the response of LN4 towards each sound pulse demonstrates that the response to P2 did not show significant differences across the P3-test and remained between 1.6±0.2 and 2.0±0.3 AP/pulse (p=0.5575, Friedman test, N=5, n=5). (Fig. 63D). In response to P3, the LN4 activity increased from 1.2±0.2 to a peak of 2.4±0.2 AP/pulse when P3 increased from 5 to 20 ms, it then remained at about 2.1±0.0 AP/pulse for all longer P3 durations. Overall, the tuning curves for P2 and P3 were very similar and like the overall activity of LN4 (Fig. 63C) reflected the tuning of the behaviour.

The sequential filtering in the pattern recognition circuit as revealed by the P3-test

To compare the tuning curves of the spiking neurons, I normalized their spiking activity to the activity elicited by the 'normal chirp' and plotted the curves (Fig. 64A). The activity of AN1, LN2 and LN3 increased over the course of the P3-test as the duration of P3 increased, however they did not show filter properties matching the phonotactic response. In comparison, only the LN4 tuning curve showed a good match to the phonotactic behaviour.

Processing of P3-chirps by the delay-line and coincidence-detection circuit

Representative example recordings of the 5 neurons are aligned to the P3-chirps (Fig. 64B), to elucidate the possible flow of auditory information in the circuit proposed by Schöneich et al. (2015). I will focus on the responses of the delay-line neuron LN5, the coincidence-detector LN3 and the feature-detector LN4.

As P1 and P2 were not altered the initial responses of all neurons were very similar throughout the test. The first phasic onset activity of LN2 in response to P1 was very consistent throughout the test and triggered the initial stereotyped inhibition in LN5. The LN2 response to the second sound pulse P2 was quite variable; therefore a precise link to the stereotyped time course of INH2 in LN5 is not obvious. In response to a short P3 of 5 ms LN2 generated a single spike only (Fig. 64B), nonetheless the third inhibition INH3 in LN5 was fully expressed (Fig. 64B, P3-5, LN5, green arrowhead). This indicates that few LN2 spikes can have a substantial effect on LN5. Furthermore the amplitude of INH3 remained the same, even when LN2 activity increased to a burst of 4.0±0.1 AP as for P3-25 ms and also for the long lasting LN2 activity elicited by P3-80. This may further indicate that the exact timing of the first LN2 spikes in response to a sound pulse is crucial to drive the inhibition in LN5.

Apart from the normal chirp, at medium and long P3 in LN5 the time course of the third

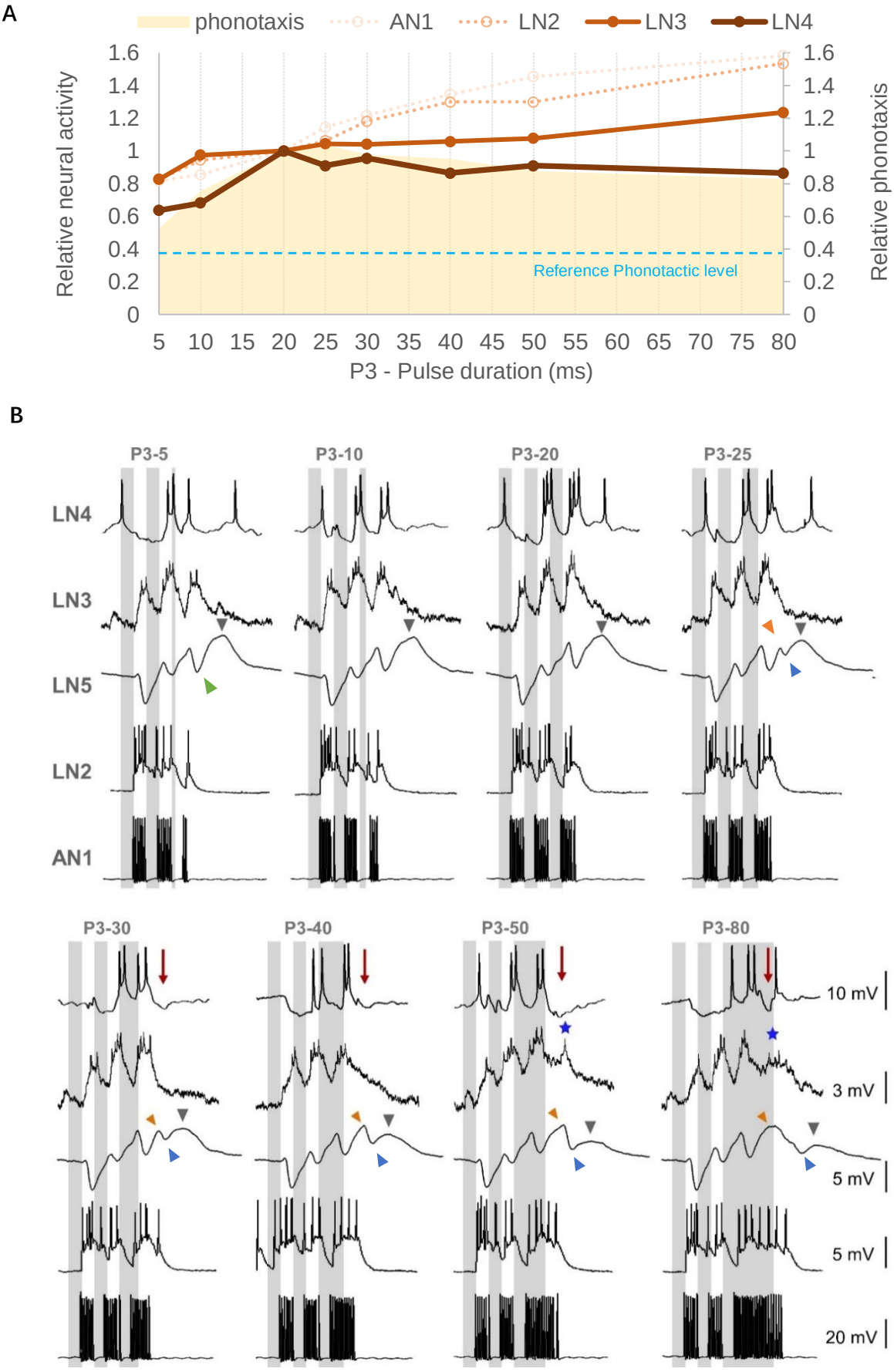

Fig. 64 Sequential processing of P3-chirps by the pattern recognition circuit.

Fig. 64 Sequential processing of P3-chirps by the pattern recognition circuit. A. The tuning curves of the spiking neurons AN1, LN2, LN3 and LN4 and the phonotactic response to P3-chirps. The response elicited by the normal chirp in the neurons and for phonotaxis were set as 1, activity evoked by other chirps is calculated as the relative change compared to 1. The tuning curves of AN1 and LN2 (dotted lines) and of LN3 (orange) do not show any temporal selectivity. The tuning curve of LN4 (brown) follows the phonotactic tuning. The reference level indicates the phonotactic response elicited by a 2-pulse chirp. **B.** The recordings of LN4, LN3, LN5, LN2 and AN1 are aligned to the sound pulses, which are indicated as grey bars, chirps are labelled on top of each column. LN5 traces are averaged from 18 recordings. For LN5, orange arrowheads indicate the additional rebound peak elicited by medium and long P3. Blue arrowheads indicate the repolarization following the extra peak during rebound3. Grey arrowheads indicate PIR3 at the end of the response. For LN3, blue stars indicate the extra EPSP/burst of spikes elicited by long P3. For LN4, red arrows indicate the inhibition following the excitatory response to the third sound pulse (P3) for medium and long pulses.

rebound changed and the neuron received an additional inhibition (Fig. 64B, blue arrowheads) that formed the extra peak (Fig. 64B, orange arrowheads), which was not directly linked to LN2 spike activity. It reveals an underlying network activity that controls the LN5 activity, beyond the direct response to the sound pulses.

Activity of LN3 is driven by spiking input from AN1 and the graded input from LN5. Even short P3 of 5 and 10 ms lead to a pronounced depolarisation and spiking of LN3, due to the coincidence of AN1 spikes with the second rebound in LN5. For P3-20 to P3-25, the response of LN3 to P3 increased in intensity since more spikes of AN1 coincided with PIR2 of LN5. For P3-50 and P3-80, the extra burst of spikes generated in LN3 (blue stars) may be related to the coincidence between the extra rebound and the long continuous spike activity in AN1. In comparison to the LN5 membrane potential, also LN3 showed a gradual maintained depolarisation over the time course of the chirps, which was similar to the overall depolarisation seen in LN5, and supports the conclusion that LN3 continuously receives a graded input from LN5, not only in time with the peak of the rebounds.

As LN4 is driven by inhibition from LN2 and excitation from LN3 its response depends on the relative intensity of both inputs. Short P3 of 5 and 10 ms elicited a depolarisation with 1-2 spikes. For P3 of 20 and 25 ms the burst of spikes elicited became similar to the bursts elicited by P2 (Fig. 64B). This response with two subsequent pronounced depolarisations and bursts of spikes represents the characteristic LN4 activity coming with the best phonotactic response. In case of the P3-test this typical LN4 activity was also generated by chirps with long P3-pulses linking it to the maintained phonotaxis. For P3-30 to P3-80 the second burst of spikes in LN4 (Fig 30B, e.g. P3-50, red arrows) did not follow the duration of the sound pulse P3, it rather was terminated before the end of the sound pulse, indicating a filter for pulse duration, which may be due to inhibition from ongoing spike activity in LN2. In case of P3-80 however, did the extra spike activity of LN3 (blue star) overcome the inhibitory input from LN2 (red arrow) and it elicited an excitation of LN4 at the end of the chirp.

Comparing the neuronal and behavioural responses to the P1-, P2- and P3-test pattern

When comparing the tuning curves of phonotactic responses towards the P1- and P2-tests, it is clearly shown that even when pulse P1 was as short as 5 ms the phonotactic response was already strong (Fig. 65A). From the peak at P1 and P2 of 10-20 ms, the phonotactic response dropped sharply when P1 or P2 was 30 ms and the response was as low as the reference level

A

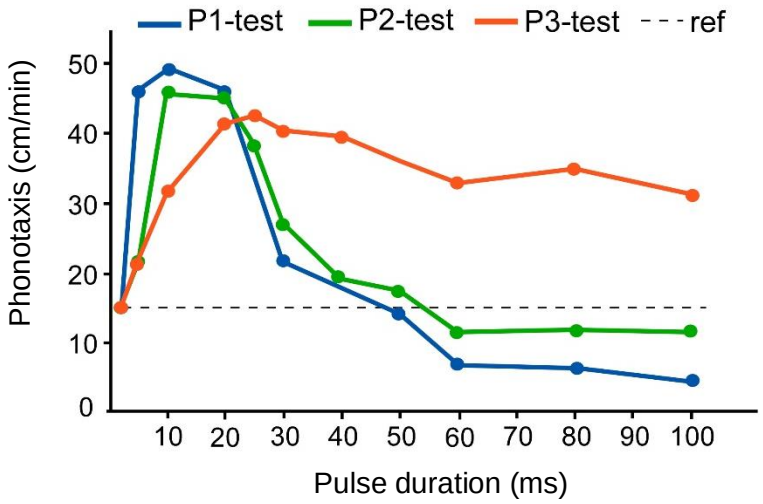

B

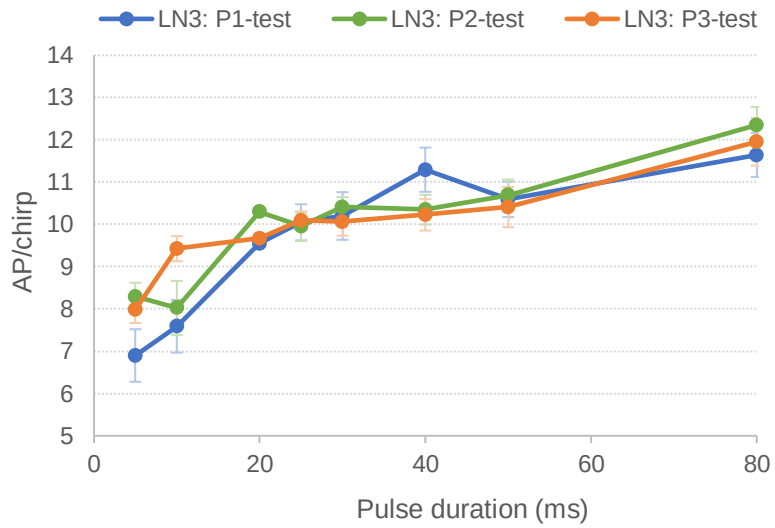

C

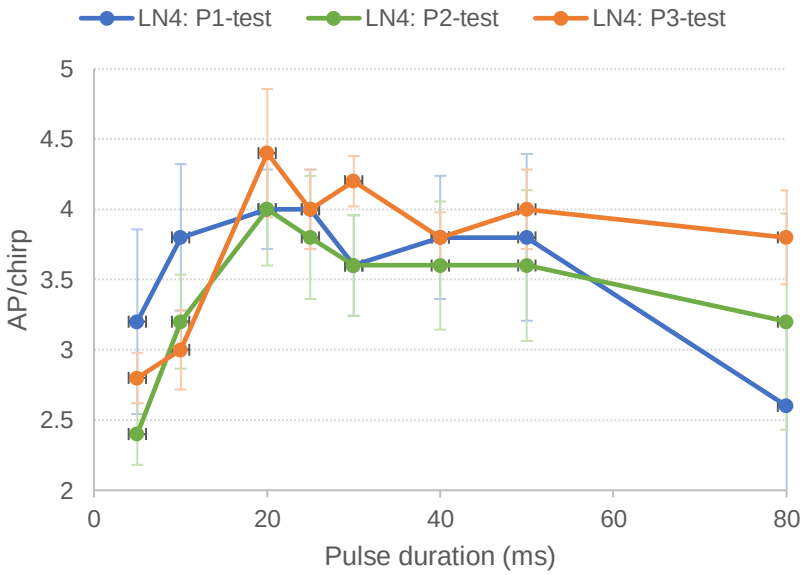

Fig. 65 Comparison of the tuning of phonotaxis, of LN3 and LN4 activity for the P1-, P2- and P3-tests

Fig. 65 Comparison of the tuning of phonotaxis, of LN3 and LN4 activity for the P1-, P2- and P3-tests. A. Phonotactic tuning to P1, P2 and P3-tests. The level of the phonotactic response to the reference chirp (2-pulses chirp) is shown as a dotted line. **B.** Comparison of the LN3 tuning between P1-, P2- and P3-tests. The tuning of LN3 to P1-chirps is in blue, for P2-chirps in green and for P3-chirps in orange. The number of spikes was averaged from 5 animals, 13 repeats. Error bars represent standard error means (SEM). **C.** Comparison of the LN4 tuning between P1-, P2- and P3-tests. The tuning of LN4 to P1-chirps is in blue, for P2-chirps in green and for P3-chirps in orange. The number of spikes was averaged from 5 animals, 5 repeats. Error bars represent standard error of the means (SEM).

from P1-40 and P2-40. In case of the P3-test the build-up to the maximum response was more gradual, however the chirps with long P3 did not result in a reduced phonotactic response, as chirps with long P1 and long P2 did (Fig. 65A). The differences exhibited among the three tuning curves indicated that P1, P2 and P3 weighed differently in a 3-pulses chirp for the phonotactic response.

However, the different phonotactic tuning curves were not reflected in the tuning curves of LN3 or LN4 as represented by the number of spikes per chirp (Fig. 65B, C). The tuning curves of LN3 to the P1-, P2- and P3-tests exhibited a very similar increase when the duration of the varied pulses was increased (Fig. 65B). This may indicate that the three pulses did not contribute differently to the activity of LN3 as seen in the phonotactic response. The three tuning curves of LN4 to the P1-, P2- and P3-test showed overall very similar shape with minor differences (Fig. 65C), indicating that the changing one of three sound pulses may make slightly different contribution to LN4 activity.

Within the range of 5 to 20 ms, both LN3 and LN4 activity elicited by P1-, P2- and P3-tests reflected the phonotactic response. The tuning curves of LN4 to medium and long pulses did not increase as the pulses increased in duration, indicating some pulse duration selectivity in LN4. However, the tuning curves for the P1- and P2-tests did not show a sharp reduction in their activity neither in LN3 or in LN4 in response to chirps containing pulses longer than 25 ms as seen in the phonotactic responses. Overall, neither the activity of LN3 nor LN4 exhibits a similar tuning as the phonotactic responses (Fig. 65B and C). This may be an indication that 1. The number of spikes per chirp may be not sufficient as a parameter coding the changes in pulse duration. Or 2. Other neurons with different filtering properties for pulse duration selectivity may also contribute to the tuning of the network. 3. The looped auditory test regime had an impact on the tuning of the neuronal responses.

Response of the pattern recognition network neurons to chirps with all pulses varied: PD-test

In the PD-test using chirps with 4 pulses the duration of all 4 pulses was systematically changed at the same time in the range of 5 to 100 ms (Fig. 37B). For the PD-test recordings of the ascending interneuron AN1 and of the feature detector LN4 were obtained in different animals, AN1 was recorded 8 times in 8 animals and LN4 was recorded 5 times in 4 animals (Fig. 66). The test will reveal, how the neuronal and network properties seen in the previous tests will

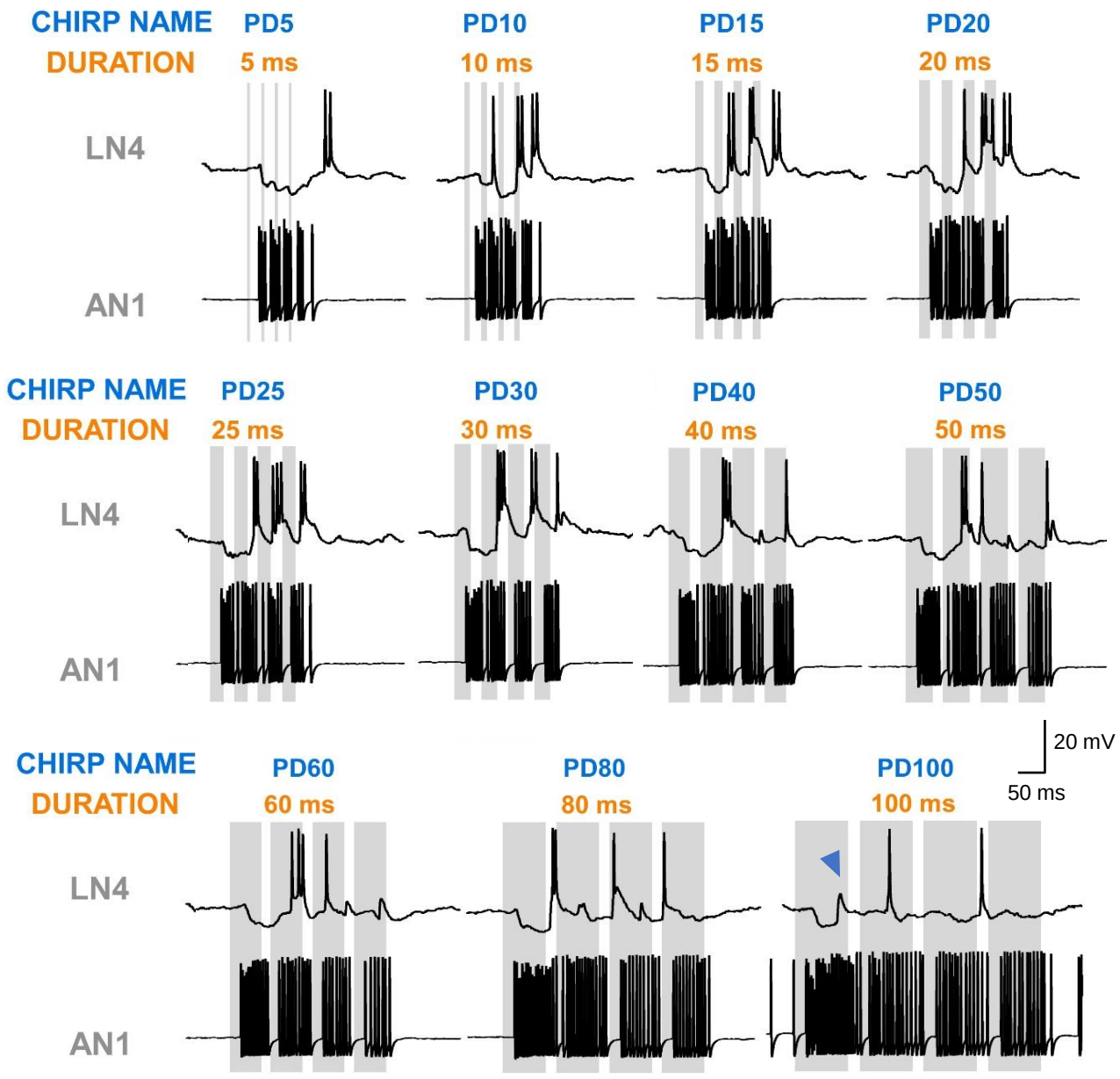

Fig. 66 Response of AN1 and LN4 to the chirps in the PD-test. Example activity of AN1 and LN4 in response to chirps with duration of all pulses varied (PD-test). The chirps were composed of four pulses with pulse intervals constant at 20 ms. The duration of the pulses was changed from 5, 10, 15, 20, 25, 30, 40, 50, 60, 80 to 100 ms, corresponding chirps are labelled as PD5, PD10, PD20, PD25, PD30, PD40, PD50, PD60, PD80 and PD100. The names of the tested chirps are given above each chirp.

affect the filtering of the chirps when all pulses have been altered in the same way.

As in the previous experiments, AN1 spike activity reflected the temporal pattern of the sound pulses across all PD-tests. It responded with a latency of 19.0±0.1 ms and generated a phasic-tonic burst of spikes (Fig. 66, AN1). The phasic part was prominent for short pulses, whereas the tonic part became obvious when long pulses of 80-100 ms were presented. There was no tuning of AN1 activity to the different PD stimuli, the number of spikes per chirp increased linearly from 16.2±1.5 AP/chirp (PD-5) to 52.4±9.4 AP/chirp (PD-100) as the duration of the pulses increased (R^2=0.9807, PD10: 20.8±1.1 AP/chirp; PD15: 23.6±1.5 AP/chirp; PD20: 25.6±2.1 AP/chirp; PD25: 26.2±1.5 AP/chirp; PD30: 29.0±2.4 AP/chirp; PD40: 34.2±2.3 AP/chirp; PD50: 37.6±3.6 AP/chirp; PD60: 41.6±3.3 AP/chirp; PD80: 47.8±7.6 AP/chirp). The activity of the AN1 presented, shows a high background activity, which - differently to other recordings - obscured the pulse intervals for short PD. This may have been due to acoustic noise or motor activity of the animal.

LN4 responded to the first sound pulse of a PD chirp consistently with IPSPs, regardless of the pulse duration. When the pulse duration was 5 ms (PD5), each pulse evoked an IPSP, which summed up over time and kept the neuron hyperpolarised for the duration of the chirp. A burst of spikes was only generated when the inhibition stopped, having a latency of 103.1±7.7 ms to the onset of the chirp. Chirps composed of pulses with a duration of 10 ms did not reliably elicit a burst of spikes for P1 and P2, the spiking responses was delayed and occurred only to the third and fourth pulse (Fig. 66). As pulse duration increased from 15 to 30 ms (PD15, PD20, PD25 and PD30), LN4 responded to each of the last three pulses with a prominent depolarisation and a burst of 2-3 spikes. The initial hyperpolarisation was still at its maximum just before the depolarisation in response to the second sound pulse occurred. As pulse duration further increased to 80 ms (PD40, PD50, PD60 and PD80), the excitatory LN4 responses became gradually diminished and inhibition dominated the response. The hyperpolarisation elicited by the first pulse lasted longer and only gradually waned before a depolarisation and burst of spikes occurred in response to the second pulse (PD40-PD60). As seen in the previous experiments and by Kostarakos and Hedwig (2015), the depolarisation generated by these long sound pulses was considerably shorter than the duration of the pulse, and points towards the effect of the inhibition or an intrinsic property of the network as a filter for pulse duration. For all long pulses the response to the third and fourth sound pulse was an inhibition mixed with EPSPs and sparse spiking, they did not induce a distinct depolarisation or burst of spiking in

LN4, and activity was considerably lower as compared to PD25, although the overall duration of the chirp at PD100 was 4 times longer. When PD100 was presented, the membrane potential recovered from the initial inhibition before the end of the first sound pulse (Fig. 66, blue arrowhead) and a depolarisation or spiking response was elicited. Spikes and depolarisation were only rarely elicited by the following three sound pulses.

To quantify the response of LN4, I measured the total number of spikes elicited by each chirp in 4 animals (N=4, n=5); this parameter was also used in previous studies (Wohlers and Huber 21982, Kostarakos and Hedwig 2012). Fig. 67 shows the phonotactic response of *G. bimaculatus* to chirps with different PDs (orange area) and the average number of spikes elicited by a chirp (AP/chirp) in LN4 (blue curve).

The phonotactic behaviour shows a sharp increase for pulse durations from 5 to 20 ms. The peak response is at PD20 with a lateral deviation of 24 cm/min, the response then drops in a similar sharp way to PD40 with a response of 25 mm/min, and remains at this level for PD50 to PD100. Overall, the behavioural data reveal a clear band-pass tuning with a best response at PD20, corresponding to the normal chirp pattern.

In comparison as the PD increased from 5 to 25 ms, the number of AP/chirp generated by LN4 increased from 1±0.5 AP/chirp to 7±0.5 AP/chirp, respectively, (Fig. 67A). The maximum response with 7±0.5 AP/chirp, was evoked by PD-25. As the pulse duration increased to 40 ms, the response decreased to 4±0.2AP/chirp and when PD increased from 40 ms to 100ms, the activity in LN4 slowly decreased to 3 AP/chirp. Statistical data analysis indicates that the response of LN4 was significantly different for chirps with short pulse duration (PD-5) and long pulse durations (PD100) when compared to the 'normal chirp' (PD-20) (PD-20 vs. PD-5: 6.8±0.6 vs. 1±0.5, p=0.0004; PD-20 vs. PD-100: 6.8±0.6 vs. 3±0.3, p=0.0312, Friedman test, n=5). Although the peak of LN4 activity is shifted to 25 ms pulse duration, overall, the resulting band-pass tuning of the LN4 response to different pulse durations matches closely with the tuning of the phonotactic behaviour (Fig. 67A).

The processing of different pulse duration is an accumulative process

The total number of spikes (AP/chirp) reflects the overall response of LN4 to a chirp. I therefore asked if the band-pass tuning is also reflected in the LN4 response to each sound pulse within a chirp. Since the first sound pulse always elicited an IPSP in LN4, I only analysed the bursts

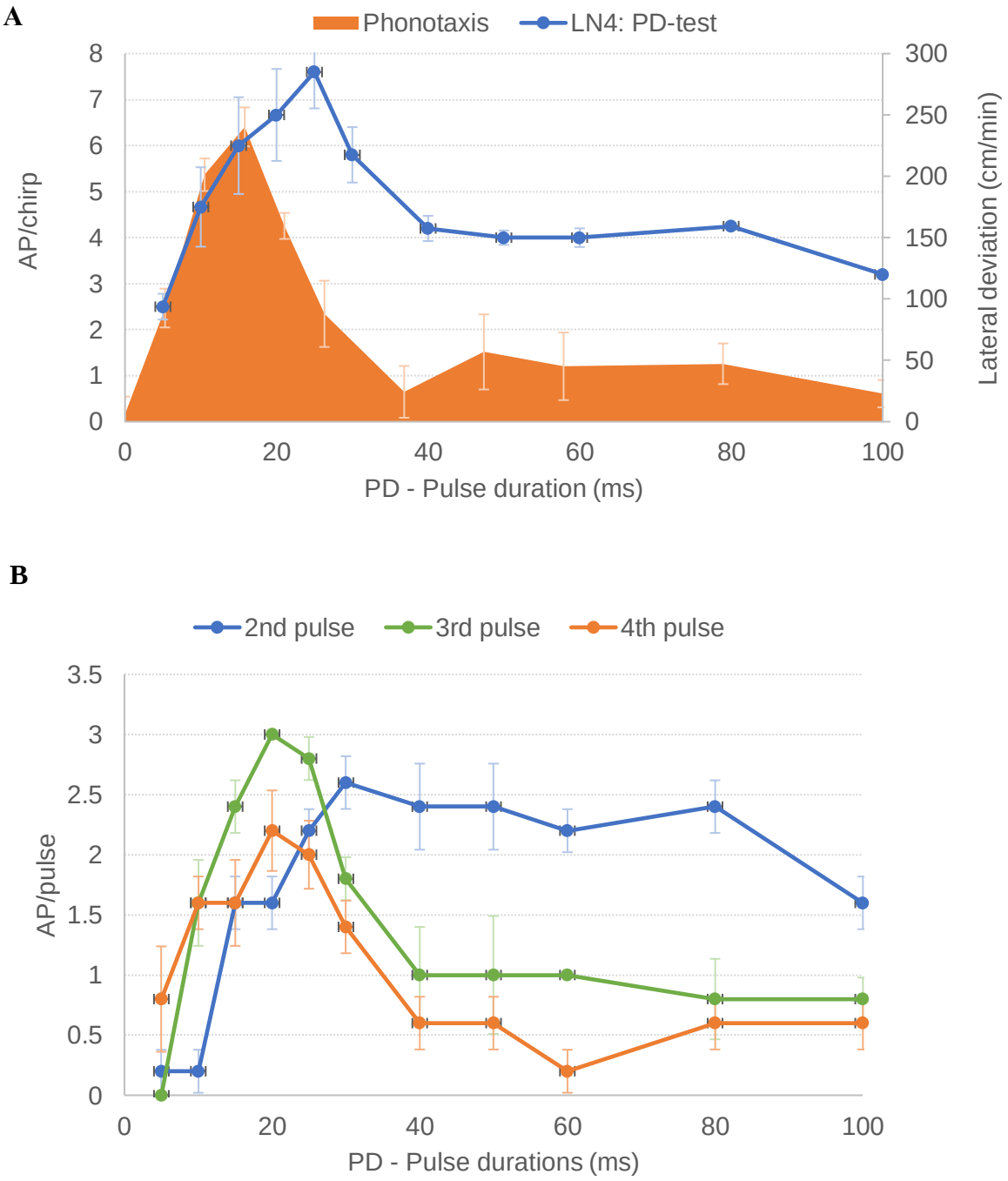

Fig. 67 The tuning curves of LN4 to the PD-chirps and to individual pulses of the PD-chirps. **A.** Tuning curve of LN4 activity (AP/chirp) in response to PD-chirps. The data is averaged from 4 animals and 5 repeats. The phonotactic response is derived from experiment by Adam Bent (unpublished). Error bars indicate the standard error mean (SEM). **B**. Tuning curve of LN4 in response to the last three sound pulses of the PD chirps. Activity elicited by the second sound pulse (blue), the third sound pulse (green) and the last sound pulse in orange. Data averaged from 4 animals and 5 repeats. Error bars indicate the standard error of the mean (SEM).

of spikes in response to the last three pulses (Fig. 67B).The number of spikes generated by LN4 in response to the second pulse increased as PD increased from 5 to 30 ms (blue line). The maximum response (2.6±0.2 AP/Pulse) to the second pulse was elicited by PD30 chirps. When the second pulse P2 was 5 ms (0.2±0.2 AP/Pulse) and 10 ms (0.2±0.2 AP/Pulse) the LN4 response was significantly lower than the response to a pulse of 20 ms duration (p=0.0149, p=0.0149, Dunnett's multiple comparison, n=5). As PD increased from 25 to 80 ms, the response curve for the second pulse plateaued and on average 2 AP/Pulse were elicited, at PD100 the response dropped slightly to 1.6±0.2 AP/Pulse.

A much sharper tuning of LN4 activity occurred in response to both the third and the fourth sound pulse (Fig. 67B). The third pulse (green line) did not elicit any spike at a PD of 5 ms. As PD increased to 20 ms, the response to the third pulse increased and peaked at PD20 with 3±0.0 AP/Pulse. With further increasing PD the response sharply declined to 1.0 AP/Pulse at PD40 and slightly fell below this level at PD100 with 0.8 AP/Pulse. The responses at PD30, PD60, PD80 and PD100 were all significantly lower than the response to PD20 (20ms vs. 30ms: 3±0.0 vs. 1.8±0.2, p=0.0183; 20ms vs. 60ms: 3±0.0 vs. 1±0.0, p=0.0001; 20ms vs. 80ms: 3±0.0 vs. 0.8±0.2, p=0.0197; 20ms vs. 100ms: 3±0.0 vs. 0.8±0.2, p=0.0019, Dunnett's multiple comparison, n=5). The LN4 activity in response to the third pulse reveals a band-pass tuning that closely resembles the overall LN4 tuning curve (Fig. 67A, blue) and especially the behavioural tuning (Fig. 67A, orange). This suggests that in particular the response to the third sound pulse could be decisive for the tuning of phonotactic behaviour.

As for LN4 responses to the fourth pulse, the overall activity of LN4 was lower than that to the second and third pulse. A rise in activity was observed as the pulse duration increased from 5 ms to 20 ms (Fig. 67B, orange line). The maximum activity occurred when the pulse duration was 20 ms (2.2±0.3 AP/Pulse). A gradual decrease in the number of AP/Pulse followed, and at PD-60 it was only 0.2±0.2 AP/Pulse, and significantly lower than the response at PD-20 (20ms vs. 60ms: 2.2±0.3 vs. 0.2±0.2, p=0.0176). A low response was also observed at 40, 50, 80 and 100 ms pulse duration. For long PDs a sharper tuning was observed as compared to the third pulse. Overall, also the tuning to the fourth pulse followed the tuning of the behavioural response.

The tuning curves suggests that the temporal filtering of the pulse patterns is a sequential process with the responses to all pulses contributing in a specific way and shaping the final tuning curve. In comparison, the tuning curve of LN4 (Fig. 67A) with the relative high activity

for PDs larger than PD20 may be shaped by the response to the second sound pulse (Fig. 66B, blue line), as the response to the second pulse remains high for long pulse durations. The specific filtering of LN4 activity is due to the decrease in spike activity (Fig. 67A) when PD was longer than 25 ms is rather due to the lower responses elicited by the third and fourth pulse. The response to all three pulses (P2-P4) contributes the sharp rising phase of the overall tuning. The sharper tuning to the third and fourth pulses is likely related to the inhibitory input to LN4 and is consistent with the observation that effective phonotactic behaviour can only be reliably induced by chirps composed of at least three pulses (Hedwig and Sarmiento-Ponce 2017). This may suggest that three pulses are required as the minimal unit for LN4 to detect and discriminate conspecific patterns.

The responses of the pattern recognition circuit to the attractive and non-attractive chirp patterns

As an outcome obtained from the three turning curves of the phonotactic behaviour to the P1-, P2- and P3-tests, two chirp patterns containing identical pulses, but with reversed pulse sequences, were demonstrated to be either attractive or non-attractive to female *G. bimaculatus* (Fig. 36C and 37C). The attractive pattern is a sequence of 3 pulses with 5, 20 and 50 ms duration, whereas the non-attractive pattern is the reverse sequence with pulses of 50, 20 and 5 ms duration. Here, responses of the pattern recognition neurons were recorded in 10 animals to the two patterns and to a normal pattern with three 20 ms pulses (Fig. 68).

In response to the normal chirp AN1 and LN2 reliably copied the sound pattern (Fig. 68A, left), LN5 showed the typical membrane potential oscillations with sequences of inhibition and three increasing post-inhibitory rebounds. LN3 responded with depolarisations and spike activity, increasing with each pulse and a subthreshold EPSP at the end of the chirp, linked to the final rebound in LN5. LN4 activity started with a typical inhibition, followed by two pronounced suprathreshold depolarisations with burst of 2-3 spikes and a delayed excitation at the end of the response.

In response to ‘attractive chirp’ (5-20-50 ms) (Fig. 68A, middle), AN1 and LN2 again copied the sound pattern. Due to the short first pulse (5 ms) the first inhibition of LN5 was not as strong as in response to the normal chirp and lead to a weak PIR1. Its coincidence and additive effect with the AN1 response to P2 made LN3 respond with 3 spikes to sound pulse P2. The second rebound PIR2 coincided with the extended response of AN1 to P3 and resulted

A

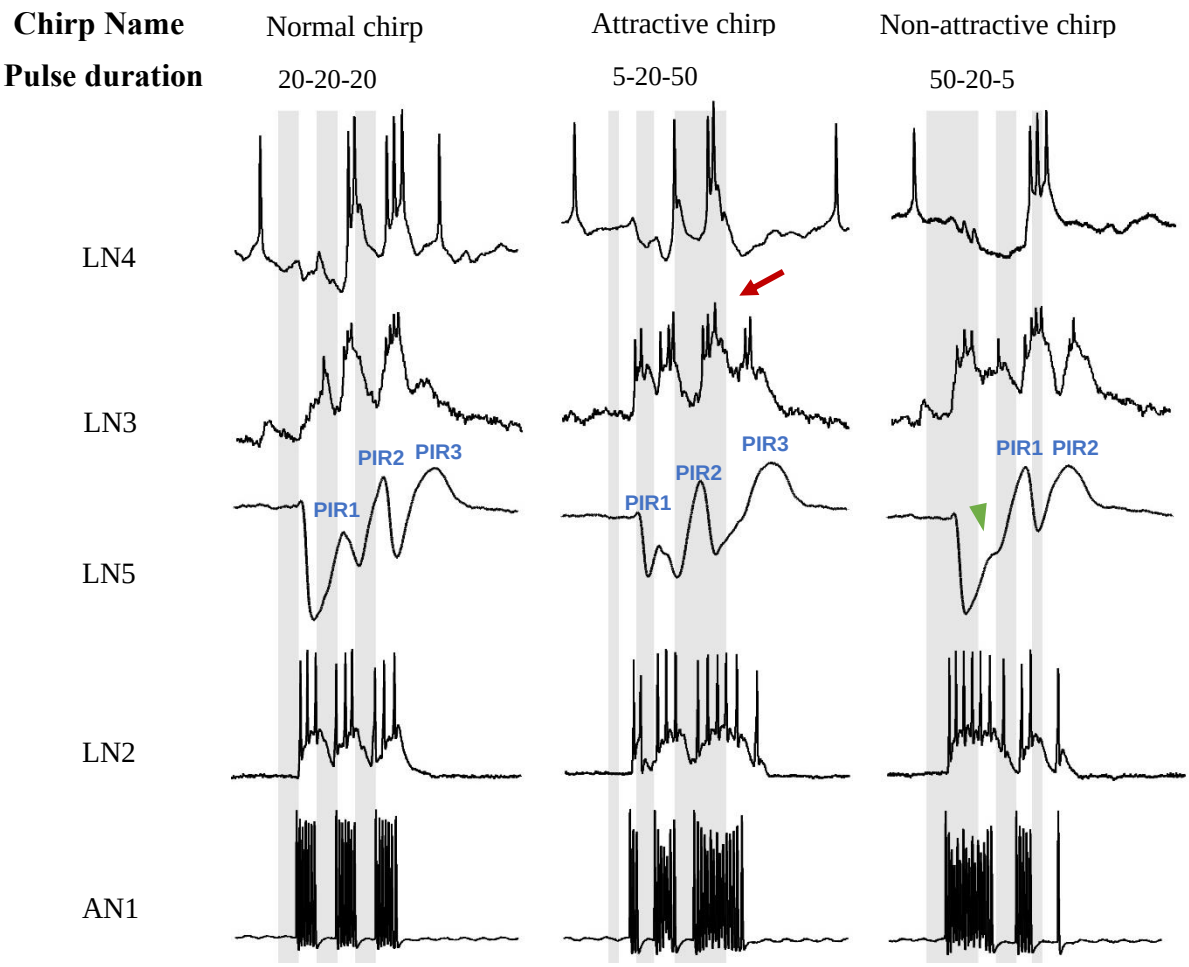

B

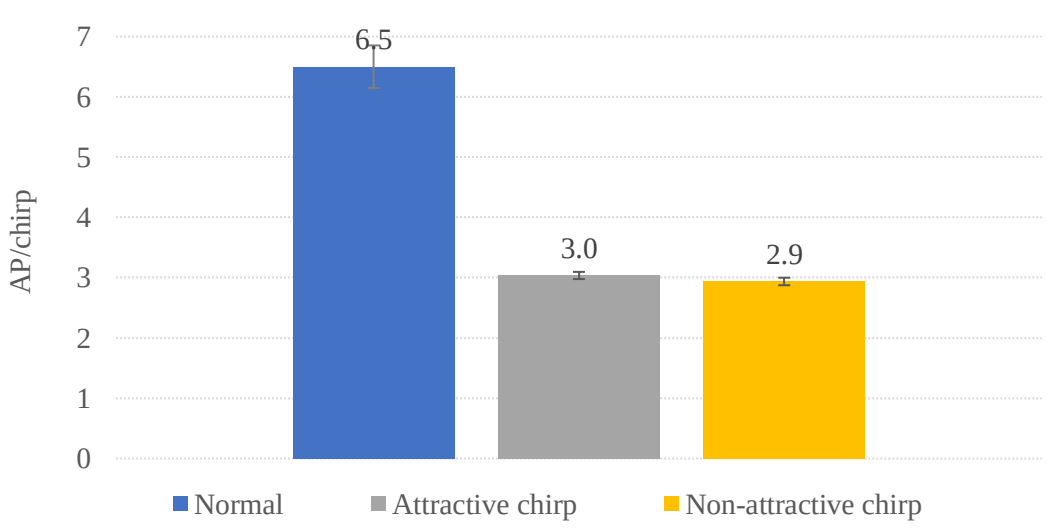

Fig. 68 The activity of the five neurons elicited by the attractive and the non-attractive patterns.

Fig. 68 The activity of the five neurons elicited by the attractive and the non-attractive chirp patterns. A. Response of the five neurons to normal, attractive and non-attractive chirps. The recordings of LN4, LN3, LN5, LN2 and AN1 are aligned to the sound pulses, indicated by grey bars. Chirps and the duration of individual pulses are labelled at top of each column. For LN4, LN3, LN2 and AN1, one example recording is shown, for LN5, the traces are averaged from 18 recordings. For LN5, PIR1, PIR2 and PIR3 are labelled on top of each peak. Green arrowhead indicates the deflection in the first rebound elicited by the non-attractive chirp. For LN3, red arrow indicates the bi-phasic spiking activity elicited by long P3 in the attractive chirp. **B.** AP/chirp elicited by the normal, attractive and non-attractive chirps. Blue bar indicates Normal chirp, grey bar the attractive chirp and yellow bar the non-attractive chirp. Mean activity is labelled on top of each bar. Error bars indicate standard error of the mean (SEM).

in a pronounced depolarisation and spike activity in LN3, which resulted in biphasic response with two bursts of activity (Fig. 68A, red arrow), as observed for the P3-test. The responses of LN3 to P2 and P3 drove LN4 and it responded with two suprathreshold depolarisations to the 'attractive chirp', embedded in an overall inhibitory response. The depolarisation elicited by the 50 ms sound pulse P3 was shorter (24.2±0.2 ms) than the duration of the stimulus, as observed in previous experiments.

When the non-attractive chirp (50-20-5 ms) was presented, AN1 and LN2 again copied the pattern (Fig. 68A, right). In response to the 50 ms pulse neuron LN5 showed a typical inhibition like to a 20 ms pulse. However, when the membrane depolarised during the rebound, an extra deflection in its membrane potential occurred, with a latency of 71.2±0.8 ms to P1 (43.1±0.6 ms after the onset of inhibition). LN3 generated a biphasic depolarisation and LN4 activity started with a pronounced inhibition. The AN1 activity in response to the 20 ms pulse coincided with the PIR1 rebound of LN5, driving a strong depolarisation with 4 APs in LN3 and a pronounced depolarisation in LN4. The second rebound PIR2 of LN5 had a similar amplitude as the first, however, due to the short duration of the third pulse (5 ms) AN1 spike activity did not elicit a strong spiking response in LN3. Subsequently neuron LN4 did not respond to the short pulse. Compared to the normal chirp, LN5 generated only two post-inhibitory rebounds and LN4 responded to the 'non-attractive chirp' with a pronounced inhibition followed by only one burst of spikes.

In comparison the attractive chirp and the non-attractive chirp elicited different responses in LN4. Both the normal chirp and the attractive chirp elicited a similar activity pattern in LN4, with two subsequent suprathreshold depolarisations; although the first depolarisation for the attractive chirp was weaker than the response elicited by the normal chirp. The response to the non-attractive chirp was dominated by inhibition and only caused one burst of spikes corresponding to the second sound pulse.

On average, the normal chirp elicited 6.5±0.4 AP/chirp, whereas both the attractive chirp and the non-attractive chirp elicited approximately 3 APs in LN4 (attractive chirp: 3.0±0.1 AP/chirp; non-attractive chirp: 2.9±0.1AP/chirp) (Fig. 68B). This demonstrates: 1. Besides the overall number of spikes per chirp, moreover the actual timing and pattern of the LN4 activity may be relevant for phonotactic tuning; or 2. The looped acoustic stimulation regime (see Materials and Methods) in my experiments may have had an impact on the neuronal activity. As a control, it may require to repeat the behavioural tests in a corresponding way, different to

the sequenced behavioural tests reported previously (Hedwig and Sarmiento-Ponce, 2017).

In both attractive and non-attractive chirps, two sound pulses (P1 and P3) were varied. For the attractive chirp, the first pulse is shortened, and the last pulse is elongated, while for the non-attractive chirp, the first pulse is elongated and the last pulse is shortened. To determine whether the response of the network to the attractive and non-attractive chirps depends more on a short or a long pulse, I compared the chirps with only one pulse varied (Fig. 69). When comparing P1-50 and P3-50 to the normal chirp, the spiking activity of LN4 was not affected regardless the position of the long pulse (P1-50: 3.8±0.6 AP/chirp; P3-50: 4.0±0.3 AP/chirp; Normal chirp: 4.1±0.3 AP/chirp; p>0.999, Friedman test test) (Fig. 69A). Although a long pulse did not affect the number of spikes generated in LN4 when positioned at the end of a chirp, it indeed affected the responses of LN4 when it was at the beginning of a chirp, which was not reflected in the overall number of spikes per chirp. Therefore, a long pulse did not affect the number of spikes generated in LN4 significantly whether it is P1 or P3. In response to the short pulse (5 ms), however, less spikes were generated in LN4 compared to the normal chirp no matter whether the short pulse was P1 or P3 (P1-5: 3.2±0.7 AP/chirp; P3-5: 2.8±0.2 AP/chirp; Normal chirp: 4.1±0.3 AP/chirp; p=0.042, Friedman test) (Fig. 69B).

Accordingly, it can be assumed that the existence of one short pulse (<20 ms) is sufficient to reduce the overall number of spikes elicited in LN4 by the whole chirp, but one long pulse (>20 ms) is not. Although single long pulse is not sufficient to elicit a different level of spiking activity in LN4 by its own compared to the normal chirp (based on the results from P1-, P2- and P3- tests), successive long pulses significantly reduced the spike number of LN4, which may be due to the accumulative effect (based on the results of PD-test). Therefore, the differences observed in the responses of LN4 elicited by the attractive, the non-attractive and the normal chirps mainly determined by the short pulse presents in the chirp although the long pulse also contributed. This effect is due to the weakened coincidence between the AN1 activity and the small PIR elicited by the short pulse.

Major conclusions

1. The responses of LN3 to chirps composed of short pulses were in accordance with the phonotactic behaviour, whereas the responses to chirps containing long pulses were not.

2. The responses of LN4 to chirps containing short pulses reflected the phonotactic behaviour,

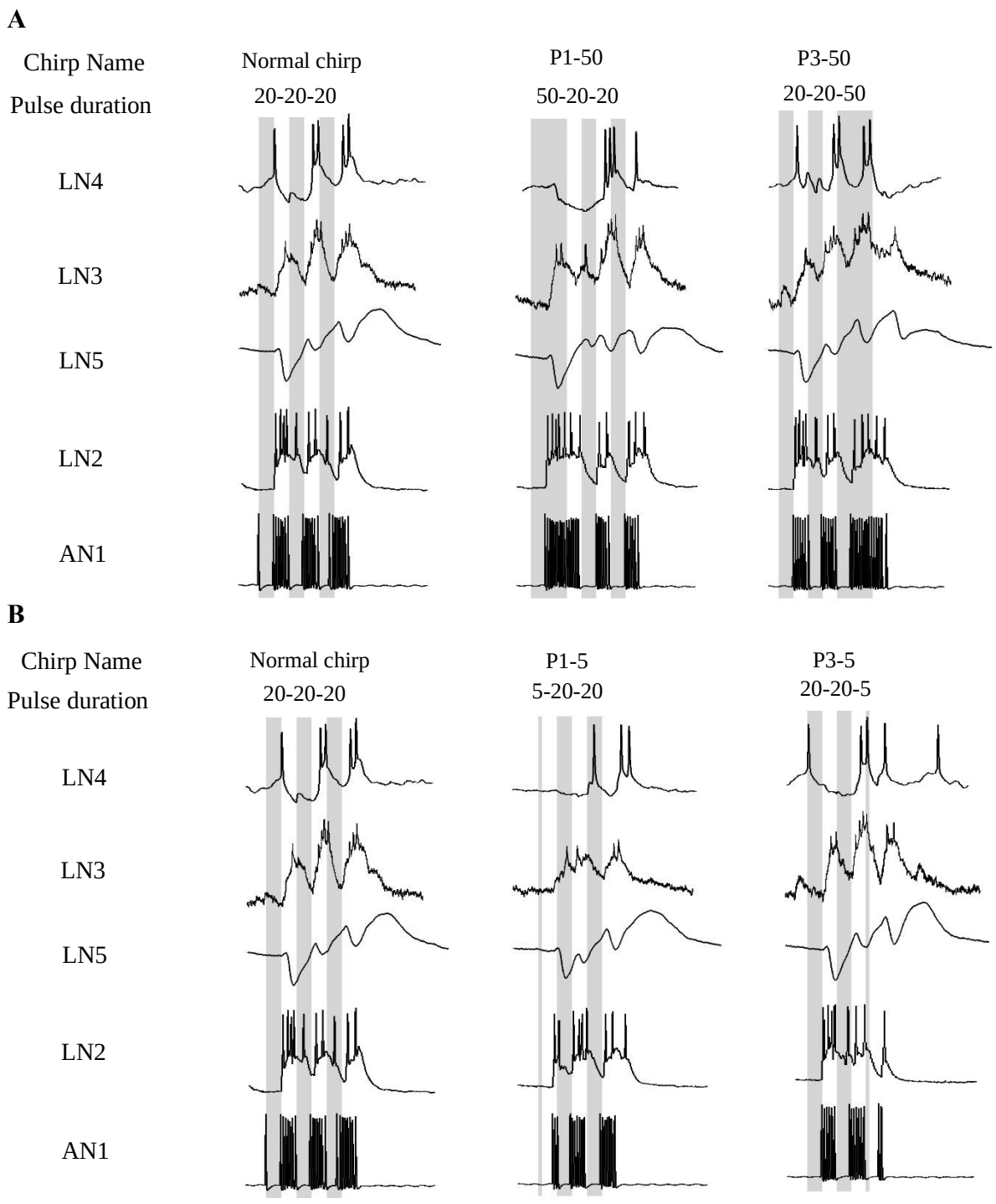

Fig. 69 The comparison of chirps with short or long P1/P3. A. The responses of the neurons to a chirp with long pulse at the beginning or the end. **B.** The responses of the neurons to a chirp with short pulse at the beginning or the end. The name of the chirps and the duration of the three sound pulses are on top of the neuronal activity. The sound pulses are in grey bars.

whereas the responses to chirps containing long pulses lack this similarity to the phonotactic tuning.

3. The circuit can tolerate a single long pulse within a chirp. Based on the PD test, the selectivity to long pulses in LN4 begins at the response to the 3rd sound pulse within a chirp

4. The effect of long pulses on the activity of the pattern recognition circuit may be linked to the gradual increase of the PIRs (the slopes) which can be altered by additional bumps occurring during the rebound.

5. The effect of the varied pulses is accumulative within a chirp when they present successively.

6. Individual pulses or intervals contribute differently to pattern recognition as they are embedded in the temporal sequence of neural processing.

7. The pattern recognition circuit is sensitive to detect changes in the pulse intervals but less sensitive to detect changes in the duration of a single pulse.

DISCUSSION

When listening to a male calling song in a natural environment, female crickets are exposed to stereotypical sequences of sound pulses and intervals. While the auditory pathway detects the species-specific calling song pattern to initiate phonotactic responses, it depends on neuronal filter mechanisms adapted and tuned to selectively respond to the species-specific pulse durations and intervals. In this chapter I analyze how the neurons of the pattern recognition network in the brain of *G. bimaculatus* process pulses of different durations.

When tested with different pulse periods, the phonotactic response of females breaks down for very short and very long pulse periods (Weber and Thorson 1989, Hedwig 2016). As the pattern recognition mechanism is based on a delay-line and coincidence detector network (Schöneich et al. 2015), Hedwig and Sarmiento-Ponce (2017) analyzed to what degree altering the duration of a single sound pulse in an otherwise normal chirp pattern of 3 sound pulses would affect the phonotactic response. Their experiments revealed that sound pulses of 10-20 ms are most efficient to elicit phonotaxis while responses are low and continuously decline for pulses longer than 30 ms. The system however, tolerates long pulse durations at the end of a chirp and very short pulses at the start. The specific tuning curves allowed to design an attractive and a non-attractive chirp pattern, in which a short, normal and long pulses are played in reverse

order.

Rational of the analysis of neuronal activity

AP/chirp was calculated as the parameter representing the neuronal activity

I recorded the neurons of the pattern recognition network in the brain of female *G. bimaculatus* and used acoustic stimulus patterns following Hedwig and Sarmiento-Ponce (2017). AP/chirp was calculated to compare the different level of responses in my experiments as in the previous experiments (Schöneich et al. 2015; Kostarakos and Hedwig, 2015). The reasons why AP/chirp was used as the parameter in my research are: 1. According to the analyses I did on the other parameters as described in the Method part, no single parameter reflected the phonotactic tuning better than AP/chirp. Beside of AP/chirp, I also analysed other parameters such as the number of bursts generated, the spike frequency and the interval between the bursts. Although the number of bursts of spikes generated in LN4 showed differences in response to the attractive and non-attractive chirps, it did not reflect the differences of the phonotactic responses in the P1, P2 and P3 tests. Nevertheless, this parameter may still need more detailed analyses. 2. According to the hypothesis proposed by Schöneich et al. (2015), LN4 serves as the feature detector, its activity might represent the output of the pattern recognition circuit and might be relevant to drive neurons controlling phonotactic walking behavior. Therefore, although the timing of the initial inhibition *and* the spike bursts may also contribute, AP/chirp was used in my experiment to represent the level of neuronal activity.

Presentation of chirp patterns in a looped mode

A mismatch occurred between the neuronal activity of LN4 and the phonotactic tuning obtained by Hedwig and Sarmiento-Ponce (2017) in P1-, P2-, P3-tests and the attractive/non-attractive tests. The activity of LN3 and LN4 analysed for the pulse duration tests derived from the same recordings which matched the behavioural tuning in the interval tests. The mismatch of neuronal and behavioural tuning seen in the pulse tests cannot be explained by the small sample size of the LN3 and LN4 recording.

The most crucial difference in the stimulus presentation in my experiments and the previous behavioural tests (Hedwig and Sarmiento-Ponce 2017) was that I did not present each of the different chirp patterns continuously in a long sequence, but rather looped the patterns, i.e. in one loop each chirp pattern was presented once and the loops were repeated several times

while the recordings lasted. This approach considered the limited recording times of the auditory neurons and may explain the discrepancies observed for the pulse tests. In the behavioral study, each chirp was repeated for 60 times before changing to the next chirp and the phonotactic response was an averaged value. The sequenced paradigm presenting species-specific chirps could possibly introduce a neuromodulatory change in the phonotactic network (Poulet and Hedwig 2005), which may not occur when chirps are presented in a looped mode. Preliminary results from Adam Bent (unpublished) showed that when presenting the looped sound paradigms, the phonotactic response did not show differences in response to the normal and chirps with long pulses. It will be interesting to test the behavioral response systematically and statistically to the looped patterns to allow a better comparison.

When the chirps (normal, attractive, non-attractive) were played in a loop-mode, the potential neuromodulatory effect on the phonotactic behaviour may be relevant. A recent behavioural assay conducted in the lab (Adam Bent, not published) using the looped paradigm as in my study provided preliminary results that the attractive and the non-attractive patterns do not give different results for the phonotactic behaviour. This is in accordance with my results on the neuronal level tuning shown in Fig. 67 and indicates that the acoustic stimulation paradigm may have a significant effect on the auditory tuning observed at the level of the behavior and the neuronal responses.

Response properties of the AN1 neuron

My recordings of the AN1 neuron revealed its spike activity reliably copied the pulse patterns presented. Its tuning curves to the different pulse tests increased with the duration of the test pulse and did not indicate any preference for a particular chirp pattern. This confirms previous reports on the coding properties of AN1 (Wohlers and Huber 1982, Schildberger 1984, Kostarakos and Hedwig 2012), and my data from the interval tests. However, while in the interval test short intervals of 5-10 ms were not properly resolved by AN1 spike activity, in the pulse duration tests even short 5 ms pulses elicited a pronounced AN1 burst of spikes. This links in with short sound pulses at the start of a chirp in the P1-test phonotaxis were efficiently elicited.

Response properties of the LN2 neuron

For all tested chirps, LN2 revealed a phasic-tonic response towards the first sound pulse, however its activity was rather tonic and decreased towards the second and third pulse. Its prolonged depolarization in response especially to the first sound pulse (P1) could contribute

to blur the coding of the second (P2) and third pulse (P3) in its spike activity. Also, Schöneich et al. (2015) show a gradual decline of the LN2 membrane potential, however long depolarizing responses like in my recordings have not been reported before. The LN2 response pattern comes with functional implications for the responses of the feature detector LN4.

The tuning of LN2 is not different to the tuning of AN1 and does not reveal a preference for any of the tested chirp patterns. When comparing LN2 activity with the tuning of phonotactic behavior, also Kostarakos and Hedwig (2012) report no evidence for filtering of the chirp patterns at the level of LN2. Like AN1 also LN2 responded to short 5 ms sound pulses with a brief burst of spikes when these occurred at the beginning of a chirp; responses to short pulses in the middle or end of a chirp however, did not stand out in its spike activity. In terms of pattern recognition, this particular feature corresponds to the phonotactic behavior, which in the P1-test was high to chirps with the first pulse being 5 ms, but it was considerably lower and close to the reference threshold, when the second or third pulse were so short like in the P2- and P3-tests.

Response properties of the LN5 neuron

The overlaid averages of the LN5 responses demonstrate that its post-inhibitory rebound always started from the peak of the inhibition. When P3-80 was presented, the rebound in response to P3 gradually increased and developed a broad maximum reaching the peak with a latency of about 85 ms, i.e. 65 ms after the end of the pulse. This is slightly different to the timing of the events described by Schöneich et al. (2015), who reported that the rebound would be at its maximum with a latency of 63 ms (43 ms after the end of a pulse).

For medium and long sound pulses, distortions were observed in the time course of the rebound potentials which developed into an extra rebound peak. These peaks occurred independently of the pulse onset but were coupled to the offset of the sound pulses. In the P1-test, it occurred about 29.9 ms to the offset of P1 (P1-25: 31.6 ms and P1-30: 30.2 ms; P1-40: 29.9 ms; P1-50: 29.4 ms; P1-80: 28.2 ms). In the P2-test, the delay was about 28.3 ms to the offset of P2 (P2-25: 28.2 ms; P2-30: 28.5 ms; P2-40: 27.9 ms; P2-50: 27.8 ms and P2-80: 28.9 ms). In P3-test, the extra peak occurred with a lightly longer delay at 35.2 ms after the offset of P3 (P3-25: 35.6 ms; P3-30: 34.8 ms; P3-40: 35.8 ms; P3-50: 34.4 ms). Given these differences in the delay time, the extra peak in all three tests occurred within the range that covers the time when a pulse of a normal chirp pattern would occur (20-40 ms to the offset of the sound pulse).

As these extra peaks were coupled to the end of the sound pulses, the inhibitory input to LN5 might be from some other intrinsic network activity influencing the rebound of LN5 rather than from LN2. The pulse duration which triggered this intrinsic network activity to shape the extra rebound peak was different in P1- and P2- tests. For example, the amplitude of the extra peak was always below PIR1 when P1 was between 25 to 50 ms and only exceeded PIR1 for P1-80 (Fig. 40C). While when P2 was 40 ms the extra peak already reached the same potential as PIR1 and exceeded it at P2-50 and P2-80 (Fig. 49C). This pronounced extra peak was observed when the third sound pulse was as short as 30 ms (Fig. 58C). It indicates that the threshold for distortion in the rebound potential caused by a long sound pulse depends on the processing of the preceding sound pulses.

When the duration of the first or second sound pulse (P1, P2) increased from 5 to 20 ms, the LN5 membrane potential revealed an overall increase of its depolarization over the time course of a chirp; this effect decreased for long sound pulses (Fig. 42 and 51). Like for the interval tests it revealed a band-pass like tuning, comparing this overall increase of the membrane potential in LN5 with the behavioral tuning curves showed a good match for all three pulse-tests (Fig. 43, 52 and 61). It was better than for any other parameter analyzed and points towards the relevance of this feature of the LN5 response, which has not yet been considered in previously. In all three tests the tuning of the average slope always showed a better representation of the behavioural response for medium and long pulses than for short pulses (Fig. 43, 52 and 61). This may imply that beside of the output from LN5, additional mechanisms may also be involved in driving the phonotactic response for short pulses. The tuning of the average slope may be linked to an inhibition driven conductance leading to the build-up of the membrane potential of LN5 during the postinhibitory rebound. Inhibition activated currents like I_h play a crucial role in the timing of centrally generated motor patterns and the central processing of rhythmic auditory signals (Felix, et. al. 2011, Kopp-Scheinpflug, et. al. 2011).

Interplay between LN2 and LN5

According to the delay-line and coincidence detector mechanism, each depolarization and burst of spikes of LN2 causes an inhibition in LN5 (Fig. 70A), the LN2-mediated inhibition is directly relevant for the inhibition-activated conductance of LN5.

In response to the first sound pulse (P1) the inhibition of LN5 was always well pronounced. It started with a latency of 26.4 ms (Table 1), and then built up over 10-13 ms to

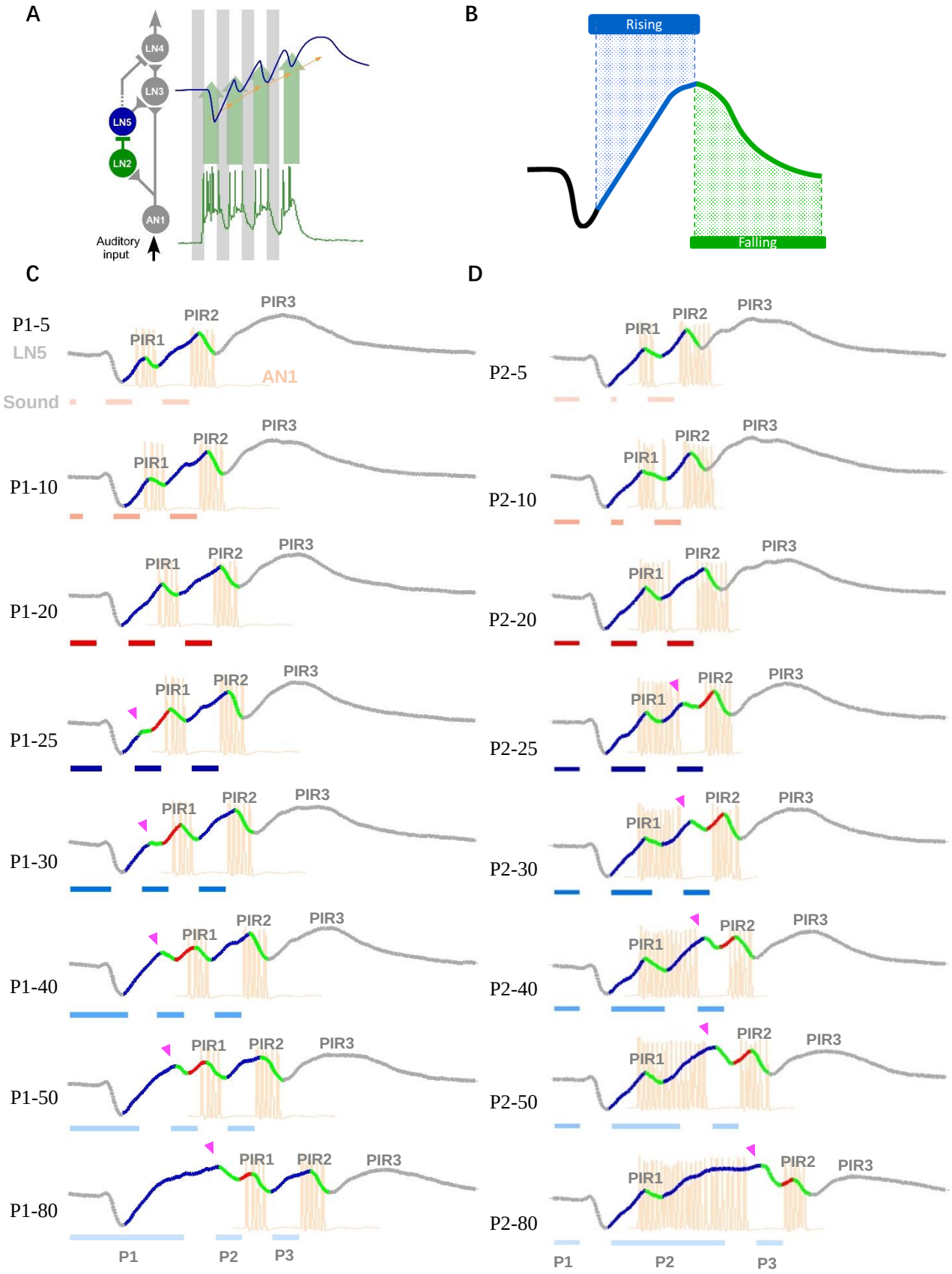

Fig. 70 The inhibitory connection between LN2 and LN5 and the coincidence between AN1 and different phases of the post-inhibitory rebound in LN5

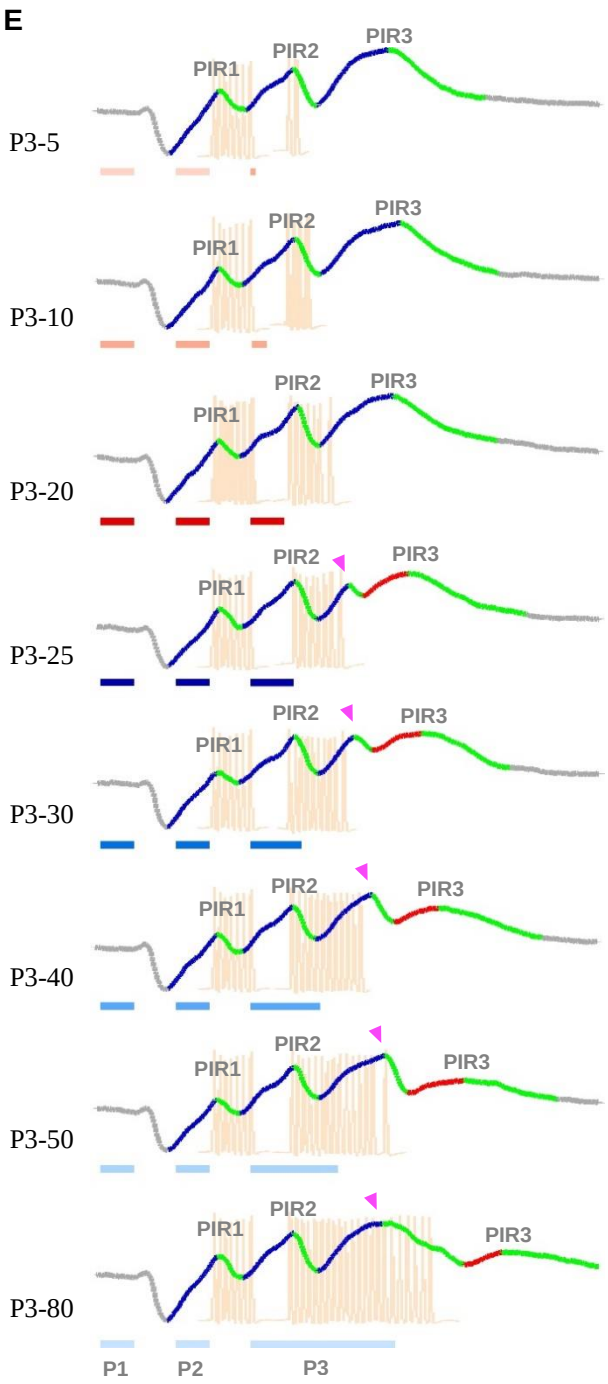

Fig. 70 The inhibitory connection between LN2 and LN5 and the coincidence between AN1 and different phases of the post-inhibitory rebound in LN5. A. Activity of LN2 and corresponding inhibition in LN5 in response to a 4-pulses chirp. The sound pulses were in grey bars. LN2 activity is in green and LN5 activity is in blue. The green arrows indicate the inhibition forwarded to LN5. The yellow arrows indicate the change of the membrane potential of the adjacent PIRs (slope between PIRs). Both LN2 and LN5 activity are redrew based on actual recording. **B.** Schematic drawing of the rising and falling phases of the post-inhibitory rebound in LN5. The rising phase is in blue and the falling phase is in green. **C.** Coincidence of AN1 and LN5 in different phases of the post-inhibitory rebound in response to the P1-test. **D.** Coincidence of AN1 and LN5 in different phases of the post-inhibitory rebound in response to the P2-test. **E.** Coincidence of AN1 and LN5 in different phases of the post-inhibitory rebound in response to the P3-test. Sound patterns are given below the LN5 recordings. AN1 activity to the last two pulses in each chirp are in purple. The first two rebounds are colored since these are the parts coinciding with AN1 activity while other parts of the LN5 activity are in grey. The rising phases of the rebounds are in blue and the falling phases are in green. In response to P1-25 to P1-80 and P2-25 to P2-80, the secondary rising phase due to the extra peak was colored in red. The falling phase may be naturally occurring, or the falling phase initiated by the subsequent inhibition. The pink arrowheads indicate the additional peak in the rebound during the P1- and P2-test. The name of each chirp is listed to the left of each test pattern. The LN5 activity is averaged from 18 recordings.

its peak (INH1) and did not reveal a summing of individual IPSPs. When considering the responses of LN5 and LN2 to the first sound pulse (P1) in all three tests, the peak of the inhibition did not dependent on pulse duration, even when the varied sound pulse was only 5 ms (Fig. 41). In this case, LN5 generated a pronounced inhibition, although the spike response of LN2 to these short pulses was only 1 to 2 spikes. LN2 spike activity occurred with a latency of 22.2 ms, allowing 4.1 ms for the inhibitory effect on LN5 to build up. Therefore, only the first 3 spikes of LN2 firing at high rate (236.2±6.5 Hz) which may be crucial for triggering the inhibition in LN5.

Although LN2 apparently inhibits LN5, at *long* P2 and P3 the rebound of LN5 developed while tonic spike activity of LN2 was still high. This implicates that at this time the LN5 conductance driving the rebound is stronger than the conductance driving the inhibition. During normal chirps the second sound pulse (P2) always occurred during the rising phase of the rebound, and the subsequent inhibition was always smaller than the inhibition to the first pulse (P1). Reasons for this could be that the LN2 spike activity was weaker and the rebound inward current would diminish the effect of the inhibition. However, LN2 activity of 1-2 spikes driven by short P3, was sufficient to elicit a pronounced inhibition although the rebound potential of LN5 was close to is maximum. Overall the inhibition of LN5 mediated by the third sound pulse (P3) was stronger than the inhibition mediated by the second pulse. This may be related to the inward current driving the rebound loosing strength at the end of a chirp which increased the inhibitory effect of LN2 on the LN5 membrane potential. Overall the interplay between LN2 mediated inhibition and LN5 rebound potentials appears to be complex, and may only be resolved if the underlying conductance were known in more detail.

The timing of LN5 and AN1 activity in P1-, P2- and P3-tests

Schöneich et al. (2015) proposed that the tuning curve of the coincidence detector LN3 and the feature detector LN4 originate from the level of overlapping activity between the delay-line (LN5) and the direct line (AN1), which apparently shifts with the pulse period tested. Also in my recordings, AN1 spike activity coincided with LN5 activity, but due to the nature of the fixed delays in the circuit, the start of AN1 activity always overlapped with the peak rebound activity of LN5. This becomes obvious when both responses are aligned with their characteristic latency to the first sound pulse. The post-inhibitory rebounds of LN5 can be divided into rising and falling phases of the membrane potential (Fig. 70A).

When P1 was varied from 5 ms to 20 ms (P1-5 to P1-20), the activity of AN1 elicited by the second sound pulse (P2) started during the rising phase of PIR1 (Fig. 70B,C, blue) and also covered the falling phase of the rebound, caused by the subsequent inhibition. For P1 longer than 25 ms an additional rebound occurred, resulting in an extra peak before PIR1. AN1 activity in response to P2, however did not overlap with this additional rebound. It rather coincided with the rising phase of the membrane potential preceding PIR1 (Fig. 70C, red) and also with its falling phase. Also the AN1 response to pulse P3 always coincided with the rising phase of PIR2 (Fig. 70C blue) as well as its falling phase (Fig. 70C). A similar situation occurred for AN1 and LN5 activity in the P2-test (Fig. 70D). For P2-5 to P2-20 the start of AN1 spike activity coincided with the end of the rising and the start of the falling phase of the PIR1 rebound (blue and green trace). When pulse P2 was longer than 20 ms, the AN1 spike activity in response to P2 coincided with the rising phase of PIR1, with the falling phase of PIR1 and the rising phase of the extra rebound (Fig. 70D, P2-25 to P2-80, blue lines). AN1 activity elicited by pulse P3 coincided with the rising phase preceding of PIR2 and the subsequent falling phase (Fig. 70D, P2-25 to P2-80, red lines). In response to chirps of the P3-test, when P3 was longer than 20 ms, the initial activity of AN1 to pulse P3 coincided with the rising phase preceding PIR2, the falling phase of PIR2 and also the rising phase of the additional rebound (pink arrowheads) (Fig. 70E, P3-25 to P3-80, blue lines).

The alignment of the recordings demonstrates that the start of any AN1 response overlapped with the peak of the LN5 activity. In none of the tests did AN1 activity overlap with the extra rebound in LN5, and all the falling phases of the post-inhibitory rebound which coincided with AN1 activity were caused by the incoming inhibition. As the latency of the AN1 response is about 19 ms and PIR1 and PIR2 occur with a latency of 25.7 and 26.2 ms, there is a time interval of about 7 ms for AN1 spike activity to overlap with the rising phase of the LN5 rebound, within this interval AN1 generate 2-3 spikes. The initial overlap and coincidence between AN1 spike activity and the LN5 rebound is fixed due to the processing delays in the circuit and is an essential property of it. The interaction of AN1 spike activity and the subsequent falling or rising LN5 rebound activity depends on the duration of the sound pulses. AN1 activity however always coincided with different amplitudes of the peak rebound potentials, which may contribute to different levels of gain in the coincidence detector LN3.

Response properties of the LN3 neuron

LN3 activity and the interplay of AN1 spike activity and LN5 rebound potentials

The dendritic recordings of LN3 showed an increasing depolarisation of the membrane potential over the time course of the chirps, which is very similar to the overall development of the LN5 rebounds and membrane potential. Especially in response to long sound pulses (e.g. P1-50) LN 5 generated extra rebound depolarizations, which are subsequently reflected in additional LN3 activity (Fig. 46B, 55B and 64B), but were not directly coupled to the sound pattern or AN1 activity. Also, following the LN5 depolarization in response to the last sound pulse (P4), the LN3 activity revealed subthreshold EPSPs with a latency of 68.6±0.9 ms to P3, which are not coupled to any AN1 spike activity and can be assigned to the graded input from the LN5 neuron (Schöneich et al. 2015). This indicates that the LN3 membrane potential is driven by graded transmission from the non-spiking LN5 neuron not only at the peaks of the rebounds but throughout a chirp. Graded synaptic transmission with transmitter release driven by the membrane potential of the presynaptic neuron is a common feature of non-spiking neurons in the insect sensory-motor system (Pearson and Fourtner 1975, Burrows and Siegler 1978, Burrows 1979).

As the membrane potential of LN5 increased over the time course of the normal chirps, also the three bursts of spikes in LN3 successively increased in intensity. The response of LN3 to the second pulse (P2) was always stronger than its response to the first pulse (P1). The response to the first sound pulse was mediated by AN1 input only, while for P2 the coincidence of AN1 activity with the LN5 rebound occurred, leading to a stronger response of LN3. The LN3 activity elicited by P3, showed a similar intensity as the second burst of spikes. This may be due to the inputs received from AN1 in response to P2 and the post-inhibitory rebound caused by P1 already reached the limit in generating spikes, so even though the depolarization of LN3 was still increasing, the number of spikes generated in response to P3 did not increase.

Pulse duration filtering property of LN3

Considering the coincidence of AN1 and LN5 inputs and the activity of LN3 indicates a pulse duration filter, which has not been pointed out before. When the first sound pulse (P1) of the chirps was extended to 80 ms, it correspondingly elicited a long AN1 spike activity and a long rebound potential in LN5. LN3 activity reflected the long sound pulse with a maintained depolarization generating few scattered spikes (see P1-80). However, when the duration of the second (P2) or third pulse (P3) increased, the LN3 depolarization and spike activity did not follow the long duration of the sound pulse (see P2-80 and P3-80, Fig. 53B and 62B) but showed a biphasic activity. In response to the 80 ms pulse LN3 initially depolarized for 39.3±0.5 ms

and generated a burst of spikes lasting 19.0±0.6 ms before an additional depolarisation and spike burst was generated. Since the AN1 activity was ongoing during the entire duration of the sound pulses, the biphasic response of LN3 may be credit to the extra rebound in the membrane potential in LN5; it may also be shaped by the same network activity that shaped the extra peak of the LN5 rebound elicited by long sound pulses (e.g P2-50 and P3-50) (Fig. 49C and 58C).

The depolarization of LN3 should be due to the coincidence of AN1 spike activity with the peak of the LN5 rebound potential. Based on the latencies of the responses to the second sound pulse (AN1: 18.4 ms and LN5: 25.7ms, Table 1) this coincidence of AN1 spike activity and the rising rebound of LN5 lasts for about 7.3 ms and may cover 3 AN spikes; its additive effect likely drives the pronounced but rather short depolarization and spike activity in LN3. The short time course of the LN3 spike response to sound pulses may be determined by the short time of coincidence between AN1 spike activity and the LN5 rebound depolarisation, while the subsequent drop in LN5 membrane potential may contribute to the decline of the LN3 depolarization before the sound pulse has finished. If the short LN3 response to the long sound pulses is not determined by the degree of AN1 and LN5 coincidence, then an additional inhibitory input to LN3 may be required to explain the neuron's response pattern. Either way the short LN3 response indicates a duration filter, which limits the effective time for the processing of a sound pulse. This may have further functional implications for the auditory response at the next level of processing by the feature detector LN4.

Response properties of the LN4 neuron

Based on intracellular recordings, it is generally difficult to assign particular filter properties to an individual neuron, as these require a careful analysis and comparison of the synaptic input signals and the output generated. In the recordings of the LN4 neurons, the inhibitory and excitatory synaptic inputs and the neurons output activity are discernible and reveal at least partially the neuronal filter mechanism.

LN2 inhibition and LN3 excitation shape the LN4 activity

At the level of LN4 the inhibitory input from LN2 and the excitatory input from LN3 interact and shape its response, which in previous tests closely matched the tuning of the phonotactic behavior (Kostarakos and Hedwig 2012, Schöneich et al. 2015). LN4 characteristically responded to the first pulse of a chirp with a pronounced inhibition, which increased with the duration of the first pulse (P1). Spikes were only generated in response to the second (P2) and

third sound pulse (P3) leading to a very long latency of its spike response when the start of the chirp is considered, corresponding to the data reported by Kostarakos and Hedwig (2012). The excitatory input from LN3 has to be strong enough to overcome the inhibition elicited by LN2, which only happens to the second and the third response due to the coincidence-detection mechanism increasing the activity of LN3. While for the last pulse LN2 activity is low and the LN4 response is extended in duration.

The pulse duration filtering property of LN4

For the range of attractive sound pulses of 15 to 30 ms, LN4 activity showed the typical short suprathreshold depolarizations, which overcame the prominent initial and ongoing inhibition. Increasing the duration of the second and third sound pulse, did not lead to an extended excitatory response of LN4 (see P2-50 or P3-50). The membrane potential rather generated a short suprathreshold depolarization and a burst of 2-3 spikes and then rapidly repolarized. When long sound pulses were presented, already the excitatory response that was forwarded from LN3 was cut short providing the basis for the short LN4 response. The inhibitory input from LN2 will additionally contribute to limit and sharpen the LN4 depolarization to long sound pulses. The inhibition dominates the response and suppresses the spike activity of the feature detector. This limited the excitatory LN4 response to long pulses, in line with a pulse duration filter. There was no evidence, that the additional activity of LN3, driven by the additional LN5 rebounds (see P2-50 or P2-80), had an effect on LN4 spike activity. Due to inhibition, this additional LN3 activity was filtered out at the level of LN4, making the LN4 response more specific. The short response of LN4 towards long sound pulses indicates a network and cellular processing mechanisms that is sensitive to pulse duration. The sharp pulse duration filter that is obvious at the level of LN4 has not been described before, although elements of this mechanism were apparent in previous recordings (Kostarakos and Hedwig 2012, 2015), demonstrating that the short spiking activity of LN4 neurons, in response to a long sound pulse, is embedded in an ongoing inhibition, which may contribute to terminate the LN4 depolarization.

The interplay of inhibition and excitation became prominent for chirp patterns in which the duration of all sound pulses was varied, while the intervals were kept at 20 ms, i.e. the normal length (PD-tests). For the range of attractive sound pulses of 15 to 30 ms, LN4 activity showed the typical short suprathreshold depolarizations, which overcome the prominent initial and ongoing inhibition. The LN4 spike bursts matched the duration of the sound pulses for 15 and 20 ms pulses, however the bursts remained short and did not follow the increasing duration

of the sound pulses in the test. For long sound pulses the inhibition dominated the response and suppressed the spike activity of the feature detector; corresponding responses were reported by (Kostarakos and Hedwig 2012). This situation is also very similar to the filter properties of the grasshopper AN4 interneuron, in which the start of each sound pulse triggers an inhibition (Ronacher and Stumpner 1988, Stumpner and Ronacher 1994). In normal song patterns the inhibition of AN4 occurred only at the start of the syllables. However, if the syllables became very short, like in case of males singing with one hind leg only, this inhibition was retriggered and blocked the excitatory response of the neuron. Overall in case of the grasshopper the tuning of the AN4 neuron matched the tuning of the behavioral response, indicating that this filter effect might contribute to the discrimination of normal song patterns and of patterns generated by males singing with one hind-leg only.

Excitation and inhibition shape the activity of the feature detector

Two different mechanism are central to the pattern recognition process. First a well-timed addition of excitatory synaptic inputs at the level of the coincidence detector LN3, which based on the temporal overlap between AN1 activity and the LN5 post-inhibitory rebound increases LN3 activity, at the species-specific pulse pattern. Second, a subtraction based on LN2 inhibitory and LN3 excitatory synaptic inputs at the level of the feature detector LN4 sharpens the response to sound pulse patterns. The impact of the inhibition efficiently blocks any spiking response to the first sound pulse of a chirp, and it further limits the duration of the feature detector response to the following sound pulses revealing a filter mechanism for pulse duration. An impression obtained from the feature detector responses may be that it's pronounced suprathreshold depolarizations coupled with short high frequency bursts of spikes, may be a crucial element for pattern recognition. The pattern recognition system seems to be limited in generating these responses: long pulse durations and long intervals apparently suppress LN4 activity, short intervals are not resolved and short pulses are only effective at the start of a chirp. This narrows and constrains the generation of LN4 suprathreshold depolarizations in responses to sound pulses to the range of normal species-specific pulse patterns.

The response of LN4 to different pulse durations indicates that - ideally - for a given pulse period the number of spikes generated by LN4 cannot be increased by increasing the duration of the sound pulse above the normal duration, as the response of LN4 is duration limited. Increasing the pulse duration would also increase the inhibitory effect of LN2 on the LN4 response, both effects will shape the tuning of LN4 when the duty cycle of a pulse pattern

is tested. Increasing the overall activity of LN4 is however possible by increasing the number of pulses per chirp, and - within a narrow range - may be a way to enhance the attractiveness of a chirp pattern. When comparing the responses to the individual sound pulses, the response of LN4 demonstrated the different weighing of the 3 responses as the first pulse always elicits an inhibition, while the second and third pulse show different degrees of excitation, depending on the duration of the pulses.

Linking feature detection to phonotactic behaviour

We do not yet know how the output of the pattern recognition network is forwarded and transformed into a motor command for phonotaxis but can speculate. The situation is complex, as phonotactic steering behavior reveals motor responses to each sound pulse in a chirp (Hedwig and Poulet 2004, 2005), while pattern recognition requires at least two pulses to detect the pulse period and three pulses to effectively drive phonotactic behavior. As the feature detector LN4 generates bursts of spikes only for a very limited range of pulse intervals and pulse durations, these bursts of spikes may be crucial to drive any interneurons that initiate phonotactic behavior. This final level of integration might be similar to the integration of spike bursts over time as a mechanism explaining the tuning of phonotaxis (Nabatiyan et al. 2003). However, different to the initial proposal it occurs only after high level auditory processing and filtering, which removes any non-specific auditory responses. The phonotactic behavior is under a "motivational" control, the nature of this decision process therefore may only be revealed in animals performing phonotactic behavior, while the auditory neurons in the brain are studied. In both PI and PD tests, the selectivity of LN4 responses to different pulse duration and interval show a qualitative very similar tuning as the band-pass tuning of phonotactic behaviour. The reliable discrimination of the normal chirp pattern (i.e. PD20 and PI20) within a series of chirps containing shorter or longer pulses or intervals by LN4 not only supports its role as a feature detector but also points towards the possibility that the difference of only 1 or 2 spikes in LN4 may be sufficient for generating different levels of output to the descending/command neurons controlling phonotactic behaviour.

The accumulative effect of pulses

According to the conclusions drawn in this Chapter, the filtering of LN4 to pulses is an accumulative process, and at least three pulses are required for LN4 to respond differently compared to its response to the normal chirp. This is in accordance to the results obtained both

from the P1-, P2-, P3-tests and the PD-test. For example, the chirp P1-50 failed to elicit different level of activities in LN4 compared to the normal chirp whereas the chirp PD-50 did. And the changes start to show at the response to the 3rd pulse for PD test. To interpret how does this effect accumulate in the circuit, we first need to recap the response properties of the neurons to long pulses. As the feature detector of the pattern recognition circuit, the activity of LN4 originates from the additive inputs from the coincidence detector LN3 and the inhibitory neuron LN2. The excitatory inputs from both AN1 and LN5 determine the response level in LN3. As described before (Fig. 42, 51 and 60), the increasing rate of the membrane potential of the adjacent PIRs (slope between PIRs) in LN5 is reduced when a single pulse (P1 or P2) was elongated. It can be expected that with successive long pulses the slope between PIRs in LN5 would further reduce, which causes an accumulation of the detrimental effect on its coincidence to AN1 activities and lead to reduced responses in LN3 and LN4.

Therefore, the reduction of the slope between PIRs caused by a single long pulse is not sufficient for the system to discriminate it from the normal chirp at the feature detector level. Only when this reduction has been accumulated to a certain level can the difference be told at LN4 in the form of spike number.

CHAPTER 5: GENERAL DISCUSSION

Main findings and comparison of the results to the previous work

The main findings of my research are summarized in Fig. 71. The results from my experiments demonstrated that varying single intervals within a chirp would lead to a reduction in LN4 activity regardless the position within a chirp of the varied interval. Either a shorter or a longer interval is able to diminish the response level of the pattern recognition circuit, which matches the phonotactic response. However, the mechanisms underlying were different. For single short intervals, the response level of the pattern recognition circuit was reduced due to integrated responses to the two sound pulses, while for single long intervals, the reduction in response level comes from the direct and the delayed pathways coinciding to different degrees (Fig. 71). Both diminishing effects are accumulated along consecutive varied intervals as tested in the PI test, which further reduces the LN4 responses when the duration of the intervals falls out of the normal range of the calling song. This further reduction in LN4 activity reflects the phonotactic response to a better extend (Fig. 71). Therefore, change in the duration of a single interval within a chirp is sufficient to alter the response level of the feature detector LN4 (Chapter 3).

The situation for varying the duration of sound pulses is different (Fig. 71). A single short pulse within a chirp can reduce the response level of LN4, which matches the phonotactic response. However, the underlying physical mechanism are different when the short pulse occupies in different positions within the chirp. When the short pulse locates at the beginning of a chirp, the PIR1 was not strong enough for generating a burst of spikes in LN4 when coinciding with AN1 activity at the level of LN3. However, when the short pulse locates at other positions (P2 and P3), it is the AN1 activity elicited by this pulse that was too short to elicit strong activity in LN4. On the other hand, single long pulse within a chirp fails reduce the response level of LN4, which does not reflect the phonotactic response (Fig. 71). The postinhibitory rebound still coincides with the AN1 activity although the amplitude is gradually decreased as the sound pulse P1 or P2 increased in duration. This decrease in the PIR amplitude caused by single long pulse is not sufficient to result in a lower response in LN4 compared to a normal pulse. However, the effect can be accumulated along consecutive long pulses within a chirp and become prominent as shown in the PD test. The results showed at least 3 successive long pulses are required to alter the response level of LN4, which matches the behavioural response (Fig. 71). Therefore, different from changing single intervals, varying the duration of single pulses within a chirp may not be sufficient to alter the response level of the feature

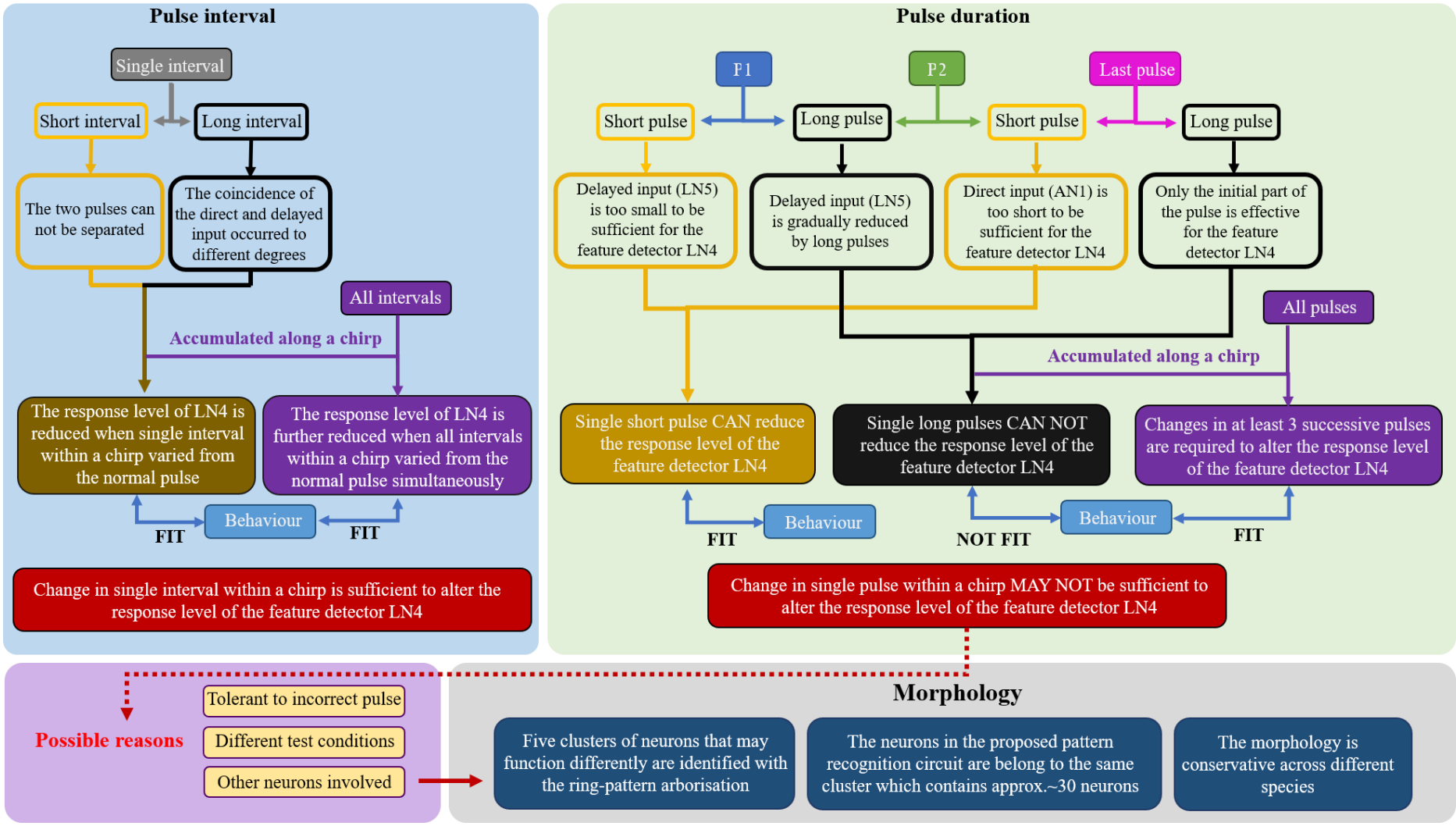

Fig. 71 Main findings and comparisons between neural and behavioural studies

Fig. 71 Main findings and comparisons between neural and behavioural studies. Summaries of the main findings in each chapter. Blue panel shows the main findings in Chapter 3 (Interval tests); green panel for Chapter 4 (Pulse tests) and grey panel for Chapter 2 (Anatomy of the neurons) and purple panel shows the possible reasons for the discrepancy between previous behavioural study and the neural responses in Chapter 4. In both blue and green panels, yellow squares indicate the processing of single short interval/pulse and black squares indicate the processing of single long interval/pulse in tests with individual interval/pulses varied (I1-, I2-, P1-, P2- and P3-tests). Purple squares indicate the processing of a sequence of varied intervals/pulses (PI- and PD- tests).

detector LN4 (Chapter 4).

The neuronal activity, therefore, does not fully reflect the phonotactic behaviour obtained by Hedwig and Sarmiento-Ponce (2017). The possible reasons could be as follows: 1. The sound patterns used in my experiment were played in a looped mode which was different from the behavioural studies (discussed in the Discussion of Chapter 4). 2. The neuronal circuit is more tolerant to long pulses than long intervals since a single long interval is sufficient to reduce the response level of the neurons whereas a single long pulse is not. 3. Other neurons may also be involved in filtering long pulses (Fig. 71). This is supported by the revealing of the five clusters of neurons within the neuropil shown in Chapter 2.

As discussed above, the discrepancies between the neuronal and the behavioural responses are generated by different levels of tolerance to single pulses and intervals and the accumulative effect. Besides, the shifted overlapping between AN1 and the peak of the postinhibitiory rebound of LN5 as described by Schoneich et al (2015) was not seen except when intervals being 80 ms in my results (in I1-80 or I2-80, the coincidence occurred at the falling phase of the rebound). The overlap elicited by chirps other than I1-80 and I2-80 in my results always occurred to the peak of the postinhibitory rebound. This is due to the fact that: 1. In the previous experiments (Schöneich et al 2015), the shift between the peak of PIR and AN1 activity was seen when the neurons were challenged by chirps with varied pulse period, i.e. the duration of the sound pulses and intervals are changed simultaneously. It can be assumed that this shift is credit more to the changes in intervals than pulse duration according to the conclusion of my research. 2. The peaks of the postinhibitory rebound in my results are determined by the interference with the subsequent inhibition. The natural peak of the PIR occurred with a latency of about 80 ms, whereas it previously was reported to be about 60 ms. This therefore led to the shift to occur even when the intervals were shorter than 80 ms in the previous study. This discrepancy in the latency of the peak of the postinhibitory rebound may also indicate the existence of multiple neurons function similarly as LN5 in the neuropil.

Another important findings regarding the response of LN5 is that the membrane potential continuously increased over a normal chirp (‘the slopes’ described in Chapter 3 and Chapter 4), which has not been reported before. This increase matches the tuning of phonotactic behaviour. It indicates that the ongoing underlying conductance in LN5 also contribute to pattern recognition, and that the graded response of LN5 may contribute to a neuromodulatory effect controlling phonotactic behaviour.

Acoustic communication and auditory pathways in insects

Finding and recognizing mates is a difficult challenge for insects living in complex environments. In several groups of insects, mainly in the Hemiptera and Orthoptera, acoustic communication evolved as a way to support mate attraction. It involves the sender to generate a species-specific acoustic signal and the receiver to detect and recognize the signal, and either generate a response signal or approach the sender guided by the sound. Hearing organs evolved in different taxa at different parts of the insect's body, and subsequently the auditory pathways have a different central organization. In acoustically communicating insects, the projections of thoracic auditory interneuron to the brain and local auditory brain neurons so far have only been characterized in few species of grasshoppers, bushcrickets and crickets (Stumpner and v. Helversen 2001, Hedwig and Stumpner 2016).

In all species the ascending auditory interneurons project towards the brain however with different characteristics. In grasshoppers on each side of the CNS there are about 12 ascending neurons (Stumpner and Ronacher 1991,1994) which terminate in the dorsal and lateral posterior protocerebrum, close to the surface of the brain (Rehbein 1976, Hedwig and Elsner 1985, Boyan et al. 1993). In the best studied bushcricket (*Ancistrura nigrovittata*) about 6 ascending neurons enter the protocerebrum dorsally and project ventrally, towards local auditory brain neurons in the lateral anterior ventral protocerebrum. Only one ascending interneuron (AN1) seems to forward auditory information of the male calling song to the brain (Stumpner 1999, Stumpner and Molina 2006, Ostrowski and Stumpner 2010, 2013, Stumpner and Nowotny 2014). In crickets only 2 ascending interneurons provide the brain with auditory information regarding male calling song (AN1) and bat avoidance (AN2), they enter the protocerebrum dorsally and project towards the anterior ventral protocerebrum. This small number of ascending interneurons may be related to the narrow frequency band of their calling songs. Local auditory neurons form a ring-like arborisations pattern around the AN1 terminals, from which they may project towards the contralateral ring-like neuropil, towards the lateral accessory lobes or other areas in the protocerebrum. (Boyan and Williams 1982, Schildberger 1984, Zorovic and Hedwig 2011, Kostarakos and Hedwig, 2012). Thus bushcrickets and crickets share an overall similarity in the layout of their auditory pathway in the brain, whereas this is very different in grasshoppers.

The group staining of the neurons in the ring-like neuropil demonstrate the close spatial relationship of the auditory neurons with neurites in very close proximity, which likely forms

the structural basis for synaptic processing in the pattern recognition network. A total of about 50 local neurons from 5 populations of cell bodies project into the neuropil. The identified pattern recognition neurons may exist in multiple copies and further processing properties of the network may be provided by these neurons. A pool of neurons contributing to pattern recognition may also form the basis for the evolutionary adaptation to different species-specific song patterns.

So far, the selectivity for the temporal patterns of the species-specific calling songs of different cricket species was demonstrated in species like *G. bimaculatus* (Hedwig and Poulet 2004, Doherty and Pires 1987), *Scapsipedus marginatus* (Murphey and Zaretsky 1972), *Acheta domesticus* (Stout et al. 1983), *Teleogryllus oceanicus* (Pollack and Hoy, 1979), *Gryllus campestris* (Thorson et al. 1982). Exploring the lay-out and morphology of the auditory neurons in other species is crucial to determine whether a different structural organization of the auditory neuropil in different species contributes to the selectivity. I also stained the auditory neuropil in both *T. oceanicus* and *T. commodus* and found the ring-like auditory neuropil shows the same overall morphology and seems to be conserved in the in different species, as is the structure of the AN1 neuron (Hennig 1988). However, the number of cell bodies in the clusters may be different. For example there were 18 cell bodies stained in the cluster ant-C in both *T. oceanicus* and *T. commodus* whereas 30 cell bodies were labelled in *G. bimaculatus*.

For different insect species e.g. locust (Kurylas et al 2008), moth (Løfaldli et al. 2010) and ant (Habenstein et al. 2020) digital brain maps have been created, which delineate the major neuropil structures. For the cricket such an approach would provide insight on how the ring-like neuropil relates to the other neuropil structures in the brain and what neuropil structure lies in the center of the ring.

Furthermore, in some model systems like Drosophila neuronal labelling techniques based on genetically encoded tracers allow to specifically label particular neurons or lines of neurons. However, such genetic labbeling techinque are not ubiquitously applicable to other organisms like crickets. By improving the surface staining technique, further exploration both of the spatial organisation and of the temporal tuning in the neurons with cell bodies located in different places and by loading calcium indicators may become possible.

Auditory pattern recognition in insects

One line of insect neurobiological research aims to analyze the neuronal mechanisms underlying the processing of species-specific sound signals (Huber et al. 1989, Gerhardt and Huber 2002). This leads to the fundamental question, how sensory processing and the control of behaviour is linked to the activity of the nervous system. Can we identify neurons which represent the characteristic behavioural response to an acoustic stimulus pattern or at least elements of it in their activity pattern? Will there be high level feature detectors that specifically respond to species-specific signals (Konishi 1991, Martin 1994)? Insects with their rather "simple" nervous system and the possibility to record and identify individual neurons provide a promising approach to deal with these fundamental questions. In crickets, central to this approach is the aim to identify where in the nervous system does the processing of auditory signals occur? What kind of neuronal processing mechanisms are involved underlying species-specific pattern recognition? How is the processing of the auditory signals linked to adaptive motor responses? My PhD thesis focused on the neuronal mechanisms of auditory pattern recognition in crickets, which have been a model system in neurobiological research since several decades (Huber et al. 1989, Horch et al. 2017).

Concepts of auditory pattern recognition in crickets,

Over the years several concepts have been put forward to explain the neural mechanisms underlying pattern recognition (Weber and Thorson 1989, Hedwig 2014, Kostarakos and Hedwig 2015). These are not completely different, and to some degree propose similar mechanisms.

Thoracic Filter Mechanism: A thoracic filter mechanism was proposed by Wiese and Eilts (1985), based on the reciprocal inhibition of the local bilateral ON1 neurons in combination with a postulated postinhibitory rebound. It was assumed that during acoustic stimulation with the normal pulse pattern, the time course of the inhibition between the ON1 neurons would cover the interval between the pulses. The timing of the subsequent postinhibitory rebound would summate with the ON1 response to the next sound pulse. Due to the time course of the inhibition and the rebound, the system would respond best to pulse periods in the range of 25-40 Hz, corresponding to the pulse pattern of the cricket calling song. Further intracellular recordings of the ON1 neurons however, did not provide substantial evidence for a postinhibitory rebound (Wohlers and Huber 1982, Zhang and Hedwig 2019). Although this hypothesis for a thoracic filter mechanism was not verified, it proposed a combination of inhibition and postinhibitory rebound that later in a very different form, would be identified in

the brain.

Cross-Correlation Analysis: This concept proposed that auditory pattern recognition is based on a comparison of the response to the acoustic signal with an internal activity template. Alexander (1962) suggested that the central pattern generator network controlling the generation of song patterns in male cricket might also be present in the female nervous system. By comparing the neuronal response to the acoustic signal to the CPG activity as an internal template, a feature detector could be established that would respond best, when both activity patterns matched (Hoy 1978). In *T. oceanicus* Pollack and Hoy (1979) demonstrated that females would also steer towards a song model with a random organization of the three different pulse intervals, which occur in a very stereotypical way in the species calling song. Their results argued against recognition resulting from a comparison of the auditory signal with an internal template. Moreover, recent research has demonstrated that the CPG for singing in male *G. bimaculatus* is housed in the abdominal ganglia (Jacob and Hedwig, 2019; Schöneich and Hedwig 2012), whereas the pattern recognition network locates in the brain of female crickets (Schildberger et al. 1989, Kostarakos and Hedwig, 2012; Schöneich et. al, 2015). The CPG and the pattern recognition circuit are not similar regarding the morphology or the physiological activity of the neurons involved. Therefore, there is no evidence that the pattern recognition network in the female nervous system mirrors the CPG for singing in males to support the concept of cross-correlation (Kostarakos and Hedwig 2015). In a different approach pattern recognition based on a cross-correlation analysis with an internal template of the song pattern, was also used in a theoretical approach. This demonstrated that cross-correlating the song pattern over different time windows with an internal template of that signal could explain the different tuning curves of phonotactic behavior in *T. oceanicus* and *T. commodus,* which show a period filter and a pulses filter, respectively (Henning 2003). The nature of the internal template however was not specified.

Low-pass and High-pass Filters: A concept that dominated the field for some time was the filter mechanism proposed by Schildberger (1984). Field crickets like *G. bimaculatus* or *G. campestris* show a band-pass tuning of their phonotactic behavior. Females respond best to the pulse periods of the species-specific calling song (25-40 ms) but phonotaxis declines strongly in response to shorter or longer pulse periods. The response properties of local auditory brain neurons indicated that a combination of high- and low-pass filter brain neurons could form the band-pass response properties matching the tuning of female phonotaxis (Schildberger 1984).

Low-pass neurons would respond to low pulse repetition rates and high-pass neurons to high pulse rates, and sequential processing by both filters would establish the band-pass selectivity, as in the phonotactic behavior. A similar concept had been proposed for temporal selectivity in the anuran brain (Rose and Capranica, 1983), but it was also regarded as a cumbersome solution for neural processing (Weber and Thorson 1989).

Auto-correlation analysis: A mechanism using a delayed pathway and a coincidence detector was mentioned by Weber and Thorson (1989). This concept suggested that an acoustic signal of repetitive pulses leads to a direct and a delayed activity in a direct and in the auditory pathway. The neuronal responses are subsequently integrated by a coincidence detector. If the pulse period matches the delay in the pathway both responses will coincide and will elicit a strong response of the coincidence detector, while pulse periods different from the delay will lead to lower responses. Behavioural support for this approach came first from experiments in bushcrickets, which provided evidence for oscillatory neuronal activity contributing to pulse rate recognition (Bush and Schul 2006). Only song patterns that were shifted by a complete pulse period were still efficient in eliciting a phonotactic response.

Pattern recognition based on a delay-line and coincidence detector mechanism has been strongly supported by Schöneich et al. (2015), and my experiments confirm and extend the insight into the functional properties of the network. The results allow two main conclusions regarding the neural filter properties: These can either be intrinsic based on the properties of individual neurons like in LN5. Due to the time course of its inhibitory response and the postinhibitory rebound it provides a delayed excitation for the processing of sound pulses and it also generates an overall graded depolarisation matching the species-specific pulse pattern. The recordings also reveal filter mechanisms as result of network connectivity, as encountered in the coincidence detector neuron LN3 and the feature detector LN4. The coincidence detector LN3 integrates two excitatory inputs, i.e. AN1 spike activity and the graded rebound input from LN5, and its response increases when these inputs coincide. Inhibitory and excitatory inputs shape the responses of the feature detector. They allow pronounced depolarisations only to occur at the species-specific pulse rate and limit the response to long pulse durations (Kostarakos and Hedwig 2012).

The role of inhibition

For the processing of pulse patterns inhibition plays a central role. AN1 forwards an excitatory

activity pattern copying the temporal structure of the pulses to the pattern recognition network, and LN2 functions as an inverter that closely follows the activity of AN1 and forwards inhibition to the subsequent neurons. Its inhibition has two central functions, it drives the postinhibitory rebound in LN5 and it contributes to the balanced processing of excitation and inhibition in LN4. A central role of inhibition for temporal auditory processing also occurs in other auditory systems. In Phaneopterine bushcrickets the 200 ms chirps of the male calling song elicit an inhibition in local brain neurons, lasting for about 500 ms. The duration of the inhibition closely matches the time interval, after which a male trigger signal and the female response would occur. The time course of the inhibition may be part of a temporal filter adapted to the time course of the duet song patterns (Stumpner and Nowotny 2014).

An inhibitory neuron similar to the role of LN2 was proposed by Crawford (1997) and Large and Crawford (2002) for an interval selective circuit in the mesencephalon of the mormyrid fish *Pollimyrus adspersus*. In this model an inhibitory neuron, would cause an inhibition leading to a subsequent postinhibitory rebound in a postsynaptic neuron. Inhibition driving a postinhibitory rebound has also been proposed to underlie the processing of temporal patterns in bats (Covey and Faure 2005) and seems to be a fundamental neural feature to enhance postinhibitory activity (Dodla et al. 2006).

Time course of the post-inhibitory rebound – the basis for delayed excitation

A rebound driven by inhibition allows delaying an excitatory response over a time interval of many milliseconds as compared to structural axonal delay lines described in binaural temporal processing, which can cover only a sub-millisecond range (Carr and Konishi 1988). It may therefore not be surprising, that it is a common mechanism underlying the processing of temporal auditory patterns. Postinhibitory rebound is an intrinsic property of the postsynaptic neuron. In response to a single sound pulse the PIR in neuron LN5 of *G. bimaculatus* develops from an initial inhibition over a time course of 89.4 ms to its maximum amplitude. The hyperpolarization-activated currents (I_h) driving the rebound have not been characterized in crickets. The I_h current is linked to the regulation of excitability and to the generation and timing of rhythmic motor activity and was first recognized in the heart and in motoneurons (Santoro and Baram 2003, Wahl-Schott 2009). It is based on the widely spread hyperpolarization-activated cyclic nucleotide-gated (HCN) channels, which also occur in insects (Jackson et al. 2007). In cockroaches they contribute to the spontaneous circadian pacemaker activity in the medulla (Wei and Stengl 2012). These cation (Na^+/K^+) channels are

activated upon membrane hyperpolarization while the opening of the channels is additionally facilitated by binding to cAMP. Functional diversity of I_h-channels is generated by four different genes in vertebrates, it is suggested that in bees splice variants of the single gene could generate a similar diversity (Santoro and Baram 2003, Gisselmann et al. 2003). One may speculate that diversity of I_h channels in the cricket taxon could lead to different time courses of the postinhibitory rebound in LN5 and thereby contribute to different species-specific phonotactic tuning. As the genomes of *G. bimaculatus* and *Laupala kohalensis* have recently been sequenced (Ylla et al. 2020) more information on the HCN channels in crickets will now be available.

Furthermore, as the channel properties are modulated by binding to cAMP, these channels might provide the basis for a modulatory change in phonotactic behavior, which occurs for a time period of seconds, after females have been exposed to the species-specific calling song (Poulet and Hedwig 2005). HCN channels in the cockroach are blocked by DK-AH269 (Wei and Stengl 2012). Altering the cAMP levels in female crickets or applying DK-AH269 might be a way to test the function of HCN channels in phonotaxis.

Coincidence detection

Coincidence detection is not just the summation of two excitatory inputs, but moreover the processing of inputs which have occurred at a specific moment in time and which simultaneously arrive at the coincidence detector, like in the Jeffress model of directional auditory processing in the barn owl (Joris et al. 1998, Konishi 2006). By extending this principle over a wider time scale of delays, processing of delayed signals with direct inputs allows for the systematic analysis of repetitive auditory pulse patterns. In the cricket the coincidence between a delayed postinhibitory rebound in LN5 and the direct activity of AN1 at the level of the coincidence detector LN3 boost the activity of the coincidence detector, when both inputs coincide. This principle of auditory processing has been proposed and/or demonstrated in a variety of auditory systems dealing with sequences of acoustic signals. In the inter-click-interval sensitive circuit proposed by Crawford (1997) and Large and Crawford (2002) the delayed rebound matches the natural range of inter-click-intervals in the fish species, providing an effective filter for click intervals. For pulse duration sensitive neurons in bats Covey and Faure (2003) and Sayegh et al. (2011) propose a similar principle based on the coincidence of an excitatory on-response, and a rebound excitation that marks the end of a pulse, the off-response. A particular pulse duration would be identified by the coincidence of

the on- and off-response, tuning to different pulse duration would be achieved by a delayed on-response. Thus the coincidence detection of direct and delayed signals appears to be a common theme and fundamental element in the processing of temporal patterns.

Feature detection by interaction of inhibition and excitation

Whereas the coincidence-detector integrates two excitatory inputs, the interaction of a leading inhibition and subsequent excitation shapes the neural response to sound pulses at the level of the feature detector LN4. In *G. bimaculatus* this interaction sets up a filter for the pulse repetition rate, it also demonstrates characteristics of a pulse duration filter and shows similarities to auditory processing in other systems. In the grasshopper *Chorthippus biguttulus* the AN4 neuron responds to a normal syllable with a leading inhibition followed spiking activity. Females do not orient to syllables interrupted by short 2-4 ms gaps, which are produced by males singing with one hind leg only. When stimulated with such "gappy" syllables, the AN4 response is dominated by inhibition, as each restart of the syllables triggers a leading inhibition. The tuning of the neural response corresponds to the tuning of the female behavior. The leading inhibition may also support the discrimination of sex-specific song features like the steep onset of male syllables as compared to the shallow onset of female syllables (Stumpner and Ronacher 1994, Krahe et al. 2002).

A pulse rate depending shift in the balance of inhibition and excitation is also a characteristic of interval counting neurons in anurans (Rose 2014, Rose et al. 2015) and leads to excitatory responses in mid-brain auditory neurons which are selective for the species-specific pulse rate of 30-40Hz as in advertisement calls, while inhibition dominates at lower and excitation is reduced at higher pulse rates.

Interaction of a maintained inhibition and phasic excitation, which in this case is not coupled to a post-inhibitory rebound, has been outlined as a mechanism sensitive to pulse duration in midbrain auditory neurons of frogs (Leary et al. 2008). In this case the excitatory response occurs during an ongoing inhibition. The balance of the inhibitory and excitatory input will determine if the excitation can overcome the inhibition, and the inhibition may also sharpen the excitatory response. In the cricket, when the activity of the coincidence detector is enhanced its input to LN4 will overcome the inhibition in the feature detector and it will drive a short pronounced suprathreshold depolarization. This depolarization is limited in time and does not follow the duration of long sound pulses. Thus, like in frogs the balance of inhibition

and excitation provides a pulse duration filter, as indicated in the recordings by Kostarakos and Hedwig (2012).

Future possibilities to analyze the system

Besides the deeper insight into the system, my experiments also demonstrate the limitations of an approach using single intracellular recordings to analyse high level sensory processing. The analysis can provide correlations between the neuronal activity/tuning and the tuning of the behavior in order to identify candidate neurons and processing mechanisms, however it cannot demonstrate the functional significance of a single neurons. Ideally a causal analysis would be aimed at allowing to manipulate the activity of single neurons or neuronal groups while the crickets perform phonotactic behavior. This could demonstrate if and to what degree the activity of the manipulated neuron contributes to the behavior. Although my experiments were performed with crickets walking on a trackball, they only rarely showed phonotactic behavior once the head capsule was opened, and altering neuronal activity during phonotaxis episodes was not possible. In similar experiments Schildberger and Hörner (1988) showed that manipulating the activity of AN1 will lead to changes in the walking direction of the cricket. In a different experimental set up Nolen and Hoy (1984) demonstrated by intracellular current injection that the activity of the AN2 neuron is sufficient and necessary to initiate phonotactic avoidance steering. Ideally one would like to induce phonotaxis or alter the tuning of phonotaxis by manipulating the activity of single neurons. The efficiency of such an approach however might be limited, as several neurons contribute to processing. In other species like Drosophila genetic tools are available to knock-out neurons or to reversibly silence or active specific sets of neurons in temperature sensitive mutants. These options are not yet available in crickets but would contribute to a more causal functional analysis of phonotactic behavior.

For a deeper understanding of the pattern recognition system a characterization of the synaptic connections within the network would be required, to confirm the current indirect assumptions based on latencies and activity patterns. Simultaneous intracellular recordings of the pattern recognition neurons will be very difficult to achieve, due to the small size of the neurons and the very lateral position of their cell bodies. Further insights might be gained by using a connectomics approach based on tracing of neuronal connections within stacks of electron microscopic sections as recently pioneered in the central nervous system of *Drosophila melanogaster* larvae and flies (Zarin et al 2019, Shan Xu et al. 2020). Connectomics could provide more detailed information on excitatory neuronal connections between the pattern

recognition neurons, however, it would not allow to specify the types of synapses involved, the dynamics of the neuronal processing or clarify the role of neuromodulators on processing in the network. However in combination with the data obtained from intracellular recordings deeper insight into the function of the system could be obtained.

In this regard in-vivo imaging may be further developed to approach the dynamics of processing in the pattern recognition network on a cellular and population level. Calcium sensitive dyes like Oregon Green or Fluo-6, can be delivered into the auditory neuropil by iontophoretic injections through the intact sheath of the brain with surface electrodes (Isaacson and Hedwig 2017). Preliminary results demonstrated specific auditory responses to the calling song pattern. Refined procedures may provide more detailed understanding of auditory processing at the population level and reveal to what degree the neurons projecting into the ring-like neuropil contribute to auditory processing. In Drosophila and other species a range of transgenic lines is available to specifically label neurons with genetically encoded Calcium indicators like GCaMPs to demonstrate neuronal activity with optical imaging. The development of these molecular genetic techniques in crickets would provide a powerful tool for the analysis of auditory processing. The genome of crickets (e.g. *G. bimaculatus*) has recently been sequenced (Ylla et al. 2020), so these option may become available in the near future. The current downside of calcium imaging at high special resolution is that it will require sophisticated two-photon microscopy with a temporal resolution of 1-2 Hz, which is not appropriate to resolve fast neuronal activity.

Besides gathering more detailed data on the cellular properties and connectivity of the pattern recognition network, using the current information on neuronal responses of the identified neurons in a modelling approach has provided a deeper understanding of the system (Clemens et al. 2020). It demonstrated the relevance of the delay-line mechanism and of inhibition in the network, and also showed that by fine tuning the neuronal parameters the wide range of pattern recognition preferences of extant crickets can be reproduced. Thus the delay-line and coincidence detection together with the processing of inhibition and excitation at the level of the feature detector may represent a neural framework that was relevant for the evolution of pattern recognition in crickets.

Pattern recognition and the control of phonotaxis

Besides the progress we have made in understanding pattern recognition a crucial part of the

analysis is still lacking: How does the pattern recognition process initiate and control the phonotactic walking behavior. As a consequence of pattern recognition descending neurons will need to be activated to initiate phonotactic walking behavior. So far no clear link has been established between the pattern recognition network and such interneurons. Descending neurons with auditory responses have been identified in crickets (Staudacher and Schildberger 1998, Zorović and Hedwig 2013) but their activity pattern is not sufficient to "explain" phonotactic walking. Also a descending command neuron for walking has been identified (Böhm and Schildberger 1992) but its activity pattern is not tightly linked to phonotactic behavior. One may expect that the feature detector neuron LN4, which gives the best tuning to the cricket song pattern, will be involved in driving the descending motor command. Its sparse coding of the pulse pattern would require that the LN4 bursting spike activity is integrated over a longer time course to generate a signal that could activate a descending pathway for phonotactic walking. Tuning of the descending neuron to the species-specific calling song could be achieved by integrating the spike activity of LN4 over a longer time scale, as proposed by Nabatiyan et al. (2003) for pattern recognition based on the repetition rate of spike bursts. The resulting command signal for walking however would not be appropriate to explain the rapid steering responses of females towards individual sound pulses of the chirps. Thus, a second parallel pathway for auditory steering will be required (Poulet and Hedwig 2005, Gabel et al. 2015). Currently the emerging picture is not yet conclusive to clearly close the loop between auditory processing and phonotactic motor control.

BIBLIOGRAPHY

Alexander R (1962) Evolutionary change in cricket acoustical communication. *Evolution,* 16(4):443–467

Andersen P and Eccles J (1962) Inhibitory phasing of neuronal discharge. *Nature*, *196*(4855), 645-647.

Böhm H and Schildberger K. (1992) Brain neurones involved in the control of walking in the cricket *Gryllus bimaculatus*. *J Exp Biol,* 166(1):113–130.

Boyan G (1981) Two-tone suppression of an identified auditory neurone in the brain of the cricket *Gryllus bimaculatus* (De Geer). *J Comp Physiol*, 144(1):117–25.

Boyan G (1984) Neural mechanisms of auditory information processing by identified interneurones in Orthoptera. *J Insect Physiol*, 30(1):27–41.

Boyan G and Williams J (1981) Descending interneurones in the brain of the cricket. *Naturwissenschaften,* Springer; 68(9):486–7.

Boyan G and Williams J (1982) Auditory neurones in the brain of the cricket *Gryllus bimaculatus* (De Geer): ascending interneurones. *J Insect Physiol,* 28(6):493–501.

Boyan G, Williams L and Meier T (1993) Organization of the commissural fibers in the adult brain of the locust. *J Comp Neurol,* 332(3):358–77.

Burrows M and Siegler M (1976). Transmission without spikes between locust interneurones and motoneurones. *Nature*, *262*(5565), 222-224.

Burrows M and Siegler M (1978). Graded synaptic transmission between local interneurones and motor neurones in the metathoracic ganglion of the locust. *J Physiol, 285*(1), 231-255.

Bush S and Schul J (2006) Pulse-rate recognition in an insect: evidence of a role for oscillatory neurons. *J Comp Physiol A*, 192(2):113–121

Carew T (2000) Behavioural Neurobiology Sinauer Associates Inc, Sunderland Massachusetts

Carr C and Konishi M (1988) Axonal delay lines for time measurement in the owl's brainstem. *PNAS,* 85(21):8311–5.

Clemens J, Schöneich S, Kostarakos K, Hennig R and Hedwig B (2020) A small,

computationally flexible network produces the phenotypic diversity of song recognition in crickets *BioRxiv* 221655.

Covey E and Faure P (2005) Neural mechanisms for analyzing temporal patterns in echolocating bats. in *Auditory Signal Processing: Physiology, Psychoacoustics, and Models.* Pressnitzer D, de Cheveign´ e A, McAdams S and Collet L (Eds) Springer; p. 250–256.

Crawford J (1997) Feature-detecting auditory neurons in the brain of a sound-producing fish. *J Comp Physiol,* 180(5):439–50.

Dodla R, Svirskis G and Rinzel J (2006) Well-timed, brief inhibition can promote spiking: postinhibitory facilitation. *J Neurophysiol,* 95(4):2664–77.

Doherty J and Pires A (1987) A new microcomputer-based method for measuring walking phonotaxis in field crickets (*Gryllidae*). *J Exp Biol*, *130*(1), 425-432.

Eisner N and Popov A (1978) Neuroethology of acoustic communication. In *Advances in insect physiology* (Vol. 13, pp. 229-355). Academic Press.

Felix R, Fridberger A, Leijon S, Berrebi A and Magnusson A (2011) Sound rhythms are encoded by post-inhibitory rebound spiking in the superior paraolivary nucleus. *J Neurosci,* 31(35):12566–78.

Fullard, J and Yack J (1993). The evolutionary biology of insect hearing. *Trends Ecol Evol*, *8*(7), 248-252.

Gabel E, Kuntze J and Hennig R (2015) Decision making and preferences for acoustic signals in choice situations by female crickets. *J Exp Biol,* 218(16):2641–50.

Gerhardt H and Huber F (2002) Acoustic communication in insects and anurans: common problems and diverse solutions. University of Chicago Press.

Gisselmann G, Warnstedt M, Gamerschlag B, Bormann A, Marx T and Neuhaus E (2003) Characterization of recombinant and native I h-channels from *Apis mellifera. Insect Biochem molec,* 33(11):1123–34.

Givois V and Pollack G (2000) Sensory habituation of auditory receptor neurons: implications for sound localization. *J Exp Biol*, *203*(17), 2529-2537.

Habenstein J, Amini E, Grübel K, Jundi B and Rössler W (2020) The brain of Cataglyphis ants: neuronal organization and visual projections. *J Comp Neurol,* 1-28.

Hartbauer M, Radspieler G and Römer H (2010) Reliable detection of predator cues in afferent spike trains of a katydid under high background noise levels. *J Exp Biol*, *213*(17), 3036-3046.

Hedwig B (2006) Pulses, patterns and paths: neurobiology of acoustic behaviour in crickets. *J Comp Physiol A,* 192: 677-689.

Hedwig B (2014) Insect Hearing and Acoustic Communication. Springer, ISBN 978-3-642-40462-7

Hedwig B (2016) Sequential Filtering Processes Shape Feature Detection in Crickets: A Framework for Song Pattern Recognition, *Front Physiol,* 7, 46.

Hedwig B (2017) Trackball systems for analysing cricket phonotaxis. In *The Cricket as a Model Organism.* Springer, Tokyo. Chapter 19, pp: 303-312.

Hedwig B and Elsner N (1985) Sound production and sound detection in a stridulating acridid grasshopper (*Omocestus viridulus*). In: Kalmring K and Elsner N (eds) *Acoustic and vibrational communication in insects*. Parey Hamburg, pp: 61-72.

Hedwig B and Poulet J (2005) Mechanisms underlying phonotactic steering in the cricket *Gryllus bimaculatus* revealed with a fast trackball system. *J Exp Biol, 208*(5), 915-927.

Hedwig B and Poulet J (2004) Complex auditory behaviour emerges from simple reactive steering. *Nature*, *430*(7001), 781-785.

Hedwig B and Sarmiento-Ponce E (2017) Song pattern recognition in crickets based on a delay-line and coincidence-detector mechanism. *P Roy Soc B*, *284*(1855), 20170745.

Hedwig B and Stumpner A (2016) Central neural processing of sound signals in insects. In: Pollack G, Mason A, Popper A and Fay R (eds), *Springer Handbook of Auditory Research: Insect Hearing*, Chapter 8, pp: 177-214, DOI 10.1007/978-3-319-28890-1_8

Hennig R (1988) Ascending auditory interneurons in the cricket *Teleogryllus commodus* (Walker): comparative physiology and direct connections with afferents. *J Comp Physiol A,* 163(1):135–43.

Hennig R (2003) Acoustic feature extraction by cross-correlation in crickets? *J Comp Physiol A*, 189(8):589–598

Horch H, Mito T, Ohuchi H, Popadić A and Noji S (eds) (2017) The Cricket as a Model

Organism Development, Regeneration and Behaviour. Springer Tokyo Japan.

Hoy R (1978) Acoustic communication in crickets: a model system for the study of feature detection. Federation Proceedings. p. 2316–23.

Huber F, Moore T and Loher W (Eds) (1989) Cricket behavior and neurobiology. Cornell University Press, Ithaca, NY. Ithaca and London: Cornell University Press.

Isaacson M and Hedwig B (2017) Neuroanatomical and functional labeling by tracer electrophoresis through the nerve sheath. *Sci Rep*, 7(1), 1-6.

Jackson H, Marshall C and Accili E (2007) Evolution and structural diversification of hyperpolarization-activated cyclic nucleotide-gated channel genes. *Physiol Genomics*, 29(3):231–45.

Jacob P and Hedwig B (2019) Structure, activity and function of a singing-CPG interneuron controlling cricket species-specific acoustic signaling. *J Neurosci*, 39 (1) 96-111.

Joris P, Smith P and Yin T (1998) Coincidence detection minireview in the auditory system: 50 years after Jeffress. *Neuron*, 21:1235–8.

Kandel E, Frazier W and Wachtel H (1969) Organization of inhibition in abdominal ganglion of Aplysia. I. Role of inhibition and disinhibition in transforming neural activity. *J Neurophysiol*, *32*(4), 496-508.

Knepper M and Hedwig B (1997) NEUROLAB, a PC-program for the processing of neurobiological data. *Comp Meth Prog Biomed,* 52, 75–77.

Konishi M (1991) Deciphering the brain's codes. *Neural Comput*, 3(1):1–18.

Konishi M (2006) Listening with two ears. Scientific American. Nature Publishing Group; 16:28–35.

Kopp-Scheinpflug C, Tozer A, Robinson S, Tempel B, Hennig M and Forsythe I (2011) The sound of silence: ionic mechanisms encoding sound termination. *Neuron*, *71*(5), 911-925.

Kostarakos K and Hedwig B (2012) Calling song recognition in female crickets: Temporal tuning of identified brain neurons matches behaviour. *J Neurosci,* 32: 9601-9612

Kostarakos K and Hedwig B (2015) Pattern recognition in field crickets: Concepts and neural evidence. *J Comp Physiol A*, 201: 73-85.

Kostarakos K and Hedwig B (2017) Surface electrodes record and label brain neurons in insects. *J Neurophysio*, *118*(5), 2884-2889.

Krahe R, Budinger E and Ronacher B (2002) Coding of a sexually dimorphic song feature by auditory interneurons of grasshoppers: the role of leading inhibition. *J Comp Physiol A,* 187(12):977–85.

Kurylas A, Rohlfing T, Krofczik S, Jenett A and Homberg U (2008) Standardized atlas of the brain of the desert locust, *Schistocerca gregaria*. *Cell Tissue Res,* 333(1):125–45.

Kutsch W and Otto D (1972). Evidence for spontaneous song production independent of head ganglia in *Gryllus campestris L. J Comp Physiol, 81*(1), 115-119.

Large E and Crawford J (2002) Auditory temporal computation: interval selectivity based on post-inhibitory rebound. *J Comput Neurosci,* 13(2):125–42.

Laufer B (1927) Insect-musicians and cricket champions of China. *Anthropology Leaflet*. JSTOR; 1–27.

Leary C, Edwards C and Rose G (2008) Midbrain auditory neurons integrate excitation and inhibition to generate duration selectivity: an in vivo whole-cell patch study in anurans. *J Neurosci*, 28(21):5481.

Løfaldli B, Kvello P and Mustaparta H (2010) Integration of the antennal lobe glomeruli and three projection neurons in the standard brain atlas of the moth *Heliothis virescens*. *Front Syst Neurosc*, 4:5.

Marsat G and Pollack G (2006) A behavioral role for feature detection by sensory bursts. *J Neurosci*, *26*(41), 10542-10547.

Martin K (1994) A brief history of the “feature detector.” *Cereb cortex*, 4(1):1–7.

Murphey R and Zahetsky M (1973) Orientation to the calling song by female crickets, *Scapiepidut margmatiu* (*Gryllidae*). *J exp Biol,* 56, 335-53.

Nabatiyan A, Poulet J, Polavieja G and Hedwig B (2003) Temporal pattern recognition based on instantaneous spike rate coding in a simple auditory system. *J Neurophysiol*, 90, 2484-2493.

Nolen T and Hoy R (1984) Initiation of behavior by single neurons: the role of behavioral context. *Science*, 226(4677):992–4.

Ostrowski T and Stumpner A (2010) Frequency processing at consecutive levels in the auditory system of bush crickets (*Tettigoniidae*). *J Comp Neurol*, 518(15):3101–16.

Ostrowski T and Stumpner A (2013) Processing of ultrasound in a bush cricket's brain. *Physiol Entomol,* 38:33–44.

Pearson K and Fourtner C. (1975) Nonspiking interneurons in walking system of the cockroach. *J neurophysiol*, *38*(1), 33-52.

Pollack G and Hoy R (1979) Temporal pattern as a cue for species-specific calling song recognition in crickets. *Science*, 204(4391):429.

Popov A and Shuvalov V (1977) Phonotactic behavior of crickets. *J Comp Physiol A*, 119(1):111–26.

Poulet J and Hedwig B (2005) Auditory orientation in crickets: Pattern recognition controls reactive steering. *PNAS*, 102 (43): 15665-15669.

Rehbein H (1976) Auditory neurons in the ventral cord of the locust: morphological and functional properties. *J Comp Physiol A,* 110(3):233–50.

Rheinlaender J, Kalmring K, Popov AV and Rehbein H (1976) Brain projections and information processing of biologically significant sounds by two large ventral-cord neurons of *Gryllus bimaculatus* DeGeer (Orthoptera, Gryllidae). *J Comp Physiol A*, 110(3):251–69.

Roesel von Rosenhof (1748) Der Monatlich-Herausgegebenen Insecten-Belustigung.

Ronacher B (2019) Innate releasing mechanisms and fixed action patterns: basic ethological concepts as drivers for neuroethological studies on acoustic communication in Orthoptera. *J Comp Physiol A*, 205(1):33–50.

Ronacher B and Stumpner A (1988) Filtering of behaviourally relevant temporal parameters of a grasshopper's song by an auditory interneuron. *J Comp Physiol A*, *163*(4), 517-523.

Rose G (2014) Time computations in anuran auditory systems. *Front Physio*, 5:206.

Rose G and Capranica R (1983) Temporal selectivity in the central auditory system of the leopard frog. *Science,* 219(4588):1087–9.

Rose G, Hanson J, Leary C, Graham J, Alluri R and Vasquez-Opazo G (2015) Species-specificity of temporal processing in the auditory midbrain of gray treefrogs: interval-counting neurons. *J Comp Physiol A*, 201(5):485–503.

Santoro B and Baram T (2003) The multiple personalities of h-channels. *Trends Neurosci*, 26(10):550–4.

Sayegh R, Aubie B and Faure P (2011) Duration tuning in the auditory midbrain of echolocating and non-echolocating vertebrates. *J Comp Physiol A*, 197(5):571–83.

Schildberger K (1984) Temporal selectivity of identified auditory neurons in the cricket brain. *J Comp Physiol A*, 155(2):171–85.

Schildberger K (1988) Behavioral and neuronal mechanisms of cricket phonotaxis. *Cell Mol Life Sci*, 44(5):408–15.

Schildberger K and Hörner M (1988) The function of auditory neurons in cricket phonotaxis I. Influence of hyperpolarization of identified neurons on sound localization. *J Comp Physiol A*, 163(5):621–31.

Schildberger K, Huber F and Wohlers D (1989) Central auditory pathway: neuronal correlates of phonotactic behavior. In: Huber F, Moore TE and Loher W, editor. Cricket behavior and neurobiology. Cornell University Press; p. 423–58.

Schöneich S and Hedwig B (2012) Cellular basis of singing motor pattern generation in the field cricket (*Gryllus bimaculatus* deGeer). *Brain Behav*, 2(6), 707-725.

Schöneich S, Kostarakos K and Hedwig B (2015) An Auditory Feature Detection Circuit for Sound Pattern Recognition. *Sci Adv*, 1(8) e1500325.

Siegler M (1984). Local interneurones and local interactions in arthropods. *J Exp Biol*, *112*(1), 253-281.

Spencer W and Kandel E (1961). Electrophysiology of hippocampal neurons: IV. Fast prepotentials. *J neurophysiol*, *24*(3), 272-285.

Staudacher E and Schildberger K (1998) Gating of sensory responses of descending brain neurones during walking in crickets. *J Exp Biol,* 201(4):559–72.

Stiedl O, Stumpner A, Mbungu D, Atkins G and Stout J (1997) Morphology and physiology of local auditory interneurons in the prothoracic ganglion of the cricket *Acheta domesticus*. *J Exp Zool,* 279(1):43–53.

Stumpner A (1999) Comparison of morphology and physiology of two plurisegmental sound-activated interneurones in a bushcricket. *J Comp Physiol A*, 185(2):199–205.

Stumpner A and Molina J (2006) Diversity of intersegmental auditory neurons in a bush cricket. *J Comp Physiol A*, 192(12):1359–76.

Stumpner A and Ronacher B (1991) Auditory interneurones in the metathoracic ganglion of the grasshopper *Chorthippus biguttulus*: I. Morphological and physiological characterization. *J Exp Biol*, 158(1):391–410.

Stumpner A and Ronacher B (1994) Neurophysiological aspects of song pattern recognition and sound localization in grasshoppers. *Am Zoolo*, 34(6):696–705.

Stumpner A and von Helversen D (2001) Evolution and function of auditory systems in insects. *Naturwissenschaften*. Springer; 88(4):159–70.

Murphey R (1972). Orientation to calling song by female crickets, *Scapsipedus marginatus* (Gryllidae). *J Exp Biol*, *56*(2), 335-352.

Thorson J, Weber T and Huber F (1982) Auditory behavior of the cricket II. Simplicity of calling-song recognition in *Gryllus*, and anomalous phonotaxis at abnormal carrier frequencies. *J Comp Physiol A*, 146(3):361–78.

Tschuch G (1976) Der Einfluss synthetischer Gesaenge auf die Weibchen von *Gryllus bimaculatus* deGeer. *Zoo JB Physiol*, 80:383–8.

Verburgt L, Ferreira M and Ferguson, J (2011) Male field cricket song reflects age, allowing females to prefer young males. *Anim Behav*, *81*(1), 19-29.

Wahl-Schott C and Biel M (2009) HCN channels: structure, cellular regulation and physiological function. *Cell Mol Life Sci*, 66(3):470–94.

Walikonis R, Schoun D, Zacharias D, Henley J, Coburn P and Stout J (1991) Attractiveness of the male *Acheta domesticus* calling song to females. *J Comp Physiol A*, *169*(6), 751-764.

Weber T and Thorson J. (1989) Phonotactic behavior of walking crickets. In: Huber F, Moore T and Loher W, editor. *Cricket behavior and neurobiology* Cornell University Press, Ithaca, NY. Ithaca and London: Cornell University Press, p. 310–39.

Wei H and Stengl M (2012) Ca^{2+} dependent ion channels underlying spontaneous activity in insect circadian pacemaker neurons. *Eur J Neurosci* 36:3021-3029

Wendler G, Dambach M, Schmitz B and Scharstein H (1980). Analysis of the acoustic orientation behavior in crickets (*Gryllus campestris L.*). *Naturwissenschaften*, *67*(2), 99-101.

Wiese K and Albrecht S (1990). A time constant in the auditory pathway of the cricket Gryllus bimaculatus related to the naturally used period of chirp repetition. In *Sensory Systems and Communication in Arthropods* (pp. 395-401). Birkhäuser, Basel.

Wiese K and Eilts K (1985) Evidence for matched frequency dependence of bilateral inhibition in the auditory pathway of *Gryllus bimaculatus*. Zoologische Jahrbücher Abteilung für allgemeine Zoologie und Physiologie der Tiere. Gustav Fischer Verlag, 89(2):181–201.

Wohlers D and Huber F (1982) Processing of sound signals by six types of neurons in the prothoracic ganglion of the cricket, *Gryllus campestris L. J Comp Physiol A*, 146(2):161–73.

Xu C, Januszewski M, Lu Z, Takemura S, Hayworth K, Huang G, Shinomiya K, Maitin-Shepard J, Ackerman D, Berg S, Blakely T, Bogovic J, Clements J, Dolaf T, Hubbard P, Kainmueller D, Katz W, Kawase T, Khairy K, Leavitt L, Li P, Lindsey L, Neubarth N, Olbris D, Otsuna H, Troutman E, Umayam L, Zhao T, Ito M, Goldammer J, Wolff T, Svirskas R, Schlegel P, Neace E, Knecht Jr. C, Alvarado C, Bailey D, Ballinger S, Borycz J, Canino B, Cheatham N, Cook M, Dreher M, Duclos O, Eubanks B, Fairbanks K, FinleyS, Forknall N, Francis A, Hopkins G, Joyce E, Kim S, Kirk N, Kovalyak J, Lauchie S, Lohff A, Maldonado C, Manley E, McLin S, Mooney C, Ndama M, Ogundeyi O, Okeoma N, Ordish C, Padilla N, Patrick C, Paterson T, Phillips E, Phillips E, Rampally N, Ribeiro C, Robertson M, Rymer J, Ryan S, Sammons M, Scott A, Scott A, Shinomiya A, Smith C, Smith K, Smith N, Sobeski M, Suleiman A, Swift J, Takemura S, Talebi I, Tarnogorska D, Tenshaw E, Tokhi T, Walsh J, Yang T, Horne J, Li R, Parekh R, Rivlin P, Jayaraman V, Ito K, Saalfeld S, George R, Meinertzhagen I, Rubin G, Hess H, Scheffer L, Jain V and Plaza S (2020) A Connectome of the Adult Drosophila Central Brain. *BioRxiv* 911859.

Yager D (1999) Structure, development, and evolution of insect auditory systems. *Microsc Res Tech*, *47*(6), 380-400.

Ylla G, Nakamura T, Itoh T, Kajitani R, Toyoda A, Tomonari S, Bando T, Ishimaru Y, Watanabe T, Fuketa M, Matsuoka Y, Noji S, Mito T and Extavour C (2020) Cricket genomes: the genomes of future food. BioRxiv 2020.07.07.191841.

Zarin A, Mark B, Cardona A, Litwin-Kumar A and Doe C (2019) A Drosophila larval premotor/motor neuron connectome generating two behaviors via distinct spatio-temporal muscle activity. B*ioRxiv,* 617977.

Zhang, X and Hedwig B (2019) Bilateral auditory processing studied by selective cold deactivation of cricket hearing organs. *J Exp Biol*, 222(21).

Zorović M and Hedwig B (2011) Processing of species-specific auditory patterns in the cricket brain by ascending, local and descending neurons during standing and walking. *J Neurophys*, 105: 2181–2194.

Zorović M and Hedwig B (2013). Descending brain neurons in the cricket *Gryllus*

bimaculatus (de Geer): auditory responses and impact on walking. *J Comp Physiol A*, *199*(1), 25-34.